Development of Peptide-Polymers for Drug and Gene Delivery to the Central Nervous System

David S. Chu

A dissertation submitted
in partial fulfillment of the
requirements for the degree of

Doctor of Philosophy

University of Washington

2014

Reading Committee:

Suzie Pun, Chair

Robert Rostomily

Patrick Stayton

Program Authorized to Offer Degree:

Bioengineering

University of Washington

Abstract

Development of Peptide-Polymers for Drug and Gene Delivery to the Central Nervous System

David S. Chu

Chair of the Supervisory Committee
Professor Suzie H. Pun, Ph.D.
Bioengineering

Diseases of the central nervous system are largely untreatable, with most current treatment strategies palliative. Current therapeutic strategies are limited by drugs of low potency, poor pharmacokinetics, and poor biodistribution following systemic administration. Diseases of the central nervous system are amongst the most debilitating and difficult to treat, significantly affecting the productivity and livelihood of those afflicted. In this work, polymeric display of bioactive peptides is used to rationally design novel therapeutics aimed at treating several central nervous system disorders. These materials address several limitations of peptides, such as poor proteolytic stability, rapid clearance, and low efficacy, via conjugation to polymeric backbones, improving pharmacokinetics and increasing peptide activity through multivalency and avidity. Three classes of materials were explored: cationic polymers for gene delivery; thrombin-inhibiting polymers for spinal cord injury and regeneration; and pro-apoptotic polymers for treating glioblastoma multiforme. Chapter 1 provides a short introduction towards using peptide-polymers as alternative therapeutics for many neurological disorders. Chapter 2 summarizes the use of living radical polymerization techniques for the development of synthetic gene delivery vectors. In Chapters 3-7, the inclusion of peptides into polymeric constructs were shown to (1) increase peptide bioactivity relative to free peptide, (2) tune peptide release and mediate enzyme-triggered polymer degradation, and (3) mediate cellular targeting via modulation of peptide ligand density. Chapter 8 concludes with recommendations for future work based on these findings.

TABLE OF CONTENTS

Page

LIST OF FIGURES

Figure Number Page

LIST OF TABLES

Table Number Page

ACKNOWLEDGEMENTS

This thesis was accomplished with the love and support of family, friends, coworkers, and mentors. I cannot express enough appreciation for the guidance and knowledge I received during my graduate school education, but I want to highlight and acknowledge many of the individuals that were instrumental towards my development in graduate school.

I would like to first thank my advisor Dr. Suzie Pun. She has served as an exemplary mentor and leader for our research group. Under her guidance, I gained invaluable knowledge regarding scientific thinking, experimental planning, group management, and project design. It has been an unbelievable blessing to work with an advisor that prioritizes my personal and career goals while advocating strongly on my behalf. It truly has been a privilege to work with and learn so much from such a talented and caring mentor. I will always cherish my training with her and look forward to our continued friendship.

I would like to thank the other members of my supervisory committee, Dr. Robert Rostomily, Dr. Patrick Stayton, and Dr. Andrew Boydston, for their guidance and advice. Their scientific input regarding relevant clinical needs, polymer and nanoparticle design, and chemical synthesis and characterization challenged and enriched my scientific understanding, refined my project design, and reinforced my scientific knowledge. I appreciated having supportive committee members that significantly contributed to my intellectual development.

Additionally, I would like to acknowledge and individually thank many of my labmates, both current and past, with whom I have spent many years work and socializing:

- Ester Kwon, my first mentor in the lab, who established high standards for scientific success. Her blend of scientific skepticism and grounded perspective on research shaped my graduate school expectations while her incredible lab sacrifices motivated me to be better lab citizen.

- Russell Johnson, my co-first mentor, who initially developed the peptide-polymer platform. His leadership, happy demeanor, and willingness to mentor younger students set high expectations for group leadership. I appreciated the long conversations about college football, family life, and professional development.

- Katherine Wang, one of my closest friends (and former workout buddy) in the group, who demonstrated work-life balance is achievable despite long work hours. Her endless support and words of motivation, both before and after her graduation, pushed me through the challenges of graduate school. I could not have made it without her support.

- Julie Shi, a wonderful and close collaborator in the lab, who expertly blended personal productivity with group leadership. Her endless optimism, cheer, and perseverance despite research setbacks remains remarkable to me. I learned immensely from working closely with her for several years and will always remember the years we effectively served together as the parents of the lab. Also, her baked goods significantly improved many rough days ($p < 0.001$).

- Joan Schellinger, an amazing chemistry knowledge bank and awesome officemate, whose willingness and devotion towards teaching chemistry to us hapless graduate students is leading to the successful completion of many PhDs. She handled collaborative projects involving many lab members with class and patience, defining excellence in mentorship and teaching. Added friendship bonus: mutual appreciation of beer and all-you-can-eat KFC.

- Maryelise Cieslewicz, a great (and token white) commiserating labmate, whose help with biological and animal work was really appreciated. I enjoyed the long conversations about the challenges of science, graduate school, and professional development. I thank her for taking a lot of the lab responsibility my last year to really help me finish my studies.

- Leslie Chan, my fellow Canto, who helped me immensely with several animal studies. I thank her for being a fun labmate, good friend, and equally (or most) importantly for understanding the greatness that is chicken chowdown.

- Kevin Tan, my closest friend in lab, whose support and perspective carried me through the good and bad times. Though I can't understand or appreciate fashion, I appreciate his efforts to teach me the intricacies of design and aesthetics. His endorsement of chili cheese fries, fried chicken, and Big Macs will always be much appreciated.

- Christine Wang, a wonderful officemate, coworker, and friend, who was always willing to hang out and appreciate the glory of chicken and wine Tuesdays. And $5 wing Mondays. And Well Wednesdays. And Tea Thursdays. And all the other great nights. When "child" completes her PhD, I will feel all the pride of a proud parent.

- Hua Wei, a great polymer chemistry resource, who defined the meaning of productivity. His interests developing polymers with advanced architectures significantly influenced my perspective in material design.

- Chayanon Ngambenjawong, a loyal friend and coworker, who kept me company during late nights in lab and became my (semi-willing) protégé. He provided endless entertainment with his proclivity for napping anywhere at all times and the "guess what Chay is saying" inadvertent trivia games. But honestly, I could not have completed this work without him and I am incredibly thankful for all his help.

- Michael Bocek, a brilliant undergraduate mentee, who went through the trenches of research with me. I appreciate his long hours, problem-solving abilities, and most significantly his appreciation of German beer after tough (and not so tough) days.

- Bob Lamm, the third of the Kamei lab/Bruin trifecta, who has been a great and reliable friend during our short time together. I value his friendship, devotion, and overall concern about the lab environment.

- Tae Hee Kim, Maja Zavaljevski, Nataly Kacherovsky, Paul Elias, and Yilong Chen: great postdocs/research scientists, who helped keep the lab productive and functional. I learned a lot both personally and professionally from these individuals and will cherish our time together.

- Josh Pahang, a very hard working undergrad, who helped significantly with my work. I appreciate his hard work in lab, our long conversations about life and sports, and his insights into the college football world.

- Jen Choi and Peter Carlson, two exceptional undergraduates, for their contributions to the gene delivery projects and for their personal friendships. I appreciate the hard work, dedication, and personal sacrifice.

- Gary Liu and Brynn Livesay, who brought back youthful energy, enthusiasm, and excitement to the lab. I appreciate your contributions and dedication towards making the lab a fun and positive work environment.

I'd also like to acknowledge my incredible family. My parents taught me through example how hard work, determination, loyalty, and persistence can lead to successful and fulfilling careers and family lives. They loved me unconditionally and have always been the most caring parents, prioritizing my personal success and happiness. I cannot thank them enough for their personal sacrifices to privilege me with such a great upbringing; I truly could not have asked for better parents.

I also want to thank my partner Eric who has been with me through all good and rough times of graduate school. He put up with my long hours and the difficult times during graduate school while always finding a way to cheer me up when the hardships would dampen my mood. His dedication and affection helped carry me through the difficulties and challenges of graduate school.

Finally, I'd like to acknowledge many friends inside and outside of the graduate program. Drs. Bilal Ghosn and Anthony Convertine – thanks for the many science (and life) conversations; they were enlightening and I learned so much from each of you. Shivang Dave – one of the most energetic, positive individuals I've ever meet; thanks for always finding time to give me a pep talk, quote of the day, or words of encouragement. Susan Liu and John Katahara – thanks for all the good times, the fried chicken and football weekends, and for being awesome, caring friends. And to my best friend Talia, who always makes me laugh and puts my life in perspective when things are rough.

DEDICATION

to my parents Chact and Miranda
and my sister Karen
for watching over and guiding me through life,
in person and in spirit

Chapter 1

DESIGN OF PEPTIDE-BASED THERAPEUTICS FOR NEUROLOGICAL DISEASES

1.1 Introduction

Most neurological disorders currently lack effective therapeutics and remain largely untreatable. Significant barriers towards development of effective therapeutics include poor drug penetration into the central nervous system (CNS) due to the blood brain barrier (BBB), limited neuroregenerative capacity of the CNS, and limited understanding of disease development. Many clinically-approved drugs only provide palliative and symptomatic care while failing to address the disease causes. Biologic therapeutics, such as peptides and nucleic acids, can potentially significantly improve the prognosis in many of these diseases and overcome shortcomings of current small-molecule therapies. Therefore, development of effective biologic and bio-mimetic materials is needed.

This collective work aims to: (1) rationally design peptide-based nonviral vectors for gene delivery to the central nervous system; (2) develop peptide-functionalized polymers to improve spinal cord injury recovery; and (3) investigate novel pro-apoptotic polymers for treatment of glioblastoma multiforme. We developed a flexible peptide-polymer platform allowing for modular design of materials, improved pharmacokinetics of peptide-grafted therapeutics, environmentally-responsive degradation and drug release, and exploration of multivalency and polymer architecture for altered peptide bioactivity. The living radical polymerization technique reversible addition-fragmentation chain transfer (RAFT) polymerization was used to synthesize various copolymers with near-statistical incorporation of monomer units and low polydispersity. Chapter 2 highlights the use of living radical polymerization techniques for the investigation and development of nonviral gene delivery vectors. Chapters 3 and 4 focus on the development of peptide-based non-viral vectors for gene delivery. Chapter 5 highlights thrombin-inhibiting polymers for intraspinal hydrogel administration following spinal cord injury. Chapters 6 and 7 focus on the development of pro-apoptotic polymers and demonstrates potential effects of multivalency on peptide bioactivity. Finally, Chapter 8 highlights potential future directions stemming from the previously

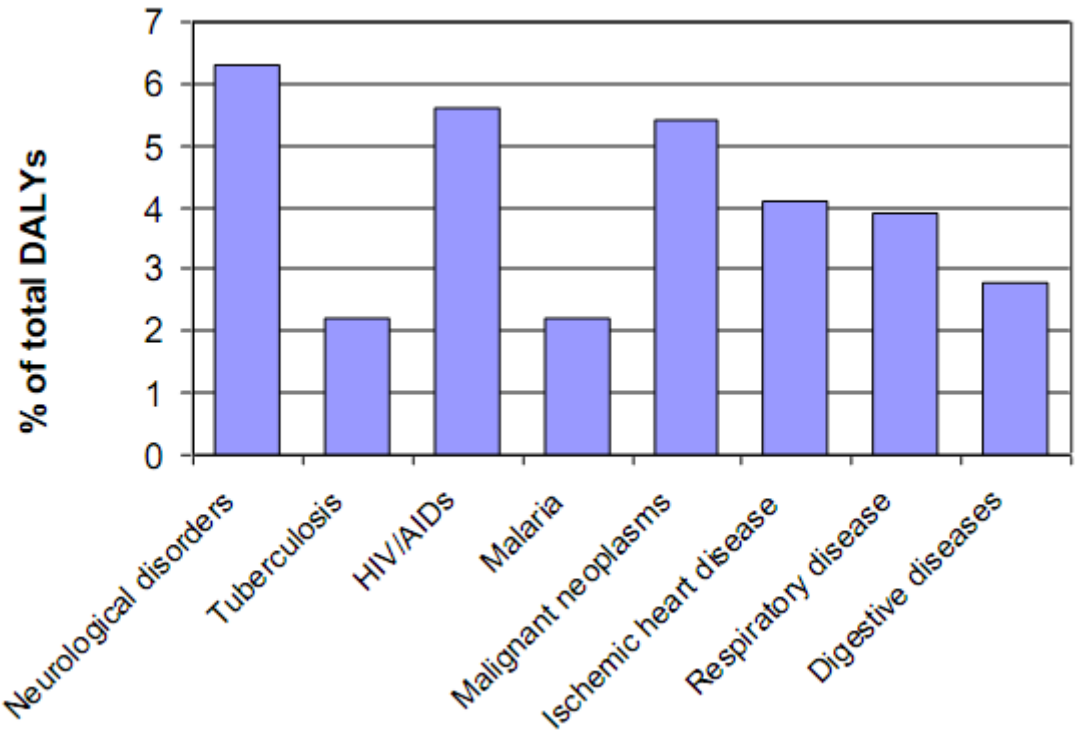

Figure 1.1. By percentage of total DALYs (disability adjusted life years), neurological disorders compromise a percentage of global disease burden exceeding that of HIV/AIDS, malignant neoplasms, and ischemic heart disease.[1]

presented works. Chapter 1 serves to give an overview of the design and motivation for the current work described here.

1.2 Diseases of the central nervous system

Neurological diseases are amongst the most pervasive and debilitating diseases. An estimated 100 million Americans are afflicted by neurological disease,[2] primarily chronic pain, at great annual cost. According to the World Health Organization, the global neurological disease burden exceeds HIV/AIDS, ischemic heart disease, and respiratory diseases (Figure 1.1). This section will highlight three classes of disorders addressed in this work: neurodegenerative diseases, spinal cord injury, and glioblastoma multiforme.

1.2.1 Neurodegenerative diseases of the brain

Neurodegenerative diseases, such as Alzheimer's and Parkinson's disease, are crippling, irreversible conditions that progressively lead to dementia and loss of motor and brain function. In the United States, over 5 million individuals suffer from Alzheimer's at estimated direct annual costs exceeding $200 billion.[3] Risk factors for neurodegenerative diseases vary from primarily age-related risk (Alzheimer's) to genetic factors (Huntington's disease).[4] These diseases involve progressive loss of function and subsequent death of various neuronal populations. Still poorly understood, these diseases lack curative therapies. Some drugs currently approved for use in treating various neurodegenerative diseases include: (1) L-DOPA, a dopamine analogue for increasing neurotransmitter concentration, providing symptomatic relief for dopaminergic neuron loss;[5] (2) acetylcholinesterase inhibitors, which maintain higher acetylcholine neurotransmitter concentrations to compensate for cholinergic neuronal loss;[6] (3) and NMDA receptor antagonists, which reduce glutamate excitotoxicity.[7] Despite providing symptomatic relief, none have significantly slowed or reversed disease development.

Neurotrophic factors play a major role in the development, maintenance and survival of neurons and their supporting cells. Highly-potent neurotrophic factors promote survival of neurons in degenerative diseases, making them attractive candidates in neurodegeneration treatments;[8] however, clinical translation is limited due to difficulties in protein delivery and poor pharmacokinetics in the CNS. Direct intraventricular infusion of neurotrophic factors was associated with significant side effects including Schwann cell hyperplasia and neuropathic pain.[9] An alternative strategy uses gene delivery vectors to modulate neurotrophic factor expression in the brain;[10] transfecting neurons in the brain may sustain elevated neurotrophic factor levels. Developing safe and effective vectors to modulate gene expression in the brain is therefore an attractive therapeutic strategy.

1.2.2 Spinal cord injury

Neurological trauma, such as brain and spinal cord injuries from motor vehicle accidents, are common, with 12,000 new cases of non-lethal spinal cord injury annually in the US.[2] The resulting damage from the primary trauma coupled with the poor innate regenerative capacity of the nervous

system frequently leads to significant physical impairment, with estimated direct lifetime medical costs of $1.5-4.5 million for individuals injured at age 25.[2] Following initial trauma, a period of primary and secondary injury occurs that significantly impacts functional recovery.[11] Inflammatory responses to spinal cord injury lead to scarring that physically obstructs the spinal column and limits neural network recovery. Methods to mitigate inflammation-related neurotoxicity following injury have shown promise in animal models.[11] Corticosteroids like methylprednisolone have been administered within 6-8 hrs of injury to reduce inflammatory responses; however, recent studies suggest minimal clinical benefits but significant health risks associated with its immunosuppressive properties.[12] Therefore, alternative strategies locally modulating the natural inflammatory response may be clinically relevant.

1.2.3 Glioblastoma multiforme

Nearly 70,000 new primary brain tumors are diagnosed annually.[2] Glioblastoma multiforme (GBM), a highly invasive stage IV cancer, is the most common primary malignant brain tumor with median survival of less than six months when left untreated.[13] Characterized by pervasive intrusion into adjacent neural tissue, strong chemotherapeutic resistance, and anti-apoptotic phenotype, it is one of the most challenging cancers to treat.[13] Surgical resection in combination with radiochemotherapy can extend median survival to over one year;[14] however high rates of tumor recurrence in sites directly adjacent to the surgical resection suggests residual cancer cells in the neighboring tissues rapidly re-form tumors. Locoregional therapy has been well-studied for chemotherapeutic delivery to GBM since it bypasses the BBB, permitting high drug concentrations in tissues adjacent to the main tumor mass. GLIADEL® Wafers, polymeric drug-eluting wafers implanted in the surgical resection cavity, slightly improve median survival by several months.[15] Convection-enhanced delivery (CED) strategies for direct drug delivery into the brain parenchyma suffer from highly variable drug distribution and high rates of adverse side effects.[16] Development of potent therapeutics that can be locally administered following surgical resection could lead to improved clinical outcome.

1.3 Drug and gene delivery for central nervous system disorders

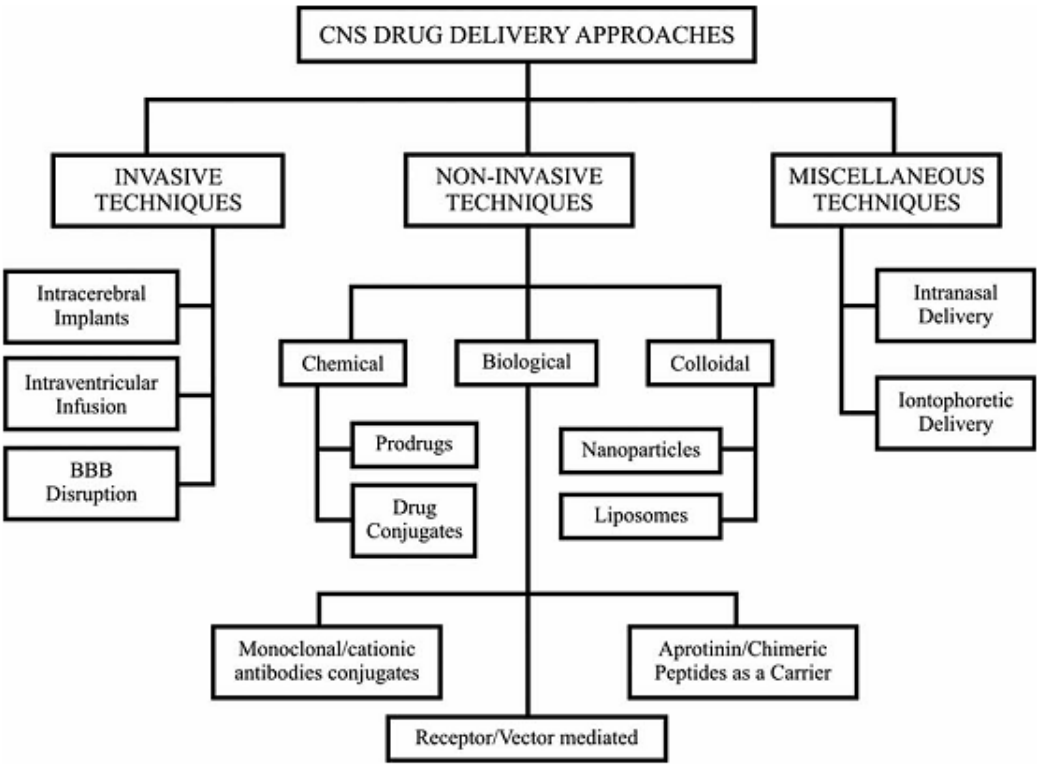

Figure 1.2. Summary of CNS drug delivery approaches.[17]

Many different approaches towards therapeutic delivery to the CNS have been investigated (Figure 1.2). Small molecules comprise most clinically-approved drugs for CNS diseases due to their potential to passively penetrate the BBB.[18] Strong correlations between lipophilicity and drug penetration through the BBB following systemic administration have been demonstrated; however, nearly all small molecule drug candidates are excluded almost completely from the CNS due to the BBB, significantly hindering drug development.[19] Effective delivery of larger biologic drug candidates, therefore, remains a significant challenge.

Biologics, such as proteins and nucleic acids, have significant advantages over traditional small molecule drugs. Nucleic acid-based therapeutics, such as small interfering RNA (siRNA) and gene therapies, have nearly limitless potential for disease treatment through direct modulation of gene expression in target tissues.[10] Nucleic acid delivery to the CNS has been primarily investigated with adeno-associated viruses due to their high transduction efficiency and innate neural tropism, but concerns over immunogenicity and safety limit clinical translation.[20]

Development of effective nonviral delivery vectors can potentially lead to potent and safe nucleic acid therapeutics.

Proteins and peptides have highly specific functionality that allows for complex signaling and potent activity. Compared to small-molecule drugs, peptides and proteins have decreased off-target interactions and significantly more druggable targets since they can be designed to interact with nearly limitless epitopes;[21] small-molecule drugs must by nature be designed to fit small protein folds, greatly limiting therapeutic targets. Passive immunotherapy,[22] neurotrophic factor delivery,[8] and protein-toxin bioconjugates are several protein delivery applications under investigation for CNS disorders.

1.4 Peptide-polymers as therapeutic molecules

Peptides are a promising class of therapeutic agents for a wide range of biomedical applications. As subunits of proteins, peptides have similar function to full-length proteins but are significantly smaller, simplifying chemical synthesis while allowing for facile incorporation of specific functional groups for bioconjugation. Additionally, when administered systemically, the smaller size of peptides improves tissue penetration while typically decreasing immunogenicity.[21] Peptides are biodegradable and therefore are expected to be highly biocompatible. Additionally, phage display techniques allow for rapid discovery of functional peptide sequences.[23]

With established stepwise solid-phase peptide synthesis techniques, a nearly limitless library of functional peptides can be synthesized. The flexibility of these molecules can be extended by (1) site-specific functionalization or bioconjugation of peptides through incorporation of bioorthogonal functional groups, (2) tailoring the activity and stability of peptide sequences through rational design and incorporation of unnatural amino acids and amino acid analogues,[24] and (3) tuning proteolytic degradation via incorporation of substrate sequences. As such, peptides have been explored for many therapeutic and materials applications, including anticancer agents,[25,26] targeted drug delivery,[27,28] and environmentally-responsive biomaterials.[29,30]

However, significant challenges hinder development of peptides as stand-alone therapeutics. In complex extracellular environments like serum, peptide half-life is short due to poor proteolytic stability.[24] Additionally, their small size results in low circulation half-life from rapid renal clearance. With higher conformation freedom, peptides often have lower activity than protein

analogues.[21] Polymer conjugation can be used to improve the pharmacokinetic profile and alter the biodistribution of grafted peptides; conjugation decreases immunogenicity, prolongs plasma half-life by decreasing renal filtration, and enhances proteolytic stability.[31] Additionally, polymer conjugation can be used for passive targeting of tumors via the enhanced permeability and retention (EPR) effect,[32] improving solubility of hydrophobic sequences,[33] and cellular targeting through the conjugation of targeting ligands.[34] Finally, controlling the molecular weights of polymer carriers can tune release rates from depot or hydrogel formulations for sustained drug release.

The development of living radical polymerization techniques has greatly expanded the library of polymers that can be synthesized for drug delivery applications. Materials can be synthesized with controlled architectures, molecular weights, and narrow polydispersity. Peptide functionalization of polymers combines the activity of peptides with stabilization and improved pharmacokinetics of polymers, thereby making peptide-polymer hybrid materials an interesting new class of materials for drug delivery applications.

1.5 Future perspectives

The development of new biologics-based therapies can potentially address currently ineffective drug regimens for CNS diseases. Peptide-functionalized polymers provide attractive platforms for drug and gene delivery via rational design and optimization of potent, modular polymer carrier systems. These hybrid materials combine attractive pharmacokinetic and architectural properties of polymeric systems with the functionality of distinct peptide sequences to create novel biomaterials.

1.1 References

(1) World Health Organization.: *Neurological disorders: public health challenges*; World Health Organization: Geneva, 2006.

(2) PhRMA: Neurological Disorders: A report on disorders of the brain, spinal cord and nerves. *Medicines in Development* **2013**.

(3) Alzheimer's, A.: 2013 Alzheimer's disease facts and figures. *Alzheimers Dement* **2013**, *9*, 208-245.

(4) Emard, J. F.; Thouez, J. P.; Gauvreau, D.: Neurodegenerative diseases and risk factors: a literature review. *Soc Sci Med* **1995**, *40*, 847-858.

(5) National Collaborating Centre for Chronic, C.: National institute for health and clinical excellence: guidance. In *Parkinson's disease: national clinical guideline for diagnosis and management in primary and secondary care*; Royal College of Physicians (UK): London, 2006.

(6) Pohanka, M.: Cholinesterases, a target of pharmacology and toxicology. *Biomed Pap Med Fac Univ Palacky Olomouc Czech Repub* **2011**, *155*, 219-129.

(7) Lipton, S. A.: Paradigm shift in neuroprotection by NMDA receptor blockade: memantine and beyond. *Nat Rev Drug Discov* **2006**, *5*, 160-170.

(8) Levy, Y. S.; Gilgun-Sherki, Y.; Melamed, E.; Offen, D.: Therapeutic potential of neurotrophic factors in neurodegenerative diseases. *BioDrugs* **2005**, *19*, 97-127.

(9) Weissmiller, A.; Wu, C.: Current advances in using neurotrophic factors to treat neurodegenerative disorders. *Transl Neurodegener* **2012**, *1*, 1-9.

(10) Bergen, J. M.; Park, I. K.; Horner, P. J.; Pun, S. H.: Nonviral approaches for neuronal delivery of nucleic acids. *Pharm Res* **2008**, *25*, 983-998.

(11) Liverman, C. T.; Institute of Medicine (U.S.). Committee on Spinal Cord Injury.: *Spinal cord injury: progress, promise, and priorities*; National Academies Press: Washington, DC, 2005.

(12) Walters, B. C.; Hadley, M. N.; Hurlbert, R. J.; Aarabi, B.; Dhall, S. S.; Gelb, D. E.; Harrigan, M. R.; Rozelle, C. J.; Ryken, T. C.; Theodore, N.: Guidelines for the management of acute

cervical spine and spinal cord injuries: 2013 update. *Neurosurgery* **2013**, *60 Suppl 1*, 82-91.

(13) Holland, E. C.: Glioblastoma multiforme: the terminator. *Proc Natl Acad Sci USA* **2000**, *97*, 6242-6244.

(14) Stupp, R.; Hegi, M. E.; Gilbert, M. R.; Chakravarti, A.: Chemoradiotherapy in malignant glioma: standard of care and future directions. *J Clin Oncol* **2007**, *25*, 4127-4136.

(15) Westphal, M.; Hilt, D. C.; Bortey, E.; Delavault, P.; Olivares, R.; Warnke, P. C.; Whittle, I. R.; Jääskeläinen, J.; Ram, Z.: A phase 3 trial of local chemotherapy with biodegradable carmustine (BCNU) wafers (Gliadel wafers) in patients with primary malignant glioma. *Neuro Oncol* **2003**, *5*, 79-88.

(16) Debinski, W.; Tatter, S. B.: Convection-enhanced delivery for the treatment of brain tumors. *Expert Rev Neurother* **2009**, *9*, 1519-1527.

(17) Pathan, S. A.; Iqbal, Z.; Zaidi, S. M.; Talegaonkar, S.; Vohra, D.; Jain, G. K.; Azeem, A.; Jain, N.; Lalani, J. R.; Khar, R. K.; Ahmad, F. J.: CNS drug delivery systems: novel approaches. *Recent Pat Drug Deliv Formul* **2009**, *3*, 71-89.

(18) Pardridge, W. M.: Drug and gene delivery to the brain: the vascular route. *Neuron* **2002**, *36*, 555-558.

(19) Begley, D. J.: Delivery of therapeutic agents to the central nervous system: the problems and the possibilities. *Pharmacol Therapeut* **2004**, *104*, 29-45.

(20) Burger, C.; Gorbatyuk, O. S.; Velardo, M. J.; Peden, C. S.; Williams, P.; Zolotukhin, S.; Reier, P. J.; Mandel, R. J.; Muzyczka, N.: Recombinant AAV viral vectors pseudotyped with viral capsids from serotypes 1, 2, and 5 display differential efficiency and cell tropism after delivery to different regions of the central nervous system. *Mol Ther* **2004**, *10*, 302-317.

(21) Góngora-Benítez, M.; Tulla-Puche, J.; Albericio, F.: Multifaceted roles of disulfide bonds. peptides as therapeutics. *Chem Rev* **2013,** *114*, 901-926.

(22) Aisen, P. S.; Vellas, B.: Passive immunotherapy for Alzheimer's disease: what have we learned, and where are we headed? *J Nutr Health Aging* **2013**, *17*, 49-50.

(23) Vodnik, M.; Zager, U.; Strukelj, B.; Lunder, M.: Phage display: selecting straws instead of a needle from a haystack. *Molecules* **2011**, *16*, 790-817.

(24) Sato, A. K.; Viswanathan, M.; Kent, R. B.; Wood, C. R.: Therapeutic peptides: technological advances driving peptides into development. *Curr Opin Biotech* **2006**, *17*, 638-642.

(25) Sanderson, R. J.; Hering, M. A.; James, S. F.; Sun, M. M. C.; Doronina, S. O.; Siadak, A. W.; Senter, P. D.; Wahl, A. F.: In vivo drug-linker stability of an anti-CD30 dipeptide-linked auristatin immunoconjugate. *Clin Cancer Res* **2005**, *11*, 843-852.

(26) Ellerby, H. M.; Arap, W.; Ellerby, L. M.; Kain, R.; Andrusiak, R.; Del Rio, G.; Krajewski, S.; Lombardo, C. R.; Rao, R.; Ruoslahti, E.; Bredesen, D. E.; Pasqualini, R.: Anti-cancer activity of targeted pro-apoptotic peptides. *Nat Med* **1999**, *5*, 1032-1038.

(27) Kwon, E. J.; Bergen, J. M.; Park, I. K.; Pun, S. H.: Peptide-modified vectors for nucleic acid delivery to neurons. *J Control Release* **2008**, *132*, 230-235.

(28) Wu, C.; Lo, S. L.; Boulaire, J.; Hong, M. L.; Beh, H. M.; Leung, D. S.; Wang, S.: A peptide-based carrier for intracellular delivery of proteins into malignant glial cells in vitro. *J Control Release* **2008**, *130*, 140-145.

(29) Dasgupta, A.; Mondal, J. H.; Das, D.: Peptide hydrogels. *RSC Advances* **2013**, *3*, 9117-9149.

(30) Mart, R. J.; Osborne, R. D.; Stevens, M. M.; Ulijn, R. V.: Peptide-based stimuli-responsive biomaterials. *Soft Matter* **2006**, *2*, 822-835.

(31) Vincent, M. J.; Dieudonne, L.; Carbajo, R. J.; Pineda-Lucena, A.: Polymer conjugates as therapeutics: future trends, challenges and opportunities. *Expert Opin Drug Del* **2008**, *5*, 593-614.

(32) Maeda, H.; Bharate, G. Y.; Daruwalla, J.: Polymeric drugs for efficient tumor-targeted drug delivery based on EPR-effect. *Eur J Pharm Sci* **2009**, *71*, 409-419.

(33) Schluep, T.; Cheng, J.; Khin, K. T.; Davis, M. E.: Pharmacokinetics and biodistribution of the camptothecin-polymer conjugate IT-101 in rats and tumor-bearing mice. *Cancer Chemoth Pharm* **2006**, *57*, 654-662.

(34) Levine, R. M.; Scott, C. M.; Kokkoli, E.: Peptide functionalized nanoparticles for nonviral gene delivery. *Soft Matter* **2013**, *9*, 985-1004.

Chapter 2

APPLICATION OF CONTROLLED RADICAL POLYMERIZATION FOR NUCLEIC ACID DELIVERY

David S.H. Chu, Joan G. Schellinger, Julie Shi, Anthony J. Convertine, Patrick S. Stayton, Suzie H. Pun

Abstract

Nucleic acid-based therapeutics can potentially address otherwise untreatable genetic disorders and have significant potential for a wide range of diseases. Therapeutic gene delivery can restore protein function by replacing defunct genes to restore cellular health while RNA interference (RNAi) can mask mutated and harmful genes.

Cationic polymers have been extensively studied for nucleic acid delivery applications due to their self-assembly with nucleic acids into virus-sized nanoparticles and high transfection efficiency *in vitro*, but toxicity and particle stability have limited their clinical applications. The advent of controlled radical polymerization has improved the quality, control and reproducibility of synthesized materials. Controlled radical polymerization yields well-defined, narrowly disperse materials of designable architectures and molecular weight, allowing study of the effects of polymer architecture and molecular weight on transfection efficiency and cytotoxicity for improved design of next-generation vectors. Robust methods such as atom transfer radical polymerization (ATRP), reverse addition-fragmentation chain transfer polymerization (RAFT), and ring-opening metastasis polymerization (ROMP) have been used to engineer materials that specifically enhance extracellular stability, cellular specificity, and decrease toxicity. This chapter reviews findings from structure-function studies that have elucidated key design motifs necessary for the development of effective nucleic acid vectors. In addition, polymers that are biodegradable, form supramolecular structures, target specific cells, or facilitate endosomal release are also discussed. Finally, promising materials with *in vivo* applications ranging from pulmonary gene delivery to DNA vaccines are described.[1]

---

[1]Reprinted, slightly modified, with permission from Chu et al (2012) *Acc Chem Res* **45**(7):1089-1099.

2.1 Introduction

Nucleic acid-based therapeutics have been investigated as treatments for hereditary, acquired, and infectious disease. Nucleic acid-based drug candidates include plasmids that induce gene expression and small, interfering RNA (siRNA) which silences target genes. Viral-based delivery methods utilize engineered viruses that provide high efficiency nucleic acid delivery. However, concerns regarding vector immunogenicity, oncogenicity, and nucleic acid loading capacity limit clinical potential. Synthetic materials offer advantages such as high loading capacity, ease of synthesis and formulation, and low immunogenicity but suffer from poor delivery efficiency and significant toxicity; as such, there are no clinically-approved materials to date. Ideal synthetic vectors emulate viruses, packaging nucleic acids for cellular uptake and protection from nucleases, targeting cells of interest, escaping the endo-/lysosomal degradative pathway, and releasing the payload in the cytosol or nucleus.

Living radical polymerization techniques provide flexible methods for synthesizing well-defined polymers with narrow polydispersity, controllable molecular weight (MW), complex architecture, and multifunctional properties. Tight control over polymer structure allows study of structure-function relationships and identification of key variables.

2.2 Controlled radical polymerization

Recent advances in state-of-the-art controlled radical polymerization methodology have the potential to revolutionize the development of "smart" multifunctional drug delivery systems. The most widely investigated CRP techniques include stable free radical polymerization (SFRP), atom transfer radical polymerization (ATRP), and reversible addition-fragmentation chain transfer (RAFT) (Figure 2.1). SFRP, best exemplified by nitroxide-mediated systems (NMP), is based on the persistent radical effect which employs a stable free radical to reversibly terminate the majority of active propagating chains in a dormant non-propagating species.[1,2] While SFRP has been shown to provide good control for a range of styrenic monomers, poor control is often observed for other monomer classes. In addition, long polymerization times and high temperatures are often required in order to reach high monomer conversions.

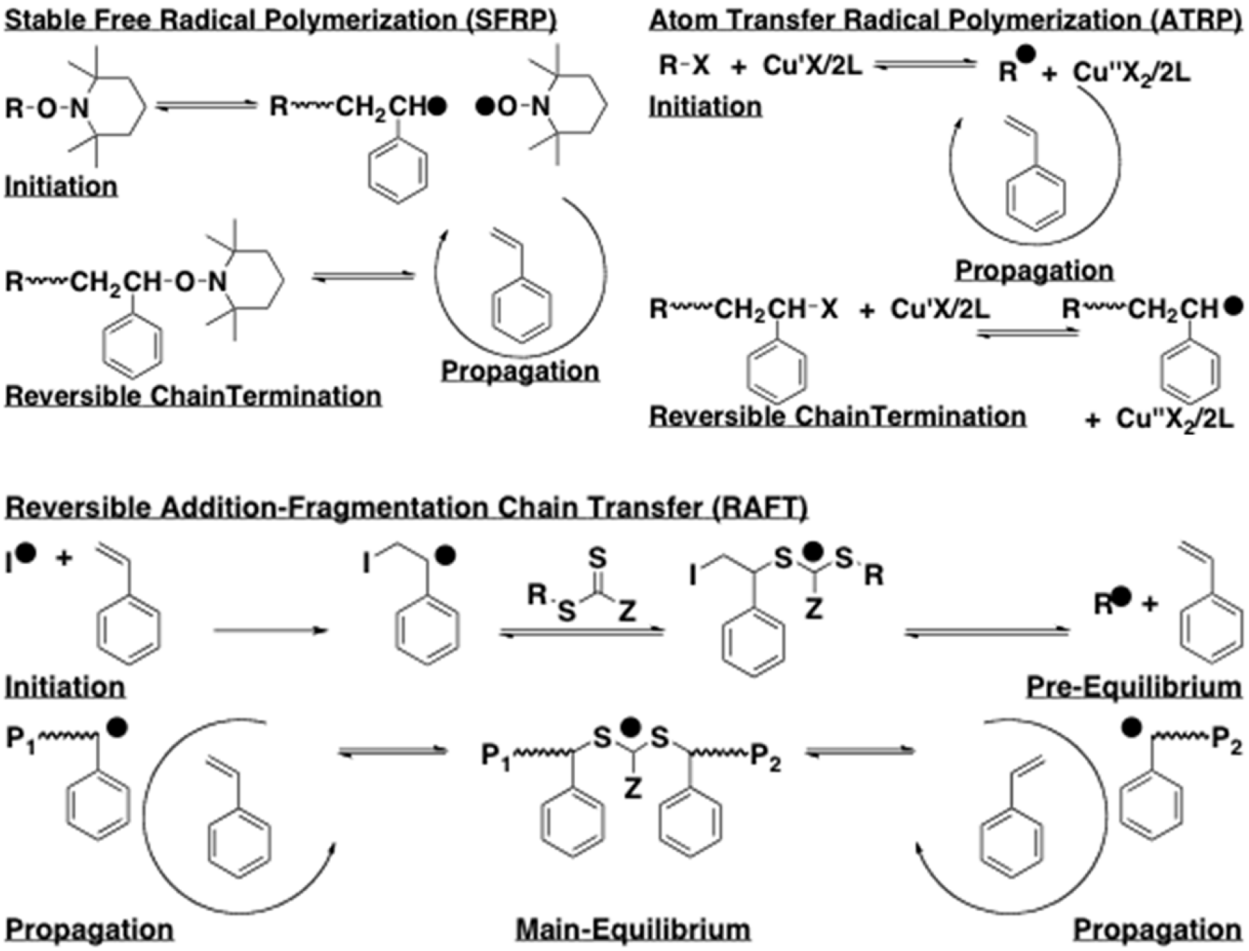

Figure 2.1. Controlled radical polymerization of styrene by (a) stable free radical polymerization (SFRP) in the presence of the nitroxide mediator TEMPO (b) copper-catalyzed atom transfer radical polymerization (ATRP) and (c) reversible addition-fragmentation chain transfer (RAFT) in the presence of a dithiobenzoate-based chain transfer agent (CTA).

ATRP is generally considered to be more widely applicable than SFRP in that most monomers containing an active double bond are amenable to controlled polymerization. Similar to SFRP, this technique employs a reversible deactivation step in order to reduce the instantaneous concentration of active propagating radicals.[3] In the case of ATRP, this equilibrium is established through the reversible homolytic cleavage of a terminal alkyl halide initiator catalyzed by a transition metal catalyst. ATRP provides a powerful method for preparing complex polymer architectures (e.g. blocks, brushes, stars) from commercially available starting materials. Additionally, polymerizations can be conducted over a wide range of temperatures and conditions

to yield telechelic materials suitable for secondary conjugation steps. Perhaps the most significant limitation of ATRP at present is the need for a metal catalyst, which for many biotechnology applications must be reduced to very low levels.

In contrast to SFRP and ATRP that impart living character to radical polymerizations by establishing a low equilibrium concentration of active propagating radicals, RAFT is based on a rapid degenerate chain transfer process.[4-7] The versatility of RAFT lies in the elegant simplicity of the technique, broad chemical compatibility, and ease of use. RAFT employs a thiocarbonyl thio compound as a degenerate chain transfer agent (CTA). Through a series of chain transfer steps, polymerizations proceed in a controlled process with most polymer chains containing well-defined end groups at their alpha and omega chain termini. By simple manipulation of the initial monomer, CTA, and initiator stoichiometry, it is possible to prepare near-monodisperse materials over a range of predefined MWs. Following polymerization of a given monomer(s), the resultant macroCTA can be isolated for use in subsequent block (co)polymerization steps. Because this methodology does not require the use of any toxic metal catalysts, it is particularly well-suited for use in biotechnology applications. The RAFT process also provides a means by which polymers with discrete orthogonal chemical functionalities can be easily prepared by employing functionalized RAFT chain transfer agents.

2.3 Polymer structure and delivery

In this section, we summarize work investigating the relationship between polymer structure and the effectiveness of materials as nucleic acid carriers. While many of these topics have been addressed using materials synthesized by conventional polymerization (e.g. Wolfert et al),[8] this chapter focuses on conclusions drawn from materials prepared by living polymerization.

a. Polymer composition

The chemical composition of polycations has been reported extensively to be a major factor in gene delivery efficiency and cytotoxicity.[9,10] Some key factors include the type of cationic charge center, charge density, presence of hydrogen bonding partners for nucleic acids, and balance between hydrophobicity/hydrophilicity.

Table 2.1. Some common monomers used in living polymerizations

Abbreviation	Structure	Full Name	Poly. Type	References
AEAEMA	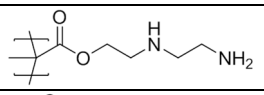	2-(2-aminoethylamino) ethyl methacrylate	ATRP	16
AEAHPMA	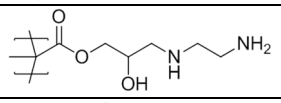	3-(2-aminoethylamino) 2-hydroxylpropyl methacrylate	ATRP	16
AEMA	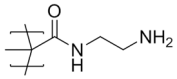	2-aminoethyl methacrylamide	ATRP RAFT	12, 15, 16, 30
AHPMA	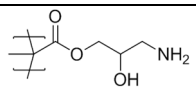	3-amino-2-hydroxypropyl methacrylate	ATRP	16
APMA	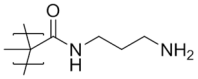	3-aminopropyl methacrylamide	RAFT	15, 30, 50, 51
BMA	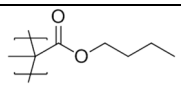	butyl methacrylate	RAFT	36, 52, 54, 56
CBMA	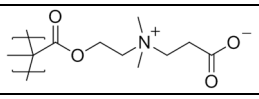	carboxybetaine methacrylate	ATRP	31
DMAEMA	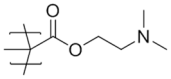	2-(dimethylamino) ethyl methacrylate	ATRP RAFT	12-14, 18-21, 32, 33, 35, 36, 41, 44-47, 52-54, 56, 57, 60
DMAPMA	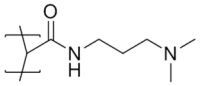	*N*-[3-(dimethylamino)propyl] methacrylamide	RAFT	27, 51
GAPMA	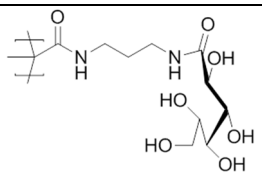	3-gluconamidopropyl methacrylamide	RAFT	15
GMA	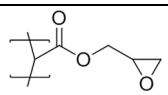	glycidyl methacrylate	ATRP	38, 39, 55
HEMA	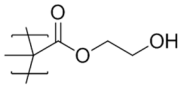	2-hydroxyethyl methacrylate	ATRP	18, 20, 22
HPMA	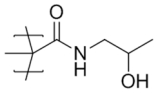	*N*-(2-hydroxypropyl) methacrylamide	RAFT	24, 25, 27, 34, 38, 40, 42, 50, 51
MPC	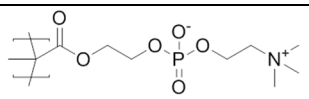	2- methacryloyloxyethyl phosphorylcholine	ATRP RAFT	30, 47
OEGMA	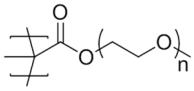	oligo(ethylene glycol) methacrylate	ATRP	31, 38, 39, 45
PAA	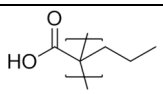	propylacrylic acid	RAFT	36, 52, 54, 56
SBMA	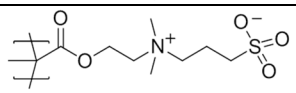	sulfobetaine methacrylate	ATRP	31

Some commonly used monomers in living polymerization of polycations include APMA (primary amine) and DMAEMA (tertiary amine). Table 2.1 lists full names and structures of monomers discussed in this review. Monomers containing primary amines can be easily guanidinylated to introduce an alternative charge center.[11] DMAEMA is one of the most frequently used monomers; polymers of DMAEMA (pDMAEMA) have average pKa ~ 7.5 and are partially protonated at physiologic pH, allowing for self-assembly with nucleic acids through electrostatic complexation and buffering of acidifying endosomes, thereby delaying or even preventing lysosome degradation of vehicles. One study compared polycations with varying ratios of primary (AEMA) and tertiary (DMAEMA) amine-containing monomers that were synthesized by RAFT and showed similar transfection efficiencies for all polycations.[12] Another study compared the gene delivery efficiencies of polycations composed of tertiary and quaternary amines by using DMAEMA monomers followed by alkylation to quaternary amines.[13,14] Conversion of tertiary amines to quaternary amines resulted in stronger nucleic acid binding, higher zeta potential of polyplexes, higher toxicity, and lower transfection efficiency. The decreased transfection efficiency was attributed to reduced buffering capacity of the resulting polymers.

The effect of spacing between charge group and polymer backbone has been investigated by comparing polymers synthesized using AEMA, APMA and AHMA monomers that contain 2-, 3-, and 6-carbon spacers, respectively.[12,15] As spacer group lengths increase, polymers become both more effective at gene delivery and also more cytotoxic, likely due to increased accessibility of the charge group. Zhuo and colleagues synthesized pAEMA and pAEAEMA polymer analogues that introduced hydroxyl groups and showed that polymers containing hydroxyl groups exhibited stronger nucleic acid binding and reduced cytotoxicity.[16] The observed effects were attributed to hydrogen bonding to nucleic acids and decreased surface charge, respectively. Hydrogen bonding between hydroxyl groups and nucleotide base amines has been shown to be the dominant thermodynamic contributor to DNA binding.[17] Binding free energy contributions from hydrogen bonding are unaffected by salt concentration while electrostatic contributions significantly decrease with increasing salt.

Finally, incorporation of hydrophilic, charge-neutral monomers such as carbohydrates, HEMA or OEGMA in polycations has been shown to reduce polymer cytotoxicity.[15,18] In some cases, increases in transfection efficiency can also be achieved because higher charge ratios can be used without compromising cell viability.[18]

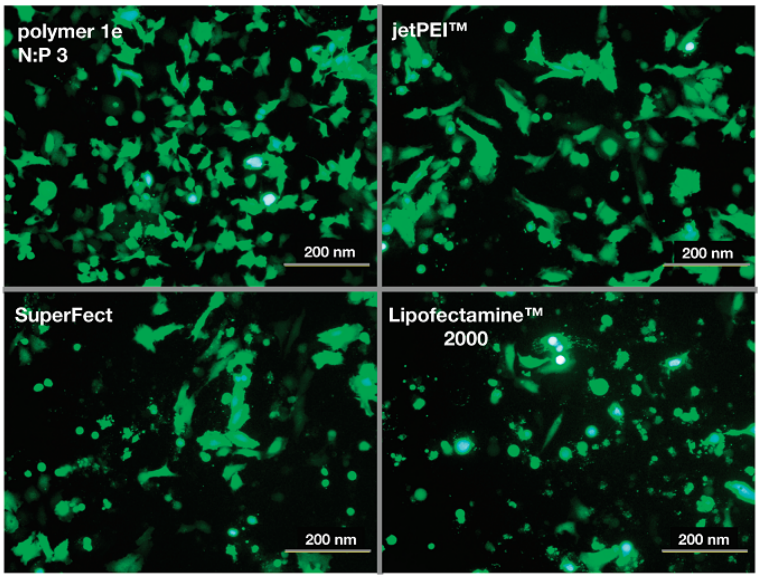

Figure 2.2. Fluorescence microscope images of HeLa cells transfected with complexes of oligolysine-grafted polymers (1e), jetPEI, Superfect, and Lipofectamine 2000.[23]

b. Polymer molecular weight

The effect of MW on gene delivery has been tested using several DMAEMA-based polycations synthesized by ATRP, including linear block copolymers,[18] grafted DMAEMA block copolymers,[14,19,20] and star-shaped copolymers.[21] The effective polycation MW can be varied by changing the DMAEMA block length[14,18,19,21] or by increasing the number of grafted DMAEMA blocks of a specific size.[20] In all studies, DNA condensation and optimized gene transfection efficiency increased with the DMAEMA block length until toxicity became a limiting factor. Cytotoxicity of polymers also generally increased with polymer MW.[14,18,19] These trends were observed with DMAEMA blocks copolymerized with poly(caprolactone) (PCL),[19] pHEMA,[20] or hydroxypropyl cellulose (HPC),[14] indicating that the cationic DMAEMA segment drives both the delivery efficiency and cytotoxicity of the materials.

The trends of higher transfection efficiency and cytotoxicity with increasing MW have been reported for other polycations synthesized by living polymerization, including pAEMA and pAPMA polymers.[15,22] The Pun and Emrick groups have also shown similar trends in polymers synthesized from oligolysine macromonomers.[23,24] Poly(cyclooctene-*g*-pentalysine) synthesized

by ring-opening metathesis polymerization (ROMP) are more effective at gene delivery with increasing MW. The highest MW copolymer tested (202 kDa) gave the best overall gene expression with efficiencies comparable to commercial reagents such as jetPEI, SuperFect and Lipofectamine 2000 (Figure 2.2) while exhibiting low cytotoxicity.[23] HPMA-oligolysine copolymers with varying MW synthesized by RAFT polymerization demonstrated transfection efficiency comparable to PEI at high MW (78kDa) but also trends of increasing cytotoxicity with higher MW.[24]

In summary, transfection efficiency and cytotoxicity tends to increase with polymer MW; polymer length therefore generally needs to be optimized for these two factors. Synthesis of materials by living polymerization can reproducibly produce well-defined materials with desired MW. Shi et al compared HPMA-oligolysine polymers synthesized by free radical and RAFT polymerization and found similar transfection efficiency at the target mass to charge ratios; however, the IC_{50} values of the free radical polymers was nearly 10-fold lower than that of the RAFT polymers.[25] Jonsson and Linse showed by Monte Carlo simulations that high MW polyelectrolytes can form increased interaction with macroions; thus, polyplexes from higher MW polycations may prevent premature release of DNA by providing additional stabilization.[26] However, another observed trend is the associated increase in cytotoxicity as polymer MW is increased. Polyplexes formed with lower MW polymers are more easily reversible, while complexes from high MW polymers are less dynamic, which can then lead to crosslinking of DNA and exposure of excess positive charge.[8] Microinjected polyplexes formed with high MW polymers showed poor transfection efficiency attributed to highly slyplexes that may inhibit transcription. Scales et al showed that as the length of DMAPMA in DMAPMA-HPMA block copolymers increase, there is a decreased amount of soluble complex due to cross-bridging of complexes, leading to aggregation.[27] Interestingly, as the HPMA block increased in length, shorter DMAPMA blocks were required for efficient complexation into soluble particles. Furthermore, Kissel and co-workers showed that high MW polymers adsorbed highly to the cell surface due to high binding affinity towards the plasma membrane, leading to aggregate formation, membrane disruption, and eventually cell death by necrosis.[28]

c. Polymer architecture and transfection efficiency

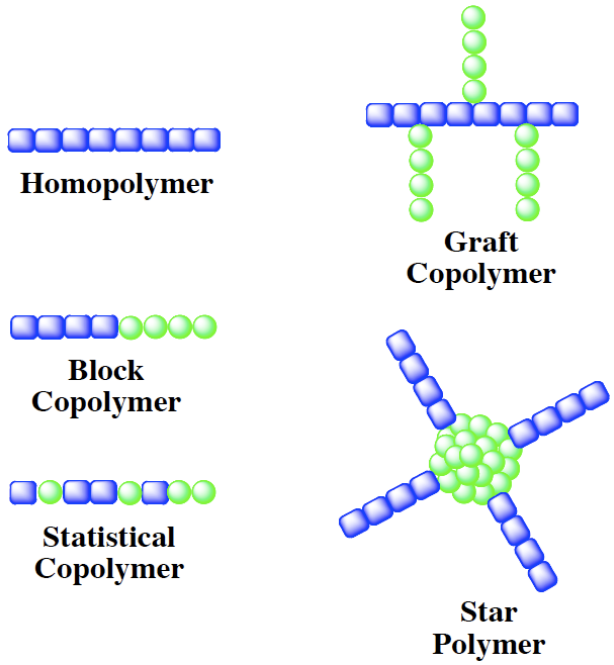

Figure 2.3. Various polymer architectures.

Polymers with controlled architectures including homopolymers, block copolymers, random or statistical copolymers, graft copolymers and star-shaped polymers can also be synthesized by living polymerization (Figure 2.3). The reader is referred to a recently published and thorough review that focuses on the preparation of various polymeric architectures using living radical polymerization.[29] This review will emphasize effects of polymer architecture on nucleic acid delivery.

The effect of block versus random copolymer architectures has been recently investigated by the Narain group (Figure 2.4).[15,30] Primary amine-containing monomers were used to copolymerize with either carbohydrate monomer GAPMA or zwitterionic phospholipid MPC. With both systems, random copolymers were less cytotoxic than their block copolymer analogues, likely due to reduced charge density. Random copolymers containing GAPMA were more effective for gene delivery compared to corresponding block copolymers but the opposite was observed with MPC monomers. The block glycopolymers were hypothesized to form core-shell structures with buried charge, as opposed to polyplexes formed from random copolymers with more accessible surface charge. The accessible charge facilitates cellular uptake of polyplexes.[15]

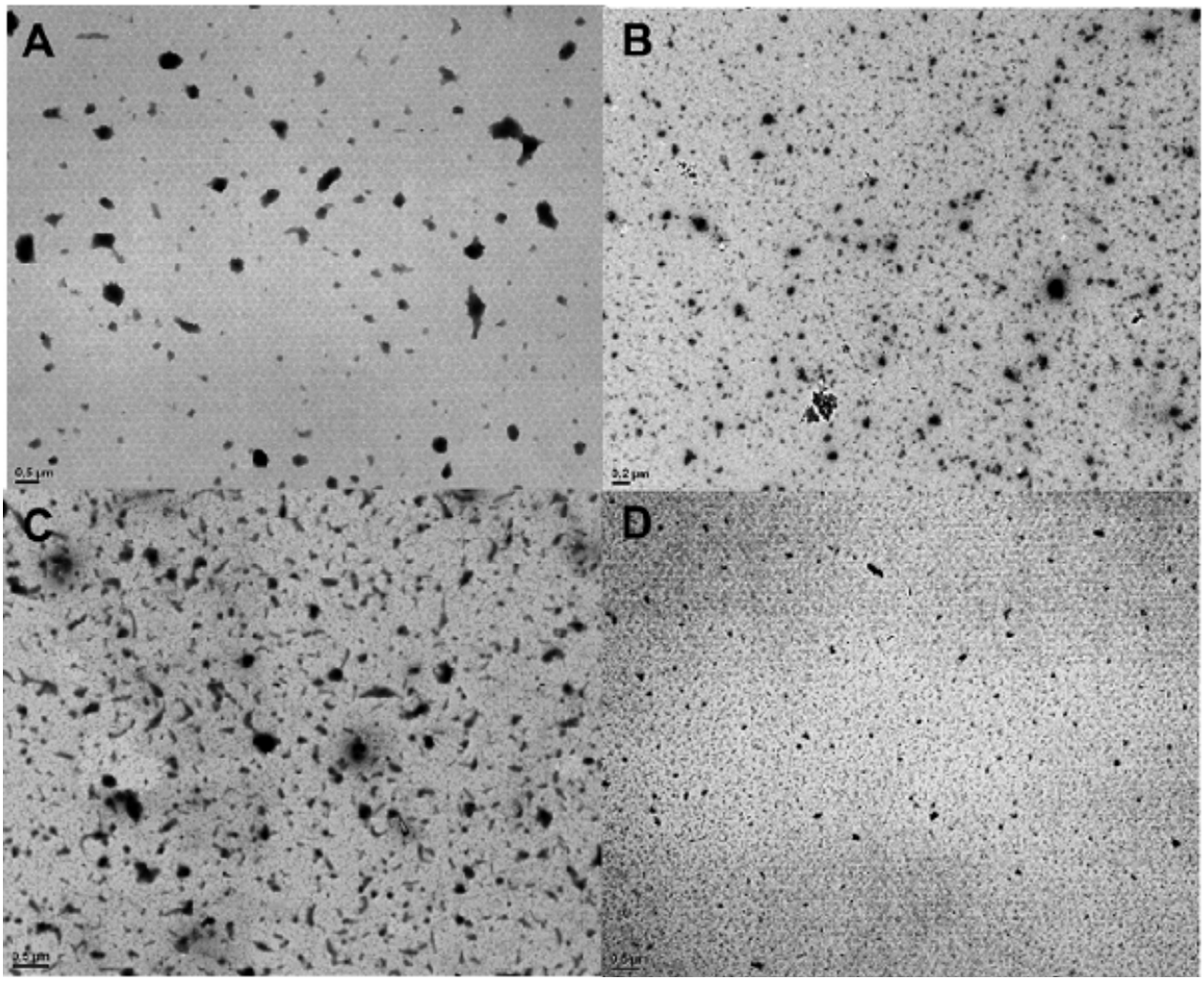

Figure 2.4. TEM images of polyplexes comparing polyplexes formulated with statistical (A, C) and block (B, D) phospholipid-containing polycations.[30]

Certain zwitterionic polymers have been previously reported to exhibit high resistance to protein adsorption due to formation of hydration shells.[31] Polyplexes formed from statistical MPC polymers may similarly resist protein interactions necessary for cellular uptake and transfection. Therefore, while random copolymers of hydrophilic monomers and cationic monomers may offer reduced toxicity compared to block copolymers, the chemical structure of the hydrophilic monomer also significantly affects *in vitro* nucleic acid delivery efficiency.

Graft or branched polymer structures generally have shown higher transfection efficiencies and lower toxicities than their linear counterparts. Reports of grafting pDMAEMA onto backbones

of pHEMA,[20] HPC,[14] dextran,[13] and chitosan[32] via ATRP show these grafted structures transfected better and were less cytotoxic than high MW pDMAEMA. In addition, Xu et al showed that HPC-*g*-pDMAEMA copolymers were more effective even with lower cation incorporation compared to linear pDMAEMA.[14] One potential reason for this phenomenon could be that these grafted structures can enhance the electrostatic interaction of the cationic pDMAEMA side chains with nucleic acids or the cell membrane. Hyperbranched DMAEMA also showed much higher transfection than linear DMAEMA of a similar MW without increased cytotoxicity.[33] Polymers with graft oligolysines also exhibit higher transfection efficiency compared to linear poly-L-lysine (PLL).[23,34]

Recently, we reported the synthesis and evaluation of cyclic pDMAEMA for gene delivery.[35] Cyclic pDMAEMA complexed DNA more tightly, forming smaller polyplexes compared to linear analogs. Transfection efficiency, however, was comparable between linear and cyclic architectures. Interestingly, cyclic pDMAEMA was significantly less toxic than linear pDMAEMA, having both lower dose-dependent toxicity and reduced plasma membrane permeabilization. Toxicity of cationic vectors is a significant barrier towards translation of non-viral vectors; therefore, these results suggest cyclic polymers are a promising architecture for gene delivery applications.

2.4 Supramolecular structures

Most polycations have been shown to condense nucleic acids into compact spherical or toroidal nanoparticles. Block copolymers that form micellar structures may provide advantages such as increased particle stability, decreased surface charge resulting in reduced cytotoxicity, and the ability to co-deliver additional therapeutics encapsulated in the micellar core.

Several groups investigated the synthesis of micellar systems for nucleic acid delivery including mPEG-*b*-(PCL-*g*-DMAEMA),[19] DMAEMA-*b*-(DMAEMA-*co*-PAA-*co*-BMA),[36] DMAEMA-*b*-PCL-*b*-DMAEMA,[37] OEGMA-*b*-(GMA-*g*-TEPA),[38] PCL-*b*-(OEGMA-*co*-(GMA-*g*-TEPA)).[39] mPEG-*b*-(PCL-*g*-DMAEMA) micelles showed efficiency comparable to polyethylenimine (PEI) in HeLa cells and exceeded PEI and Lipofectamine 2000 in HepG2 cells. However, these materials demonstrated substantial DMAEMA-dependent toxicity.

DMAEMA-*b*-(DMAEMA-*co*-PAA-*co*-BMA) micelles efficiently delivered siRNA to cells

with over 90% knockdown of target genes at optimized conditions.[32] High siRNA delivery efficacy is attributed to the pH-responsive, membrane-lytic second block as a means of efficient endosomal escape. The stability of the micelle is also pH dependent, with destabilization occurring with decreasing pH. It was shown that the micellar structure encourages siRNA binding, and that loss of micelle structure leads to weak siRNA binding. Thus, the high efficiency can be attributed to simultaneous release of siRNA during micelle destabilization and activation of membrane-lytic activity in the endosomes.

Zhu et al (2010) demonstrated dual drug delivery by encapsulating a small molecule drug (paclitaxel) with anti-neoplastic activity in the core of micellar nucleic acid delivery vehicles composed of DMAEMA-*b*-PCL-*b*-DMAEMA triblocks.[37] When paclitaxel was co-delivered with VEGF siRNA, VEGF knockdown was close to 85% and was higher than siRNA or paclitaxel alone.

Wei et al (2012) investigated OEGMA-*b*-(GMA-*g*-TEPA) copolymers, synthesized via tandem RAFT/ATRP by novel double-headed initiators, containing either reducible or non-reducible bonds between the hydrophilic OEGMA and cationic GMA-*g*-TEPA blocks.[38] Copolymers efficiently packaged DNA into core-shell polyplexes < 50 nm in diameter that demonstrated excellent colloidal salt stability over 20 hrs. Reducible copolymers had an order of magnitude increased transfection efficiency compared to non-reducible analogs, attributed to intracellular reduction that mediates OEGMA shell deshielding and cytosolic DNA release. Terminal display of the Tet1 targeting ligand mediated significantly enhanced transfection efficiency of neuron-like differentiated PC-12 cells compared to untargeted analogs.

Wei et al (2013) investigated polymers containing PCL, OEGMA, and GMA-*g*-TEPA arranged in either di- or triblock architectures.[39] All architectures efficiently condensed DNA to form core-shell polyplexes < 100 nm in diameter and mediated up to 8-fold higher transfection efficiency than PEI in serum-containing media *in vitro*. PCL-*b*-(OEGMA-*co*-(GMA-*g*-TEPA)) block-statistical copolymers had higher transfection efficiency than either PCL-*b*-OEGMA-*b*-(GMA-*g*-TEPA) or PCL-*b*-(GMA-*g*-TEPA)-*b*-OEMGA triblocks. Additionally, the block-statistical polymer mediated efficient siRNA delivery, achieving ~80% GAPDH reporter gene knockdown.

Additionally, synthetic polymers have been combined with viral vectors as hybrid gene delivery vehicles. Cationic polymers self-assemble with electronegative viral capsids, reducing

host immune recognition and allowing for facile re-targeting of viruses. Wang et al reported that adenoviruses coated with HPMA-oligolysine copolymers had 6-fold higher transduction efficiency in cells that did not express receptors for adenovirus.[40] Polymer-coated viruses maintained high transduction efficiency in serum and protected viruses from neutralized antibodies compared to naked virus.

2.5 Polymer degradability

Polymer degradability is an important feature for *in vivo* applications. Three main methods of introducing degradability into polymers synthesized via controlled radical polymerization are: (1) disulfide linkages, which can be degraded by glutathione in the reducing environment of the cytosol; (2) acid-labile linkages, such as esters, which can be hydrolyzed in the endo-/lysosomal compartments; and (3) enzymatically-degradable elements, which can be degraded by specific proteolytic enzymes.

Disulfide bonds are the most commonly employed degradable linkage in controlled polymerization reactions due to the ease of introducing thiols or disulfide bonds into the initiator or chain transfer agent. For example, reducible pDMAEMA polymers were synthesized by oxidation of thiol-terminated DMAEMA oligomers prepared by RAFT polymerization using a difunctional CTA. In another approach, reducible linkages were introduced in HPMA-oligolysine copolymers via an amino acid analogue containing an internal disulfide.[25] Polyplexes of the reducible copolymers were much less toxic than their non-reducible analogue, but suffered decreased transfection efficiency.

Other strategies for introducing degradability into the polymer structure include the use of acid-labile linkages and enzymatically-degradable segments. Lin et al. synthesized via ATRP block copolymers of poly(ethylene glycol) (PEG) and pDMAEMA connected through a cyclic orthoester linkage.[41] Transfection with acid-labile PEG-*a*-pDMAEMA polyplexes was better than with its acid-stable counterpart, PEG-*b*-pDMAEMA, at high amine to phosphate (N/P) ratios. Enzymatically-degradable polymers, such as chitosan, can also be attractive alternative for more specific and controlled degradation. Chitosan, which can be degraded by lysozyme, was used as a backbone and copolymerized with side chains of pDMAEMA via ATRP for endosomal

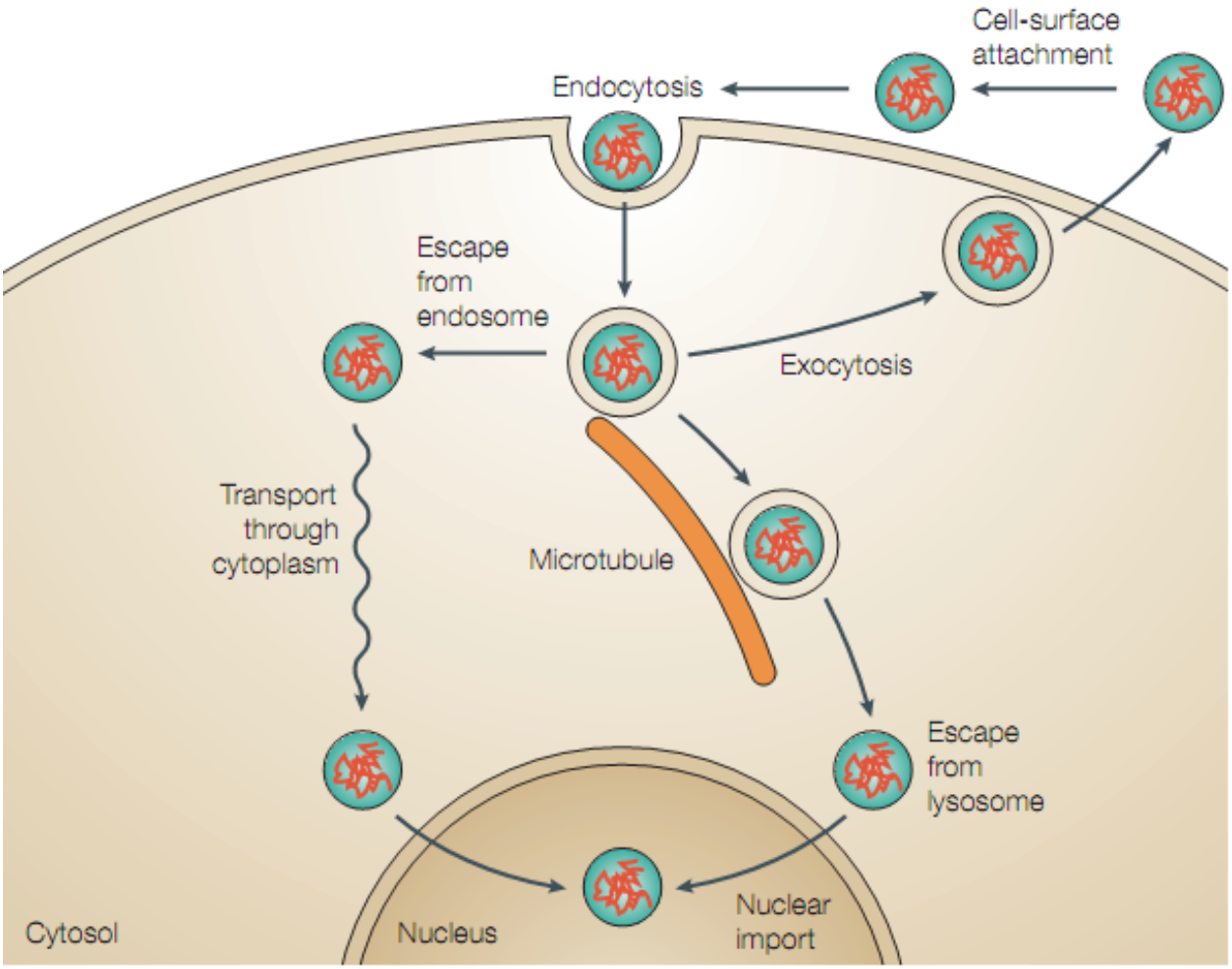

Figure 2.5. Barriers to gene delivery.[61]

buffering.[32] Additionally, the use of enzymatically-cleavable linker sequences has shown the possibility of specific enzymatic degradation within polyplex formulations. Recently, copolymers of HPMA and oligolysine monomers linked by an amino acid sequence that is recognized by the endo-/lysosomal protease cathepsin B were reported.[42] Transfection of these copolymers in HeLa and NIH/3T3 cells were comparable to non-degradable copolymers synthesized with (D)-amino acids but with reduced cytotoxicity.

In general, polymers synthesized with these degradable features show decreased cytotoxicity *in vitro*, but transfection efficiency is only on par or even reduced compared to non-degradable analogues. Therefore, optimization of these degradable segments requires further study.

2.6 Polymer functionalities

There are several barriers to the successful delivery of nucleic acids (Figure 2.5). Non-viral vectors must overcome the following obstacles: (1) stability in serum for intravenous injection, (2) specificity for the cell- or tissue-of-interest, (3) escape from endo-/lysosomal degradation, and (4) successful release of active payload. Thus, multiple strategies have been explored for building in polymer functionalities to improve transfection efficiency, specifically addressing several of these barriers.

2.6.1. Serum stability

Colloids instability and resulting aggregation should be avoided in applications requiring systemic delivery of polyplexes. Salt and serum-induced polyplex aggregation can lead to opsonization of particles or pulmonary embolism.

The major strategy to improve polyplex stability is the incorporation of hydrophilic polymers (such as HPMA, PEG or zwitterionic polymers) that serve as steric stabilizers,[43] minimizing protein adsorption to particles and particle aggregation.[23,30,44-46] In general, these copolymers, regardless of specific architecture and form of hydrophilic modification, show significantly decreased cytotoxicity and enhanced colloidal stability relative to their respective homopolymers. For example, MPC-AEMA and MPC-APMA copolymers showed low protein adsorption likely due to the zwitterionic MPC component.[30] However, *in vitro* transfection efficiency relative to their respective homopolymers is also typically reduced.[44,45,47]

While the hydrophilic shielding limits *in vitro* efficacy, *in vivo* it has proven valuable. One aerosolized formulation of OEGMA-*co*-DMAEMA demonstrated 7-fold greater bulk pulmonary transfection compared to PEI.[45] pDMAEMA-*b*-PEG used for intranasal delivery of DNA vaccines showed immune response comparable to and higher than PEI and DMAEMA homopolymer, respectively.[44]

2.6.2. Targeting

Effective cell targeting of polyplexes increases specific delivery to target tissues thereby reducing

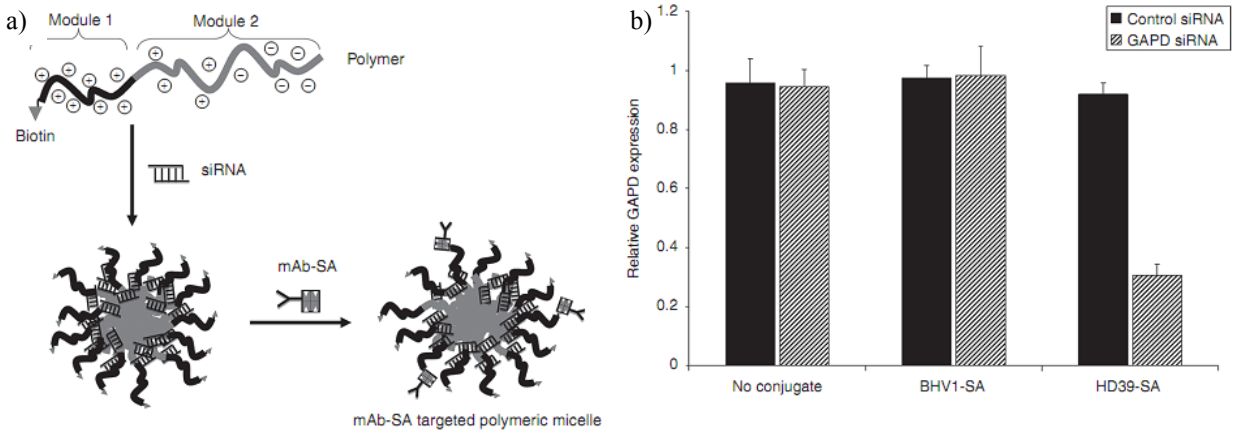

Figure 2.6. (a) Structure and (b) GAPD knockdown efficacy of antibody-conjugated polymeric micelles in CD22+ lymphoma cells measured using real time RT-PCR.[54]

off-target effects. Polyplexes, typically with a positive surface charge, electrostatically associate with electronegative cellular membranes, leading to non-specific uptake.[48] Modifying polymers with ligands while including domains for charge shielding targets polyplexes to receptors expressed on the cell or tissue of interest.

Folate is a small molecule ligand of the folate receptor that is commonly overexpressed in cancer and has been shown to be an effective targeting ligand for drug carriers.[49] Several groups have incorporated folate into polymers synthesized by living polymerization.[50-53] Folate-targeted polyplexes showed enhanced siRNA delivery in cells with upregulated folate receptor expression compared to control cells, with specific targeting demonstrated by decreased silencing when treated competitively with free folate.

Biotin-DMAEMA-*b*-(DMAEMA-*co*-PAA-*co*-BMA) micelles, functionalized with streptavidin-Anti-CD22 monoclonal antibody conjugates, demonstrated highly specific targeting against CD22+ lymphoma.[54] These micelles were used to deliver siRNA and specifically reduced target gene expression by 70% (Figure 2.6).

2.6.3 Endosomal release

Another major barrier to efficient transfection is entrapment of polyplexes in endo-/lysosomal organelles. Some approaches to increasing endosomal release are the use of protonatable amines

to buffer the acidifying endosome, often referred to as the "proton sponge effect,"[14,32,55] the incorporation of hydrophobic groups to destabilize endosomal membrane,[56,57] and the incorporation of membrane-lytic peptides to disrupt endosomal membranes.[58]

Endosomal buffering is the result of the accumulation of protons brought into the endosome via an ATPase.[59] Tertiary amine-containing polymers, such as PEI, are increasingly protonated in acidifying endosomes, causing osmotic swelling of the endosome and ultimate release of endosomal contents. For example, Ma et al synthesized PEG-*b*-PGMA diblock copolymers via ATRP and grafted small oligoamines, such as low MW PEI, to encourage endosomal buffering of these vectors.[55] Although the transfection of these polymers was less efficient than PEI alone, high buffering capacity and low binding ability was correlated to high transfection ability. As discussed in section IIIa, DMAEMA monomers contain a tertiary amine that also buffers in endosomal pH. This review has highlighted select examples of DMAEMA-containing polymers synthesized for nucleic acid delivery.[12-14,18,32,60] Because polymerized DMAEMA also induces cytotoxicity, DMAEMA content in polycations needs to be optimized to balance between transfection efficiency and cytotoxicity.

Another promising method for endosomal release is the use of hydrophobic groups that become membrane-lytic via a pH-sensitive trigger. Convertine et al synthesized copolymers of DMAEMA, PAA, and hydrophobic BMA via RAFT that undergo a pH-induced conformational change.[56] At pH 7, positively-charged DMAEMA and negatively-charged PAA mask the hydrophobicity of BMA; at lower pH, the polymer undergoes a conformational change, exposing the BMA hydrophobic residues and thus rendering the polymer hydrophobic and hemolytic. These polymers showed significant activity of delivered siRNA.

Endosomalytic peptides mediate direct membrane disruption, typically inducing pore formation and resulting in release of endosomal contents. Schellinger et al synthesized diblock copolymers containing the endosomalytic peptide melittin in one block and a statistical HPMA-oligolysine copolymer in the other.[58] Optimal polyplex formulations using the melittin polymers mediated > 100-fold increase luciferase expression compared to HPMA-oligolysine polyplexes. These promising melittin polymers mediated 35-fold higher bulk luciferase expression *in vivo* compared to the base HPMA-oligolysine copolymer.

2.7 In vivo results

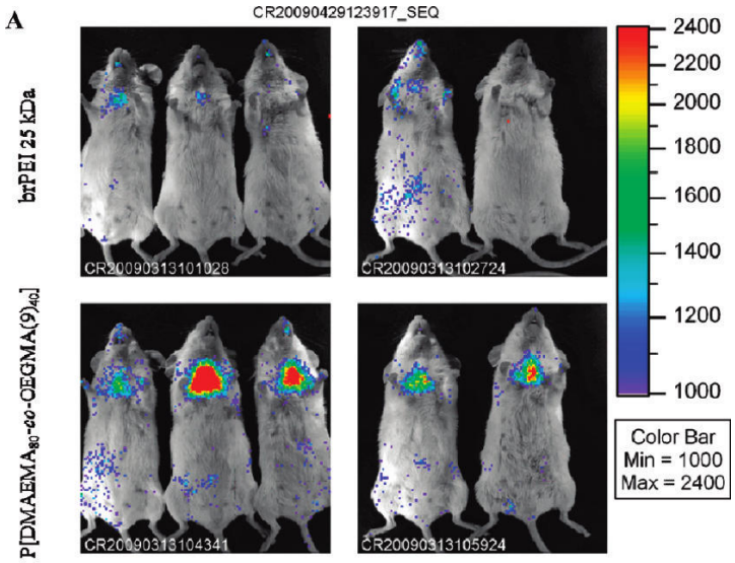

Figure 2.7. *In vivo* bioluminescence images of Balb/c mice after intratracheal application of OEGMA-*co*-DMAEMA block copolymers delivering luciferase transgene.[45]

Despite extensive development of polymeric nucleic acid delivery systems over the past two decades, clinical translation of these materials is in its nascency. Noted drawbacks of tested polymers include poor *in vivo* stability, high cytotoxicity, and low delivery efficiency. The development of living radical polymerization techniques for gene delivery allows for controlled architectures and rationally-designable materials. This section highlights some examples of promising and recent *in vivo* results using such materials.

Ternary complexes of PCL-*g*-pDMAEMA polyplexes coated with folate-targeted poly(glutamic acid)-*g*-mPEG yielded enhanced transgene delivery to tumor xenograft models compared to untargeted ternary complexes.[53] Administration of binary complexes of PCL-*g*-pDMAEMA polyplexes without the mPEG coating resulted in animal death within several hours of administration likely due to erythrocyte toxicity, demonstrating the importance of hydrophilic shielding with targeting. In another report, OEGMA-*co*-DMAEMA polyplexes were aerosolized and administered directly to the pulmonary tract. The optimal copolymer formulation showed a 7-fold bulk increase in luciferase transgene expression compared to PEI polyplexes (Figure 2.7).[45] A similar material, DMAEMA-*b*-PEG, was used for DNA delivery for vaccination against HIV-1.[42] When administered intranasally to mice, DMAEMA and DMAEMA-*b*-PEG copolymers showed stimulation of TNF-α and IL-10 production, enhancing the immunogenicity of the DNA

vaccine, while PEI did not. Since DMAEMA-*b*-PEG *in vitro* was shown to be significantly less toxic than homoDMAEMA, this makes for an attractive DNA vaccine vector.

2.8 Conclusions/future perspectives

Application of controlled radical polymerization techniques has allowed for detailed structure-function analysis and optimization of existing vectors. More importantly, these approaches allow for reproducible and controlled synthesis of desired materials. With increasing understanding of effective motifs, controlled radical polymerization provides a robust means to design and implement future materials meeting the properties of low cytotoxicity, high stability, and high transfection efficiency required for nucleic acid delivery applications.

2.9 Acknowledgments

This work was supported by NIH R01NS064404, NIH R01EB002991, and the Center for Intracellular Delivery of Biologics (Life Sciences Discovery Fund Grant 2496490).

2.10 References

(1) Georges, M.K.; Veregin, R.P.N.; Kazmaier, P.M.; Hamer, G.K.: Narrow molecular resins by a free-radical polymerizaiton process. *Macromolecules* **1993**, *26*, 2987-2988.

(2) Georges, M. K.; Veregin, R. N. P.; Kazmaier, P. M.; Hamer, G. K.: Taming the free radical polymerization process. *Trends Polym Sci* **1994**, *2*, 66-72.

(3) Coessens, V. M. C.; Matyjaszewski, K.: Fundamentals of atom transfer radical polymerization. *J Chem Educ* **2010**, *87*, 916-919.

(4) Boyer, C.; Bulmus, V.; Davis, T. P.; Ladmiral, V.; Liu, J.; Perrier, S. b.: Bioapplications of RAFT polymerization. *Chem Rev* **2009**, *109*, 5402-5436.

(5) Moad, G.; Rizzardo, E.; Thang, S. H.: Living radical polymerization by the RAFT process -

a second update. *Aust J Chem* **2009**, *62*, 1402-1472.

(6) Lowe, A. B.; McCormick, C. L.: Homogeneous controlled free radical polymerization in aqueous media. *Aust J Chem* **2002**, *55*, 367-379.

(7) Moad, G.; Rizzardo, E.; Thang, S. H.: Toward living radical polymerization. *Acc Chem Res* **2008**, *41*, 1133-1142.

(8) Wolfert, M. A.; Dash, P. R.; Nazarova, O.; Oupicky, D.; Seymour, L. W.; Smart, S.; Strohalm, J.; Ulbrich, K.: Polyelectrolyte vectors for gene delivery: influence of cationic polymer on biophysical properties of complexes formed with DNA. *Bioconjug Chem* **1999**, *10*, 993-1004.

(9) Davis, M. E.; Pun, S. H.; Bellocq, N. C.; Reineke, T. M.; Popielarski, S. R.; Mishra, S.; Heidel, J. D.: Self-assembling nucleic acid delivery vehicles via linear, water-soluble, cyclodextrin-containing polymers. *Curr Med Chem* **2004**, *11*, 179-197.

(10) De Smedt, S. C.; Demeester, J.; Hennink, W. E.: Cationic polymer based gene delivery systems. *Pharm. Res.* **2000**, *17*, 113-126.

(11) Qin, Z.; Liu, W.; Li, L.; Guo, L.; Yao, C.; Li, X.: Galactosylated N-2-hydroxypropyl methacrylamide-b-N-3-guanidinopropyl methacrylamide block copolymers as hepatocyte-targeting gene carriers. *Bioconjug Chem* **2011**, *22*, 1503-1512.

(12) Zhu, C. H.; Jung, S.; Si, G. Y.; Cheng, R.; Meng, F. H.; Zhu, X. L.; Park, T. G.; Zhong, Z. Y.: Cationic methacrylate copolymers containing primary and tertiary amino side groups: controlled synthesis via RAFT polymerization, DNA condensation, and in vitro gene transfection. *J Polym Sci Pol Chem* **2010**, *48*, 2869-2877.

(13) Wang, Z. H.; Li, W. B.; Ma, J.; Tang, G. P.; Yang, W. T.; Xu, F. J.: Functionalized nonionic dextran backbones by atom transfer radical polymerization for efficient gene delivery.

Macromolecules **2011**, *44*, 230-239.

(14) Xu, F. J.; Ping, Y.; Ma, J.; Tang, G. P.; Yang, W. T.; Li, J.; Kang, E. T.; Neoh, K. G.: Comb-shaped copolymers composed of hydroxypropyl cellulose backbones and cationic poly((2-dimethyl amino)ethyl methacrylate) side chains for gene delivery. *Bioconjug Chem* **2009**, *20*, 1449-1458.

(15) Ahmed, M.; Narain, R.: The effect of polymer architecture, composition, and molecular weight on the properties of glycopolymer-based non-viral gene delivery systems. *Biomaterials* **2011**, *32*, 5279-5290.

(16) Ma, M.; Li, F.; Yuan, Z. F.; Zhuo, R. X.: Influence of hydroxyl groups on the biological properties of cationic polymethacrylates as gene vectors. *Acta Biomater* **2010**, *6*, 2658-2665.

(17) Prevette, L. E.; Kodger, T. E.; Reineke, T. M.; Lynch, M. L.: Deciphering the role of hydrogen bonding in enhancing pDNA−polycation interactions. *Langmuir* **2007**, *23*, 9773-9784.

(18) Xu, F. J.; Li, H.; Li, J.; Zhang, Z.; Kang, E. T.; Neoh, K. G.: Pentablock copolymers of poly(ethylene glycol), poly((2-dimethyl amino)ethyl methacrylate) and poly(2-hydroxyethyl methacrylate) from consecutive atom transfer radical polymerizations for non-viral gene delivery. *Biomaterials* **2008**, *29*, 3023-3033.

(19) Guo, S.; Huang, Y.; Wei, T.; Zhang, W.; Wang, W.; Lin, D.; Zhang, X.; Kumar, A.; Du, Q.; Xing, J.; Deng, L.; Liang, Z.; Wang, P. C.; Dong, A.; Liang, X. J.: Amphiphilic and biodegradable methoxy polyethylene glycol-block-(polycaprolactone-graft-poly(2-(dimethylamino)ethyl methacrylate)) as an effective gene carrier. *Biomaterials* **2011**, *32*, 879-889.

(20) Jiang, X.; Lok, M. C.; Hennink, W. E.: Degradable-brushed pHEMA-pDMAEMA synthesized via ATRP and click chemistry for gene delivery. *Bioconjug Chem* **2007**, *18*,

2077-2084.

(21) Xu, F. J.; Zhang, Z. X.; Ping, Y.; Li, J.; Kang, E. T.; Neoh, K. G.: Star-shaped cationic polymers by atom transfer radical polymerization from beta-cyclodextrin cores for nonviral gene delivery. *Biomacromolecules* **2009**, *10*, 285-293.

(22) Yang, J.; Zhang, P.; Tang, L.; Sun, P.; Liu, W.; Sun, P.; Zuo, A.; Liang, D.: Temperature-tuned DNA condensation and gene transfection by PEI-g-(PMEO(2)MA-b-PHEMA) copolymer-based nonviral vectors. *Biomaterials* **2010**, *31*, 144-155.

(23) Breitenkamp, R. B.; Emrick, T.: Pentalysine-grafted ROMP polymers for DNA complexation and delivery. *Biomacromolecules* **2008**, *9*, 2495-2500.

(24) Johnson, R. N.; Chu, D. S.; Shi, J.; Schellinger, J. G.; Carlson, P. M.; Pun, S. H.: HPMA-oligolysine copolymers for gene delivery: optimization of peptide length and polymer molecular weight. *J Control Release* **2011**, *155*, 303-311.

(25) Shi, J.; Johnson, R. N.; Schellinger, J. G.; Carlson, P. M.; Pun, S. H.: Reducible HPMA-co-oligolysine copolymers for nucleic acid delivery. *Int J Pharm* **2011**, *427*, 113-122.

(26) Jonsson, M.; Linse, P.: Polyelectrolyte-macroion complexation. I. Effect of linear charge density, chain length, and macroion charge. *J Chem Phys* **2001**, *115*, 3406-3418.

(27) Huang, F. Q.; Scales, C. W.; Li, N.; Vasilieva, Y. A.; Ray, J.; Convertine, A. J.; McCormick, C. L.: Corona-stabilized interpolyelectrolyte complexes of SiRNA with nonimmunogenic, hydrophilic/cationic block copolymers prepared by aqueous RAFT polymerization. *Macromolecules* **2006**, *39*, 6871-6881.

(28) Fischer, D.; Bieber, T.; Li, Y.; Elsasser, H. P.; Kissel, T.: A novel non-viral vector for DNA delivery based on low molecular weight, branched polyethylenimine: effect of molecular weight on transfection efficiency and cytotoxicity. *Pharm Res* **1999**, *16*, 1273-1279.

(29) Xu, F. J.; Yang, W. T.: Polymer vectors via controlled/living radical polymerization for gene delivery. *Prog Polym Sci* **2011**, *36*, 1099-1131.

(30) Ahmed, M.; Bhuchar, N.; Ishihara, K.; Narain, R.: Well-controlled cationic water-soluble phospholipid polymer-DNA nanocomplexes for gene delivery. *Bioconjug Chem* **2011**, *22*, 1228-1238.

(31) Ladd, J.; Zhang, Z.; Chen, S.; Hower, J. C.; Jiang, S.: Zwitterionic polymers exhibiting high resistance to nonspecific protein adsorption from human serum and plasma. *Biomacromolecules* **2008**, *9*, 1357-1361.

(32) Ping, Y.; Liu, C. D.; Tang, G. P.; Li, J. S.; Li, J.; Yang, W. T.; Xu, F. J.: Functionalization of chitosan via atom transfer radical polymerization for gene delivery. *Adv Funct Mater* **2010**, *20*, 3106-3116.

(33) Newland, B.; Tai, H. Y.; Zheng, Y.; Velasco, D.; Di Luca, A.; Howdle, S. M.; Alexander, C.; Pandit, A.; Wang, W. X.: A highly effective gene delivery vector-hyperbranched poly(2-(dimethylamino)ethyl methacrylate) from in situ deactivation enhanced ATRP. *Chem Commun* **2010**, *46*, 4698-4700.

(34) Johnson, R. N.; Burke, R. S.; Convertine, A. J.; Hoffman, A. S.; Stayton, P. S.; Pun, S. H.: Synthesis of statistical copolymers containing multiple functional peptides for nucleic acid delivery. *Biomacromolecules* **2010**, *11*, 3007-3013.

(35) Wei, H.; Chu, D. S.; Zhao, J.; Pahang, J. A.; Pun, S. H.: Synthesis and evaluation of cyclic cationic polymers for nucleic acid delivery. *ACS Macro Lett* **2013**, *2*, 1047-1050.

(36) Convertine, A. J.; Diab, C.; Prieve, M.; Paschal, A.; Hoffman, A. S.; Johnson, P. H.; Stayton, P. S.: pH-Responsive polymeric micelle carriers for siRNA drugs. *Biomacromolecules* **2010**, *11*, 2904-2911.

(37) Zhu, C. H.; Jung, S.; Luo, S. B.; Meng, F. H.; Zhu, X. L.; Park, T. G.; Zhong, Z. Y.: Co-delivery of siRNA and paclitaxel into cancer cells by biodegradable cationic micelles based on PDMAEMA-PCL-PDMAEMA triblock copolymers. *Biomaterials* **2010**, *31*, 2408-2416.

(38) Wei, H.; Schellinger, J. G.; Chu, D. S.; Pun, S. H.: Neuron-targeted copolymers with sheddable shielding blocks synthesized using a reducible, RAFT-ATRP double-head agent. *J Am Chem Soc* **2012**, *134*, 16554-16557.

(39) Wei, H.; Volpatti, L. R.; Sellers, D. L.; Maris, D. O.; Andrews, I. W.; Hemphill, A. S.; Chan, L. W.; Chu, D. S. H.; Horner, P. J.; Pun, S. H.: Dual responsive, stabilized manoparticles for efficient in vivo plasmid delivery. *Angew Chem Int Edit* **2013**, *52*, 5377-5381.

(40) Wang, C.-H. K.; Chan, L. W.; Johnson, R. N.; Chu, D. S.; Shi, J.; Schellinger, J. G.; Lieber, A.; Pun, S. H.: The transduction of Coxsackie and Adenovirus Receptor-negative cells and protection against neutralizing antibodies by HPMA-co-oligolysine copolymer-coated adenovirus. *Biomaterials* **2011**, *32*, 9536-9545.

(41) Lin, S.; Du, F.; Wang, Y.; Ji, S.; Liang, D.; Yu, L.; Li, Z.: An acid-labile block copolymer of PDMAEMA and PEG as potential carrier for intelligent gene delivery systems. *Biomacromolecules* **2007**, *9*, 109-115.

(42) Chu, D. S.; Johnson, R. N.; Pun, S. H.: Cathepsin B-sensitive polymers for compartment-specific degradation and nucleic acid release. *J Control Release* **2012**, *157*, 445-454.

(43) Zhulina, E. B.; Borisov, O. V.; Priamitsyn, V. A.: Theory of steric stabilization of colloid dispersions by grafted polymers. *J Colloid Interface Sci* **1990**, *137*, 495-511.

(44) Qiao, Y.; Huang, Y.; Qiu, C.; Yue, X.; Deng, L.; Wan, Y.; Xing, J.; Zhang, C.; Yuan, S.; Dong, A.; Xu, J.: The use of PEGylated poly [2-(N,N-dimethylamino) ethyl methacrylate] as a mucosal DNA delivery vector and the activation of innate immunity and improvement of HIV-1-specific immune responses. *Biomaterials* **2010**, *31*, 115-123.

(45) Üzgün, S.; Akdemir, O.; Hasenpusch, G.; Maucksch, C.; Golas, M. M.; Sander, B.; Stark, H.; Imker, R.; Lutz, J. F.; Rudolph, C.: Characterization of tailor-made copolymers of oligo(ethylene glycol) methyl ether methacrylate and N,N-dimethylaminoethyl methacrylate as nonviral gene transfer agents: influence of macromolecular structure on gene vector particle properties and transfection efficiency. *Biomacromolecules* **2009**, *11*, 39-50.

(46) Venkataraman, S.; Ong, W. L.; Ong, Z. Y.; Joachim Loo, S. C.; Ee, P. L.; Yang, Y. Y.: The role of PEG architecture and molecular weight in the gene transfection performance of PEGylated poly(dimethylaminoethyl methacrylate) based cationic polymers. *Biomaterials* **2011**, *32*, 2369-2378.

(47) Lam, J. K. W.; Ma, Y.; Armes, S. P.; Lewis, A. L.; Baldwin, T.; Stolnik, S.: Phosphorylcholine-polycation diblock copolymers as synthetic vectors for gene delivery. *J Control Release* **2004**, *100*, 293-312.

(48) Jewell, C. M.; Lynn, D. M.: Surface-mediated delivery of DNA: cationic polymers take charge. *Curr Opin Colloid In* **2008**, *13*, 395-402.

(49) Lu, Y. J.; Low, P. S.: Folate-mediated delivery of macromolecular anticancer therapeutic agents. *Adv Drug Deliv Rev* **2002**, *54*, 675-693.

(50) York, A. W.; Huang, F.; McCormick, C. L.: Rational design of targeted cancer therapeutics through the multiconjugation of folate and cleavable siRNA to RAFT-synthesized (HPMA-s-APMA) copolymers. *Biomacromolecules* **2010**, *11*, 505-514.

(51) York, A. W.; Zhang, Y.; Holley, A. C.; Guo, Y.; Huang, F.; McCormick, C. L.: Facile synthesis of multivalent folate-block copolymer conjugates via aqueous RAFT polymerization: targeted delivery of siRNA and subsequent gene suppression. *Biomacromolecules* **2009**, *10*, 936-943.

(52) Benoit, D. S.; Srinivasan, S.; Shubin, A. D.; Stayton, P. S.: Synthesis of folate-functionalized

RAFT polymers for targeted siRNA delivery. *Biomacromolecules* **2011**, *12*, 2708-2714.

(53) Guo, S.; Huang, Y.; Zhang, W.; Wang, W.; Wei, T.; Lin, D.; Xing, J.; Deng, L.; Du, Q.; Liang, Z.; Liang, X. J.; Dong, A.: Ternary complexes of amphiphilic polycaprolactone-graft-poly (N,N-dimethylaminoethyl methacrylate), DNA and polyglutamic acid-graft-poly(ethylene glycol) for gene delivery. *Biomaterials* **2011**, *32*, 4283-4292.

(54) Palanca-Wessels, M. C.; Convertine, A. J.; Cutler-Strom, R.; Booth, G. C.; Lee, F.; Berguig, G. Y.; Stayton, P. S.; Press, O. W.: Anti-CD22 antibody targeting of pH-responsive micelles enhances small interfering RNA delivery and gene silencing in lymphoma cells. *Mol Ther* **2011**, *19*, 1529-1537.

(55) Ma, M.; Li, F.; Chen, F. J.; Cheng, S. X.; Zhuo, R. X.: Poly(ethylene glycol)-block-poly(glycidyl methacrylate) with oligoamine side chains as efficient gene vectors. *Macromol Biosci* **2010**, *10*, 183-191.

(56) Convertine, A. J.; Benoit, D. S. W.; Duvall, C. L.; Hoffman, A. S.; Stayton, P. S.: Development of a novel endosomolytic diblock copolymer for siRNA delivery. *J Control Release* **2009**, *133*, 221-229.

(57) Guo, S.; Qiao, Y.; Wang, W.; He, H.; Deng, L.; Xing, J.; Xu, J.; Liang, X. J.; Dong, A.: Poly(ε-caprolactone)-graft-poly(2-(N, N-dimethylamino) ethyl methacrylate) nanoparticles: pH dependent thermo-sensitive multifunctional carriers for gene and drug delivery. *J Mater Sci* **2010**, *20*, 6935-6941.

(58) Schellinger, J. G.; Pahang, J. A.; Johnson, R. N.; Chu, D. S.; Sellers, D. L.; Maris, D. O.; Convertine, A. J.; Stayton, P. S.; Horner, P. J.; Pun, S. H.: Melittin-grafted HPMA-oligolysine based copolymers for gene delivery. *Biomaterials* **2013**, *34*, 2318-2326.

(59) Behr, J. P.: The proton sponge: a trick to enter the cells the viruses did not exploit. *CHIMIA* **1997**, *51*, 34-36.

(60) Dai, F.; Sun, P.; Liu, Y.; Liu, W.: Redox-cleavable star cationic PDMAEMA by arm-first approach of ATRP as a nonviral vector for gene delivery. *Biomaterials* **2010**, *31*, 559-569.

(61) Pack, D. W.; Hoffman, A. S.; Pun S.; Stayton, P. S.: Design and development of polymers for gene delivery. *Nat Rev Drug Discov* **2005**, *4*, 581-593.

Chapter 3

OPTIMIZATION OF TET1 LIGAND DENSITY IN HPMA-*CO*-OLIGOLYSINE COPOLYMERS FOR TARGETED NEURONAL GENE DELIVERY

David S.H. Chu, Joan G. Schellinger, Michael J. Bocek, Russell N. Johnson, Suzie H. Pun

Abstract

Targeted gene delivery vectors can enhance cellular specificity and transfection efficiency. We demonstrated previously that conjugation of Tet1, a peptide that binds to the GT1b ganglioside, to polyethylenimine results in preferential transfection of neural progenitor cells *in vivo*. In this work, we investigate the effect of Tet1 ligand density on gene delivery to neuron-like, differentiated PC-12 cells. A series of statistical, cationic peptide-based polymers containing various amounts (1-5 mol%) of Tet1 were synthesized via one-pot reversible addition fragmentation chain transfer (RAFT) polymerization by copolymerization of Tet1 and oligo-L-lysine macromonomers with *N*-(2-hydroxypropyl)methacrylamide (HPMA). When complexed with plasmid DNA, the resulting panel of Tet1-functionalized polymers formed particles with similar particle size as particles formed with untargeted HPMA-oligolysine copolymers. The highest cellular uptake in neuron-like differentiated PC-12 cells was observed using polymers with intermediate Tet1 peptide incorporation. Compared to untargeted polymers, polymers with optimal incorporation of Tet1 increased gene delivery to neuron-like PC-12 cells by over an order of magnitude but had no effect compared to control polymers in transfecting NIH/3T3 control cells.[1]

[1]Reprinted with permission from Chu et al (2013). *Biomaterials* **34**(37):9632-9637.

3.1 Introduction

Gene delivery can potentially treat a range of neurological diseases inadequately addressed by current therapeutics. Delivery of genes expressing various neurotropic factors have been studied for neuroprotection and axonal regeneration following central nervous system (CNS) injury or for delayed progression of amyotrophic lateral sclerosis, Huntington's and Parkinson's.[1-3] Of the available delivery technologies, adeno-associated viral vectors have been most extensively explored for CNS gene delivery applications due to their high transduction efficiency and innate neural tropism,[4] but immunogenicity, long-term safety, and cost of manufacturing remain significant concerns. Non-viral delivery systems, such as cationic polymers or liposomes, can potentially overcome such limiting barriers; however, relatively poor transfection efficiency and high cytotoxicity are remain challenges.[5]

The incorporation of targeting ligands into non-viral gene delivery vehicles have been shown to both increase gene delivery efficiency and specificity. Various ligands, such as folate,[6] transferrin,[7] and RGD sequences,[8] have been used to mediate cellular binding and internalization. It has been postulated that to achieve specificity *in vivo*, the density of targeting ligands must be controlled.[9] Recent work reported that intermediate levels of ligand density in folate,[10] transferrin,[11] and antibody-targeted nanoparticles[12] conferred the highest level of tissue specificity *in vivo*.

Current approaches towards multivalent decoration of polymeric nanoparticles typically involve grafting of ligands onto the polymer carrier. However, control and reproducibility of synthesis remains a challenge for these approaches, leading to incomplete coverage or varied surface functionalization of nanoparticles.[13] We have developed an approach to controllably incorporate ligands into a polymeric construct through direct copolymerization of functionalized ligand monomers, allowing direct control over material properties. This method allows for control over ligand density, orientation of display, and architectural display in the final polymeric construct, overcoming some limitations of grafting approaches.

We recently reported the synthesis and optimization of well-defined, narrowly disperse oligo-L-lysine-HPMA cationic polymers utilizing reverse addition-fragmentation chain transfer (RAFT) polymerization to copolymerize HPMA with methacrylamido-functionalized peptide macromonomers.[14] Polymers displaying multiple peptide entities can be easily synthesized using

this approach, and incorporation of water-soluble peptides can be controlled based on feed ratios.[15,16] This platform can therefore be used to probe the effect of targeting ligand density on polymer gene transfer efficiency. Tet1, a peptide identified by *in vitro* phage display, binds to GT1b gangliosides, sphingophospholipids highly expressed on neuronal cell types.[17] Tet1 has been used in applications such as peripheral neural labeling and in the delivery of PLGA nanoparticles and polymersomes to neuronal targets.[18-20] Our group has previously shown neuronal transfection *in vitro* using Tet1-modified poly(ethylenimine) (PEI) polyplexes and specific gene delivery to neural stem and progenitor cells *in vivo* upon intraventricular administration using PEGylated versions of these materials.[21,22]

We report here the synthesis and evaluation of a series of peptide-based polymers containing varying amounts of Tet1 for targeted gene delivery to neuron-like cells. We utilize RAFT polymerization for one-pot synthesis of three component peptide-polymers using Tet1 as a targeting sequence, oligolysine for DNA binding and condensation, and HPMA for colloidal stability. Polyplexes were formed by self-assembly of polycations with plasmid DNA, and characterized by YOYO-1 DNA packaging assay and particle sizing. Cellular uptake as a function of Tet1 modification as well as gene transfection efficiency was studied in cultured neuron-like cells.

3.2 Materials and methods

3.2.1 Materials

N-(2-hydroxypropyl)methacrylamide (HPMA) was purchased from Polysciences (Warrington, PA). The initiator VA-044 was purchased from Wako Chemicals (Richmond, VA). Fmoc-protected amino acids and HBTU were purchased from AAPPTec (Louisville, KY), N-succinimidyl methacrylate from TCI America (Portland, OR), and Rink Amide Resin from EMD Biosciences (Darmstad, Germany). All other materials were reagent grade or better and were purchased from Sigma-Aldrich (St. Louis, MO) unless otherwise stated. Endotoxin-free plasmid pCMV-Luc2 was prepared using the Qiagen Plasmid Giga kit (Qiagen, Hilden, Germany) according to manufacturer's recommendations.

3.2.2 Synthesis of peptide monomers

Two peptide sequences were synthesized on solid support: K_3-Tet1 (KKKHLNILSTLWKYR) and the oligolysine K_{10} (KKKKKKKKKK). Peptides were synthesized via solid phase peptide synthesis following standard Fmoc chemistry using an automated PS3 Peptide Synthesizer (Protein Technologies, Phoenix, AZ). 6-aminohexanoic acid (Ahx) was added to the N-terminus of the peptide sequences. Prior to peptide cleavage from resin, the N-termini of the peptides were deprotected and coupled with N-succinimidyl methacrylate. These methacrylamido-functionalized peptides were cleaved from resin by treatment with trifluoroacetic acid (TFA)/triisopropylsilane(TIPS)/1,3-dimethoxybenzene/ddH_2O (90:2.5:5:2.5, v/v/v/v) for 3 hrs under gentle mixing. Cleaved peptide monomers were precipitated in ice-cold ether, dissolved in methanol and re-precipitated twice in ice-cold ether. Peptide monomers were analyzed by RP-HPLC and MALDI-TOF MS and purified as necessary.

3.2.3 Polymer synthesis

A series of copolymers was synthesized with varying amounts of Tet1 peptide in the feed (0%, 1%, 3%, 5%) while holding K_{10} peptide constant at 20%. Monomers were dissolved in acetate buffer (1 M, pH 5.1) with 10% ethanol (v/v) such that the final monomer concentration of the solution was 0.5 M. The RAFT chain transfer agent (CTA) used was ethyl cyanovaleric trithiocarbonate (ECT, molecular weight 263.4 g/mol) and the initiator (I) used was VA-044. The molar ratios of total monomer:CTA:I at the start of the polymerization were 190:1:0.1. The reaction solutions were transferred to round bottom flasks, capped with a rubber septa, purged with argon for 10 min, and then submerged in a 44 °C oil bath to initiate polymerization. The polymerization was allowed to proceed for 48 hrs. The flasks were removed from the oil bath and polymers dialyzed against distilled H_2O to removed unreacted monomers and buffer salts. The dialyzed products were lyophilized dry.

3.2.4 Size exclusion chromatography

Molecular weight analysis was carried out by size exclusion chromatography. The copolymers were dissolved at 2 mg/mL in running buffer (1:1 MeOH:300 mM acetate buffer, pH 4.4) for analysis by size exclusion chromatography – multiangle laser light scattering (SEC-MALLS). Analysis was carried out on an OHpak SB-804 HQ column (Shodex, Kawasaki, Japan) in line with a miniDAWN TREOS multiangle laser light scattering detector (Wyatt, Santa Barbara, CA) and an OptiLab rEX refractive index detector (Wyatt). Absolute molecular weight averages (M_n, M_w) were calculated using ASTRA software (Wyatt).

3.2.5 Amino acid analysis

The actual incorporated amount of peptide and HPMA in the final copolymers was determined through modified amino acid analysis as previously reported.[23] Briefly, hydrolyzed polymers were derivatized with o-phthalaldehyde/β-mercaptopropionic acid and run on a Zorbax Eclipse X-18 (Agilent Technologies, Santa Clara, CA) HPLC column with pre-column derivatization to label hydrolyzed amino acids and 1-amino-2-propanol (hydrolysis product of HPMA). Calibration curves were generated using serial dilutions of (L)-lysine, (L)-histidine, and reagent grade 1-amino-2-propanol.

3.2.6 Polyplex formation

pCMV-Luc2 plasmid was diluted in ddH_2O to a concentration of 0.1 mg/mL and mixed with an equal volume of polymer (in ddH_2O) at the desired amino to phosphate (N:P) ratio. After mixing, polyplexes were allowed to form for 10 minutes at room temperature.

3.2.7 Polyplex sizing by dynamic light scattering (DLS)

Polyplexes (0.5 μg DNA, 10 μL) were formed with polymers pHT1K10, pHT3K10, pHT5K10, and pHK10 at N:P ratios of 2, 3, and 4 and were mixed with either 90 μL of ddH2O or PBS such that the final salt concentration was 150 mM. Particle size was determined by dynamic light scattering (ZetaPLUS, Brookhaven Instruments Corp, Holtsville, NY).

3.2.8 DNA condensation using YOYO-1 fluorescence quenching assay

pCMV-Luc2 plasmid was mixed with the bis-intercalating dye YOYO-1 iodide (Invitrogen, Carlsbad, CA) at a dye/base pair ratio of 1:50 and incubated at room temperature for 1 h. Polyplexes were formed at N/P ratios of 0, 1, 2, 4, 6, and 10 by complexing YOYO-1-labeled DNA with pHT1K10, pHT3K10, pHT5K10, or pHK10. Ten microliters (containing 0.5 μg DNA) of polyplex was added to each well of a 96-well plate, followed by 90 μL of ddH_2O. The fluorescence from each well was measured on a Tecan Safire^2 plate reader with excitation at 491 nm and emission at 509 nm. The fluorescence signal for each N/P ratio was normalized to the N/P 0 (uncomplexed DNA) signal.

3.2.9 Cell culture

NIH/3T3 cells and PC-12 cells were grown according to ATCC recommendations. For *in vitro* studies, PC-12 cells were seeded onto collagen-coated plates. PC-12 cells were differentiated in F12K media supplemented with 1% HS, 1% ABAM, and 100 ng/mL nerve growth factor. Media was changed every 2 days.

3.2.10 Polyplex uptake

pCMV-Luc2 plasmid was mixed with the bis-intercalating dye YOYO-1 iodide at a dye/base pair ratio of 1:50 and incubated at room temperature for 1 hr. Polyplexes were formed at N:P=3 by complexing YOYO-1 labeled DNA with pHK10, pHT1K10, pHT3K10, and pHT5K10 polymers. Labeled polyplexes were added to cells for 2 hrs at 37 ºC. Cells were washed 3 times with PBS, detached by treatment with collagenase, and then washed twice more before labeling with propidium iodide (PI) stain. Cells were analyzed for fluorescence intensity by flow cytometry using the MACSQuant Analyzer (Miltenyi Biotec, Cologne, Germany) and gating for PI- (live) cells.

3.2.11 In vitro transfection efficiency

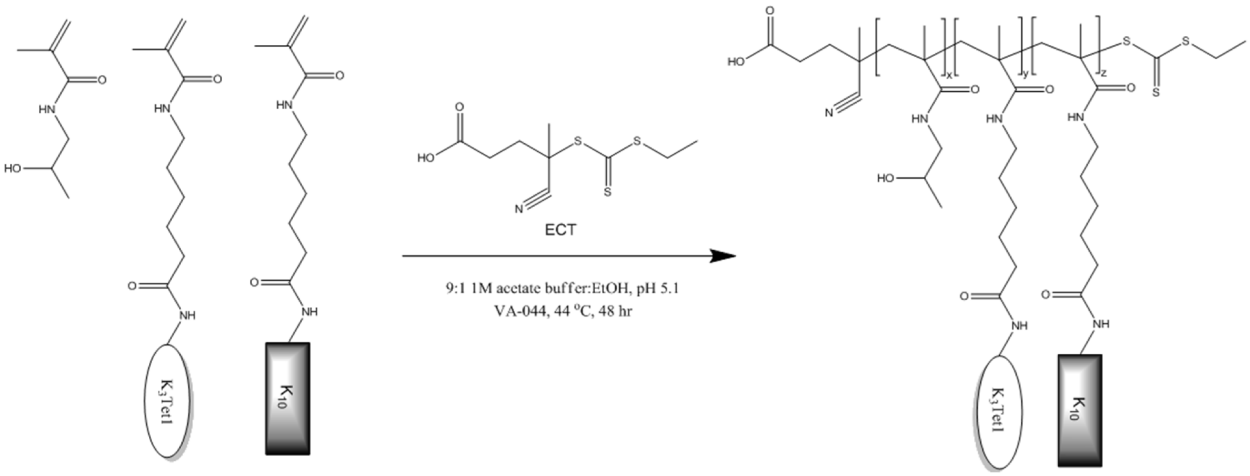

Scheme 3.1. Synthetic scheme of Tet1-*co*-oligolysine-*co*-HPMA copolymers.

PC-12 and NIH/3T3 cells were transfected as previously described. Briefly, polyplexes (1 µg DNA) were formed at 2.5, 3, and 4 N:P, diluted to 200 µL in OptiMEM (Invitrogen), and added to cells for 4 hrs. After an additional 44 hrs, luciferase expression was quantified using a luciferase assay kit (Promega, Fitchburg, WI) according to the manufacturer's instructions, except with an additional freeze-thaw cycle at -20 ºC to ensure complete cell lysis. Luminescence intensity was measured on a Tecan Safire^2 plate reader (Männerdorf, Switzerland) with 1 sec integration; total protein content was measured using a BCA Protein Assay Kit (Thermo Scientific, Rockford, IL) according to the manufacturer's instructions so luciferase activity could be normalized to the total protein content. Each sample was tested in triplicate.

3.2.12 Hemolysis assay

A hemolysis assay evaluating the membrane-lytic activity of the materials was performed as previously described.[24] Briefly, plasma was removed from freshly-drawn human blood via centrifugation. The erythrocyte layer was washed 3x with 150mM NaCl and resuspended in PBS. Polymers and polyplexes at various N/P with 1% Triton X-100 as a control were added to the erythrocyte suspensions in 96-well plates and incubated at 37 ºC for 1 hr. The plate was then centrifuged to pellet intact cells and released hemoglobin from lysed cells was measured

Table 3.1. Properties of HPMA-oligolysine copolymers

HPMA-oligolysine Copolymer	% Tet1 Mole Feed	Mn (kDa)[a]	M_w/M_n[a]	Mole % Tet1[b]	Mole % K_{10}[b]
$pHT1K_{10}$	1%	54.53	1.07	0.72	13.3
$pHT3K_{10}$	3%	79.51	1.04	2.86	14.3
$pHT5K_{10}$	5%	65.92	1.11	4.87	23.2
pHK_{10}	---	65.5	1.14	---	20.5

[a]Determined by SEC-MALLS. [b]Determined by amino acid analysis.

spectrophotometrically at 541 nm absorbance. Percent hemolysis was calculated relative to Triton X-100.

3.3 Results and discussion

3.3.1 Polymer characterization

A series of peptide-HPMA copolymers was synthesized via RAFT polymerization of peptide monomers with HPMA to investigate the effect of Tet1 peptide density on gene transfection using oligolysine-*co*-HPMA copolymers (Scheme 2.1). Monomer feed ratio and degree of polymerization were based on previous optimization studies suggesting a 4:1 HPMA to MaAhxK10 ratio at a degree of polymerization (DP) 150-190 yielded efficient vectors.[14]

The molecular weight and composition of synthesized copolymers are summarized in Table 3.1. Copolymers were synthesized with narrow polydispersities (< 1.2) and molecular weights in the 55-80 kDa range. Copolymers containing ~1, 3 and 5 mol% Tet1 and ~13-23% K_{10}, as determined by amino acid analysis, were prepared. pHK10 was used as an untargeted control for all studies.

3.3.2 Polyplex characterization

Polymers were used to formulate polyplexes (cationic polymer/plasmid DNA complexes) in either ddH_2O or PBS buffer containing physiological salt concentrations. The average hydrodynamic diameter of polyplexes was measured using dynamic light scattering (Figure 3.1). Polymers

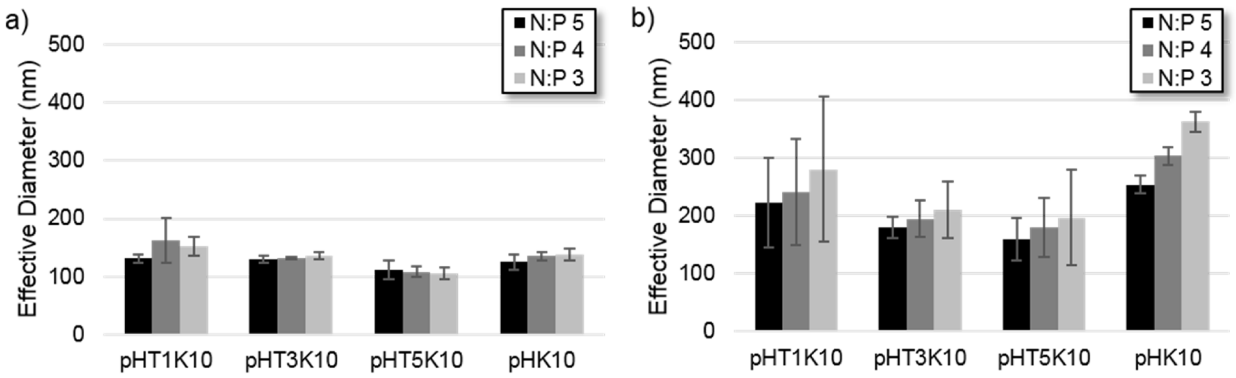

Figure 3.1. Particle size of polyplexes at various N/P ratios in (a) ddH_2O and (b) 150 mM PBS.

showed comparable polyplex size (100-150 nm) in ddH_2O regardless of Tet1 incorporation, suggesting that Tet1 incorporation does not affect particle formation. In physiological salt, 3% and 5% Tet1 polymers showed improved salt stability relative to 1% Tet1 and untargeted polymers. Inclusion of hydrophobic domains has previously been shown to improve colloidal stability.[25] Overall, relatively good salt stability is observed, with particles increasing to 200-300 nm in size in the presence of physiological salt. Particles show slight increase in size over time in PBS (Figure 3.5) but are stable against flocculation in PBS at concentrations both 20-fold higher and 50-fold lower than formulation concentrations. This correlates well previous work optimizing oligolysine-*co*-HPMA copolymers where polymers in the 60-80 kDa mass range showed good colloidal stability.[14]

To determine the effects of Tet1 incorporation on plasmid complexation and condensation, DNA condensation was monitored using YOYO-1 fluorescence quenching assay. In this assay, the condensation of plasmid DNA is labeled with a DNA-intercalating dye fluorophore YOYO-1. DNA condensation results in self-quenching of the YOYO-1 fluorescence due to electronic interactions between nearby dyes.[26] The YOYO-1 fluorescence, normalized to uncondensed plasmid, is shown in Figure 3.2 as a function of polymer DNA N/P ratio. Complexation of plasmid DNA with the various peptide-HPMA copolymers resulted in increasing YOYO-1 quenching with higher N/P ratios up to ~ N/P=6. Comparable trends in YOYO-1 fluorescence quenching are observed between the polymers, suggesting Tet1 functionalization does not affect plasmid complexation.

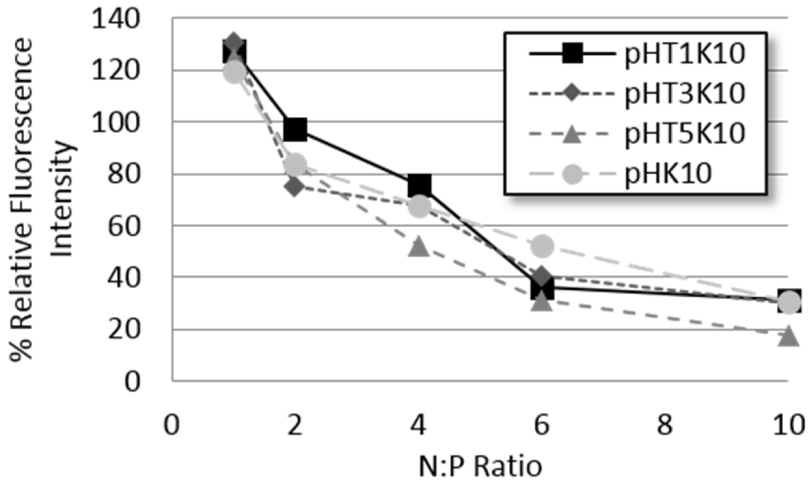

Figure 3.2. YOYO-1 fluorescence quenching assay as a measure of DNA complexation and condensation in ddH2O.

3.3.3 In vitro cellular uptake

Treatment of PC-12 pheochromocytoma cells with nerve growth factor (NGF) results in neuronal differentiation; cells acquire a neuron-like phenotype with extended neurties and reduced cell proliferation [27,28]. PC-12 cells differentiated for 6 days with NGF were therefore treated with fluorophore-labeled polyplexes (via YOYO-1 labeling) for 2 hrs at 37 ºC to determine relative cellular uptake of Tet1-targeted polyplexes. Cells were washed, stained with propidium iodide for dead cells, and then analyzed by flow cytometry to determine the relative polyplex uptake of live cells based on mean fluorescence intensity.

There is a 1.41-fold increase in mean fluorescence intensity at 2 hrs with pHT3K10 and 1.92-fold increase in intensity with pHT5K10 in 6-day differentiated PC-12 cells. pHT1K10 shows comparable cellular uptake to pHK10 (0.91-fold increase), suggesting that at very low modifications (~ 1-2 peptides per polymer chain), we observe no increase in cellular uptake. However, at higher levels (4-10 peptides per polymer), we observe increased cellular uptake as a function of increasing Tet1 modification. Similar transferrin- and bFGF-targeted poly-L-lysine nanoparticles have also shown around 2-4 fold increased cellular association while displaying over an order of magnitude increased transgene expression *in vitro*.[7]

Multivalent display of targeting ligands by polymers and nanoparticles has been shown to give significantly enhanced binding due to avidity.[29] Dendrimeric display of folate, for example, has been able to show decreased effective K_d by over 4 orders of magnitude.[30] However, recent work suggests optimal cellular specificity based on differential receptor expression benefits most from using low-affinity ligands.[31] While multivalent display of antibodies leads to effective ~pM K_d, cellular specificity is lost to high avidity due to increased binding to both target and non-target cells.[12] Instead, multivalent display of weak targeting ligands allows for super-selective targeting based on particle ligand density and cellular receptor density.[31] The observed increased cellular uptake with pHT3K10 and pHT5K10 relative to pHT1K10 suggests insufficient ligand density in pHT1K10 for effective binding to target PC-12 cells.

3.3.4 In vitro gene delivery

Gene transfection efficiency of the various Tet1-modified oligolysine-HPMA copolymers was then evaluated in neuron-like PC-12 cells and in control NIH/3T3 murine fibroblast cells. Polyplexes formulated at various charge ratios (N/P 2.5-4) were used to transfect 6-day differentiated PC-12 cells. Several charge ratios (N/P 2.5-4) were evaluated. The transfection efficiency of pHT1K10 is comparable to pHK10 for all N:P ratios tested, showing that low levels of Tet1 incorporation have no effects on transfection efficiency or cytotoxicity (Figure 3.3a). pHT3K10 and pHT5K10 showed significantly increased transfection efficiency at all three N/P ratios tested, with 11.5- and 10.7-fold higher luciferase expression at N/P 3 for pHT3K10 and pHT5K10 compared to pHK10, respectively, with no observed increase in toxicity (Figure 3.3c). At N/P 4, there was a 54.1 and 89.3-fold increase in transfection efficiency in pHT3K10 and pHT5K10 but that corresponded to a 30% and 60% reduction in cell viability, respectively, compared to a 15% drop in viability of pHK10.

The Tet1-modified oligolysine-HPMA copolymers were next tested in control NIH/3T3 cells, murine fibroblasts that express gangliosides at low levels. At N/P 3, the transfection efficiency of all materials was comparable, with no noticeable toxicity observed for any of the materials (Figure 3.3b, 3.3d). pHT1K10 and pHK10 copolymers transfected NIH/3T3 cells increasing efficiency with increasing N/P with no observable toxicity at the highest N/P tested. In contrast, polymers with higher Tet1 peptide functionalization, pHT3K10 and pHT5K10, show

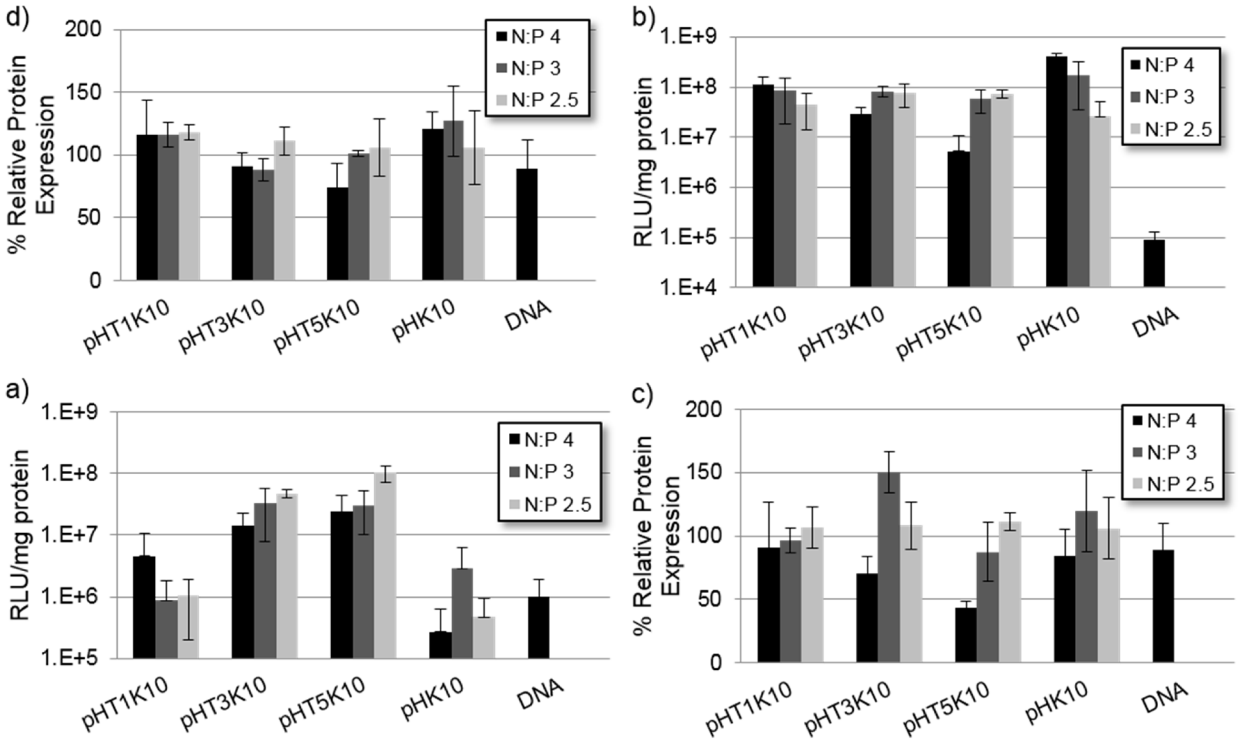

Figure 3.3. Normalized luminescence per mg protein as a measure of transfection efficiency for (a) 6-day differentiated PC-12 cells and (b) NIH/3T3 cells. Protein content normalized to untreated cells for (c) 6-day differentiated PC-12 cells and (d) NIH/3T3 cells as a measure of cellular viability.

decreased transfection efficiency at N/P 4, likely a result of decreased cellular viability at high N/P. This increased toxicity as a function of Tet1 peptide incorporation is consistent with what was observed for differentiated PC-12 cells.

Higher cytotoxicity of 3% and 5% Tet1 polymers compared to untargeted and 1% Tet1 polymer was observed in both control NIH/3T3 and target differentiated PC-12 cells, suggesting non-specific toxicity related to Tet1 peptide incorporation. Higher incorporation of Tet1 (pHT5K10 > pHT3K10) correlated with increased toxicity in a concentration-dependent manner. The Tet1 peptide sequence is relatively hydrophobic and suffers from poor solubility in water. Incubation with free Tet1 peptide alone shows no toxicity at concentrations > 100 μM (data not shown), suggesting that toxicity is not due to Tet1 peptide alone but in combination with the lysine-based polymers. Inclusion of hydrophobic domains has been shown to increase toxicity in several

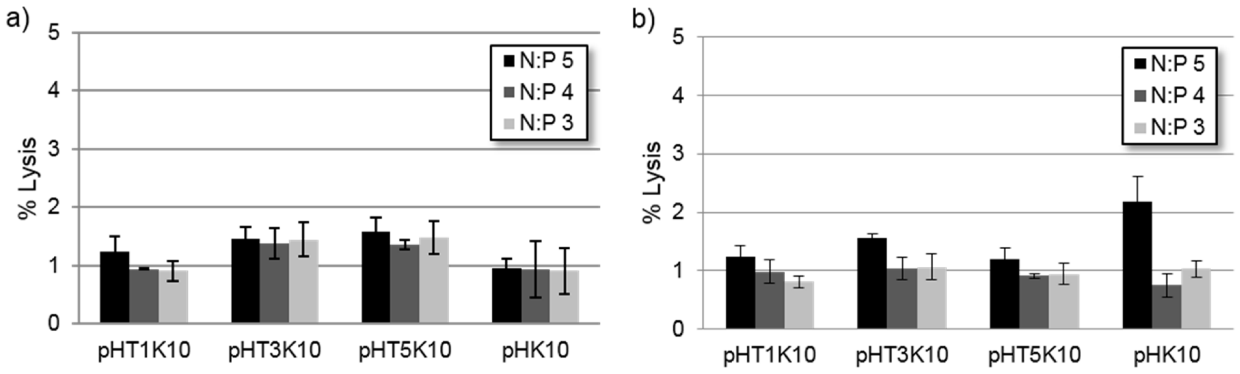

Figure 3.4. Percent hemolysis of (a) free polymer at concentrations equivalent to N/P ratios and (b) polyplexes relative to Triton X-100 control.

cationic vectors, postulated through increased membrane lyticity.[32] Polycationic polymers with increasing hydrophobicity demonstrated increasing hemolytic and antimicrobial activities.[33] Polylysines have been implicated in mitochondrial membrane disruption *in vitro* and have been implicated in induction of apoptosis via release of cytochrome c and induction of the caspase cascade.[34]

Cationic polymers typically suffer from high cytotoxicity,[35] but our group has recently reported several strategies incorporating enzymatically-labile or reducible motifs to improve biocompatibility.[36,37] Additionally, oligo-L-lysine copolymers undergo proteolytic degradation, with up to a 60% reduction in molecular weight thereby allowing for renal clearance of systemically-administered materials.[36] These strategies can be combined with optimized Tet1-targeted materials to produce efficient, biocompatible materials.

3.3.5 Hemolysis assay

To determine if Tet1 peptide was increasing transfection efficiency through increased endosomal escape, the membrane lyticity of the polymer materials was determined via hemolysis assay. Free polymer and polyplexes were incubated with freshly isolated human erythrocytes and tested for plasma membrane disruption by detecting hemoglobin release (Figure 3.4). Less than 2% hemolysis was observed at all polymer concentrations used during transfection studies. Likewise,

erythrocytes treated with polyplexes showed membrane lysis was around 1-2%, suggesting that insignificant membrane disruption is occurring even at 5% Tet1 incorporation. Therefore, observed increased transfection efficiency in 3% and 5% Tet1 copolymers is likely through increased cellular uptake and not through enhanced endosomal escape.

3.4 Conclusions

In this work, we have demonstrated the synthesis, characterization, and evaluation of Tet1-targeted HPMA-oligolysine copolymers for targeted gene delivery to neuronal cells. Incorporation of Tet1 peptide did not affect polyplex size or DNA condensation. At moderate levels of peptide incorporation, increased cellular uptake and transfection efficiency was observed in neuron-like differentiated PC-12 cells but not in NIH/3T3 fibroblast cells. However, increased toxicity not related to plasma membrane disruption was observed with pHT3K10 and pHT5K10 polymers, suggesting a balance between enhanced transfection efficiency and increased cytotoxicity. At N/P 3, over an order of magnitude increase in luciferase expression was achieved without significant increased toxicity. Overall, incorporation of Tet1 targeting ligand enhanced gene delivery efficiency to neuron-like cells.

3.5 Acknowledgements

This work was supported by NIH/NINDS 1R01 NS064404. David Chu was supported by NIH T32 CA138312. We thank Profs. Anthony Convertine and Patrick Stayton for generous donation of the ECT chain transfer agent.

3.6 References

(1) Hermens, W. T.; Verhaagen, J.: Viral vectors, tools for gene transfer in the nervous system. *Prog Neurobiol* **1998**, *55*, 399-432.

(2) Lo Bianco, C.; Schneider, B. L.; Bauer, M.; Sajadi, A.; Brice, A.; Iwatsubo, T.; Aebischer,

P.: Lentiviral vector delivery of parkin prevents dopaminergic degeneration in an α-synuclein rat model of Parkinson's disease. *P Natl Acad Sci USA* **2004**, *101*, 17510-17515.

(3) Åkerud, P.; Canals, J. M.; Snyder, E. Y.; Arenas, E.: Neuroprotection through delivery of glial cell line-derived neurotrophic factor by neural stem cells in a mouse model of Parkinson's disease. *J Neurosci* **2001**, *21*, 8108-8118.

(4) Burger, C.; Gorbatyuk, O. S.; Velardo, M. J.; Peden, C. S.; Williams, P.; Zolotukhin, S.; Reier, P. J.; Mandel, R. J.; Muzyczka, N.: Recombinant AAV viral vectors pseudotyped with viral capsids from serotypes 1, 2, and 5 display differential efficiency and cell tropism after delivery to different regions of the central nervous system. *Mol Ther* **2004**, *10*, 302-317.

(5) Pack, D. W.; Hoffman, A. S.; Pun, S.; Stayton, P. S.: Design and development of polymers for gene delivery. *Nat Rev Drug Discov* **2005**, *4*, 581-593.

(6) Morris, V. B.; Sharma, C. P.: Folate mediated l-arginine modified oligo (alkylaminosiloxane) graft poly (ethyleneimine) for tumor targeted gene delivery. *Biomaterials* **2011**, *32*, 3030-3041.

(7) Fisher, K. D.; Ulbrich, K.; Subr, V.; Ward, C. M.; Mautner, V.; Blakey, D.; Seymour, L. W.: A versatile system for receptor-mediated gene delivery permits increased entry of DNA into target cells, enhanced delivery to the nucleus and elevated rates of transgene expression. *Gene Ther* **2000**, *7*, 1337-1343.

(8) Park, J.; Singha, K.; Son, S.; Kim, J.; Namgung, R.; Yun, C. O.; Kim, W. J.: A review of RGD-functionalized nonviral gene delivery vectors for cancer therapy. *Cancer Gene Ther* **2012**, *19*, 741-748.

(9) Haun, J. B.; Hammer, D. A.: Quantifying nanoparticle adhesion mediated by specific molecular interactions. *Langmuir* **2008**, *24*, 8821-8832.

(10) Yamada, A.; Taniguchi, Y.; Kawano, K.; Honda, T.; Hattori, Y.; Maitani, Y.: Design of folate-linked liposomal doxorubicin to its antitumor effect in mice. *Clin Cancer Res* **2008**, *14*, 8161-8168.

(11) Wang, J.; Tian, S.; Petros, R. A.; Napier, M. E.; DeSimone, J. M.: The complex role of multivalency in nanoparticles targeting the transferrin receptor for cancer therapies. *J Am Chem Soc* **2010**, *132*, 11306-11313.

(12) Zern, B. J.; Chacko, A.-M.; Liu, J.; Greineder, C. F.; Blankemeyer, E. R.; Radhakrishnan, R.; Muzykantov, V.: Reduction of nanoparticle avidity enhances the selectivity of vascular targeting and PET detection of pulmonary inflammation. *ACS Nano* **2013**, *7*, 2461-2469.

(13) Hakem, I. F.; Leech, A. M.; Johnson, J. D.; Donahue, S. J.; Walker, J. P.; Bockstaller, M. R.: Understanding ligand distributions in modified particle and particlelike systems. *J Am Chem Soc* **2010**, *132*, 16593-16598.

(14) Johnson, R. N.; Chu, D. S.; Shi, J.; Schellinger, J. G.; Carlson, P. M.; Pun, S. H.: HPMA-oligolysine copolymers for gene delivery: optimization of peptide length and polymer molecular weight. *J Control Release* **2011**, *155*, 303-311.

(15) Johnson, R. N.; Burke, R. S.; Convertine, A. J.; Hoffman, A. S.; Stayton, P. S.; Pun, S. H.: Synthesis of statistical copolymers containing multiple functional peptides for nucleic acid delivery. *Biomacromolecules* **2010**, *11*, 3007-3013.

(16) Shi, J.; Schellinger, J. G.; Johnson, R. N.; Choi, J. L.; Chou, B.; Anghel, E. L.; Pun, S. H.: Influence of histidine incorporation on buffer capacity and gene transfection efficiency of HPMA-co-oligolysine brush polymers. *Biomacromolecules* **2013**, *14*, 1961-1970.

(17) Liu, J. K.; Teng, Q.; Garrity-Moses, M.; Federici, T.; Tanase, D.; Imperiale, M. J.; Boulis, N. M.: A novel peptide defined through phage display for therapeutic protein and vector neuronal targeting. *Neurobiol Dis* **2005**, *19*, 407-418.

(18) Zhang, Y.; Zhang, W.; Johnston, A. H.; Newman, T. A.; Pyykko, I.; Zou, J.: Targeted delivery of Tet1 peptide functionalized polymersomes to the rat cochlear nerve. *Int J Nanomedicine* **2012**, *7*, 1015-1022.

(19) Mathew, A.; Fukuda, T.; Nagaoka, Y.; Hasumura, T.; Morimoto, H.; Yoshida, Y.; Maekawa, T.; Venugopal, K.; Kumar, D. S.: Curcumin loaded-PLGA nanoparticles conjugated with Tet-1 peptide for potential use in Alzheimer's disease. *PLoS One* **2012**, *7*, e32616.

(20) Federici, T.; Liu, J. K.; Teng, Q.; Yang, J.; Boulis, N. M.: A means for targeting therapeutics to peripheral nervous system neurons with axonal damage. *Neurosurgery* **2007**, *60*, 911-918.

(21) Park, I. K.; Lasiene, J.; Chou, S. H.; Horner, P. J.; Pun, S. H.: Neuron-specific delivery of nucleic acids mediated by Tet1-modified poly(ethylenimine). *J Gene Med* **2007**, *9*, 691-702.

(22) Kwon, E. J.; Lasiene, J.; Jacobson, B. E.; Park, I. K.; Horner, P. J.; Pun, S. H.: Targeted nonviral delivery vehicles to neural progenitor cells in the mouse subventricular zone. *Biomaterials* **2010**, *31*, 2417-2424.

(23) Bidlingmeyer, B. A.; Cohen, S. A.; Tarvin, T. L.: Rapid analysis of amino acids using pre-column derivatization. *J Chromatogr* **1984**, *336*, 93-104.

(24) Schellinger, J. G.; Pahang, J. A.; Johnson, R. N.; Chu, D. S.; Sellers, D. L.; Maris, D. O.; Convertine, A. J.; Stayton, P. S.; Horner, P. J.; Pun, S. H.: Melittin-grafted HPMA-oligolysine based copolymers for gene delivery. *Biomaterials* **2013**, *34*, 2318-2326.

(25) Filippov, S. K.; Koňák, C.; Kopečková, P.; Starovoytova, L.; Špírková, M.; Štěpánek, P.: Effect of hydrophobic interactions on properties and stability of DNA−polyelectrolyte complexes. *Langmuir* **2010**, *26*, 4999-5006.

(26) Krishnamoorthy, G.; Duportail, G.; Mély, Y.: Structure and dynamics of condensed DNA probed by 1,1‘-(4,4,8,8-tetramethyl-4,8-diazaundecamethylene)bis[4-[[3- methylbenz-1,3-

oxazol-2-yl]methylidine]-1,4-dihydroquinolinium] tetraiodide fluorescence. *Biochemistry* **2002**, *41*, 15277-15287.

(27) Greenberg, M. E.; Greene, L. A.; Ziff, E. B.: Nerve growth factor and epidermal growth factor induce rapid transient changes in proto-oncogene transcription in PC12 cells. *J Biol Chem* **1985**, *260*, 14101-14110.

(28) Greene, L.: Nerve growth factor prevents the death and stimulates the neuronal differentiation of clonal PC12 pheochromocytoma cells in serum-free medium. *J Cell Biol* **1978**, *78*, 747-755.

(29) Davis, M. E.; Chen, Z.; Shin, D. M.: Nanoparticle therapeutics: an emerging treatment modality for cancer. *Nat Rev Drug Discov* **2008**, *7*, 771-782.

(30) Hong, S.; Leroueil, P. R.; Majoros, I. J.; Orr, B. G.; Baker Jr, J. R.; Banaszak Holl, M. M.: The binding avidity of a nanoparticle-based multivalent targeted drug delivery platform. *Chem Biol* **2007**, *14*, 107-115.

(31) Martinez-Veracoechea, F. J.; Frenkel, D.: Designing super selectivity in multivalent nano-particle binding. *Proc Natl Acad Sci USA* **2011**, *108*, 10963-10968.

(32) Incani, V.; Lavasanifar, A.; Uludag, H.: Lipid and hydrophobic modification of cationic carriers on route to superior gene vectors. *Soft Matter* **2010**, *6*, 2124-2138.

(33) Kuroda, K.; Caputo, G. A.; DeGrado, W. F.: The role of hydrophobicity in the antimicrobial and hemolytic activities of polymethacrylate derivatives. *Chemistry* **2009**, *15*, 1123-1133.

(34) Symonds, P.; Murray, J. C.; Hunter, A. C.; Debska, G.; Szewczyk, A.; Moghimi, S. M.: Low and high molecular weight poly(l-lysine)s/poly(l-lysine)–DNA complexes initiate mitochondrial-mediated apoptosis differently. *FEBS Lett* **2005**, *579*, 6191-6198.

(35) Chu, D. S.; Schellinger, J. G.; Shi, J.; Convertine, A. J.; Stayton, P. S.; Pun, S. H.: Application of living free radical polymerization for nucleic acid delivery. *Acc Chem Res* **2012**, *45*, 1089-1099.

(36) Chu, D. S.; Johnson, R. N.; Pun, S. H.: Cathepsin B-sensitive polymers for compartment-specific degradation and nucleic acid release. *J Control Release* **2012**, *157*, 445-454.

(37) Shi, J.; Johnson, R. N.; Schellinger, J. G.; Carlson, P. M.; Pun, S. H.: Reducible HPMA-co-oligolysine copolymers for nucleic acid delivery. *Int J Pharm* **2012**, *427*, 113-122.

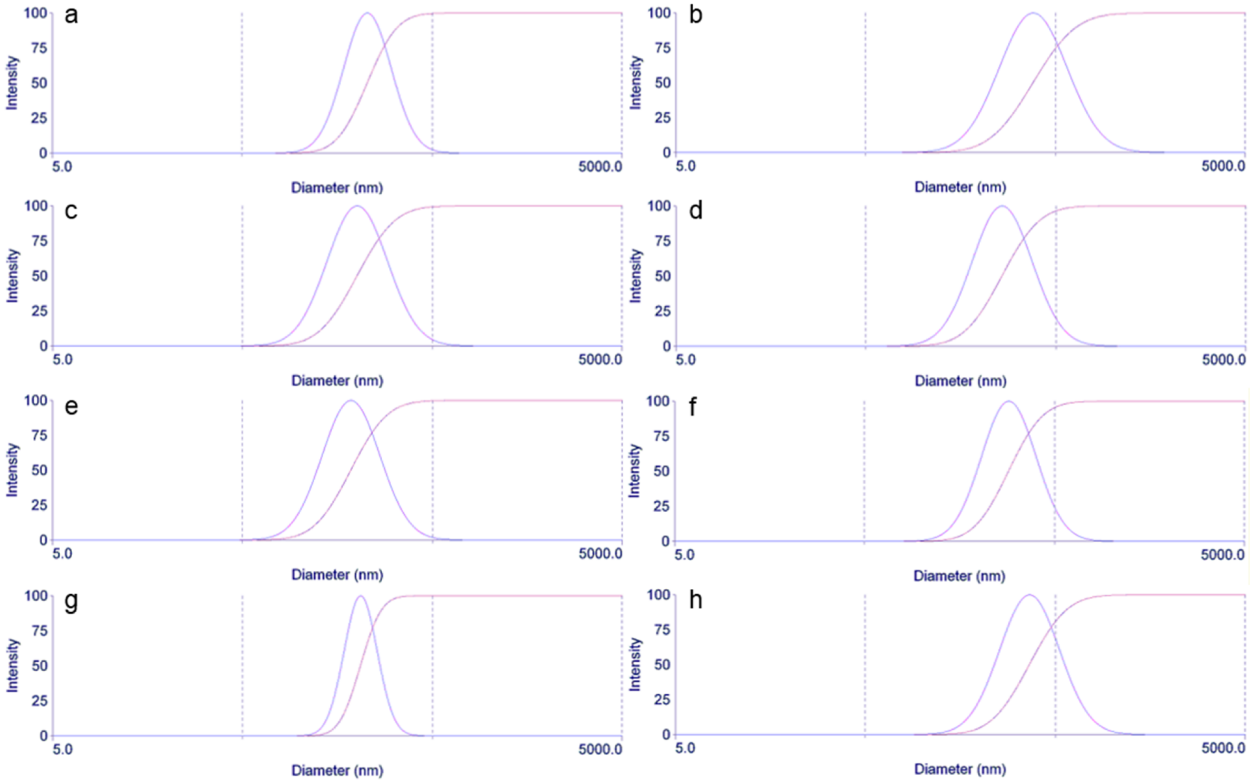

Figure 3.5. Lognormal intensity vs. size plots at time = 0 min for (a) pHT1K$_{10}$, (c) pHT3K$_{10}$, (e) pHT5K$_{10}$, and (g) pHK$_{10}$ and at time = 30 min for (b) pHT1K$_{10}$, (d) pHT3K$_{10}$, (f) pHT5K$_{10}$, and (h) pHK10. N/P = 4.

Chapter 4

CATHEPSIN-B SENSITIVE HPMA-*CO*-OLIGOLYSINE COPOLYMERS FOR ENZYMATICALLY-DEGRADABLE NUCLEIC ACID DELIVERY VECTORS

David S.H. Chu, Russell N. Johnson, Suzie H. Pun

Abstract

Degradable cationic polymers are desirable for *in vivo* nucleic acid delivery because they offer significantly decreased toxicity over non-degradable counterparts. Peptide linkers provide chemical stability and high specificity for particular endopeptidases but have not been extensively studied for nucleic acid delivery applications. In this work, enzymatically degradable peptide-HPMA copolymers were synthesized by RAFT polymerization of HPMA with methacrylated peptide macromonomers, resulting in polymers with low polydispersity and near quantitative incorporation of peptides. Three peptide-HPMA copolymers were evaluated: (i) pHCathK_{10}, containing peptides composed of the linker phe-lys-phe-leu (FKFL), a substrate of the endosomal/lysosomal endopeptidase cathepsin B, connected to oligo-(L)-lysine for nucleic acid binding, (ii) pHCath(D)K_{10}, containing the FKFL linker with oligo-(D)-lysine, and (iii) pH(D)Cath(D)K_{10}, containing all (D) amino acids. Cathepsin B degraded copolymers pHCathK_{10} and pHCath(D)K_{10} within one hour while no degradation of pH(D)Cath(D)K_{10} was observed. Polyplexes formed with pHCathK_{10} copolymers show DNA release by 4 hrs of treatment with cathepsin B; comparatively, polyplexes formed with pHCath(D)K_{10} and pH(D)Cath(D)K_{10} show no DNA release within 8 hrs. Transfection efficiency in HeLa and NIH/3T3 cells were comparable between the copolymers but pHCathK_{10} was less toxic. This work demonstrates the successful application of peptide linkers for degradable cationic polymers and DNA release.[1]

---

[1]Reprinted with permission from Chu et al (2012). *J Control Release* **157**(3):445-454.

4.1 Introduction

Polycations are frequently used as nucleic acid delivery materials because of their ability to package nucleic acids and promote cellular uptake.[1] However, polycation toxicity is frequently a limiting factor for *in vivo* application, thus impeding clinical translation.[2-4] Both nucleic acid delivery efficiency and cytotoxicity have been correlated with increasing molecular weight for several polycations.[5,6] Higher molecular weight polycations provide stronger binding to nucleic acids, resulting in improved stability in serum and circulation time after systemic delivery.[7-9] Lower molecular weight polycations are more readily displaced from their nucleic acid cargo; this release is necessary for biological activity.[10] Lower MW materials are also less toxic to cells when compared to their higher molecular weight counterparts.[11,12] Biodegradable polycations with controllable degradation have been of great interest to the nucleic acid delivery field because these materials can provide combine advantages of both high and low molecular weight polycations.

The most extensively studied degradable cationic polymers have utilized either reducible or hydrolysable bonds,[13-16] but these approaches provide limited control over the *in vivo* site of degradation. For example, poly(beta-amino esters) are degraded more quickly at neutral pH than acidic pH so that delivery vehicles would be susceptible to degradation once reconstituted in aqueous solution and administered *in vivo*.[16] Reducible linkers aim to take advantage of the highly reducing cytosolic environment for controlled intracellular degradation,[17] but extracellular reduction has been implicated as the primary site of degradation for some polymeric systems.[18] We recently synthesized reducible HPMA-*co*-oligolysine copolymers by including disulfide linkers between the HPMA backbone and oligolysine pendant peptides.[19] Although reduced cytotoxicity was observed with these materials, transfection efficiency was also significantly decreased. This was partially attributed to the instability of the disulfide bond by sulfhydryl exchange and metal-catalyzed oxidation of the free sulfhydryl groups leading to crosslinking between polymer strands.

A controlled release material with polymer degradation triggered by specific intracellular enzymatic activity is highly attractive for gene delivery applications. Enzyme-catalyzed degradation combines chemical stability and high specificity. Peptide-based linkers act as selective substrates for specific extra- or intracellular peptidases, with enzymatic specificity determined by the amino acid sequence. In addition, linkers have varying rates of enzymatic cleavage, adjustable

by changing the recognition sequence or neighboring residues,[20,21] further enabling the control of degradation. Peptide linkers have been used successfully for other biological applications, such as antibody-drug conjugates for cancer therapy[22] and degradable cross-linked scaffolds for tissue engineering,[23] but have not been extensively studied for nucleic acid delivery applications. Two groups recently reported enzymatically-cleavable linkers for release of targeting ligands,[24,25] but, to our knowledge, no reports using peptide linkers in main or side-chain architectures in gene delivery materials as an approach for specific polymer degradation are available.

In nucleic acid delivery applications, endosomal degradation of carriers has several advantages. Materials need to remain intact in the extracellular environment to protect nucleic acids from nucleases present in serum. However, polycations such as polyethylenimine (PEI) and poly-(L)-lysine (PLL) have been shown to trigger mitochondrial-mediated apoptosis after polymer interaction with the outer mitochondrial membrane.[26] Polymers that degrade prior to cytosolic release are therefore hypothesized to be less cytotoxic than non-degraded polymers. Cathepsin B is a papain-like cysteine protease with both endopeptidase and exopeptidase activity that is involved in protein degradation and turnover in cells.[10] Cathepsin B functions primarily in the endo/lysosomal compartments[27-29] and has therefore been the target for enzyme-triggered, intracellular drug delivery.[30-32] We therefore designed cationic, peptide-based polymers for nucleic acid delivery with cathepsin B linker substrates for specific endosomal degradation as a means to reduce cytotoxicity through enzyme-mediated degradation.

In this work, peptide-HPMA copolymers were synthesized via reverse addition-fragmentation chain transfer (RAFT) polymerization of HPMA with methacrylamido-peptide monomers. The peptide monomers contained an oligolysine motif that was capped with a short, four amino acid cathepsin B substrate, thereby enabling endosomal degradation of the cationic copolymers. In total, three peptide-HPMA copolymers were evaluated: (i) pHCathK_{10}, containing peptides composed of the linker phe-lys-phe-leu (FKFL), a substrate of cathepsin B, connected to oligo-(L)-lysine for nucleic acid binding; (ii) pHCath(D)K_{10}, containing the FKFL linker with oligo-(D)-lysine; and (iii) pH(D)Cath(D)K_{10}, containing all (D) amino acids. These polymers were evaluated for sensitivity to cathepsin B degradation, polyplex destabilization and DNA release, cytotoxicity and transfection efficiency.

4.2 Materials and methods

4.2.1 Materials

N-(2-hydroxypropyl)methacrylamide (HPMA) was purchased from Polysciences (Warrington, PA). The initiator VA-044 was purchased from Wako Chemicals (Richmond, VA). Fmoc-protected amino acids and HBTU were purchased from AAPPTec (Louisville, KY), N-succinimidyl methacrylate from TCI America (Portland, Oregon), and Rink Amide Resin from EMD Biosciences (Darmstad, Germany). Human liver cathepsin B was purchased from Enzo Life Sciences (Plymouth Meeting, PA). All other materials were reagent grade or better and were purchased from Sigma-Aldrich (St. Louis, MO) unless otherwise stated. Endotoxin-free plasmid pCMV-Luc2 was prepared using the Qiagen Plasmid Giga kit (Qiagen, Hilden, Germany) according to manufacturer's recommendations.

4.2.2 Synthesis of peptide monomers

Three peptides were synthesized using (D) and (L) amino acids and 6-aminohexanoic acid (Ahx): AhxFKFLAhxK_{10} (composed of only (L) amino acids); AhxFKFLAhx(D)K_{10} (composed of (L) amino acid linker with oligo-(D)-lysine); and Ahx(D)FKFLAhx(D)K_{10} (composed of only (D) amino acids). Peptides were synthesized on a solid support with Rink amide linker following standard Fmoc chemistry on an automated PS3 peptide synthesizer (Protein Technologies, Phoenix, AZ). Prior to peptide cleavage from the resin, the amino termini of the peptides were deprotected and coupled with N-succinimidyl methacrylate. These functionalized peptide monomers are respectively called MaAhxFKFLAhxK_{10}, MaAhxFKFLAhx(D)K_{10}, and MaAhx(D)FKFLAhx(D)K_{10}. Synthesized peptides were cleaved from resin by treatment of solid support with a solution of TFA/triisopropylsilane (TIPS)/1,3-dimethoxybenzene (92.5:2.5:5, v/v/v) for 2.5 hours under gentle mixing. Cleaved peptide monomers were precipitated in cold ether, dissolved in methanol and re-precipitated twice in cold ether. Each peptide monomer was analyzed by RP-HPLC and MALDI-TOF MS and shown to have greater than 95% purity after cleavage. The expected molecular weight of the peptides was 2128.82 Da. Experimentally measured molecular weights determined by MALDI-TOF MS were 2129.137 Da, 2128.526 Da,

and 2128.689 Da for MaAhxFKFLAhxK_{10}, MaAhxFKFLAhx(D)K_{10}, and MaAhx(D)FKFLAhx(D)K_{10}, respectively.

4.2.3 Cathepsin B cleavage of peptide monomers

Specific cleavage at the FKFL linker by cathepsin B was determined by adapting a method from Dubowchik *et al*.[20] For this and subsequent cathepsin B cleavage studies, human liver cathepsin B (0.351 mg/mL stock) was added to activation buffer (30 mM DTT, 15 mM EDTA) for a final concentration of 0.117 mg/mL cathepsin B, 20 mM DTT, 10 mM EDTA and incubated at 37 °C for 15 min. Reaction buffer (25 mM acetate, 1 mM EDTA, pH 5, pre-warmed at 37 °C) and peptide solution (10 mM stock) were added to the enzyme solution such that the final concentration of the reaction solution was 1.28 μg/mL cathepsin B, 24.6 mM acetate, 1.1 mM EDTA, 0.33 mM DTT, 65 μM peptide, and the reaction solution was incubated at 37 °C. Aliquots were removed at various time points and enzymatic activity stopped by addition of thioprotease inhibitor E-64 (Thermo Scientific, Waltham, MA) to a 26 μg/mL final concentration. Aliquots were analyzed qualitatively via MALDI-TOF MS.

4.2.4 Serum stability of peptide macromonomers

Linker susceptibility to serum proteases was evaluated using freshly isolated mouse serum. For each peptide, peptide (5 μL of 10 mM stock) was added to serum (120 μL, pre-incubated at 37 °C). At various time points, 20 μl aliquots of the mixture were withdrawn and 5 μL of ice-cold 15% trichloroacetic acid (w/v) was added to stop enzymatic degradation via protein precipitation. Precipitated solutions were centrifuged at 13000 rpm for 15 min and supernatants were analyzed by MALDI-TOF MS.

4.2.5 Polymer Synthesis

Three polymers were synthesized: HPMA-*co*-MaAhxFKFLAhxK_{10} (pHCathK_{10}), HPMA-*co*-MaAhxFKFLAhx(D)K_{10} (pHCath(D)K_{10}), and HPMA-*co*-MaAhx(D)FKFLAhx(D)K_{10} (pH(D)Cath(D)K_{10}). Each polymer was synthesized with target degree of polymerization (DP) of

190 with 20% mole feed peptide to yield polymers with target molecular weight of approximately 103 kDa. Monomers were dissolved in acetate buffer (1 M, pH 5.1) such that the final monomer concentration of the solution was 0.7 M. The RAFT chain transfer agent (CTA) used was ethyl cyanovaleric trithiocarbonate (ECT, molecular weight 263.4 g/mol) and the initiator (I) used was VA-044. The molar ratios of total monomer:CTA:I at the start of polymerization were 190:1:0.1. The reaction solutions were transferred to round bottom flasks, capped with a rubber septum, purged with argon for 10 min, and the submerged in a 44 °C oil bath to initiate polymerization. The polymerization was allowed to proceed for 48 hrs. The flasks were removed from the oil bath and polymers dialyzed against distilled H_2O to removed unreacted monomers and buffer salts. The dialyzed polymers were lyophilized dry.

4.2.6 Size exclusion chromatography

Molecular weight analysis was carried out by size exclusion chromatography. The copolymers were dissolved at 10 mg/mL in running buffer (150 mM acetate buffer, pH 4.4) for analysis by size exclusion chromatography-multiangle laser light scattering (SEC-MALLS). Analysis was carried out on an OHpak SB-804 HQ column (Shodex, New York, NY) in line with a miniDAWN TREOS multiangle laser light scattering detector (Wyatt, Santa Barbara, CA) and an OptiLab rEX refractive index detector (Wyatt). Absolute molecular weight averages (M_n, M_w) were calculated using ASTRA software (Wyatt).

4.2.7 Amino acid analysis

The actual incorporated amount of peptide and HPMA in the final copolymers was determined through modified amino acid analysis following the method of Bidlingmeyer and coworkers.[33] Briefly, hydrolyzed lysine and HPMA (which results in 1-amino-2-propanol) were derivatized with o-phthalaldehyde/β-mercaptopropionic acid and run on a Poroshell 120 EC-C18 (Agilent Technologies, Santa Clara, CA) HPLC column with pre-column derivatization to label hydrolyzed lysine and 1-amino-2-propanol. Calibration curves were generated using serial dilutions of (L)-lysine and reagent grade 1-amino-2-propanol.

4.2.8 Cathepsin B-mediated polymer degradation

Linker recognition and subsequent release of oligolysine side-chains from the polymer were assessed by enzymatic treatment with cathepsin B. For each polymer, cathepsin B reactions were set up as described previously with a final polymer concentration of 44 μg/mL. At various time points, aliquots were removed and E-64 was added to stop the enzymatic reaction. Solutions were analyzed by SEC and the relative differential refractive index profiles were compared. MALDI-TOF MS was also performed.

4.2.9 Polyplex formation

pCMV-Luc2 plasmid was diluted in ddH_2O to a concentration of 0.1 mg/mL and mixed with an equal volume of polymer (in ddH_2O water) at the desired amine to phosphate (N:P) ratio. After mixing, polyplexes were allowed for form for 10 minutes at room temperature. The charge densities of the oligolysine-*co*-HPMA copolymers, PEI, and PLL are approximately 290 mg/mmol N, 43 mg/mmol N, and 208 mg/mmol N, respectively.

4.2.10 Sizing of polyplexes by dynamic light scattering (DLS)

Polyplexes (0.5 μg DNA, 10 μL) were formed with pHCathK_{10}, pHCath(D)K_{10}, pH(D)Cath(D)K_{10}, branched polyethylenimine (PEI, 25 kDa, PDI ~2.5) or poly-(L)-lysine (PLL, 15-30 kDa, PDI 1.2) at 3, 4, and 5 N:P ratios and were mixed with either 90 μL of ddH_2O or PBS such that the final salt concentration was 150 mM. Particle size was determined by dynamic light scattering (ZetaPLUS, Brookhaven Instruments Corp, Holtsville, NY).

4.2.11 Polyplex destabilization by DLS

Polyplexes were formulated at 4 N:P with pHCathK_{10}, pHCath(D)K_{10}, or pH(D)Cath(D)K_{10}. The DLS instrument and cuvette with cap were pre-equilibrated at 37 °C. For each polyplex solution, cathepsin B reactions were set up as described previously with a final concentration of DNA of 5.33 μg/mL. Reaction solutions were transferred to the cuvette and capped to prevent evaporation.

Enzymatic reaction was allowed to proceed for 8 hrs at 37 °C with particle size measured every 15 min.

4.2.12 Polyplex unpackaging by YOYO-1 fluorescence quenching assay

pCMV-Luc2 plasmid was mixed with the bis-intercalating dye YOYO-1 iodide (Invitrogen, Carlsbad, CA) at a dye/base pair ratio of 1:50 and incubated at room temperature for 1 hour. Polyplexes were formed at 4 N:P by complexing YOYO-1-labeled DNA with pHCathK_{10}, pHCath(D)K_{10}, and pH(D)Cath(D)K_{10}. For each polyplex solution, cathepsin B reactions were set up as described previously with a final concentration of DNA at 5.33 μg/mL. At various time points, aliquots were removed and reaction stopped with addition of E-64, diluted to 100 μL total volume with ddH_2O, and transferred to a 96-well plate. After the final time point, the fluorescence from each well of all the plates was measured on a Tecan Safire^2 plate reader (Männerdorf, Switzerland) with excitation at 491 nm and emission at 509 nm. The fluorescence signal for each time point was normalized against a plasmid-only signal.

4.2.13 In vitro transfection efficiency

HeLa and NIH/3T3 cells were transfected as previously described.[34] Briefly, polyplexes (1 μg DNA) were formed at 3, 4, and 5 N:P, diluted to 200 uL in MEM Reduced Serum Medium (Hyclone), and added to cells for 4 hrs. After an additional 44 hrs, luciferase expression was quantified using a luciferase assay kit (Promega, Fitchburg, WI) according to the manufacturer's instructions, except with an additional freeze-thaw cycle at -20 ºC to ensure complete cell lysis. Luminescence intensity was measured on the plate reader with 1 sec integration; total protein content was measured using a BCA Protein Assay Kit (Thermo Scientific, Rockford, IL) according to the manufacturer's instructions so luciferase activity could be normalized to the total protein content. Each sample was tested in quadruplicate.

4.2.14 Cytotoxicity of polymers and polyplexes

The cytotoxicity of the polymers and polyplexes was evaluated *in vitro* using the MTS assay as

described previously.[34] Polymers of various concentrations or polyplexes at 3, 4, and 5 N:P (0.2 μg DNA) were prepared in ddH_2O water and then diluted 10-fold in MEM Reduced Serum Medium. The cells were rinsed once with PBS and incubated with 40 μL of the polymer or polyplex solution for 4 hrs. At 48 hrs, 20 μL of 3-(4,5-dimethylthiazol-2-yl)-5-(3-carboxymethoxyphenyl)-2-(4-sulfophenyl)-2*H*-tetrazolium (MTS) (Promega, Madison, WI) was added to each well. Cells were then incubated for 3 hrs and absorbance measured at 490 nm using a plate reader. For polymers, IC_{50} values were determined using a nonlinear fit (four-parameter variable slope) in GraphPad Prism v.5 (San Diego, CA). For polyplexes, cellular viability was normalized against untreated cells.

4.3 Results

4.3.1 Enzymatic degradation of peptides by cathepsin B and mouse serum

Methacrylated oligolysine (K_{10}) peptides containing the FKFL cathepsin B substrate sequence flanked on each side by a six-carbon spacer were synthesized by solid phase peptide synthesis. Three peptides were synthesized, differing only in the use of D- versus L-amino acids to impart peptidase resistance; thus, all full length peptides have MW 2128 Da. Cathepsin B-mediated peptide cleavage at the FKFL linker was monitored over 30 min enzyme incubation (Figure 4.1). Rapid recognition and specific cleavage of the MaAhxFKFLAhxK_{10} and MaAhxFKFLAhx(D)K_{10} peptides at the FKFL linker results in disappearance of the 2128 Da peak and simultaneous emergence of a 1673 Da peak corresponding to the FLAhxK_{10}/ FLAhx(D)K_{10} fragment, respectively. Fragmentation of the original peptide is complete within 15 min of enzymatic exposure. The FLAhxK_{10} peptide fragment is susceptible to exopeptidase degradation as well, with the systematic removal of C-terminal lysines over time; however, this process is considerably slower than the endopeptidase cleavage at the linker. The FLAhx(D)K_{10} fragment shows resistance to exopeptidase activity. The MaAhx(D)FKFLAhx(D)K_{10} peptide has no observable degradation within the 30 min of cathepsin B treatment.

Extracellular enzymatic stability of the peptide and specificity of the FKFL linker for intracellular peptidases was tested by exposing peptides to freshly isolated mouse serum and

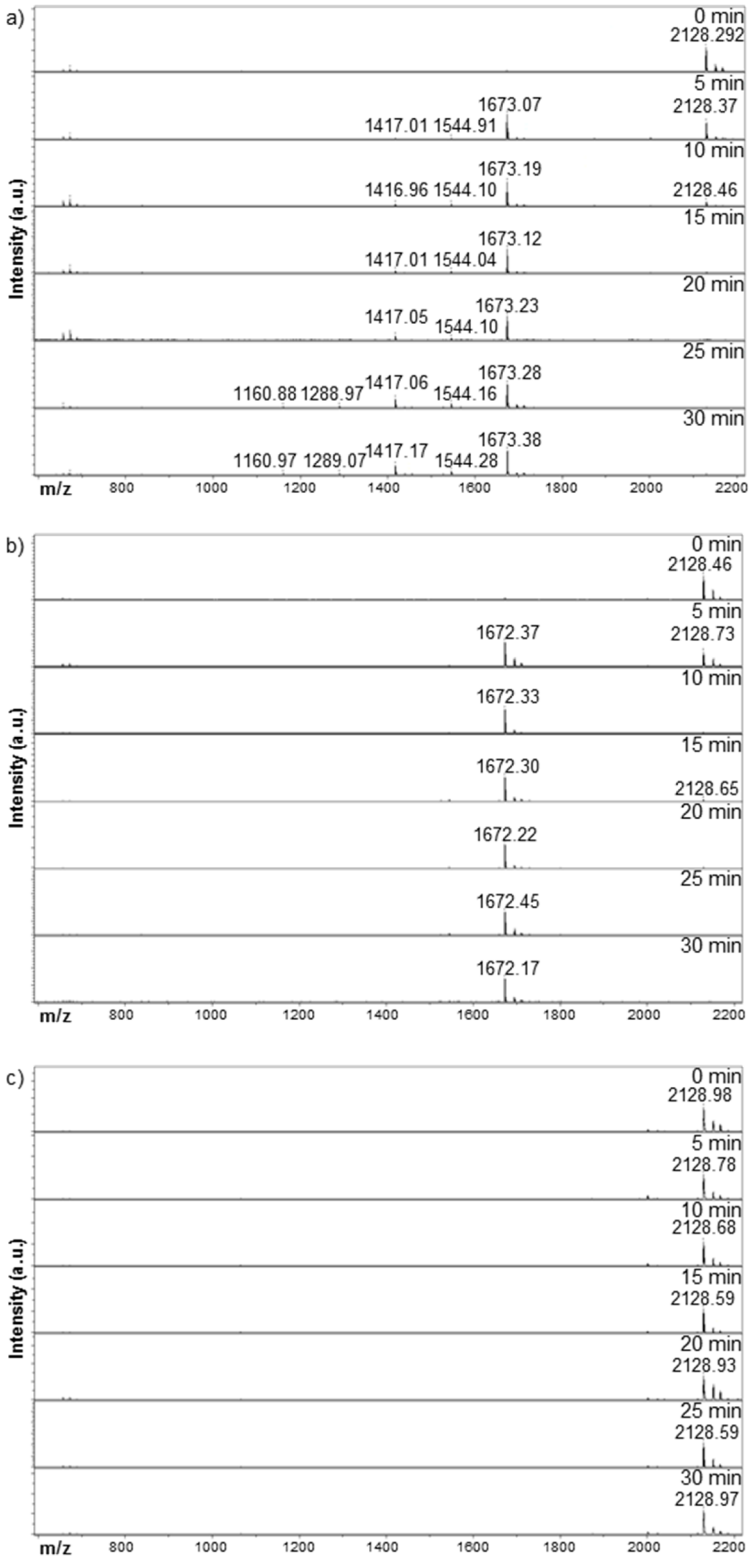

Figure 4.1. MALDI-TOF MS time-point study of cathepsin B-mediated fragmentation of (a) MaAhxFKFLAhxK$_{10}$, (b) MaAhxFKFLAhx(D)K$_{10}$, and (c) MaAhx(D)FKFLAhx(D)K$_{10}$.

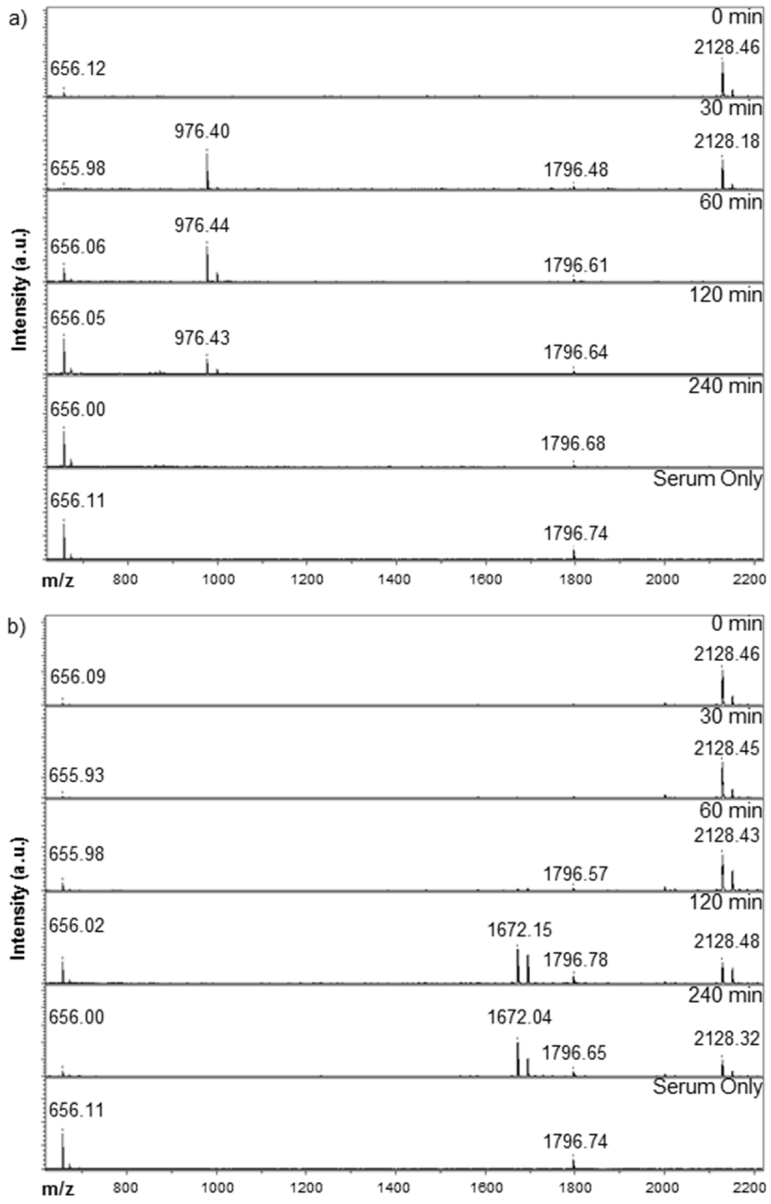

Figure 4.2. MALDI-TOF MS time-point study of mouse serum enzymatic digest of (a) MaAhxFKFLAhxK_{10}, (b) MaAhxFKFLAhx(D)K_{10}.

monitoring degradation over 4 hrs. No endopeptidase cleavage of the FKFL linker was detected but degradation of the MaAhxFKFLAhxK_{10} peptide by non-specific exopeptidase hydrolysis was observed by 1 hr post-incubation (Figure 4.2a), yielding the shortened fragment MaAhxFKFLAhxK (976 Da). In contrast, intact MaAhxFKFLAhx(D)K_{10} peptide is observed even after serum incubation for 4 hours. Some endopeptidase degraded product (1672 Da =

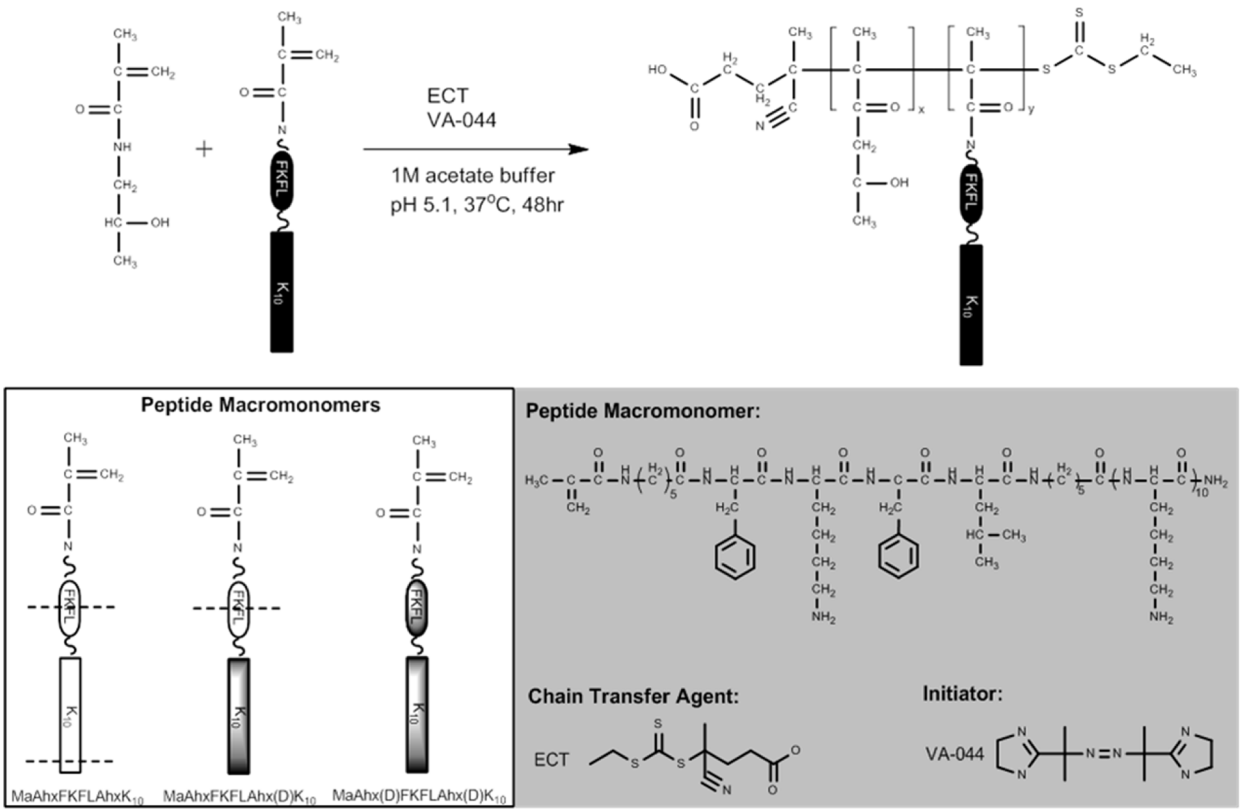

Scheme 4.1. Synthetic scheme of HPMA-*co*-oligolysine copolymers.

FLAhx(D)K_{10}) is observed at the 2 and 4 hr time points (Figure 4.2b). No FLAhxK10 fragments are observed in 2a, likely due to rapid exopeptidase degradation by the first 30 min time point. Peaks at 656 and 1796 Da correspond to matrix and a peptide found in serum, respectively.

4.3.2 Enzymatic degradation of HPMA-co-oligolysine copolymers by cathepsin B

Three HPMA-oligolysine copolymers were synthesized by RAFT polymerization of peptide monomers with HPMA as described previously.[34,35] The synthesized polymers displayed properties close to targeted values as summarized by Table 4.1. In general, the copolymers had M_n ~ 5-15% lower than expected. Polydispersity of all the copolymers was below 1.2. Amino acid analysis of the copolymers revealed peptide mole incorporation around 25-27%.

Cathepsin-B mediated degradation of HPMA-oligolysine copolymers was evaluated by treating polymers with cathepsin B and analyzing polymers at various time points by size exclusion

Table 4.1. Properties of HPMA-oligolysine copolymers

HPMA-oligolysine Copolymer	Peptide Monomer	Type of Degradation	Targeted M_n (kDa)[a]	Determined Mn (kDa)[b]	M_w/M_n[b]	Mole% Peptide Monomer[c]
pHCathK_{10}	MaAhxFKFLAhxK_{10}	Endo/exopeptidase	102.63	96.64	1.17	27.4
pHCath(D)K_{10}	MaAhxFKFLAhx(D)K_{10}	Exopeptidase Only	102.63	93.26	1.17	24.8
pH(D)Cath(D)K_{10}	MaAhx(D)FKFLAhx(D)K_{10}	None	102.63	88.57	1.18	26.0

[a]Based on Mn=[Mo]/[CTAo] x conversion x FW with no counterions. [b]Determined by SEC-MALS. [c]Determined by amino acid analysis.

chromatography (Figure 4.3). Un-degraded polymers elute from the column ~13 min. Degradation of pHCathK_{10} and pHCath(D)K_{10} occurs within 10 min and continues up to 1 hr, as evidenced by the increased elution time of lower molecular weight polymers (Figures 4.3a and 4.3b). A secondary peak simultaneously emerges, eluting around 20 min for both copolymers. This secondary peak is attributed to released peptide after endopeptidase cleavage of the FKFL linker (FLAhxK_{10}/FLAhx(D)K_{10} and respective C-terminally shortened fragments). This is supported by the shifting profile of the secondary peak in the pHCathK_{10} due to exopeptidase activity on the FLAhxK_{10} fragment compared to a stable profile in exopeptidase-resistant pHCath(D)K_{10}. This is also confirmed by MALDI-TOF MS on the reaction mixture (Figure 4.8, Figure 4.1). pH(D)Cath(D)K_{10} shows no degradation over the two hours of enzymatic treatment due to its resistance to peptidases (Figure 4.3c).

4.3.3 Polyplex sizing and colloidal stability

The HPMA-oligolysine copolymers were complexed with plasmid DNA at 3, 4, and 5 N:P ratios to form nanoparticles called "polyplexes." The average hydrodynamic diameters of polyplexes in both water and 150 mM PBS were determined by dynamic light scattering. All the HPMA-oligolysine copolymers formed polyplexes with average hydrodynamic diameter of 120 nm water (Figure 4.4a). PEI and PLL also formed slightly smaller particles around 100 nm in diameter. In PBS, HPMA-oligolysine polyplexes remain relatively stable. The average diameter of polyplexes formed at 5 N:P increased only by 25% to 150 nm. In general, increases in size are seen with decreasing N:P ratios for all materials. In contrast, PEI and PLL particles aggregate in PBS, as indicated by the increased average diameter ranging from 500 nm to over 1 micron.

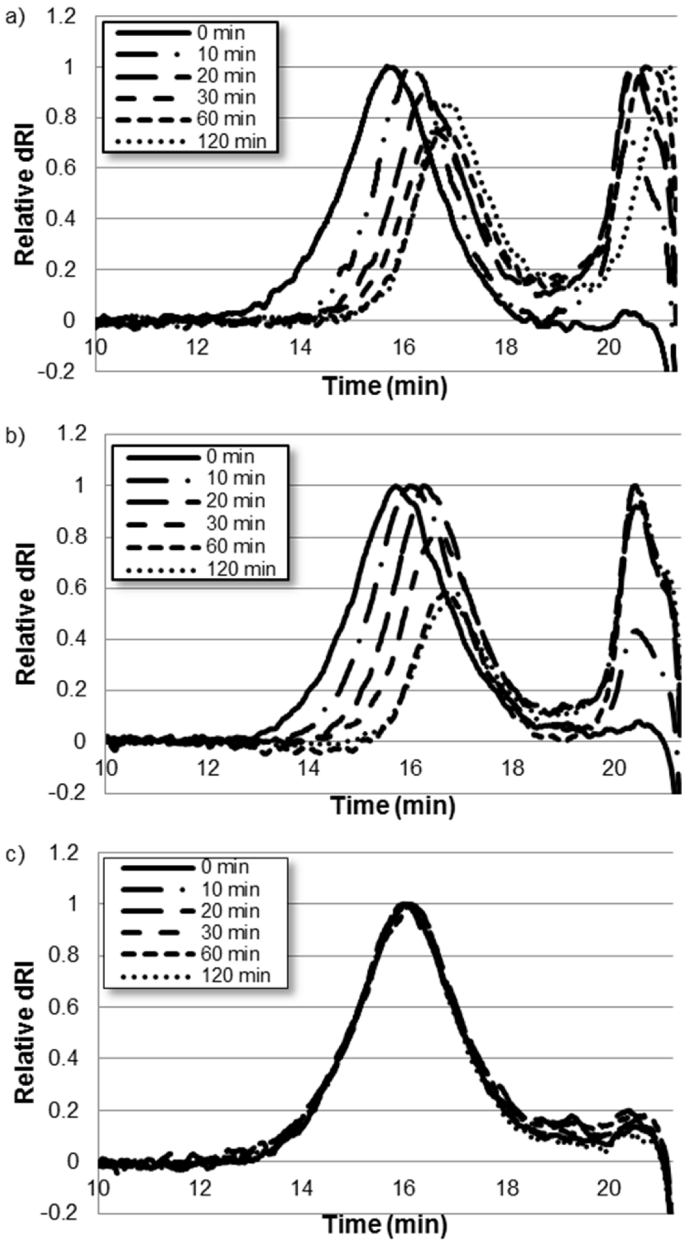

Figure 4.3. Overlaid size exclusion chromatography of cathepsin B degradation of (a) pHCathK_{10}, (b) pHCath(D)K_{10}, and (c) pH(D)Cath(D)K_{10}.

4.3.4 Cathepsin B-mediated polyplex destabilization and unpackaging

The effects of cathepsin B exposure to pHCathK_{10}, pHCath(D)K_{10}, and pH(D)Cath(D)K_{10} polyplexes were determined by monitoring particle size by DLS and DNA condensation by dye

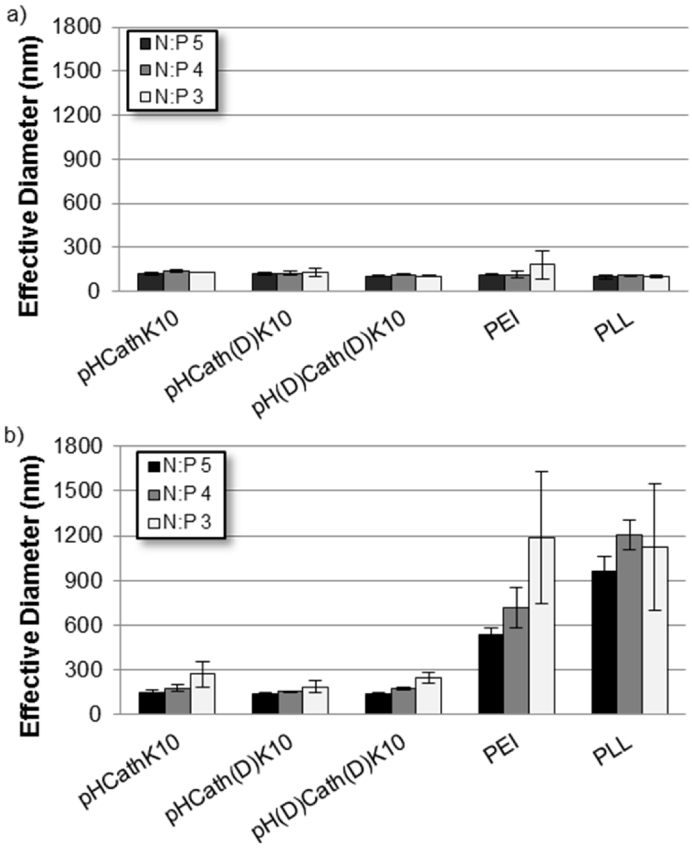

Figure 4.4. DLS sizing of polyplexes in (a) ddH_2O and (b) 150 mM PBS.

quenching assay. Polyplexes were formulated at 4 N:P and particle size measured every 15 min for 8 hrs of cathepsin B treatment (Figure 4.5a). Polyplexes formed with pHCathK_{10} show particle size increases from ~150 nm to about 500 nm over 4hrs before plateauing. pHCath(D)K_{10} shows size increases over 8 hrs up to ~600 nm in diameter. In contrast, pH(D)Cath(D)K_{10} maintain particles ~150 nm in diameter with no observable size change over 8 hrs.

To monitor DNA condensation, plasmid DNA was labeled with the DNA-intercalating fluorophore YOYO-1 before complexation with polymer at 4 N:P. Plasmid condensation results in self-quenching of the YOYO-1 fluorescence due to electronic interactions between nearby YOYO-1 molecules.[13] The YOYO-1 fluorescence, normalized to that of uncomplexed plasmid, is shown in Figure 4.5b as a function of time of cathepsin B exposure. For the first 3 hrs, all polyplex solutions have fluorescence around 10% of free plasmid indicating efficient condensation; starting around 4 hrs, the pHCathK_{10} polyplexes begin to show a trend of increasing fluorescence, up to

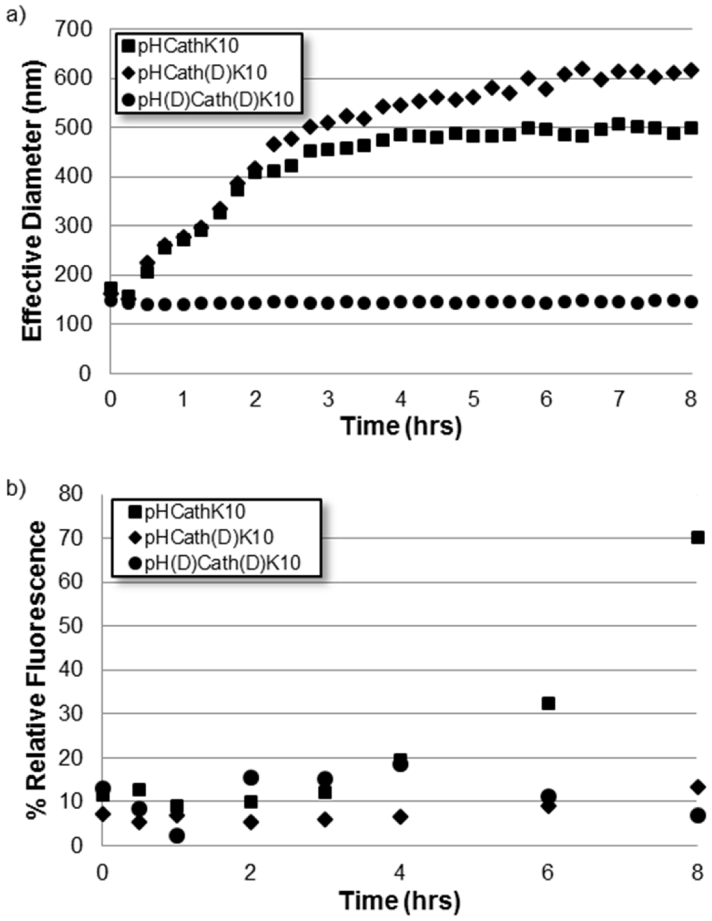

Figure 4.5. Polyplex destabilization and unpackaging of pHCathK_{10}/DNA, pHCath(D)K_{10}/DNA, and pH(D)Cath(D)K_{10}/DNA polyplexes as measured by (a) dynamic light scattering and (b) YOYO-1 fluorescence quenching assay.

70% by 8 hrs. In contrast, pHCath(D)K_{10} and pH(D)Cath(D)K_{10} did not show any significant increase in fluorescence (unpackaging) over 8 hrs.

4.3.5 Plasmid DNA delivery

Transfection efficiency of the polyplexes formed at 3, 4, and 5 N:P was tested using both HeLa and NIH/3T3 cells. The luciferase reporter transgene was used to assess gene delivery efficiency with cytotoxicity evaluated by BCA protein assay (Figure 4.6). In general, the HPMA-oligolysine copolymers transfected with higher efficiency than PLL over all N:P ratios. Efficiencies and trends

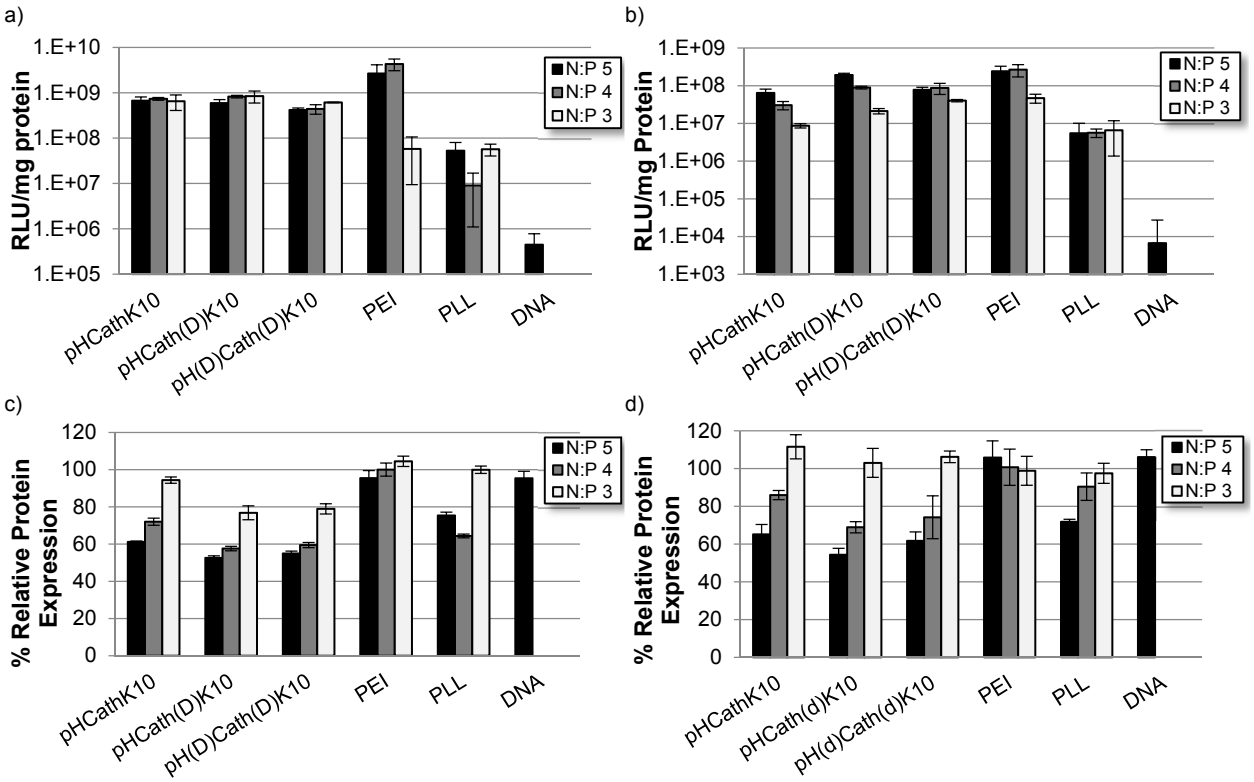

Figure 4.6. Normalized luminescence per mg protein as a measure for transfection efficiency in (a) HeLa and (b) NIH/3T3 cells. Protein expression normalized to untreated cells for (c) HeLa and (d) NIH/3T3 cells.

were cell-line dependent. HeLa cells showed no significant difference in normalized transfection between the 3, 4, and 5 N:P ratios for the copolymers while PEI shows trends of increasing efficiency with increasing N:P ratio; however, copolymer materials are still within an order of magnitude less effective than PEI in transfection efficiency for N:P ratios of 4 and 5. For NIH/3T3 cells, transfection efficiencies of HPMA-oligolysine copolymers were higher with increasing N:P ratios. pHCath(D)K_{10} showed the best transfection of the three copolymers, with normalized luciferase expression comparable to PEI.

4.3.6 Polymer Toxicity

Cytotoxicity of polymers and polyplexes was determined by MTS and BCA assay, respectively. MTS was used to determine the mitochondrial activity in HeLa and NIH/3T3 cells that had been

Table 4.2. Polymer Toxicity

	HeLa		NIH/3T3	
HPMA-oligolysine Copolymer	**IC_{50} (μg/mL)**	**IC_{50} (μM 1°N)**	**IC_{50} (μg/mL)**	**IC_{50} (μM 1°N)**
pHCathK_{10}	16.2	53	29.7	97.3
pHCath(D)K_{10}	16.3	53.5	28.7	94
pH(D)Cath(D)K_{10}	14.3	46.7	30.3	99.3
PEI	4.5	26.4	8.3	48.3
PLL	7.2	34.4	17.9	86.1

treated with the different polymers. A range of polymer concentrations was evaluated in order to determine the IC_{50} value (concentration of polymer for 50% cell survival) for each polymer in amine equivalents. The three synthesized polymers had essentially indistinguishable IC_{50} values with overlapping confidence intervals. Determined IC_{50} values were higher in general for NIH/3T3 cells than HeLa cells and HPMA-oligolysine copolymers were less toxic than both PEI and PLL (Table 4.2).

The BCA assay was conducted to determine the total amount of cellular protein in lysates of transfected cells 48 hrs after transfection. Cell viability was estimated by comparing the protein levels of transfected cells with control untreated cells. Generally, a N:P of 3 was nontoxic in all polymers screened, including PLL and PEI. Toxicity increased at higher N:P ratios for the HPMA-oligolysine polymers and PLL. A trend of decreased toxicity in the pHCathK_{10} polyplexes compared to pHCath(D)K_{10} and pH(D)Cath(D)K_{10} polyplexes for all N:P ratios in both cell types was observed ($p < 0.01$). This trend is confirmed in HeLa cells treated with polyplexes via the MTS assay (Figure 4.7).

4.4 Discussion

In previous work, we reported the synthesis of pendant peptide copolymers with HPMA synthesized by living polymerization and their application for nucleic acid delivery.[34,35] RAFT polymerization of this class of materials resulted in better controlled peptide incorporation, lower polydispersity and decreased cytotoxicity compared to similar polymers prepared by free radical polymerization.[19,36] In previous work, we found optimal polymers contained 20% by mole K_{10} with transfection efficiency of these polymers in cultured cells similar to that of branched PEI.[34]

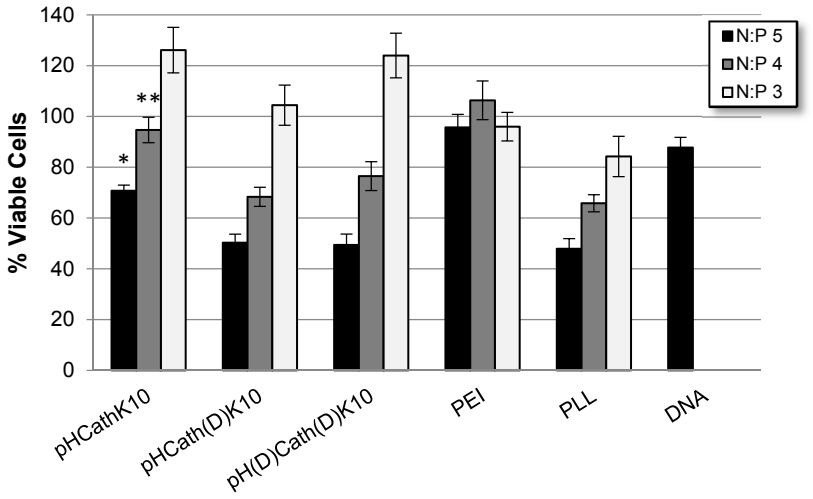

Figure 4.7. Cellular viability of HeLa cells treated with polyplexes measured via MTS assay. $pHCathK_{10}$ are significantly less toxic than $pHCath(D)K_{10}$, $pH(D)Cath(D)K_{10}$, and PLL at *N:P 5 and **N:P 4 ($p < 0.01$).

The goal of this work is to develop peptide-HPMA materials that undergo triggered endosomal-degradation and cargo release in response to specific enzymatic activity. Our strategy is to include an enzymatically cleavable linker between the peptide and the polymer HPMA backbone. Because peptide content in these polymers is high, complete cleavage would result in a 60% reduction in polymer molecular weight and the release of short oligolysine peptides from an HPMA-based polymer backbone.

Cathepsin B was selected as the targeted enzyme for its endo-lysosomal activity. With a papain-like structure, cathepsin B has two domains with the active site cleft along the interface.[37] The peptidyl substrate amino acids are conventionally named ... P2-P1-P1'-P2'..., where the peptide bond is cleaved between P1 and P1' [38]. In this study, the sequence FKFL, where F=P2, K=P1, F=P1' and L=P2', was used as the cathepsin B substrate linkage. Several studies have systematically evaluated various amino acids to optimize the substrate sequence for cathepsin B. These studies show that a phenylalanine in P2 gives the highest cathepsin B hydrolysis rate (k_{cat}/K_m).[39-41] Arginine is the most preferred amino acid for the P1 position, although a lysine in this position is also accepted with about 50% relative activity compared to arginine.[39,40] Dubowchik and Firestone utilized a lysine at P1 in their immunoconjugate BR96-Dox because of potential improved systemic stability compared to arginine.[20,42] Based on this rationale, a lysine at

P1 was also used for this work. Initially a peptide was designed with lysines in the P1' and P2' positions (peptide MaAhxFK$_{10}$) but no specific endopeptidase cleavage was observed with this substrate (data not shown). Because of reports showing that hydrophobic amino acids are preferred in both the P1' and P2' positions, the amino acids F and L were used, respectively. Phenylalanine was used at the P1' position due to reports showing optimal cathepsin B cleavage in sequences with this amino acid at P1'.[40,43] Finally, a six carbon linker (6-aminohexanoic acid) was included flanking both sides of the FKFL to provide spacers for the cathepsin substrate sequence both from the polymer backbone and the cationic K_{10} nucleic acid binding domain in attempt to provide better access to cathepsin B. The resulting peptide, MaAhxFKFLAhxK$_{10}$, was shown to be recognized by cathepsin B and cleaved within 15 min (Figure 4.1).

Cathepsin B exhibits both specific endopeptidase and exopeptidase activity, with the former dominating at pH 6-7 and the latter optimal at pH < 5.0.[44] Three peptides were therefore synthesized: MaAhxFKFLAhxK$_{10}$, which is susceptible to both endopeptidase and exopeptidase activity; MaAhxFKFLAhx(D)K$_{10}$, which is susceptible only to endopeptidase activity; and MaAhx(D)FKFLAhx(D)K$_{10}$, which is protease resistant. Sensitivity of these peptides to cathepsin B-mediated proteolysis was evaluated at pH 5.0. This pH was selected because it is representative of the late endosome milieu where both endopeptidase and exopeptidase activity would be expected.[45] At this pH, the endopeptidase activity is about 15% of optimum activity at pH ~6.2 while exopeptidase activity is about 80% of optimal activity. Degradation of the three peptides by cathepsin B followed expected patterns with faster kinetics for endopeptidase activity compared to exopeptidase activity (Figure 4.1).

Ideally, the peptide-based polymers would remain stable during circulation to protect nucleic acids from serum nucleases. In addition to nucleases, serum contains many peptidases, such as dipeptidyl peptidases and endopeptidases.[46-49] To assess serum stability, peptides were incubated with freshly isolated mouse serum (Figure 4.2). Degradation of MaAhxFKFLAhxK$_{10}$ was complete by 1 hr, resulting in the shortened MaAhxFKFLAhxK fragment. In contrast, full length MaAhxFKFLAhx(D)K$_{10}$ is detected even after a 4 hr serum incubation, although some endopeptidase degraded product (1672 Da = FLAhx(D)K$_{10}$) is observed after 1 hr. It should be noted that in the presence of cathepsin B, endopeptidase degradation of this peptide is observed within 5 min. The analogous FLAhxK$_{10}$ fragment from MaAhxFKFLAhxK$_{10}$ likely is rapidly degraded by carboxypeptidases and thus is not detected on MALDI. The MaAhxFKFLAhx(D)K$_{10}$

peptide is a promising building block for polymers used in *in vivo* applications requiring specific intracellular degradation. While stability in murine serum may not correlate to human serum, high homology in the degradomes (> 80% strict orthologues) between mice and humans suggests information regarding enzymatic substrate specificity may be gained from these serum studies.[50]

Copolymerization of the methacrylated peptides with HPMA by RAFT polymerization yielded polymers with narrow polydispersity, expected composition, and near-target molecular weights (Table 4.1). Cathepsin B-mediated degradation of polymers was evaluated at pH 5.0 by size exclusion chromatography (Figure 4.3). Accessibility of cathepsin B to linker sites incorporated in dendrimers has been shown to be restricted due to steric hindrance for some systems.[51] However, synthesized pHCathK$_{10}$ and pHCath(D)K$_{10}$ polymers susceptible to cathepsin B cleavage show rapid reduction in size within 10 min and complete cleavage of oligolysine side chains from the polymer backbone within one hour, leading to a theoretical reduction of ~60% in molecular weight. The kinetics of proteolysis for the peptide and polymers are similar as seen by comparing peptide monomer (Figure 4.1) and copolymer (Figure 4.8) fragmentation. In comparison, pH(D)Cath(D)K$_{10}$ shows complete enzymatic resistance. HPMA-*co*-MaAhxK$_{10}$ copolymers were also treated with cathepsin B and the observed MW shift over 4 hrs is comparable to 10 min with pHCathK$_{10}$ (data not shown). In addition to rapid copolymer size reduction, labile side-chains can potentially increase accessibility of peptide side-chains for other peptidases; this is observed in the peptide peak (~20 min) released by degradation of pHCathK$_{10}$ but not pHCath(D)K$_{10}$ (Figures 4.3a and 4.3b).

All polymers efficiently complexed DNA and formed polyplexes with diameters ~100-200 nm that are stable in physiological salt concentrations (Figure 4.4). While poly-(L)-lysine-based polyplexes are not stable in 150 mM PBS, inclusion of HPMA in the backbone of the cationic polymer prevents salt-induced aggregation.[34,36,52] Controlled polyplex unpackaging and DNA release after cellular internalization is integral to efficient gene delivery and expression.[10] Effective delivery requires extracellular and endosomal stability with cytosolic unpackaging for eventual expression. Cathepsin B-mediated unpackaging of polyplexes formed from pHCathK$_{10}$, pHCath(D)K$_{10}$ and pH(D)Cath(D)K$_{10}$ was studied by dynamic light scattering and YOYO-1 fluorescence quenching assay. pHCathK$_{10}$ and pHCath(D)K$_{10}$ polyplexes both show increasing particle size over time while pH(D)Cath(D)K$_{10}$ particles remain unchanged, suggesting enzymatically-driven polyplex destabilization. DNA packaging was also assessed through YOYO-

1 fluorescence quenching assay, which monitors DNA decondensation as YOYO-1 fluorescence is restored when these molecules are not in close proximity to each other. Decondensation of DNA from polyplexes is only observed with pHCathK$_{10}$ and not pHCath(D)K$_{10}$ or pHK10 (data not shown). Oligolysines as short as 8-mers are able to condense DNA,[24,53] so despite cleavage of oligolysine side chains from the HPMA backbone, oligolysine fragments may remain able to form relatively large and unstable, but intact, polyplexes. Since oligo-(D)-lysine is resistant to further degradation, it will remain bound to DNA thereby keeping it packaged; in contrast, oligo-(L)-lysine, subject to exopeptidase degradation, will eventually release DNA upon further degradation. This is supported by the observation that YOYO-1 fluorescence from polyplexes formed by oligo-(L)-lysine increases with time when incubated with cathepsin B but polyplexes formed by oligo-(D)-lysine do not (data not shown).

While reducible HPMA-oligolysine copolymers have significantly lower transfection efficiency compared to their non-degradable counterparts,[19] the enzymatically-cleavable polymers described here (pHCathK$_{10}$ and pHCath(D)K$_{10}$) have similar transfection efficiencies to non-degradable pH(D)Cath(D)K$_{10}$ in cultured cells (Figures 4.6a and 4.6b). Endosomal/lysosomal unpackaging may not increase transfection without compartmental escape for cytosolic release. Transfection was also evaluated in serum conditions (data not shown). Reduced transfection efficiency compared to serum-free transfections was observed, as reported previously for similar polymers.[19] No significant difference in transfection efficiency was noted between the three polymers even in serum conditions (data not shown), possibly because of altered protease activities in heat-inactivated serum. Cationic polymers have been implicated in toxicity through both necrotic and apoptotic routes.[12,26,54,55] Electrostatic interactions with the plasma membrane cause permeabilization and pore formation, triggering cellular efflux of cytosolic contents and necrosis.[54] Compromised mitochondrial and lysosomal membranes lead to release of pro-apoptotic factors cytochrome c and cathepsins, respectively, initiating apoptotic cascades.[56,57] Degradation of cationic polymers prior to cytosolic release or endo-lysosomal fusion can potentially decrease induction of apoptosis and reduce cytotoxicity. The relative toxicity pHCathK$_{10}$, pHCath(D)K$_{10}$ and pH(D)Cath(D)K$_{10}$ was evaluated in HeLa and NIH/3T3 cells using the MTS assay (Table 4.2). Results suggest similar toxicity between the three synthesized polymers regardless of enzymatic susceptibility. One possible explanation is that for free polymer the primary route of toxicity might be through plasma membrane disruption and permeabilization as implicated for PEI.[12] Therefore,

intracellularly-controlled degradation will not significantly affect toxicity. This hypothesis is supported by the observation that polyplexes formed with pHCathK_{10} are less toxic than pHCath(D)K_{10} and pH(D)Cath(D)K_{10} polyplexes at all tested charge ratios and in both HeLa and NIH/3T3 cells (Figures 4.6c and 4.6d, Figure 4.7). This result was confirmed both by protein content analysis and MTS assay of cells exposed to polyplexes. In the polyplex form, a reduced amount of free polymer is available to disrupt the cellular membrane and the effect of intracellular degradation on cytotoxicity may be more pronounced. pHCathK_{10} can be degraded additionally by exopeptidases, allowing for accelerated degradation and reduced toxicity compared to pHCath(D)K_{10}. Still, substantial toxicity is still observed with the pHCathK_{10} polyplexes formed at higher N:P ratios. One potential approach that may further reduce toxicity of future generations of these polymers is to decrease the cationic charge density by including non-charged amino acids in the nucleic acid binding sequence. High charge density has been correlated with cytotoxicity for several cationic polymers.[12,58,59]

4.5 Conclusions

In summary, peptide-based polycations that are susceptible to cathepsin B-catalyzed degradation were synthesized. The polymers were shown to undergo rapid degradation in the presence of cathepsin B. When packaged into nanoparticles by complexation with nucleic acids, linkers remain sufficiently available to fit into catalytic pockets of endopeptidases and be specifically degraded. Thus, we have demonstrated triggered nanoparticle degradation by a selective enzymatic mechanism.

4.6 Acknowledgments

This work was supported by NIH/NINDS 1R01 NS064404, NSF DMR 0706647, and the Center for Intracellular Delivery of Biologics (Life Sciences Discovery Fund Grant 2496490). We thank Profs. Anthony Convertine and Patrick Stayton for generous donation of the ECT chain transfer agent. We also thank Drs. Peter Senter and Svetlana Dororina of Seattle Genetics for their advice in linker development.

4.7 References

(1) Pack, D. W.; Hoffman, A. S.; Pun, S.; Stayton, P. S.: Design and development of polymers for gene delivery. *Nat Rev Drug Discov* **2005**, *4*, 581-593.

(2) Chollet, P.; Favrot, M. C.; Hurbin, A.; Coll, J. L.: Side-effects of a systemic injection of linear polyethylenimine-DNA complexes. *J Gene Med* **2002**, *4*, 84-91.

(3) Ward, C. M.; Read, M. L.; Seymour, L. W.: Systemic circulation of poly(L-lysine)/DNA vectors is influenced by polycation molecular weight and type of DNA: differential circulation in mice and rats and the implications for human gene therapy. *Blood* **2001**, *97*, 2221-2229.

(4) Burke, R. S.; Pun, S. H.: Extracellular barriers to in vivo PEI and PEGylated PEI polyplex-mediated gene delivery to the liver. *Bioconjug Chem* **2008**, *19*, 693-704.

(5) Grigsby, C. L.; Leong, K. W.: Balancing protection and release of DNA: tools to address a bottleneck of non-viral gene delivery. *J R Soc Interface* **2010**, *7 Suppl 1*, S67-82.

(6) Luten, J.; van Nostrum, C. F.; De Smedt, S. C.; Hennink, W. E.: Biodegradable polymers as non-viral carriers for plasmid DNA delivery. *J Control Release* **2008**, *126*, 97-110.

(7) Fischer, D.; Osburg, B.; Petersen, H.; Kissel, T.; Bickel, U.: Effect of poly(ethylene imine) molecular weight and pegylation on organ distribution and pharmacokinetics of polyplexes with oligodeoxynucleotides in mice. *Drug Metab Dispos* **2004**, *32*, 983-992.

(8) Mullen, P. M.; Lollo, C. P.; Phan, Q. C.; Amini, A.; Banaszczyk, M. G.; Fabrycki, J. M.; Wu, D.; Carlo, A. T.; Pezzoli, P.; Coffin, C. C.; Carlo, D. J.: Strength of conjugate binding to plasmid DNA affects degradation rate and expression level in vivo. *Biochim Biophys Acta* **2000**, *1523*, 103-110.

(9) Nishikawa, M.; Takemura, S.; Takakura, Y.; Hashida, M.: Targeted delivery of plasmid DNA to hepatocytes in vivo: optimization of the pharmacokinetics of plasmid DNA/galactosylated poly(L-lysine) complexes by controlling their physicochemical properties. *J Pharmacol Exp Ther* **1998**, *287*, 408-415.

(10) Schaffer, D. V.; Fidelman, N. A.; Dan, N.; Lauffenburger, D. A.: Vector unpacking as a potential barrier for receptor-mediated polyplex gene delivery. *Biotechnol Bioeng* **2000**, *67*, 598-606.

(11) de Wolf, H. K.; de Raad, M.; Snel, C.; van Steenbergen, M. J.; Fens, M. H.; Storm, G.; Hennink, W. E.: Biodegradable poly(2-dimethylamino ethylamino)phosphazene for in vivo gene delivery to tumor cells. Effect of polymer molecular weight. *Pharm Res* **2007**, *24*, 1572-1580.

(12) Fischer, D.; Li, Y.; Ahlemeyer, B.; Krieglstein, J.; Kissel, T.: In vitro cytotoxicity testing of polycations: influence of polymer structure on cell viability and hemolysis. *Biomaterials* **2003**, *24*, 1121-1131.

(13) Breunig, M.; Lungwitz, U.; Liebl, R.; Goepferich, A.: Breaking up the correlation between efficacy and toxicity for nonviral gene delivery. *P Natl Acad Sci USA* **2007**, *104*, 14454-14459.

(14) Mintzer, M. A.; Simanek, E. E.: Nonviral vectors for gene delivery. *Chem Rev* **2009**, *109*, 259-302.

(15) Meng, F. H.; Hennink, W. E.; Zhong, Z.: Reduction-sensitive polymers and bioconjugates for biomedical applications. *Biomaterials* **2009**, *30*, 2180-2198.

(16) Lynn, D. M.; Langer, R.: Degradable poly(beta-amino esters): synthesis, characterization, and self-assembly with plasmid DNA. *J Am Chem Soc* **2000**, *122*, 10761-10768.

(17) Meister, A.; Anderson, M. E.: Glutathione. *Annu Rev Biochem* **1983**, *52*, 711-760.

(18) Sun, W. C.; Davis, P. B.: Reducible DNA nanoparticles enhance in vitro gene transfer via an extracellular mechanism. *J Control Release* **2010**, *146*, 118-127.

(19) Shi, J.; Johnson, R. N.; Schellinger, J. G.; Carlson, P. M.; Pun, S. H.: Reducible HPMA-co-oligolysine copolymers for nucleic acid delivery. *Int J Pharm* **2011**, *427*, 113-122.

(20) Dubowchik, G. M.; Firestone, R. A.; Padilla, L.; Willner, D.; Hofstead, S. J.; Mosure, K.; Knipe, J. O.; Lasch, S. J.; Trail, P. A.: Cathepsin B-labile dipeptide linkers for lysosomal release of doxorubicin from internalizing immunoconjugates: model studies of enzymatic drug release and antigen-specific in vitro anticancer activity. *Bioconjug Chem* **2002**, *13*, 855-869.

(21) Hortin, G. L.; Warshawsky, I.; Laude-Sharp, M.: Macromolecular chromogenic substrates for measuring proteinase activity. *Clin Chem* **2001**, *47*, 215-222.

(22) Doronina, S. O.; Toki, B. E.; Torgov, M. Y.; Mendelsohn, B. A.; Cerveny, C. G.; Chace, D. F.; DeBlanc, R. L.; Gearing, R. P.; Bovee, T. D.; Siegall, C. B.; Francisco, J. A.; Wahl, A. F.; Meyer, D. L.; Senter, P. D.: Development of potent monoclonal antibody auristatin conjugates for cancer therapy. *Nat Biotechnol* **2003**, *21*, 778-784.

(23) Levesque, S. G.; Shoichet, M. S.: Synthesis of enzyme-degradable, peptide-cross-linked dextran hydrogels. *Bioconjug Chem* **2007**, *18*, 874-885.

(24) Wang, Y.; Mangipudi, S. S.; Canine, B. F.; Hatefi, A.: A designer biomimetic vector with a chimeric architecture for targeted gene transfer. *J Control Release* **2009**, *137*, 46-53.

(25) Grosse, S. M.; Tagalakis, A. D.; Mustapa, M. F.; Elbs, M.; Meng, Q. H.; Mohammadi, A.; Tabor, A. B.; Hailes, H. C.; Hart, S. L.: Tumor-specific gene transfer with receptor-mediated nanocomplexes modified by polyethylene glycol shielding and endosomally cleavable lipid

and peptide linkers. *FASEB J* **2010**, *24*, 2301-2313.

(26) Hunter, A. C.; Moghimi, S. M.: Cationic carriers of genetic material and cell death: a mitochondrial tale. *Biochim Biophys Acta* **2010**, *1797*, 1203-1209.

(27) Authier, F.; Metioui, M.; Bell, A. W.; Mort, J. S.: Negative regulation of epidermal growth factor signaling by selective proteolytic mechanisms in the endosome mediated by cathepsin B. *J Biol Chem* **1999**, *274*, 33723-33731.

(28) Blum, J. S.; Fiani, M. L.; Stahl, P. D.: Proteolytic cleavage of ricin A chain in endosomal vesicles. Evidence for the action of endosomal proteases at both neutral and acidic pH. *J Biol Chem* **1991**, *266*, 22091-22095.

(29) Lautwein, A.; Kraus, M.; Reich, M.; Burster, T.; Brandenburg, J.; Overkleeft, H. S.; Schwarz, G.; Kammer, W.; Weber, E.; Kalbacher, H.; Nordheim, A.; Driessen, C.: Human B lymphoblastoid cells contain distinct patterns of cathepsin activity in endocytic compartments and regulate MHC class II transport in a cathepsin S-independent manner. *J Leukoc Biol* **2004**, *75*, 844-855.

(30) Kopecek, J.; Kopeckova, P.; Minko, T.; Lu, Z.: HPMA copolymer-anticancer drug conjugates: design, activity, and mechanism of action. *Eur J Pharm Biopharm* **2000**, *50*, 61-81.

(31) Sutherland, M. S.; Sanderson, R. J.; Gordon, K. A.; Andreyka, J.; Cerveny, C. G.; Yu, C.; Lewis, T. S.; Meyer, D. L.; Zabinski, R. F.; Doronina, S. O.; Senter, P. D.; Law, C. L.; Wahl, A. F.: Lysosomal trafficking and cysteine protease metabolism confer target-specific cytotoxicity by peptide-linked anti-CD30-auristatin conjugates. *J Biol Chem* **2006**, *281*, 10540-10547.

(32) Ulbrich, K.; Subr, V.; Strohalm, J.; Plocova, D.; Jelinkova, M.; Rihova, B.: Polymeric drugs based on conjugates of synthetic and natural macromolecules. I. Synthesis and physico-

chemical characterisation. *J Control Release* **2000**, *64*, 63-79.

(33) Bidlingmeyer, B. A.; Cohen, S. A.; Tarvin, T. L.: Rapid analysis of amino acids using pre-column derivatization. *J Chromatogr* **1984**, *336*, 93-104.

(34) Johnson, R. N.; Chu, D. S.; Shi, J.; Schellinger, J. G.; Carlson, P. M.; Pun, S. H.: HPMA-oligolysine copolymers for gene delivery: optimization of peptide length and polymer molecular weight. *J Control Release* **2011**, *144*, 303-311.

(35) Johnson, R. N.; Burke, R. S.; Convertine, A. J.; Hoffman, A. S.; Stayton, P. S.; Pun, S. H.: Synthesis of statistical copolymers containing multiple functional peptides for nucleic acid delivery. *Biomacromolecules* **2010**, *11*, 3007-3013.

(36) Burke, R. S.; Pun, S. H.: Synthesis and characterization of biodegradable HPMA-oligolysine copolymers for improved gene delivery. *Bioconjug Chem* **2010**, *21*, 140-150.

(37) Guha, S.; Padh, H.: Cathepsins: fundamental effectors of endolysosomal proteolysis. *Indian J Biochem Biophys* **2008**, *45*, 75-90.

(38) Schechter, I.; Berger, A.: On the size of the active site in proteases. I. Papain. *Biochem Biophys Res Commun* **1967**, *27*, 157-162.

(39) Cezari, M. H.; Puzer, L.; Juliano, M. A.; Carmona, A. K.; Juliano, L.: Cathepsin B carboxydipeptidase specificity analysis using internally quenched fluorescent peptides. *Biochem J* **2002**, *368*, 365-369.

(40) Cotrin, S. S.; Puzer, L.; de Souza Judice, W. A.; Juliano, L.; Carmona, A. K.; Juliano, M. A.: Positional-scanning combinatorial libraries of fluorescence resonance energy transfer peptides to define substrate specificity of carboxydipeptidases: assays with human cathepsin B. *Anal Biochem* **2004**, *335*, 244-252.

(41) Hasnain, S.; Hirama, T.; Tam, A.; Mort, J. S.: Characterization of recombinant rat cathepsin B and nonglycosylated mutants expressed in yeast. New insights into the pH dependence of cathepsin B-catalyzed hydrolyses. *J Biol Chem* **1992**, *267*, 4713-4721.

(42) Dubowchik, G. M.; Firestone, R. A.: Cathepsin B-sensitive dipeptide prodrugs. 1. A model study of structural requirements for efficient release of doxorubicin. *Bioorg Med Chem Lett* **1998**, *8*, 3341-3346.

(43) Stachowiak, K.; Tokmina, M.; Karpinska, A.; Sosnowska, R.; Wiczk, W.: Fluorogenic peptide substrates for carboxydipeptidase activity of cathepsin B. *Acta Biochim Pol* **2004**, *51*, 81-92.

(44) Polgar, L.; Csoma, C.: Dissociation of ionizing groups in the binding cleft inversely controls the endo- and exopeptidase activities of cathepsin B. *J Biol Chem* **1987**, *262*, 14448-14453.

(45) Killisch, I.; Steinlein, P.; Romisch, K.; Hollinshead, R.; Beug, H.; Griffiths, G.: Characterization of early and late endocytic compartments of the transferrin cycle. Transferrin receptor antibody blocks erythroid differentiation by trapping the receptor in the early endosome. *J Cell Sci* **1992**, *103 (Pt 1)*, 211-232.

(46) Durinx, C.; Lambeir, A. M.; Bosmans, E.; Falmagne, J. B.; Berghmans, R.; Haemers, A.; Scharpe, S.; De Meester, I.: Molecular characterization of dipeptidyl peptidase activity in serum: soluble CD26/dipeptidyl peptidase IV is responsible for the release of X-Pro dipeptides. *Eur J Biochem* **2000**, *267*, 5608-5613.

(47) Erdos, E. G.; Skidgel, R. A.: Neutral endopeptidase 24.11 (enkephalinase) and related regulators of peptide hormones. *FASEB J.* **1989**, *3*, 145-151.

(48) Mentlein, R.; Gallwitz, B.; Schmidt, W. E.: Dipeptidyl-peptidase IV hydrolyses gastric inhibitory polypeptide, glucagon-like peptide-1(7-36)amide, peptide histidine methionine and is responsible for their degradation in human serum. *Eur J Biochem* **1993**, *214*, 829-835.

(49) Wang, L. H.; Ahmad, S.; Benter, I. F.; Chow, A.; Mizutani, S.; Ward, P. E.: Differential processing of substance P and neurokinin A by plasma dipeptidyl(amino)peptidase IV, aminopeptidase M and angiotensin converting enzyme. *Peptides* **1991**, *12*, 1357-1364.

(50) Puente, X. S.; Sanchez, L. M.; Overall, C. M.; Lopez-Otin, C.: Human and mouse proteases: a comparative genomic approach. *Nat Rev Genet* **2003**, *4*, 544-558.

(51) Etrych, T.; Strohalm, J.; Chytil, P.; Cernoch, P.; Starovoytova, L.; Pechar, M.; Ulbrich, K.: Biodegradable star HPMA polymer conjugates of doxorubicin for passive tumor targeting. *Eur J Pharm Sci* **2011**, *42*, 527-539.

(52) Kasuya, Y.; Lu, Z. R.; Kopeckova, P.; Minko, T.; Tabibi, S. E.; Kopecek, J.: Synthesis and characterization of HPMA copolymer-aminopropylgeldanamycin conjugates. *J Control Release* **2001**, *74*, 203-211.

(53) Mann, A.; Thakur, G.; Shukla, V.; Ganguli, M.: Peptides in DNA delivery: current insights and future directions. *Drug Discov Today* **2008**, *13*, 152-160.

(54) Hong, S.; Leroueil, P. R.; Janus, E. K.; Peters, J. L.; Kober, M. M.; Islam, M. T.; Orr, B. G.; Baker, J. R., Jr.; Banaszak Holl, M. M.: Interaction of polycationic polymers with supported lipid bilayers and cells: nanoscale hole formation and enhanced membrane permeability. *Bioconjug Chem* **2006**, *17*, 728-734.

(55) Moghimi, S. M.; Symonds, P.; Murray, J. C.; Hunter, A. C.; Debska, G.; Szewczyk, A.: A two-stage poly(ethylenimine)-mediated cytotoxicity: implications for gene transfer/therapy. *Mol Ther* **2005**, *11*, 990-995.

(56) Klemm, A. R.; Young, D.; Lloyd, J. B.: Effects of polyethyleneimine on endocytosis and lysosome stability. *Biochem Pharmacol* **1998**, *56*, 41-46.

(57) Droga-Mazovec, G.; Bojic, L.; Petelin, A.; Ivanova, S.; Romih, R.; Repnik, U.; Salvesen, G.

S.; Stoka, V.; Turk, V.; Turk, B.: Cysteine cathepsins trigger caspase-dependent cell death through cleavage of bid and antiapoptotic Bcl-2 homologues. *J Biol Chem* **2008**, *283*, 19140-19150.

(58) Allen, M. H.; Green, M. D.; Getaneh, H. K.; Miller, K. M.; Long, T. E.: Tailoring charge density and hydrogen bonding of imidazolium copolymers for efficient gene delivery. *Biomacromolecules* **2011**, *12*, 2243-2250.

(59) Hwang, S. J.; Bellocq, N. C.; Davis, M. E.: Effects of structure of beta-cyclodextrin-containing polymers on gene delivery. *Bioconjug Chem* **2001**, *12*, 280-290.

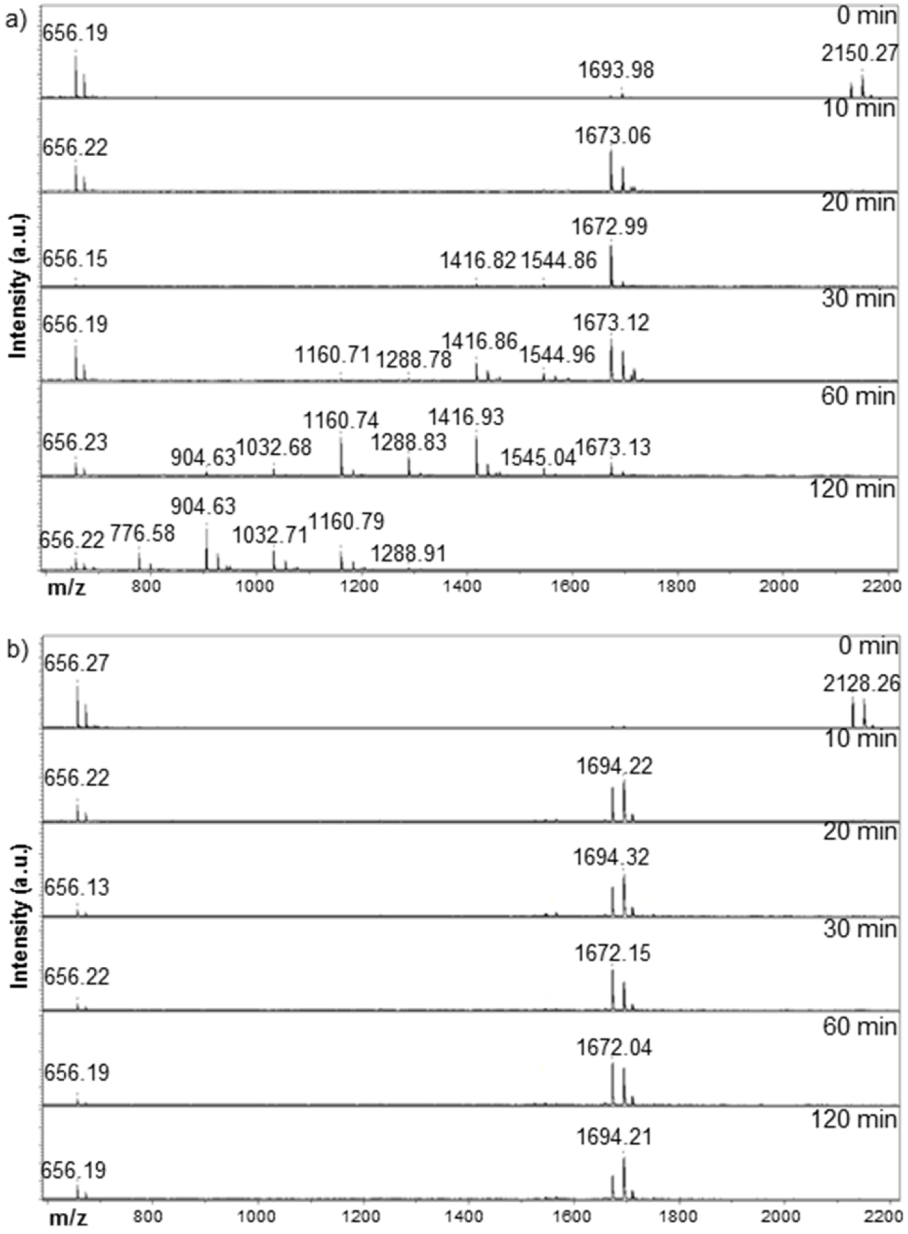

Figure 4.8. MALDI-TOF MS time-point study of cathepsin B-mediated fragmentation of (a) pHCathK_{10} and (b) pHCath(D)K_{10}.

Chapter 5

MMP9-SENSITIVE POLYMERS FOR ENVIRONMENTALLY-RESPONSIVE BIVALIRUDIN RELEASE AND THROMBIN INHIBITION

David S.H. Chu, Drew L. Sellers, Michael J. Bocek, Amanda E. Fischedick, Philip J. Horner, Suzie H. Pun

Abstract

MMP9-responsive bivalirudin-HPMA copolymers were synthesized for direct, local administration in rat spinal cord contusion injury models. Polymer-conjugated bivalirudin peptides maintained activity while demonstrating enzyme-mediated release upon MMP9 exposure and prolonged release from hyaluronic acid/methylcellulose (HAMC) hydrogels compared to free bivalirudin peptide. Localized administration of bivalirudin copolymers in vivo at the site of rat spinal cord injury decreased cellular proliferation and astrogliosis, suggesting the bivalirudin copolymer and HAMC hydrogel system are a promising therapeutic intervention for reducing immediate inflammatory responses and long term scarring.[1]

---

[1]Reproduced from Chu et al (2014). *Biomater Sci* **3**:41-45 with permission from he Royal Society of Chemistry.

5.1 Introduction

Spinal cord injuries (SCI) comprise a significant percentage of debilitating injuries, with over 250,000 Americans suffering from SCI and 12,000 new cases annually.[1] Following acute SCI from blunt trauma, thrombin, a serine protease and key component of the coagulation cascade, rapidly increases from basal picomolar levels[2] at injury sites and elevated levels are sustained for several days due to expression by endothelial and astrocytic cells.[3,4] Thrombin administered to healthy rat brains induces histological changes resembling inflammation and glial scarring,[5] indicating it may impede recovery of damaged neural networks.

Modulation of thrombin activity post-SCI is therefore a potential method for improving outcome.[3] Indeed, thrombin inhibition immediately following SCI has been shown to improve both histological and functional recovery.[6] Systemic administration of recombinant thrombomodulin (rTM), a regulator of thrombin activity, reduced glial scarring and improved locomotor recovery in rats.[7] However, systemic administration of thrombin inhibitors, particularly in a polytrauma patient, is associated with adverse outcomes. A sustained delivery of thrombin inhibitors localized to the injury site is likely to be more effective and safe.

Injectable hydrogels, typically formed from polymers that undergo a temperature transition near body temperature, have been investigated as delivery depots in the central nervous system (CNS). The Shoichet group has pioneered the use of natural biopolymer hydrogel formulations composed of hyaluronic acid and methylcellulose (HAMC) in the CNS. These materials exhibit low cellular adhesion, good biocompatibility, and tunable mechanical properties.[8] However, peptide release from hydrogels typically occurs within hours due to their low molecular weight.[9]

Bivalirudin is a clinically approved, 20-amino acid direct thrombin inhibitor.[10] N-terminal residues reversibly bind the catalytic pocket while C-terminal residues bind the fibrinogen-binding domain of thrombin. Bivalirudin is an attractive drug due to its low immunogenicity and large therapeutic window; however, poor proteolytic stability and small size results in rapid clearance. To improve peptide stability and local retention, peptides can be grafted to higher molecular weight polymers. Proteins loaded in HAMC hydrogels are released over two days,[11] providing ideal release kinetics for protein-sized bivalirudin polymers.

In this work, we developed a material formulation for localized and prolonged bivalirudin delivery following SCI and demonstrated reduced proliferation and decreased gliosis in rats treated

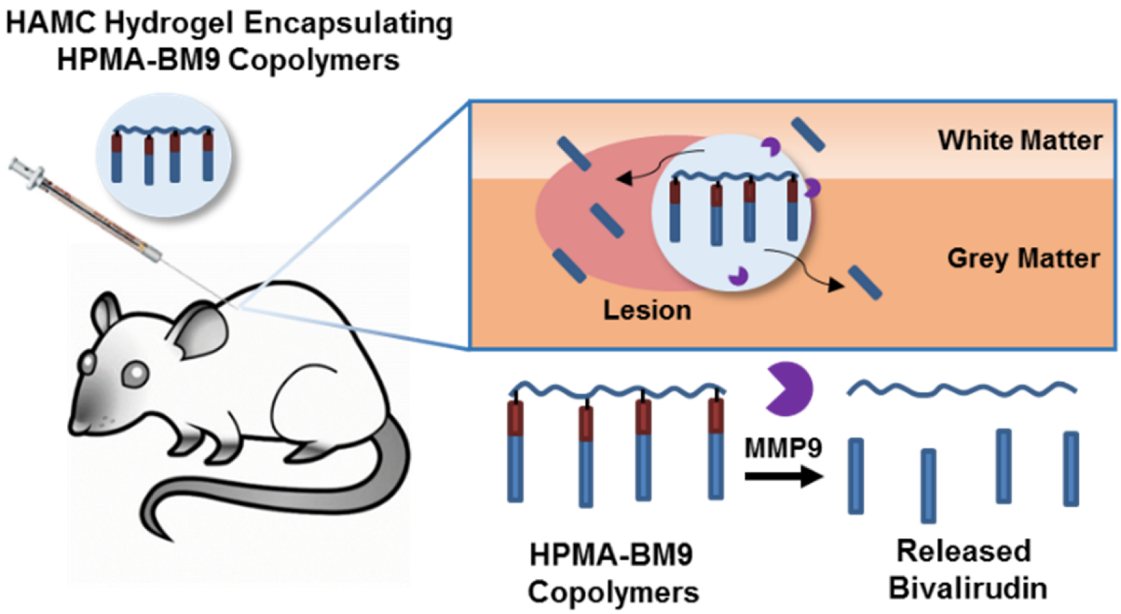

Figure 5.1. Localized depot delivery of bivalirudin through HPMA-BM9-loaded thermoresponsive hydrogels.

with these bivalirudin-release depots. Polymers displaying pendant bivalirudin were synthesized by reversible addition-fragmentation chain transfer (RAFT) polymerization of an HPMA-co-APMA polymer backbone followed by grafting of the BM9 peptide, comprised of bivalirudin fused to a protease substrate sequence for targeted proteolytic release from the polymer. Three peptide-HPMA copolymers (DP200, DP300, DP400) of varying molecular weight but comparable peptide incorporation were synthesized. The polymers were then loaded in HAMC hydrogels for localized delivery. We hypothesized that hydrogel-encapsulated, enzymatically-responsive bivalirudin polymers administered locally to the spinal cord would (1) improve bivalirudin stability and prolong residence time in the tissue through sustained hydrogel release and (2) allow for environmentally-responsive bivalirudin cleavage from polymer for enhanced tissue penetration at the site of injury after release from the hydrogel (Figure 5.1).

5.2 Materials and methods

5.2.1 Materials

N-(2-hydroxypropyl) methacrylamide (HPMA) and N-(3-aminopropyl) methacrylamide hydrochloride (APMA) were purchased from Polysciences (Warrington, PA). The initiator VA-044 was purchased from Wako Chemicals (Richmond, VA). Bivalirudin-MMP9 substrate (BM9) peptide (Ac-(D)FPRPGGGGNGDFEEIPEEYLGGGPRQITAGGC-CONH2) was synthesized by Elim Biopharmaceuticals (Hayward, CA) at >95% purity, bivalirudin peptide (Ac-(D)FPRPGGGGNGDFEEIPEEYL-COOH) was bought from Bachem (Torrance, CA) at > 98% purity, succinimidyl-4-(N-maleimidomethyl)cyclohexane-1-carboxylate (SMCC) crosslinker from Pierce (Rockford, IL), hyaluronan (1.8 MDa) from Lifecore Biomedical (Chaska, MN), and methylcellulose (4000 cP) from Sigma-Aldrich (St. Louis, MO). All other materials were reagent grade or better and were purchased from Sigma-Aldrich unless otherwise stated.

5.2.2 MMP9-mediated cleavage of BM9

The susceptibility of bivalirudin-MMP9 substrate peptide BM9 to MMP-9-mediated enzymatic cleavage was first evaluated in vitro. BM9 peptide solution (25 µL, 3.52 mg/mL) in Reaction Buffer A (500 mM TrisHCl, 5 mM CaCl2, 200mM NaCl, pH 7.7) was mixed with 5 µL of 0.1 mg/mL pre-activated MMP9 stock solution (EMD Millipore, Billerica, MA) and incubated at 37 ºC. At various time points, a 3 µL aliquot of the reaction solution was removed and mixed with 3 µL of 5 mM 1,10-phenanthroline to stop the enzymatic digest. Samples were analyzed using RP-HPLC on a Jupiter Proteo 90A analytical column (Phenomenex, Torrance, CA) following the fluorescence of tryptophan (ex/em 270/330 nm), and peptide fragmentation was determined by MALDI-TOF MS.

5.2.3 HPMA-co-APMA copolymer synthesis

Three polymers were synthesized: DP200, DP300, and DP400. Each polymer was synthesized with target degree of polymerization (DP) of 200, 300, and 400, respectively, with 10% mole feed of APMA. Monomers were dissolved in acetate buffer (1 M, pH 5.1) such that the final monomer concentration of the solution was 0.7 M. The RAFT chain transfer agent (CTA) used was ethyl cyanovaleric trithiocarbonate (ECT, molecular weight 263.4 g/mol) and the initiator (I) used was VA-044. The molar ratios of total monomer:CTA:I at the start of polymerization were 200:1:0.1,

300:1:0.1, and 400:1:0.1, respectively. The reaction solutions were transferred to round bottom flasks, capped with a rubber septum, purged with argon for 10 min, and the submerged in a 44 °C oil bath to initiate polymerization. The polymerization was allowed to proceed for 14 hrs. Polymers were dialyzed against DI H2O and lyophilized.

5.2.4 HPMA-co-APMA end terminus capping

Polymers were end-capped to remove the trithiocarbonate terminal group. HPMA-*co*-APMA copolymers (DP200, DP300, DP400) were dissolved to a final concentration of 1 mM in DMF and solutions transferred to round bottom flasks. 40 eq of 2,2′-azobis(2-methylpropionitrile) (AIBN) was added to each reaction flask; flasks were capped and purged for 15 min under argon. Samples were incubated 70 ºC for 4 hrs. After 4 hrs, polymers were recovered by precipitation 3x in diethyl ether. Elimination of the terminal trithiocarbonate group was confirmed by loss of absorbance at 310 nm.

5.2.5 BM9 peptide grafting on HPMA-co-APMA copolymers

Peptides were grafted onto the HPMA-*co*-APMA copolymers via thiol-maleimide chemistry. First, HPMA-*co*-APMA copolymers were dissolved to a concentration of 1 mM in DMF. 2 eq of SMCC (relative to total primary amines) was added and reaction proceeded for 4 hrs at room temperature. Polymers were purified by precipitation in diethyl ether 3x.

BM9 peptide was dissolved in PBS, pH 6.5 and added as a 2 eq excess to maleimide-functionalized polymers. Thiol-maleimide reaction proceeded overnight at room temperature. Polymers were purified by dialysis for 4 days against 25 mM phosphate buffer, pH 6.5 and then against distilled H2O for 3 days. Polymers were lyophilized dry.

5.2.6 Size exclusion chromatography

Molecular weight analysis was carried out by size exclusion chromatography. HPMA-*co*-APMA copolymers were dissolved at 2 mg/mL in running buffer (150 mM acetate buffer, pH 4.4) for analysis by size exclusion chromatography-multiangle laser light scattering (SEC-MALLS).

Analysis was carried out on an OHpak SB-804 HQ column (Shodex, New York, NY) in line with a miniDAWN TREOS multiangle laser light scattering detector (Wyatt, Santa Barbara, CA) and an OptiLab rEX refractive index detector (Wyatt). HPMA-BM9 copolymers were dissolved at 2 mg/mL in running buffer (100 mM phosphate buffer, 300 mM NaCl, 0.05% NaN_3 pH 7.0) with analysis carried out on a TSK-Gel G3000SWXL column (Tosoh Bioscience, King of Prussia, PA). Absolute molecular weight averages (M_n, M_w) and polydispersity index (PDI) were calculated using ASTRA software (Wyatt).

5.2.7 Amino acid analysis

The incorporated amount of peptide and HPMA in the final copolymers was determined through modified amino acid analysis following the method of Bidlingmeyer and coworkers.[12] Briefly, HPMA-BM9 copolymers were hydrolyzed by reflux for 24 hrs at 110 ºC in 6N HCl. Hydrolyzed copolymers were derivatized with o-phthalaldehyde/β-mercaptopropionic acid and run on a ZORBAX Eclipse Plus C18 (Agilent Technologies, Santa Clara, CA) HPLC column with pre-column derivatization to label glycine and 1-amino-2-propanol (results from hydrolyzed HPMA). Calibration curves were generated using serial dilutions of glycine and reagent grade 1-amino-2-propanol.

5.2.8 MMP9-mediated polymer degradation

MMP9 mediated enzymatic release of bivalirudin peptide was determined. 25 µL of 5 mg/mL polymer solution in Reaction Buffer A (500 mM TrisHCl, 5 mM CaCl2, 200mM NaCl, pH 7.7) was mixed with 5 µL of 0.1 mg/mL pre-activated MMP9 stock solution and incubated at 37 ºC. At various time points, a 5 µL aliquot of the reaction solution was removed and mixed with 5 µL of 5 mM 1,10-phenanthroline to stop the enzymatic digest. Samples were analyzed via SEC-MALLS following shifts in molecular weight distribution using the RI detector.

5.2.9 In vitro thrombin inhibition

The thrombin inhibitory effects of BM9 peptide and HPMA-BM9 copolymers were assayed using

a thrombin colorimetric activity assay. To 95.75 μL of 104.4 μM BM9 (or polymer equivalent) in thrombin reaction buffer (100 mM Tris, 150 mM NaCl, 0.1% PEG-8000, pH 7.5), 1 μL of thrombin (10 μg/mL) was added and the mixtures were incubated for 10 min at room temperature. After 10 min, 3.25 μL of thrombin substrate S-2238 (1 mg/mL) was added to each reaction and absorbance at 405 nm was read every minute for 30 minutes using a Tecan Safire2 plate reader (Männerdorf, Switzerland).

To evaluate the effects of MMP9 treatment on HPMA-BM9 polymer activity, 9.5 μL of the HPMA-BM9 polymers was mixed with 2 μL of 0.1 mg/mL pre-activated MMP9 for 30 min at 37 °C; samples treated with HAMC (1.5% methylcellulose, 0.5% hyaluronic acid in HBSS HAMC) had an additional 0.5 μL of HAMC added. Following 30 min incubation, samples were diluted with 83.8 μL of thrombin reaction buffer and 1 μL of thrombin (10 μg/mL) was added. Samples were incubated for 10 min at room temperature and then 3.25 μL of S-2238 was added and the absorbance read at 405 nm every minute for 30 minutes.

5.2.10 Hydrogel release kinetics

Release kinetics of the HPMA-BM9 copolymers and the native bivalirudin peptide from HAMC hydrogels was evaluated. Polymers were dissolved at 10 mg/mL and bivalirudin peptide at an equivalent molar peptide concentration of 4.68 mg/mL in a cold 1.5% methylcellulose (w/v), 0.5% hyaluronic acid (w/v) HBSS solution and mixed thoroughly. In triplicate, 30 μL of each HPMA-BM9 hydrogel solution was aliquoted into microcentrifuge tubes and incubated at 37 ºC overnight to ensure complete gelation. 300 μL of pre-warmed HBSS was added to each tube and tubes were incubated at 37 ºC. At various time points, 30 μL of HBSS was removed and 30 μL of fresh pre-warmed HBSS was added.

Acid-catalyzed hydrolysis of polymers followed by amine concentration determination via Fluoraldehyde assay (Pierce) was used to quantitate release. 15 μL of each sample was dissolved in 200 μL of 6N HCl, and refluxed at 110 ºC for 24 h. Hydrolyzed samples were dried using a SpeedVac (ThermoFisher Scientific, Waltham, MA) and resuspended in 100 μL of 10 mM borate, 10 mM phosphate, 0.05% sodium azide pH 8.2. To assay, 10 μL of sample was mixed with 100 μL of Fluoraldehyde reagent in 96 well round-bottom black plates. Samples were incubated in the dark for 4 min at room temperature and then fluorescence read using a plate reader at ex/em

360/456 nm.

5.2.11 Spinal cord contusion injury model

Spinal cord contusion injuries were performed on adult female Long-Evans rats as previously described.[13] Briefly, animals were anesthetized with ketamine/xylazine and a laminectomy was performed at the C4 spinous process of the lamina ipsilateral to the animal's dominant paw. The animals were then placed in a spinal frame and a contusion injury was conducted using a fourth generation Ohio State Injury Device. An electromagnetically controlled probe (0.7 mm end diameter, Ling Dynamics, Inc) was lowered to the surface of the cord just lateral to midline. The probe was oscillated on the surface of the spinal cord to achieve a common starting force of 3000 dynes for all animals. The spinal cord was displaced 0.8 mm for 14 ms to induce the injury. One hr post-injury, 1 μL (10 mg/mL) of either DP400 HPMA-BM9 copolymer or DP400 APMA-HPMA copolymer physically encapsulated in a 1.5% methylcellulose, 0.5% hyaluronic acid hydrogel (in HBSS) was administered to the site of injury. The surgical site was closed by suturing muscle in layers and closing skin with wound clips.

5.2.12 Quantification of proliferating cells

Bromodeoxyuridine (BrdU) incorporation is a commonly used as a marker for mitotically active cells. Following hydrogel administration, a single injection of BrdU (50 mg/kg, Sigma) was administered intrapertoneally. 24 hrs after injection, animals were anesthetized and perfused with saline and then 4% paraformaldehyde in 0.1M phosphate buffer. Spinal cords were removed, post-fixed overnight and transferred to 30% sucrose for cryopreservation. 1 mm coronal sections surrounding the lesion were cut, embedded in OCT medium, and flash frozen. 20 μm sections were cut and stored at -80C.

For the stereological quantitation of BrdU-labeled cells, cryostat sections were stained for diaminobenzadine (DAB) immunohistochemistry as previous reported.[14] Briefly, sections were pretreated with 50% formamide in 2x saline-sodium citrate (SSC), 2x SSC, 2N HCl, 0.1 M borate buffer, and then rinsed six times with TBS. Nonspecific labeling was blocked with TBS + 0.1% Triton X-100 and 3% normal donkey serum. A monoclonal mouse antibody against BrdU (1:400,

Boehringer Mannheim, Indianapolis, IN) was incubated with the tissue for 2 d at 4 ºC. After primary antibody incubation, sections were quenched with 0.6% H_2O_2 in TBS and tissue rinsed in TBS before incubation with a polyclonal donkey α mouse IgG secondary antibody (Accurate Chemicals, Westbury, NY; 1:200 in TBS). Sections were then rinsed with TBS and incubated with avidin-biotin complex (ABC-Elite; Vector Laboratories, Burlingame, CA). BrdU labeling was visualized using DAB (0.25 mg DAB, 0.009% H_2O_2, and 0.04% NiCl in TBS). DAB incubation was terminated by a tap water rinse, and slides were then dehydrated through alcohols and coversliped with permount. BrdU nuclei were excluded from the study if they exhibited punctate staining in part of the nucleus or the DNA appeared to be condensed.

5.2.13 Quantification of astrocytes

30 days post-injury, rats were sacrificed, spinal cords harvested, and sections processed as discussed above. To stain for astrocytes, sections were treated with rabbit αS-100β (1:10,000; Swant, Bellinzona, Switzerland) for 2 days at 4 ºC in TBS + 0.1% Triton X-100 + 5% donkey serum. Sections were rinsed twice with TBS and once with TBS + 0.1% Triton X-100 for 15 min. Sections were treated with secondary antibody donkey α rabbit conjugated to Cy5 (1:500; Jackson ImmunoResearch) for 1-2 hrs with 0.1% Tween-20. Sections were washed three times for 15 min with TBS. Slides were immediately coversliped and imaged. Cells populations within the spinal cord and lesion epicenter were calculated via fractionator Stereology (an unbiased sampling method) by Stereo Investigator (Microbrightfield, Inc.). A grid size of 400x400 μm and counting frame of 75x75 μm was used to assure unbiased sampling of a randomized grid in a 1 in 6 series of tissue sections to generate averaged populations for each animal.

5.2.14 Limb-use asymmetry test

The limb-use asymmetry test (LUAT) was used to assess forelimb preference during vertical exploration in a clear Plexiglas cylinder. Animals were scored by blinded-observers on independent and simultaneous use of their left and right forelimbs when rearing to make wall contacts.[15] Each session lasted until an animal made 20 wall contacts. To determine paw preference, an asymmetry score was calculated for each test session, asymmetry = [(affected

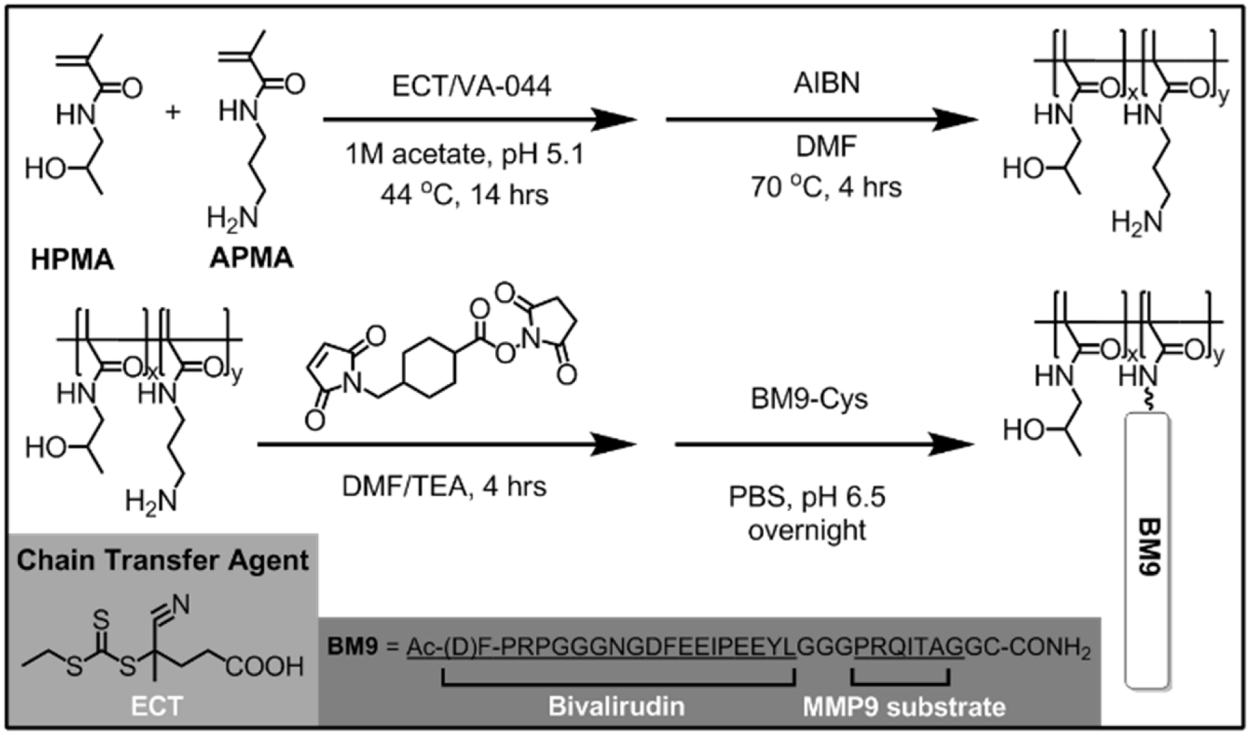

Scheme 5.1. Synthetic scheme of HPMA-BM9 copolymers.

forelimb) + .5(both forelimbs)] / 20, with a score below 0.5 indicating preference for the unaffected forelimb. No training is required for this test, and all animals prior to injury showed no paw preference (average 0.4875 ± 0.08 SD).

5.2.15 IBB forelimb usage test

Forelimb function was tested using the Irvin, Beatties and Bresnahan (IBB) forelimb scale to assess recovery of different forelimb function such as joint position, object support, digit movement and grasping technique.[16] To do this animals are videotaped while eating a spherical and doughnut shaped piece of cereal that are of similar size. The testing environment is a clear Plexiglas cylinder that is 19.5cm in diameter and 30cm in height and a mirror is placed around the cylinder, which allows for filming of an animal from any side. The week prior to injury each animal was filmed while eating each piece of cereal to determine an uninjured IBB score. Animals were then filmed only once a week for four weeks following their SCI. IBB videos are scored by evaluation of digit

Table 5.1. Properties of HPMA-BM9 copolymers

	HPMA-APMA		HPMA-BM9		
Copolymers	Mn (kDa)[a]	PDI[a]	Mn (kDa)[a]	PDI[a]	%BM9[b]
DP200	28.7	1.02	98.7	1.44	12.1
DP300	37.9	1.03	107.0	1.25	12.8
DP400	51.0	1.03	178.4	1.49	13.1

[a]Determined by GPC-MALLS. [b]Determines by amino acid analysis

usage (in slow-motion) by an observer that was blinded to the animal's experimental group. Forelimb function was scored according to a 9-point scale to assess forelimb position and movement, volar support, wrist movement, and digiti usage for cereal adjustment after SCI.

5.3 Results and discussion

We first designed the BM9 peptide, which contains bivalirudin fused to an optimized matrix metalloproteinase-9 (MMP9) peptide substrate linker, PRQITAG.[17] MMP9 was selected as the target protease for triggering bivalirudin release due to its maximal expression at 24 hrs following SCI, concurrent with upregulated thrombin expression.[18] MMP9 activity on BM9 was confirmed via MALDI-TOF MS fragmentation analysis (Figure 5.6a), with > 15% of peptide cleaved within 3 hrs (Figure 5.6b). Rapid recognition and specific cleavage of the bivalirudin-MMP9 peptide at the linker results in the emergence of a 2774 Da peak corresponding to fragmentation at the peptide linker (Table 5.2). The peptide fragment is susceptible to further C-terminal exopeptidase degradation, leading to smaller, truncated peptide fragments over time. The N-terminus of the peptide shows resistance to exopeptidase activity, likely due to acetylation of the N-terminal amine and presence of a (D)-phenylalanine as the first residue.[19,20] Cleavage at the linker sequence is expected to yield functional bivalirudin peptide.

A series of HPMA-BM9 copolymers was then synthesized as peptide carriers for localized thrombin inhibition (Scheme 5.1). The molecular weight and composition of synthesized copolymers are summarized in Table 5.1. The base HPMA-APMA polymer had a monomer feed ratio of 1:9 APMA to HPMA and were varied in size to investigate the effects of different polymer

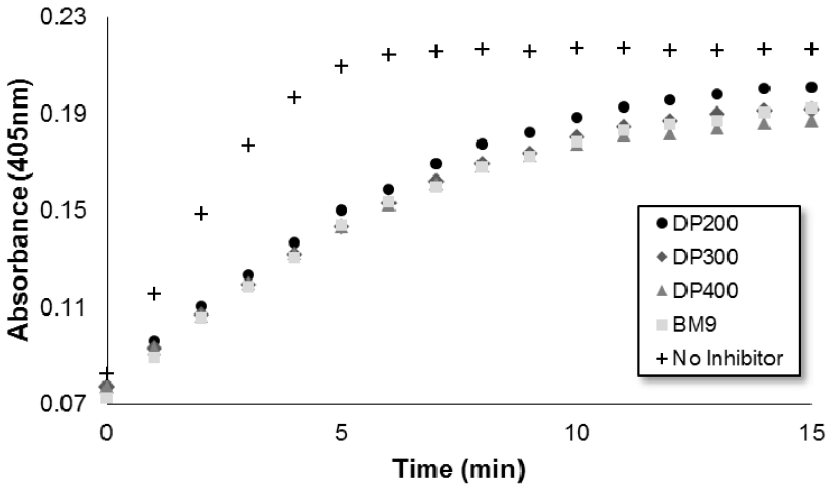

Figure 5.2. Thrombin activity measured by colorimetric substrate S-2238 as a function of time.

molecular weights. Base copolymers were synthesized with narrow polydispersities (< 1.05) and molecular weights 28-51 kDa. The primary amines of the copolymers were converted to thiol-reactive maleimide groups and BM9 peptides conjugated via a C-terminal cysteine residue. Final BM9-conjugated copolymers contained 12-13% peptide, as determined by amino acid analysis, and ranged from 100-180 kDa in molecular weight with PDI < 1.5. Polymers contain ~20-50 peptides per polymer chain depending on polymer molecular weight. Some bimodal polymer populations were observed by aqueous GPC (Figure 5.7), prominently for the DP400 copolymer, likely due to some inter-chain crosslinking during peptide bioconjugation. Alternative bioconjugation strategies with higher orthogonality, such as azide-alkyne "click" chemistries, could minimize crosslinking.

Bivalirudin activity after peptide grafting onto polymers was confirmed using a colorimetric thrombin activity assay. All three HPMA-BM9 copolymers show similar thrombin inhibition kinetics and levels as free BM9 peptide regardless of polymer sizes (~50% reduction in thrombin activity, Figure 5.8), confirming that polymer conjugation does not affect peptide activity (Figure 5.2); pre-treatment of HPMA-BM9 polymers with MMP9 minimally affects thrombin inhibition (Figure 5.9). The retained bivalirudin activity when presented on a polymer backbone is likely due to adequate spacing between the bivalirudin sequences to minimize activity loss due to steric hindrance; spacing between grafted peptides was high (~13 mol% peptide in polymer) as was

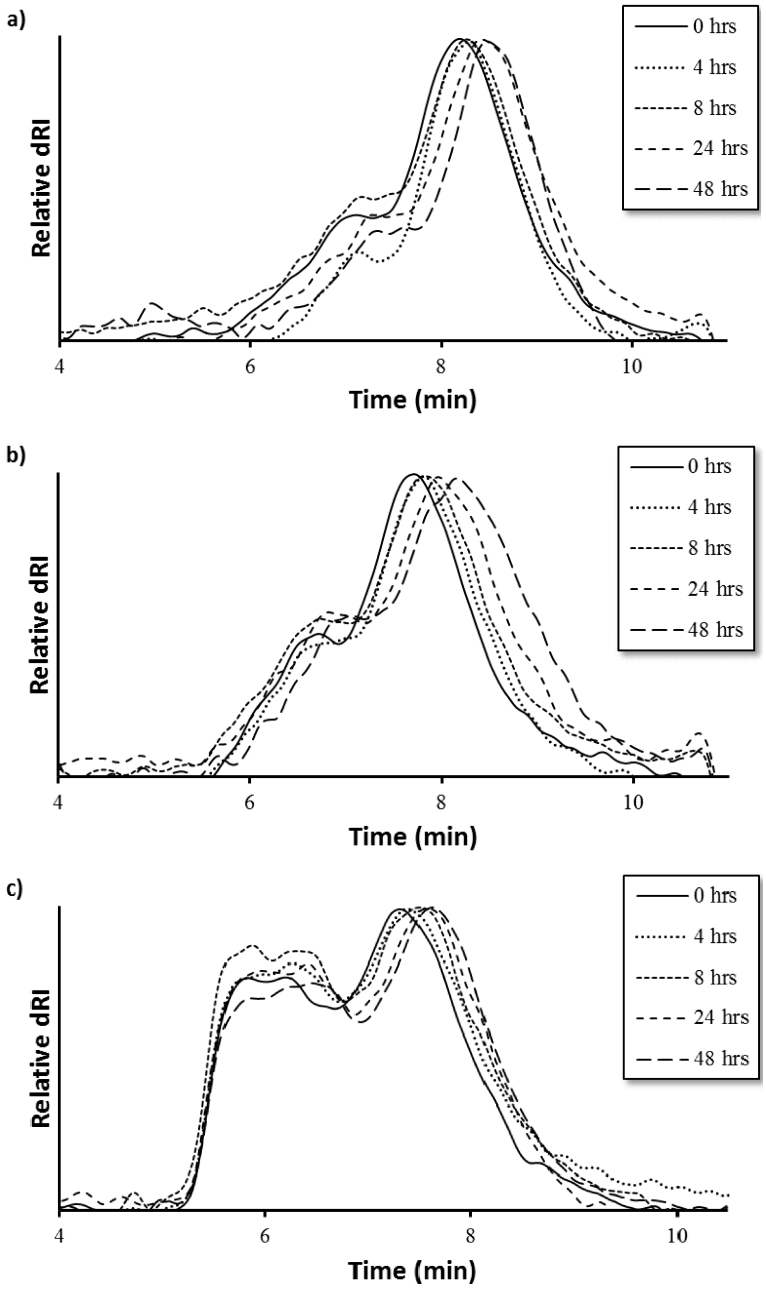

Figure 5.3. Polymer degradation as a function of elution time via size exclusion chromatography of (a) DP200, (b) DP300, and (c) DP400 HPMA-BM9 copolymers.

spacing from the polymer backbone (12 amino acid linker). Peptides do not have to be cleaved from polymeric support for activity; therefore, MMP9-mediated bivalirudin release would be expected to improve the tissue penetration of bivalirudin peptides *in vivo* but is not required for

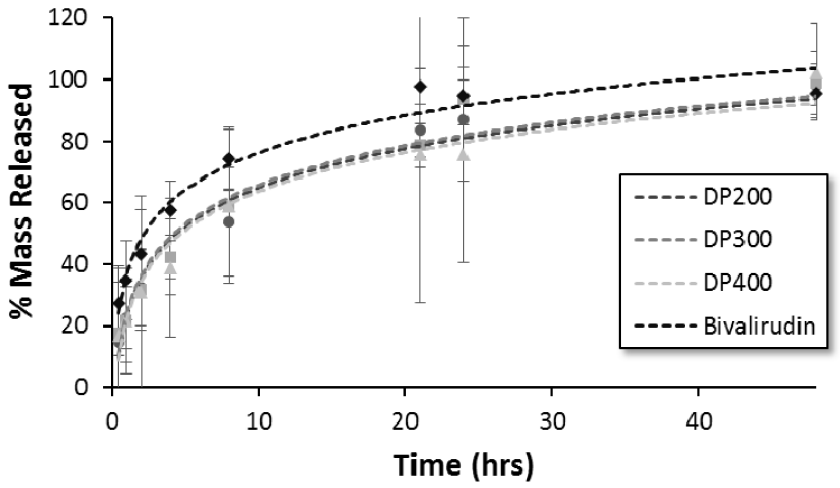

Figure 5.4. HPMA-BM9 copolymer and bivalirudin release from HAMC hydrogels as a function of time.

activity.

MMP9-mediated degradation of HPMA-BM9 copolymers was evaluated by treating polymers with MMP9 and analyzing polymers at various time points by size exclusion chromatography (Figure 5.3). Kinetics of BM9 peptide linker cleavage suggests >80% of peptide could be released within 24 hrs if similar enzyme activity is seen with polymers (Figure 5.6b). Degradation of DP200 begins within 4 hrs of incubation with MMP9 and continues for up to 24 hrs, as evidenced by increasing elution time as a function of MMP9 treatment time, indicating formation of lower molecular weight polymer populations. (Figure 5.3a). Since BM9 peptide sequences are resistant to N-terminal peptidase activity, decreasing polymer molecular weight is attributed to the release of bivalirudin peptide following linker cleavage. DP300 and DP400 polymers degrade more slowly than DP200, showing noticeable shifts in molecular weight profiles within 4 hrs that last for at least 48 hrs (Figure 5.3b and 5.3c). Slower peptide release kinetics could possibly be attributable to decreased enzymatic susceptibility due to more steric hindrance in larger polymers.

The release kinetics of HPMA-BM9 copolymers physically encapsulated in HAMC hydrogels was evaluated *in vitro*. Polymer release from the HAMC hydrogels was quantified by incubating loaded hydrogels with HBSS and then sampling at various time points to determine the

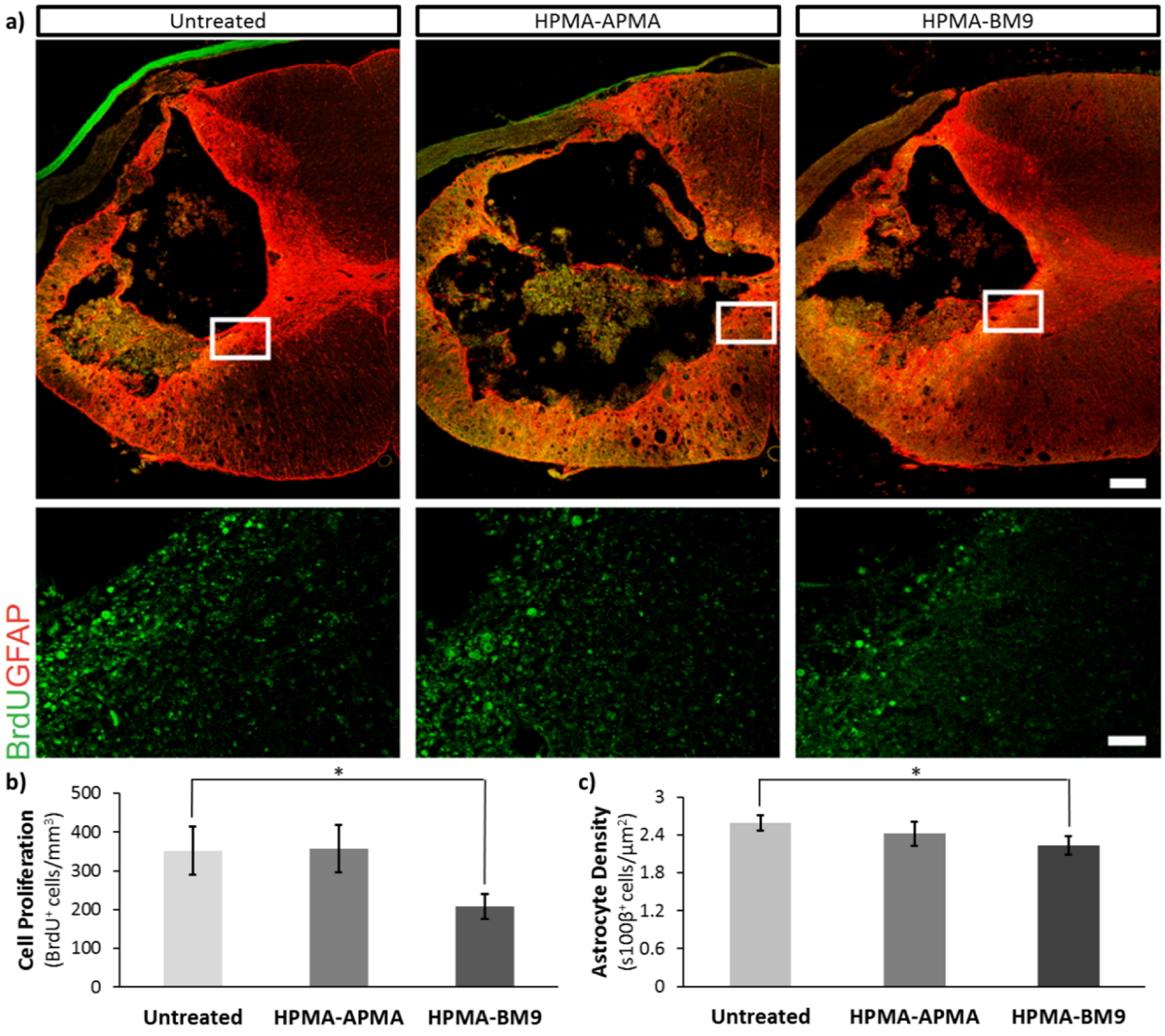

Figure 5.5. (a) Confocal images of BrdU and GFAP immunofluorescence in spinal cord sections at lesion epicenter. Bar, 100 μm. Inset shows BrdU at the lesion margin. Bar, 10 μm (b) Average BrdU+ cells as a measure of cellular proliferation in the C4 cervical vertebrae 24 hrs post-injury. (c) Average s100β+ cells as a measure of astrocyte density 30 days post-injury. *$p < 0.05$. Error bars = standard error.

amount of released polymer by hydrolyzing the various samples and assaying for amine concentration. For all three polymers, complete hydrogel release is observed within 48 hrs (Figure 5.4). Trends, though not statistically significant, of decreased release rate with increasing polymer size are observed, corresponding to expected decreased diffusivity with increased polymer size.

Importantly, BM9 copolymers show significantly delayed release compared to free bivalirudin peptide, demonstrating that peptide grafting on polymeric support decreases hydrogel release rates. Direct conjugation of the polymers to the hydrogel may be a useful alternative strategy for prolonged released in future studies. We therefore proceeded with the highest molecular weight (DP400) polymer for *in vivo* evaluation of the materials.

To study the effects of localized thrombin inhibition on spinal cord recovery, we performed a laminectomy at cervical spinal level 4 (C4) and induced a lateral hemi-contusion injury.[13] One hour following injury, rats received either no treatment, a localized intraspinal injection of DP400 base HPMA-APMA copolymer encapsulated in the HAMC hydrogel, or an injection of DP400 HPMA-BM9 polymer in a HAMC hydrogel within the lesion epicenter.

Previous studies have shown that proliferation of inflammatory cells, endogenous neural progenitors and glia is upregulated after spinal cord injury.[13,21] To examine whether bivalirudin release affects cell proliferation after SCI, 5-Bromo-2'-deoxyuridine (BrdU) was administered intraperitoneally 24 hr post-injury (PI) to label mitotically-active cells (Figure 5.5a, 5.5b). Spinal cord sections from the injury site show ~45% decreased cellular proliferation for DP400 HPMA-BM9 treated animals compared to untreated control animals and pHPMA-APMA/HAMC treated animals ($p < 0.05$). These results confirm that the HAMC hydrogel and base HPMA-APMA polymer do not affect proliferative responses. Observed differences are therefore attributable to the thrombin-inhibition effects of the bivalirudin sequence.

Since thrombin inhibition has been shown to reduce astrogliogenesis, we quantified astrocytes (s100β+ cells) proximal to the lesion epicenter (Figure 5.5c). Rats treated with HPMA-BM9 polymer showed the lowest astrocyte density, a statistically-significant ~15% decrease in astrocyte density ($p < 0.05$) compared to untreated injured animals. pHPMA-APMA/HAMC treated animals showed no signficant difference. Analysis of the area around the lesion margin delimitated by GFAP-cells showed similar trends, but the differences did not show significance despite an apparnt diffference in density. Nonetheless, BM9 was able to reduce gliosis at the lesion without collateral effects on inflammation (Iba1-cells, Figure 5.10) or cell density (nuclei, Figures 5.10, 5.11). BM9-treated rats tended to have increased oligodendroyte populations (Figure 5.11), which could serve to promote functional regeneration in the long-term.

Following injury, many signals induce reactive gliosis.[22] Astrogliosis is characterized by cellular hypertropy, hyperplasia, increased glial fibrillary acidic protein (GFAP), proliferation, and

ultimately scar formation;[23] while playing important roles in restoration of extracellular ionic homeostasis and spatially limiting inflammation, astrogliosis can also significantly interfere with functional recovery through scar formation that impairs axon regeneration, leading to Wallarian degeneration (chronic demylination), functional deficits and paralysis.[24,25] Therefore, successful reduction in reactive gliosis would serve toreduce astrocyte proliferation and density to create a post-inury environment to augment recovery without an exacerbated paralytic response, which astrocyte ablation has been shown to affect.[26] Our data show that polymer-loaded HAMC hydrogels do not have a negative impact on forelimb function or usage (Figure 5.12). Consequently, HPMA-BM9 reduced astrocyte numbers, suggesting lessened reactive gliosis during the post-injury response without collateral behavioral deficits. Since reactive gliosis is thought to impede recovery, BM9-loaded hydrogels might serve to remodel the post-injury repsonse, inducing an environment more amenable to regenerative strategies after SCI.

5.4 Conclusions

In summary, HPMA-BM9 polymers are a promising platform for the grafting and display of functional peptides. Bivalirudin-grafted polymers maintain thrombin inhibition activity but demonstrate enzyme-mediated peptide release, making them a promising new formulation for active peptide delivery. Localized delivery of DP400 copolymer encapsulated in a HAMC hydrogel decreased cellular proliferation by 45% after 24 hrs and led to decreased astrocyte density after 30 days. These results suggest the DP400 copolymer and HAMC hydrogel system are effective therapeutics for reducing the immediate inflammatory response and long term scarring response, potentially leading to improved functional recovery following neural trauma.

5.5 Acknowledgements

This work was funded by NIH 1RO1NS064404, a CDMRP SCRIP Investigator Initiated Award (SC130249) and the Craig H Neilsen Foundation (SAN 124679). D. Chu was supported by NIH T32 CA138312. We thank Drs. Patrick Stayton and Anthony Convertine for generous donation of the ECT chain transfer agent.

5.6 References

(1) Dunham, K. A.; Floyd, C. L.: Contusion models of spinal cord injury in rats. In *Animal Models of Movement Disorders : Volume II*; Lane, E. L., Dunnett, S. B., Eds.; Humana Press: London, United Kingdom, 2011; Vol. 62; pp 345-362.

(2) Turgeon, V. L.; Houenou, L. J.: The role of thrombin-like (serine) proteases in the development, plasticity and pathology of the nervous system. *Brain Res Rev* **1997**, *25*, 85-95.

(3) Citron, B. A.; Smirnova, I. V.; Arnold, P. M.; Festoff, B. W.: Upregulation of neurotoxic serine proteases, prothrombin, and protease-activated receptor 1 early after spinal cord injury. *J Neurotraum* **2000**, *17*, 1191-1203.

(4) Thuret, S.; Moon, L. D. F.; Gage, F. H.: Therapeutic interventions after spinal cord injury. *Nat Rev Neurosci* **2006**, *7*, 628-643.

(5) Nishino, A.; Michiyasu, S.; Ohtani, H.; Motohashi, O.; Umezawa, K.; Nagura, H.; Toshimoto, T.: Thrombin May Contribute to the Pathophysiology of Central Nervous System Injury. *J Neurotram* **1993**, *10*, 167-179.

(6) Sellers, D. L.; Kim, T. H.; Mount, C. W.; Pun, S. H.; Horner, P. J.: Poly(lactic-co-glycolic) acid microspheres encapsulated in Pluronic F-127 prolong Hirudin delivery and improve functional recovery from a demyelination lesion. *Biomaterials* **2014**, *10*, 8895-8902.

(7) Festoff, B. W.; Ameenuddin, S.; Santacruz, K.; Morser, J.; Suo, Z.; Arnold, P. M.; Stricker, K. E.; Citron, B. A.: Neuroprotective effects of recombinant thrombomodulin in controlled contusion spinal cord injury implicates thrombin signaling. *J Neurotraum* **2004**, *21*, 907-922.

(8) Caicco, M. J.; Zahir, T.; Mothe, A. J.; Ballios, B. G.; Kihm, A. J.; Tator, C. H.; Shoichet, M. S.: Characterization of hyaluronan-methylcellulose hydrogels for cell delivery to the injured

spinal cord. *J Biomed Mater Res A* **2013**, *101*, 1472-1477.

(9) Caicco, M. J.; Cooke, M. J.; Wang, Y.; Tuladhar, A.; Morshead, C. M.; Shoichet, M. S.: A hydrogel composite system for sustained epi-cortical delivery of Cyclosporin A to the brain for treatment of stroke. *J Control Release* **2013**, *166*, 197-202.

(10) Warkentin, T. E.; Greinacher, A.; Koster, A.: Bivalirudin. *Thromb Haemostasis* **2008**, *99*, 830-839.

(11) Vulic, K.; Shoichet, M. S.: Tunable growth factor delivery from injectable hydrogels for tissue engineering. *J Am Chem Soc* **2012**, *134*, 882-885.

(12) Bidlingmeyer, B. A.; Cohen, S. A.; Tarvin, T. L.: Rapid analysis of amino acids using pre-column derivatization. *J Chromatogr* **1984**, *336*, 93-104.

(13) Nutt, S. E.; Chang, E.-A.; Suhr, S. T.; Schlosser, L. O.; Mondello, S. E.; Moritz, C. T.; Cibelli, J. B.; Horner, P. J.: Caudalized human iPSC-derived neural progenitor cells produce neurons and glia but fail to restore function in an early chronic spinal cord injury model. *Exp Neurol* **2013**, *248*, 491-503.

(14) Horner, P. J.; Power, A. E.; Kempermann, G.; Kuhn, H. G.; Palmer, T. D.; Winkler, J.; Thal, L. J.; Gage, F. H.: Proliferation and differentiation of progenitor cells throughout the intact adult rat spinal cord. *J Neurosci* **2000**, *20*, 2218-2228.

(15) Schallert, T.; Fleming, S. M.; Leasure, J. L.; Tillerson, J. L.; Bland, S. T.: CNS plasticity and assessment of forelimb sensorimotor outcome in unilateral rat models of stroke, cortical ablation, parkinsonism and spinal cord injury. *Neuropharmacology* **2000**, *39*, 777-787.

(16) Irvine, K. A.; Ferguson, A. R.; Mitchell, K. D.; Beattie, S. B.; Beattie, M. S.; Bresnahan, J. C.: A novel method for assessing proximal and distal forelimb function in the rat: the Irvine, Beatties and Bresnahan (IBB) forelimb scale. *J Vis Exp* **2010**, DOI:10.3791/2246.

(17) Kridel, S. J.; Chen, E.; Kotra, L. P.; Howard, E. W.; Mobashery, S.; Smith, J. W.: Substrate Hydrolysis by Matrix Metalloproteinase-9*. *J Biol Chem* **2001**, *276*, 20572-20578.

(18) Noble, L. J.; Donovan, F.; Igarashi, T.; Goussev, S.; Werb, Z.: Matrix metalloproteinases limit functional recovery after spinal cord injury by modulation of early vascular events. *J Neurosci* **2002**, *22*, 7526-7535.

(19) Powell, M. F.; Stewart, T.; Otvos, L., Jr.; Urge, L.; Gaeta, F. C.; Sette, A.; Arrhenius, T.; Thomson, D.; Soda, K.; Colon, S. M.: Peptide stability in drug development. II. Effect of single amino acid substitution and glycosylation on peptide reactivity in human serum. *Pharm Res* **1993**, *10*, 1268-1273.

(20) Nguyen, L. T.; Chau, J. K.; Perry, N. A.; de Boer, L.; Zaat, S. A.; Vogel, H. J.: Serum stabilities of short tryptophan- and arginine-rich antimicrobial peptide analogs. *PLoS One* **2010**, *5*, e12684.

(21) Sellers, D. L.; Maris, D. O.; Horner, P. J.: Postinjury niches induce temporal shifts in progenitor fates to direct lesion repair after spinal cord injury. *J Neurosci* **2009**, *29*, 6722-6733.

(22) Pindon, A.; Berry, M.; Hantaï, D.: Thrombomodulin as a New Marker of Lesion-Induced Astrogliosis: Involvement of Thrombin through the G-Protein-Coupled Protease-Activated Receptor-1. *J Neurosci* **2000**, *20*, 2543-2550.

(23) Pekny, M.; Nilsson, M.: Astrocyte activation and reactive gliosis. *Glia* **2005**, *50*, 427-434.

(24) Fawcett, J. W.; Asher, R. A.: The glial scar and central nervous system repair. *Brain Res Bull* **1999**, *49*, 377-391.

(25) Cregg, J. M.; DePaul, M. A.; Filous, A. R.; Lang, B. T.; Tran, A.; Silver, J.: Functional regeneration beyond the glial scar. *Exp Neurol* **2014**, *253*, 197-207.

(26) Faulkner, J. R.; Herrmann, J. E.; Woo, M. J.; Tansey, K. E.; Doan, N. B.; Sofroniew, M. V.: Reactive astrocytes protect tissue and preserve function after spinal cord injury. *J Neurosci* **2004**, *24*, 2143-2155.

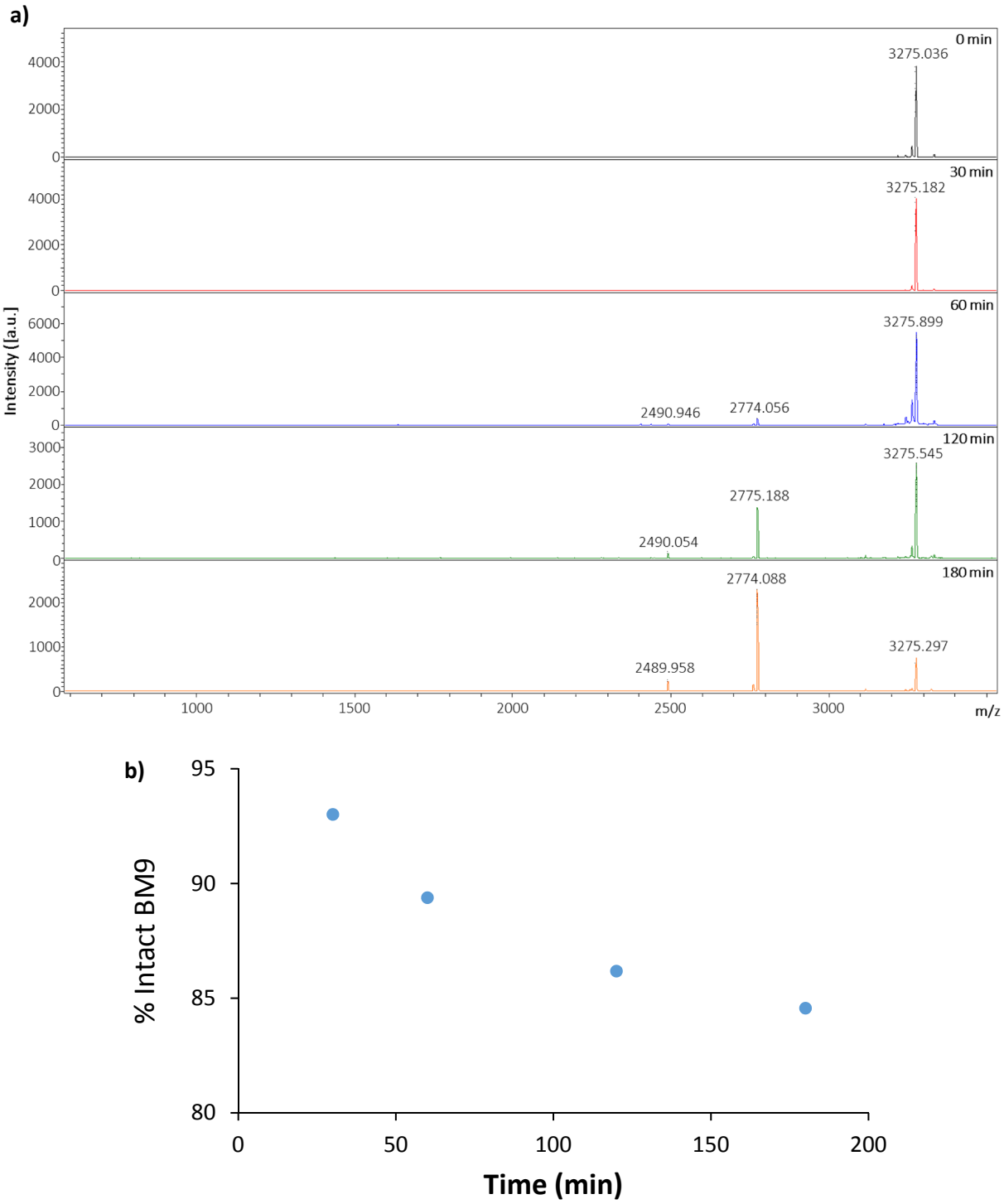

Figure 5.6. (a) MALDI-TO MS time-point study of MMP9-mediated peptide digest of BM9. (b) Kinetics of MMP9 digest of BM9 peptide by tyrosine fluorescence via RP-HPLC.

Table 5.2. Molecular weights of peptide fragments

Sequence	MW (Da)
Ac-(D)F-PRPGGGGNGDFEEIPEEYLGGG*PRQITAG*GC-CONH2	3275
Ac-(D)F-PRPGGGGNGDFEEIPEEYLGGGPRQ-COOH	2774
Ac-(D)F-PRPGGGGNGDFEEIPEEYLGGGP-COOH	2490

*Bivalirudin sequence is bolded; MMP9 linker sequence is italicized

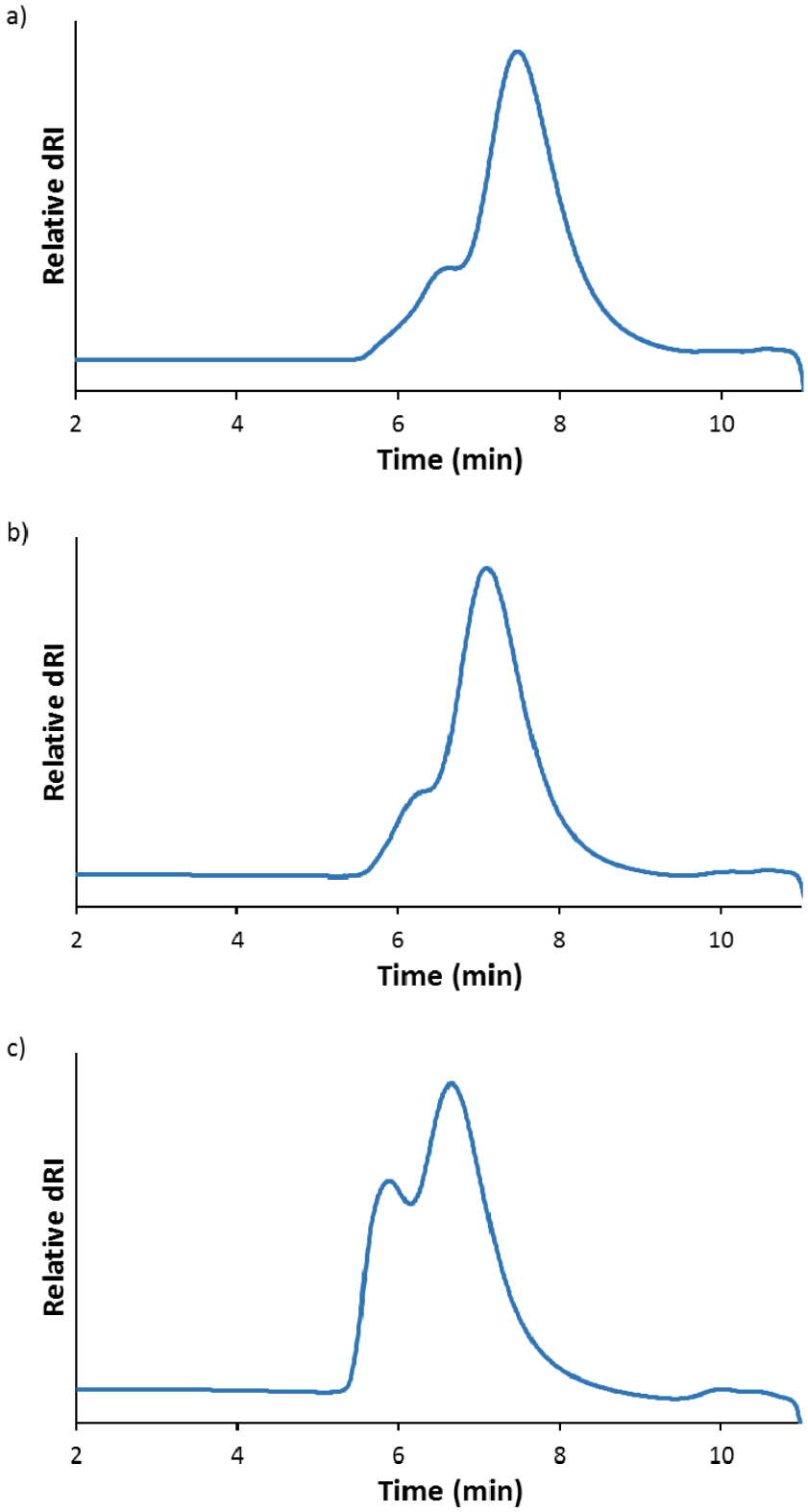

Figure 5.7. Gel-permeation chromatography traces of (a) DP200, (b) DP300, and (c) DP400 copolymers.

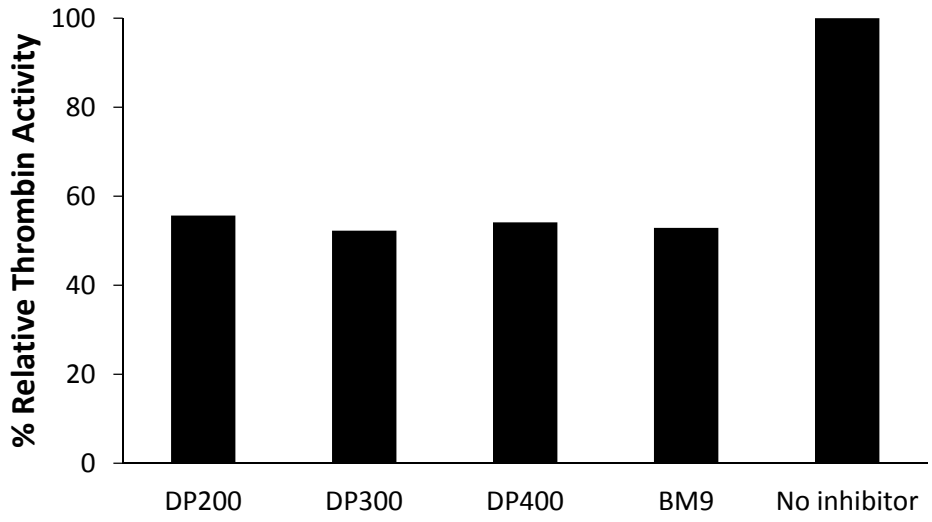

Figure 5.8. Initial relative thrombin activity measured by colorimetric substrate S-2238.

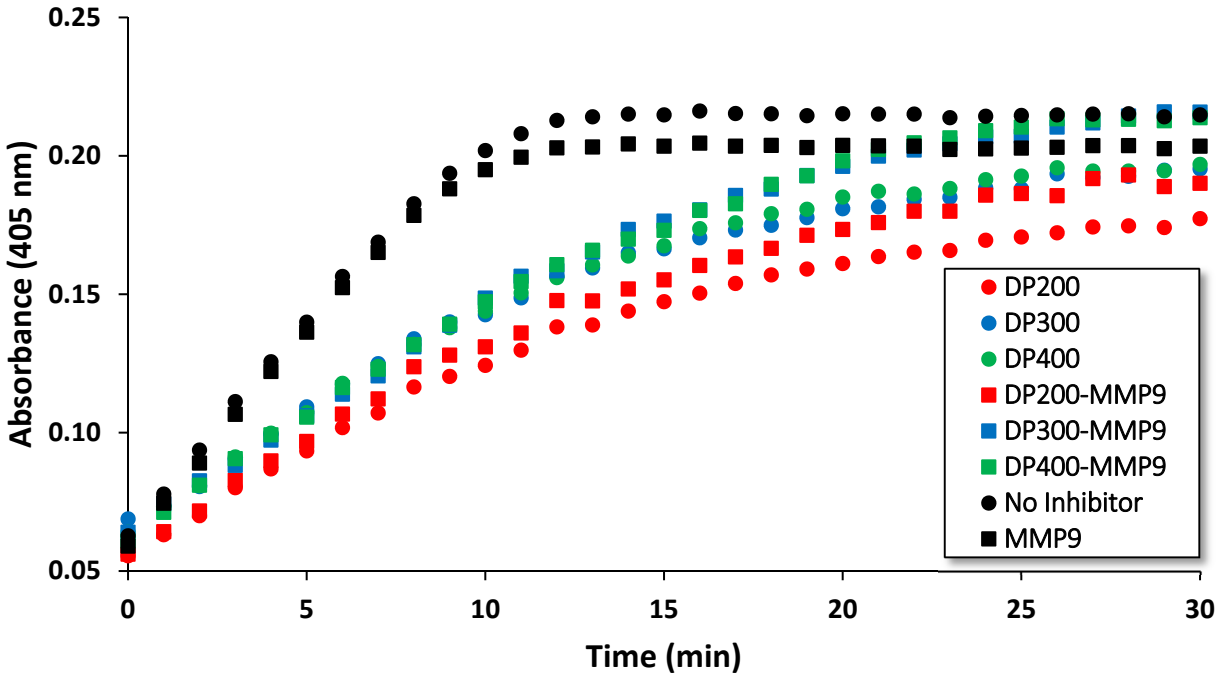

Figure 5.9. Thrombin activity assay as measured by colorimetric development of S-2238 substrate for polymers that either untreated with MMP9 (○) or treated with MMP9 for 30 min prior to addition of thrombin (□).

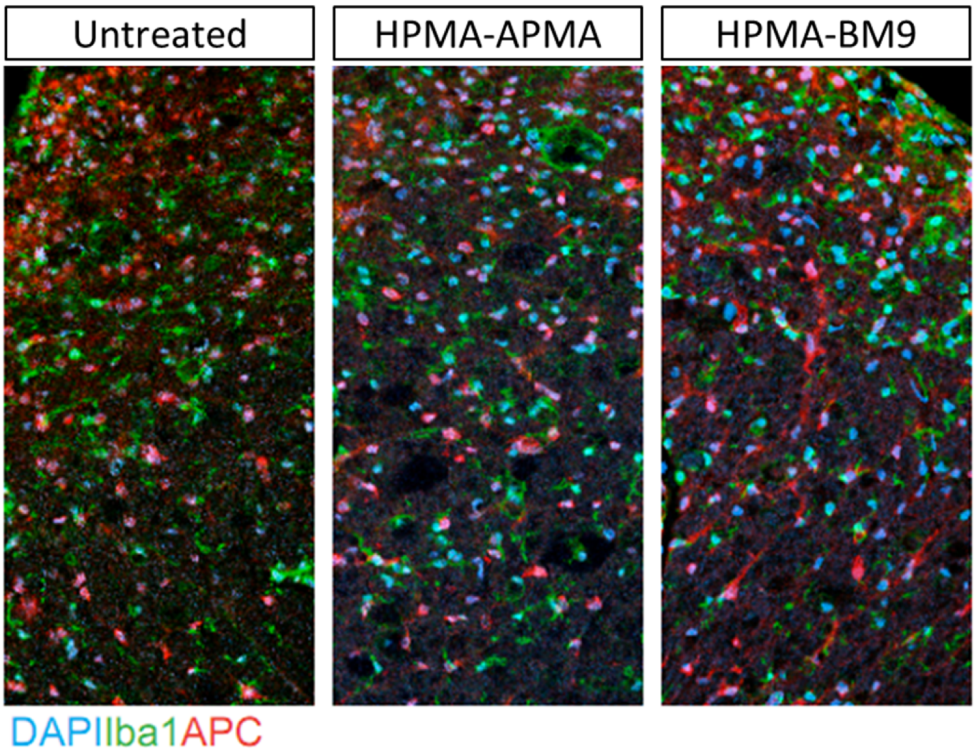

Figure 5.10. Confocal images of spinal cord sections at the lesion 30 days post-injury stained for microglia (Iba1), immature oligodendrocytes (APC), and nuclei (DAPI).

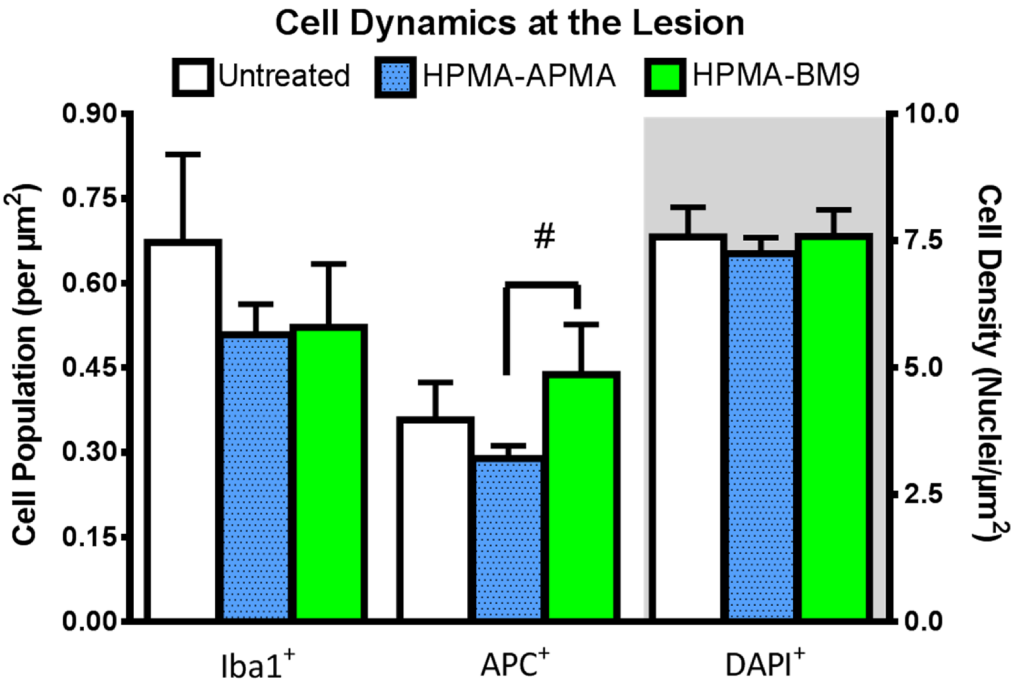

Figure 5.11. Iba^{+} (microglia), APC^{+} (immature oligodendrocytes), and DAPI^{+} (all) cells per area at the lesion 30 days post-injury. $^{\#}p < 0.08$. Error bars = standard error.

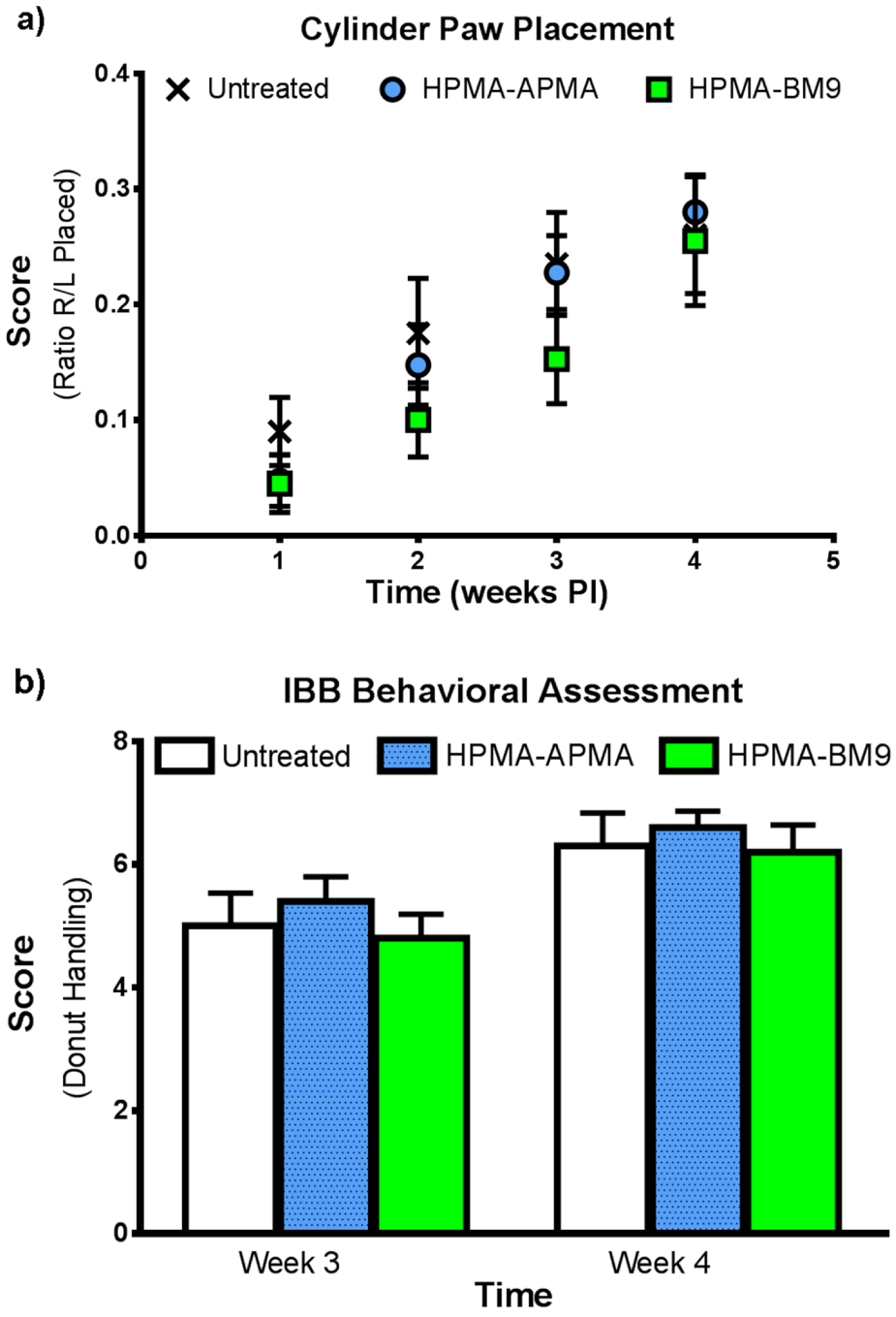

Figure 5.12. Behavioural recovery of treated rats following injury studied via (a) limb-use asymmetry tests to assess forelimb preference and (b) forelimb function via the Irvin, Beatties and Bresnahan (IBB) forelimb scale.

Chapter 6

DEVELOPMENT OF MULTIVALENT PRO-APOPTOTIC PEPTIDE-BASED POLYMERS FOR TREATMENT OF GLIOBLASTOMA MULTIFORME

David S.H. Chu, Michael J. Bocek, Julie Shi, Anh Ta, Robert C. Rostomily, Suzie H. Pun

Abstract

Several cationic antimicrobial peptides have been investigated as potential anti-cancer drugs due to their demonstrated selective toxicity towards cancer cells relative to normal cells. For example, intracellular delivery of KLA, a pro-apoptotic peptide, results in toxicity against a variety of cancer cell lines; however, the relatively low activity and small size leads to rapid renal excretion when applied in vivo, limiting its therapeutic potential. In this work, apoptotic peptide-polymer hybrid materials were developed to increase apoptotic peptide activity via multivalent display. Multivalent peptide materials were prepared with comb-like structure by RAFT copolymerization of peptide macromonomers with N-(2-hydroxypropyl) methacrylamide (HPMA). Polymers displayed a GKRK peptide sequence for targeting p32, a protein often overexpressed on the surface of cancer cells, either fused with or as a comonomer to a KLA macromonomer. In three tested cancer cell lines, apoptotic polymers were significantly more cytotoxic than free peptides as evidenced by an order of magnitude decrease in IC50 values for the polymers compared to free peptide. The uptake efficiency and intracellular trafficking of one polymer construct was determined by radiolabeling and subcellular fractionation. Despite their more potent cytotoxic profile, polymeric KLA constructs have poor cellular uptake efficiency (<1%). A significant fraction (20%) of internalized constructs localize with intact mitochondrial fractions. In an effort to increase cellular uptake, polymer amines were converted to guanidines by reaction with O-methylisourea. Guanidinylated polymers disrupted function of isolated mitochondria more than their lysine-based analogs, but overall toxicity was decreased, likely due to inefficient mitochondrial trafficking. Thus, while multivalent KLA polymers are more potent than KLA peptides, these materials can be substantially improved by designing next generation materials with improved cellular internalization and mitochondrial targeting efficiency.[1]

---

[1]Submitted for publication.

6.1 Introduction

Glioblastoma multiforme (GBM), the most common form of primary brain cancer, has a very poor prognosis, with an estimated 12-14 month life expectancy following diagnosis.[1] Systemic administration of chemotherapeutics remains challenging due to poor drug penetration past the blood brain barrier (BBB)[2] in addition to strong chemotherapeutic resistance that may be unrelated to drug efflux pumps.[3] Current therapy involving aggressive surgical resection with combination radiochemotherapy prolongs life expectancy by a mere 3-6 months.[1] Therefore, there is an urgent need to develop alternative therapeutics for GBM.

One class of potential anti-cancer agents draws inspiration from cationic antimicrobial peptides (CAP), natural host defense mechanisms widely conserved in diverse species.[4,5] These peptides eliminate a wide range of bacteria, fungi, viruses, and protozoa[6,7] by disrupting negatively-charged membranes through electrostatic interactions, leading to pore formation, cellular depolarization, and cell death.[8] Minimal bacterial resistance was developed against antimicrobial amphiphilic polymers over several hundred cellular divisions compared to rapid development of antibiotic resistance, suggesting that drug strategies based on membrane-disruption are less susceptible to drug resistance.[9] Most CAPs have low cytotoxicity towards healthy eukaryotic cells, whose cellular membranes contain high levels of zwitterionic phosphatidylcholine resulting in minimal CAP interaction. Cancer cells, however, frequently overexpress anionic phospholipids, such as phosphatidylserine and *O*-glycosylated mucins, resulting in net-negative membranes that interact with CAPs.[5,10] Therefore, many CAPs show selective toxicity towards cancer cells relative to normal cells.

Additionally, intracellular delivery of these CAPs can induce mitochondrial dysfunction.[11] Mitochondrial membranes resemble bacterial membranes and are disrupted upon exposure to CAPs, inducing cellular apoptosis through the release of cytochrome c.[11] The peptide sequence $(KLAKLAK)_2$, or "KLA", has been shown to permeabilize mitochondrial membranes in a local peptide concentration-dependent manner.[7,11] KLA has therefore been investigated as a pro-apoptotic agent in fusion peptide,[11-14] polymer conjugate,[15] and nanoparticle conjugate[16] form. These materials have been studied in several cancer cell lines and animal models both *in vitro* and *in vivo*, showing promising cancer cell killing.[13,15,16] However, the requirement for high intracellular concentrations pose a significant barrier to clinical translation.

Multivalent polymeric display can significantly increase the activity of functional peptides and drugs. Dendrimeric display of folate, for example, has been shown to increase binding avidity up to 5 orders of magnitude.[17] Likewise, multivalent display of apoptotic peptides increased activity by over an order of magnitude.[15,18] Multivalent strategies to increase peptide bioactivity can allow for rational design and optimization of materials for cancer applications.

In this work, peptide copolymers were synthesized via reverse addition-fragmentation chain transfer (RAFT) polymerization of *N*-(2-hydroxypropyl) methacrylamide (HPMA) with methacrylamido-functionalized peptide macromonomers and evaluated in several cancer lines. Two peptide sequences were used, the KLA apoptotic sequence and a GKRK targeting ligand for p32, a mitochondrial protein frequently overexpressed on the surface of tumor cells,[19] isolated from phage display. Two peptide-HPMA copolymers with differing display of the peptides were evaluated: (i) pHGcK, a copolymer of GKRK, KLA, and HPMA, and (ii) pHGfK, a copolymer of GKRK-KLA fusion peptide and HPMA. These polymers were evaluated for *in vitro* cellular toxicity, plasma membrane disruption, intracellular trafficking, and inhibition of mitochondrial respiration.

6.2 Materials and Methods

6.2.1 Materials

N-(2-hydroxypropyl)methacrylamide (HPMA) was purchased from Polysciences (Warrington, PA). The initiator VA-044 was purchased from Wako Chemicals (Richmond, VA). Fmoc-protected amino acids and HBTU were purchased from AAPPTec (Louisville, KY), N-succinimidyl methacrylate from TCI America (Portland, Oregon), and Rink Amide Resin from EMD Biosciences (Darmstad, Germany). All other materials were reagent grade or better and were purchased from Sigma-Aldrich (St. Louis, MO) unless otherwise stated.

6.2.2 Synthesis of peptide monomers

Three peptides were synthesized using (D) and (L) amino acids and 6-aminohexanoic acid (Ahx): Ahx(D)[KLAKLAK]$_2$ (composed of only (D) amino acids); AhxGKRK(D)[KLAKLAK]$_2$

(composed of (L) amino acid uptake sequence GKRK with (D)-amino acid KLA); and AhxGKRK (composed of only (L) amino acids). Peptides were synthesized on solid support with Rink amide linker following standard Fmoc chemistry on an automated PS3 peptide synthesizer (Protein Technologies, Phoenix, AZ). Prior to peptide cleavage from the resin, the amino termini of the peptides were deprotected and coupled with N-succinimidyl methacrylate. These functionalized peptide monomers are respectively called MaAhxKLA, MaAhxGKRK-KLA, and MaAhxGKRK. Synthesized peptides were cleaved from resin by treatment of solid support with a solution of TFA/H_2O/triisopropylsilane (TIPS)/1,3-dimethoxybenzene (90:2.5:2.5:5, v/v/v) for 2.5 hours under gentle mixing. Cleaved peptide monomers were precipitated in cold ether, dissolved in methanol and re-precipitated twice in cold ether. Each peptide monomer was purified to > 95% purity using RP-HPLC and analyzed by MALDI-TOF MS.

6.2.3 Polymer synthesis

Four polymers were synthesized: HPMA-*co*-(MaAhxGKRK-KLA) (pHGfK), HPMA-*co*-MaAhxKLA-*co*-MaAhxGKRK (pHGcK), and two HPMA-*co*-MaAhxGKRK copolymers (pHG35k, pHG64k). pHGfK, pHGcK, and pHG35k were synthesized with a monomer to chain transfer agent ratio of 142 and pHG64k with a ratio of 226; all polymers had 10% peptide mole feed. Monomers were dissolved in 9:1 acetate buffer (1 M, pH 5.1):ethanol (v/v) such that the final monomer concentration of the solution was 0.7 M. The RAFT chain transfer agent (CTA) used was ethyl cyanovaleric trithiocarbonate (ECT, molecular weight 263.4 g/mol) and the initiator (I) used was VA-044. The molar ratios of total monomer:CTA:I at the start of polymerization were 142:1:0.1 and 226:1:0.1, respectively. The reaction solutions were transferred to round bottom flasks, capped with a rubber septum, purged with argon for 10 min, and the submerged in a 44 °C oil bath to initiate polymerization. The polymerization was allowed to proceed for 24 hrs. The flasks were removed from the oil bath and polymers dialyzed against distilled H_2O to removed unreacted monomers and buffer salts. The dialyzed polymers were lyophilized dry.

6.2.4 Guanidinylation of peptide and polymers

15 mg of the pHGcK and pHGfK copolymers and 12 mg of AcAhxKLA were dissolved in 1 mL

of half-saturated $NaHCO_3$. 60 mg of o-methylisourea was dissolved in 1 mL of half-saturated $NaHCO_3$ and added to each solution. Guanidinylation reaction was allowed to proceed at room temperature under stirring for 3 days. After 3 days, polymer reactions were dialyzed again distilled H_2O to purify. Guanidinylated peptide was purified by RP-HPLC and analyzed by MALDI-TOF MS.

6.2.5 Size exclusion chromatography

Molecular weight analysis was carried out by size exclusion chromatography. The copolymers were dissolved at 2 mg/mL in running buffer (150 mM acetate buffer, pH 4.4) for analysis by size exclusion chromatography-multiangle laser light scattering (SEC-MALLS). Analysis was carried out on an OHpak SB-804 HQ column (Shodex, New York, NY) in line with a miniDAWN TREOS multiangle light scattering detector (Wyatt, Santa Barbara, CA) and an OptiLab rEX refractive index detector (Wyatt). Absolute molecular weight averages (M_n, M_w) were calculated using ASTRA software (Wyatt).

6.2.6 Amino acid analysis

The polymer composition was determined through modified amino acid analysis following the method of Bidlingmeyer and coworkers.[20] Briefly, hydrolyzed polymer samples were run on a ZORBAX Eclipse Plus C18 (Agilent Technologies, Santa Clara, CA) HPLC column with pre-column derivatization using o-phthalaldehyde/β-mercaptopropionic acid to label hydrolyzed amino acids and 1-amino-2-propanol (hydrolyzed HPMA). Calibration curves were generated using serial dilutions of (L)-lysine, (L)-arginine, and reagent grade 1-amino-2-propanol.

6.2.7 ^{3}H-pHGfK radiolabeling

pHGfK was ^{3}H-labeled using ^{3}H-acetic anhydride. 5 mg of polymer was dissolved in 500 µL of 5% triethylamine in N,N-dimethylformamide. 2.5 µL of H^3-acetic anhydride was added and reaction allowed to proceed under mixing for 2 hrs. Polymer was precipitated in ice-cold ether, dissolved in methanol and re-precipitated twice in ice-cold ether.

6.2.8 Polymer cytotoxicity

The cytotoxicity of the polymers was evaluated *in vitro* using the MTS assay. GL261 (murine glioma), SNB-19 (human glioblastoma), and HeLa (human cervical cancer) cells were plated overnight in 96-well plates at a density of 3000, 1500, and 2500 cells per well per 0.1 mL growth media, respectively. Polymers of various concentrations were prepared in phosphate buffered saline (PBS) and then diluted 10-fold in complete growth media. The cells were rinsed once with PBS and incubated with 100 μL of the polymer solution for 48 hrs at 37 ºC, 5% CO_2. At 48 hrs, 20 μL of 3-(4,5-dimethylthiazol-2-yl)-5-(3-carboxymethoxyphenyl)-2-(4-sulfophenyl)-2*H*-tetrazolium (MTS) (Promega, Madison, WI) was added to each well. Cells were then incubated for 3 hrs and absorbance measured at 1.5 hrs and 3 hrs at 490 nm using a plate reader (Tecan Safire^2, Männerdorf, Switzerland). IC_{50} values were determined using a nonlinear fit (four-parameter variable slope) in GraphPad Prism v.6 (San Diego, CA).

6.2.9 Hemolysis assay

A hemolysis assay was used to evaluate the membrane-lytic activity of the synthesized materials following the procedure described by Hoffman and co-workers.[21] Briefly, plasma from freshly isolated human blood was removed by centrifugation. The cell layer containing the erythrocytes was washed three times with 150 mM NaCl and resuspended into phosphate buffer at pH 7.4. 16 μL of polymer at various concentrations and 1% Triton X-100 as control were added to 184 μL of erythrocyte suspensions in a 96-well conical plate and incubated for 1 h at 37 °C. The plate was then centrifuged, pelleting intact erythrocytes, and 100 μL of supernatant transferred to a 96-well flat bottom plate. Released hemoglobin within the supernatant was measured at 541 nm absorbance and percent hemolysis was calculated relative to the Triton X-100 control. Experiments were performed in triplicate.

6.2.10 Cellular uptake and subcellular fractionation

Subcellular fractionation experiments were completed as previously described by Shi et al with minor modifications.[22] HeLa cells were seeded in 150 mm^2 dishes at 5×10^6 cells per 20 mL media

per dish 24 h prior to the start of the experiment. Radiolabeled pHGfK was added to cells for a final concentration of 1 mM polymer and incubated for 6 hrs at 37 °C, 5% CO_2. After a 6 h incubation, media was collected. Cells will be washed once with PBS, incubated with CellScrub (Genlantis, San Diego, CA) for 15 min at room temperature, washed twice in DPBS (no $MgCl_2$, $CaCl_2$), lifted off the plates in PBS, and then transferred to conical tubes. To remove dead/compromised cells, cells were washed twice with PBS, pelleting cells at 500*g* for 5 min after each wash. The cells were washed once with homogenization buffer (HB) (250 mM sucrose, 10 mM HEPES-NaOH, 1 mM EDTA, pH 7.4), pelleting the cells at 1000*g* for 6 min. The resulting pellet was then resuspended in 2.5x the wet pellet mass of HB (containing 1X protease inhibitors). Cells were homogenized with a 25-gauge needle until greater than 90% cell lysis was achieved.

Fractionation into a nuclear (N), heavy mitochondrial (HM), light mitochondrial (LM), microsomal (MF), and cytosolic (C) fractions was completed via differential centrifugation as previously described [22]. Briefly, the cell lysate was centrifuged at 1000*g* for 10 min. The resulting pellet (N) was resuspended in HB and centrifuged again. The remaining post-nuclear supernatant (PNS) was combined from both washes, and centrifuged at 3000*g*, 15,000*g*, and 100,000*g*, each with a wash step, to yield the HM, LM, MF pellets and C supernatant. For radioactivity analysis, samples were mixed with Ultima Gold XR scintillation fluid (Perkin Elmer, Waltham, MA), and then analyzed for radioactivity using a Beckman LS-6500 scintillation counter (Beckman Coulter Inc, Pasadena, CA).

6.2.11 Mitochondrial respiration assay

Mitochondria were isolated using established protocols with minor modifications.[23] Four confluent T225 flasks of SNB-19 cells were trypsinized, collected, and pelleted at 400g for 5 min at 4 °C. The cell pellet was washed twice with ice-cold Isolation Buffer (70 mM sucrose, 220 mM mannitol, 5 mM HEPES, 1 mM EGTA, pH 7.2, 0.5% (w/v) fatty-acid free BSA). The resulting pellet was resuspended in 3x the wet pellet volume in Isolation Buffer containing 1X Roche Complete Protease Inhibitor Cocktail (Roche, Basel, Switzerland). The cells were homogenized by 15 passes through a 26-gauge needle and the homogenate was centrifuged twice at 600g for 10 min at 4 °C, discarding the pellet (unbroken cells and nuclei) each time. The supernatant was centrifuged at 7000g for 10 min at 4 °C, the supernatant (lysosomes and microsomes) discarded,

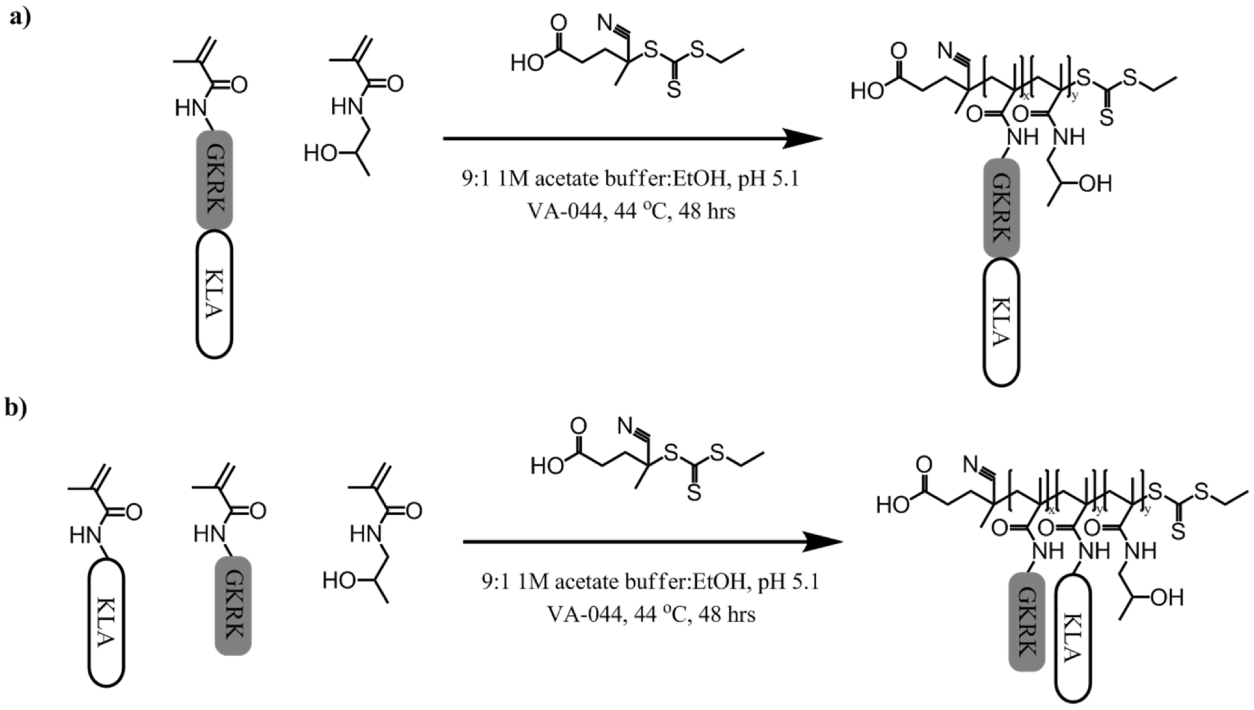

Scheme 6.1. Synthetic scheme of (a) pHGfK and (b) pHGcK.

and the pellet resuspended in Isolation Buffer and centrifuged again at 7000g for 10 min at 4 °C. The supernatant was removed, leaving a concentrated crude mitochondrial pellet. The pellet was resuspended in 120 µL of Measurement Buffer (250 mM sucrose, 15 mM KCl, 1 mM EGTA, 5 mM $MgCl_2$, 30 mM K_2HPO_4, pH 7.4).

Mitochondrial respiration was studied using the Mito-ID® O_2 Extracellular Sensor Kit (Enzo Life Sciences, Farmingdale, NY) with minor modifications to manufacturer's protocol. For each condition tested, 3 µL of mitochondria suspension was diluted to 30 µL with Measurement Buffer in a 96 well plate. 25 µL of 0.53 mM peptide or equivalent polymer concentration was added to the mitochondria solutions and incubated at room temperature for 20 min. After 20 min, 100 µL of O_2 sensor probe and 50 µL of 6.6 mM ADP/100 mM succinate in Measurement Buffer were added to each well following manufacturer's protocol. 100 µL of oil was added on top of each well and then the plate was incubated at 30 °C for 10 min prior to beginning reading fluorescence. Fluorescence at ex/em 380/650 nm was read every 1.5 min for 30 min. Materials were tested in triplicate.

Table 6.1. Properties of HPMA-Peptide Copolymers

Peptide-HPMA Copolymer	Abbrev.	Mn (kDa)[a]	M_w/M_n[a]	% GKRK[b]	% KLA[b]	% GK-KLA[b]
HPMA-*co*-MaAhxGKRK-*co*-MaAhxKLA	pHGcK	49.3	1.1	7.86	7	---
HPMA-*co*-MaAhxGKRK-KLA	pHGfK	55.7	1.18	---	---	12.13
HPMA-*co*-MaAhxGKRK	pHG35k	35.5	1.15	9.1	---	---
HPMA-co-MaAhxGKRK	pHG64k	63.6	1.2	10.2	---	---

[a]Determined by SEC-MALLS. [b]Determined by amino acid analysis.

6.3 Results and discussion

6.3.1 Polymer characterization

Two KLA-containing HPMA copolymers and two control HPMA-*co*-GKRK copolymers were synthesized via RAFT polymerization of methacrylamido-functionalized peptide monomers with HPMA to investigate the effects of multivalent display on cellular toxicity of KLA (Scheme 6.1). Polymers contained the GKRK p32 targeting sequence either as a separate comonomer (pHGcK) or fused with the KLA pro-apoptotic sequence (pHGfK). Degree of polymerization was chosen to target polymers around 50 kDa in size in order to be below the renal filtration threshold. HPMA was copolymerized to provide an inert, hydrophilic backbone.

The molecular weight and composition of the synthesized copolymers are summarized in Table 6.1. Copolymers were synthesized with narrow polydispersities (≤ 1.2). KLA-containing copolymers were around 50 kDa and control polymers lacking the KLA sequence (pHG35k and pHG64k) about 35.5 kDa and 63.6 kDa, respectively. Polymers contained 7-12% peptide, near quantitative incorporation of peptides (~10%) based on molar feed, as determined by amino acid analysis. pHG35k and pHG64k polymers served as cationic polymer controls lacking the KLA sequence.

6.3.2 Polymer cytotoxicity

The IC_{50} values (concentration of polymer for 50% growth inhibition) of acetylated KLA peptide, acetylated GK-KLA peptide (GKRK targeting sequence fused with KLA), and KLA polymers were determined in three cancer cell lines - HeLa (human adenocarcinoma), SNB-19 (human

Table 6.2. Peptide and polymer IC_{50} values

	GL261		SNB-19		HeLa	
Peptide or Polymer	**IC_{50} (μg/mL)**	**IC_{50} (μM KLA)**	**IC_{50} (μg/mL)**	**IC_{50} (μM KLA)**	**IC_{50} (μg/mL)**	**IC_{50} (μM KLA)**
KLA[1]	314.3	165.8	115.1	60.7	> 500	> 250
GK-KLA[2]	182.1	73.6	65.1	26.3	84.9	34.3
pHGcK	25.7	5.4	11.7	2.5	22.0	4.4
pHGfK	20.1	5.4	11.2	3	18.8	5.0

[1]Full peptide sequence: AcAhx-D[KLAKLAK]$_2$. [2]Full peptide sequence: AcAhxGKRK-D[KLAKLAK]$_2$

glioblastoma), and GL261 (murine glioma) - with results summarized in Table 6.2. Cell viability following incubation with a range of material concentrations was determined by MTS assay, a measure of metabolic activity. The SNB-19 cell line was most sensitive to KLA toxicity (IC_{50} = 60 μM) while the HeLa cell line was least sensitive to KLA toxicity (IC_{50} > 250 μM). The fusion peptide GK-KLA, which includes the GKRK targeting peptide to increase cell uptake, showed ~2-5-fold lower IC_{50} compared to KLA. This result confirms previous reports where conjugation of GKRK to KLA was shown to enhance mitochrondrial localization and cellular apoptosis.[16,19] Administration of the two KLA copolymers resulted in a 20-70 fold decrease in IC_{50} values compared to KLA, indicating enhanced cytotoxicity (Table 6.2); this result is consistent with prior reports of increased toxicity due to multivalent display of pro-apoptotic peptides, such as BH3,[18] KLA,[15,16] and antimicrobial peptides,[24] relative to monomeric peptides. Interestingly, the architectural display of the two peptide sequences does not affect the cytotoxicity of the polymers – pHGfK and pHGcK show nearly-identical IC_{50} values for all cell types tested despite differences in peptide display as either individual or fused sequences. This suggests that targeting ligands can be fused to KLA sequences in polymeric constructs without compromising KLA activity, simplifying material synthesis.

Cytotoxic cationic polymers can exert their toxicity through plasma and mitochondrial membrane disruption.[25] To evaluate whether the increased toxicity observed with pHGcK and pHGfK copolymers was due to the cationic nature of the polymers resulting from multivalent display of the GKRK targeting ligand, two copolymers of HPMA and GKRK were synthesized as controls. pHG35k was synthesized with the same monomer:CTA ratio as the KLA copolymers and pHG64k was synthesized with target molecular weight of 50 kDa. Neither pHG copolymer demonstrated dose-dependent cytotoxicity at mass concentrations up to 100-fold higher than the

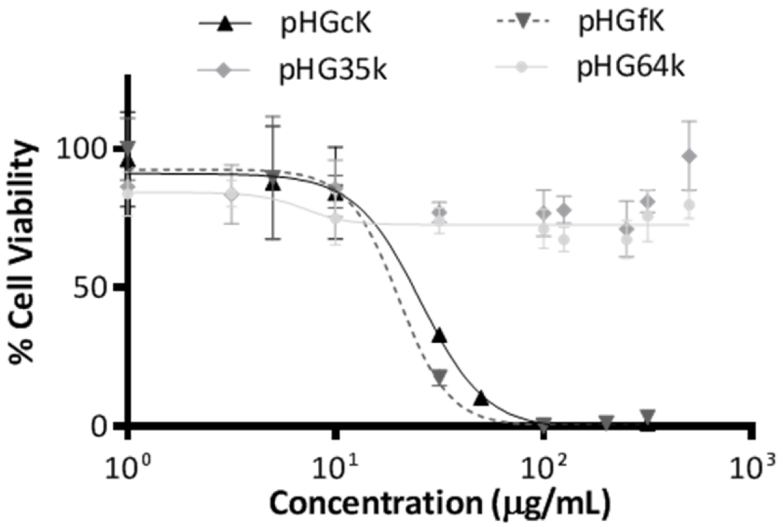

Figure 6.1. Cytotoxicity curves for various peptide-HPMA copolymers in SNB-19 cells.

IC_{50} values of the two KLA copolymers (Figure 6.1). KLA copolymer cytotoxicity is therefore likely due to the KLA sequence and not the cationic targeting sequence.

6.3.3 Hemolysis assay

To investigate the route of cellular toxicity, the ability of the pHGcK and pHGfK copolymers to lyse plasma membranes was determined via hemolysis assay. Polymers were incubated with freshly isolated human erythrocytes and tested for plasma membrane disruption by detecting hemoglobin release (Figure 6.2). Minimal hemolysis was observed for both copolymers at concentrations an order of magnitude higher than the IC_{50} values for the cancer lines. Observed cellular toxicity is therefore likely not due to direct plasma membrane disruption. Cationic polymers containing membrane-active domains have shown hemolysis at concentrations as low as 1 μg/mL.[26] High cationic charge density is correlated with plasma membrane disruption;[27] KLA materials possibly differ in membrane lytic characteristics due to lower charge density.

Interestingly, the manner of GKRK display affected the membrane-lytic behavior of the KLA-containing copolymers. pHGfK, with the GKRK sequence fused to KLA, shows significantly higher membrane-lytic behavior; at 100 μg/mL, pHGfK induces 13% hemoglobin

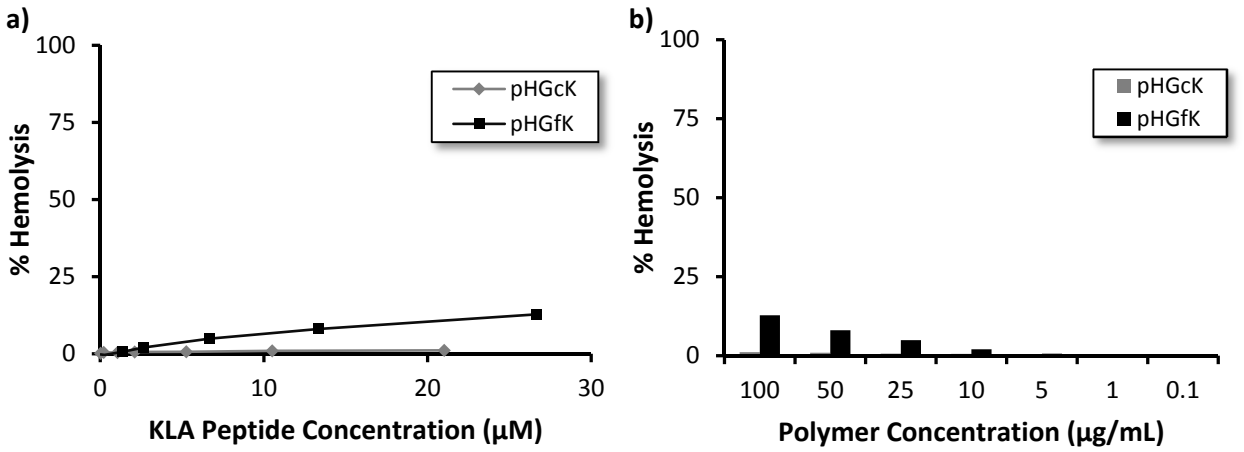

Figure 6.2. Percent hemolysis of pHGck and pHGfK polymers relative to Triton X-100 control in (a) KLA molar concentration and (b) polymer mass concentration.

release when incubated with erythrocytes, whereas pHGcK induces < 2% hemoglobin release at the same mass concentration (Figure 6.2b). However, despite differences in hemolytic activity, the IC_{50} values are similar. pHGcK has more charge delocalization due to spatial separation of the GKRK and KLA sequences along the polymer backbone; comparatively, the two sequences are fused together in pHGfK. This could lead to differences in membrane specificity and lytic activity. We previously have shown that 60 kDa HPMA-oligolysine copolymers demonstrated differences in cytotoxicity based on pendant oligolysine chain length despite keeping the overall charge/mass ratio constant.[28] Therefore, molecular architecture may play a significant role in cytotoxicity.

6.3.4 Cellular uptake and intracellular trafficking

The cellular uptake and intracellular localization of pHGfK were investigated through subcellular fractionation of radiolabeled polymer. ^{3}H-labeled pHGfK was incubated with HeLa cells for 6 hrs at 37 ºC and then cells were washed, lysed, and relative radioactivity measured in the various fractions. Less than 3% of polymer was found to be cell associated, with about 2% surface bound and less than 1 % internalized after 6 hrs (Figure 6.3a). Low cellular association and poor internalization therefore pose significant barriers towards the efficacy of these polymers. Similarly, low uptake was seen with the cationic polymer PEI, where 5% cellular association was observed

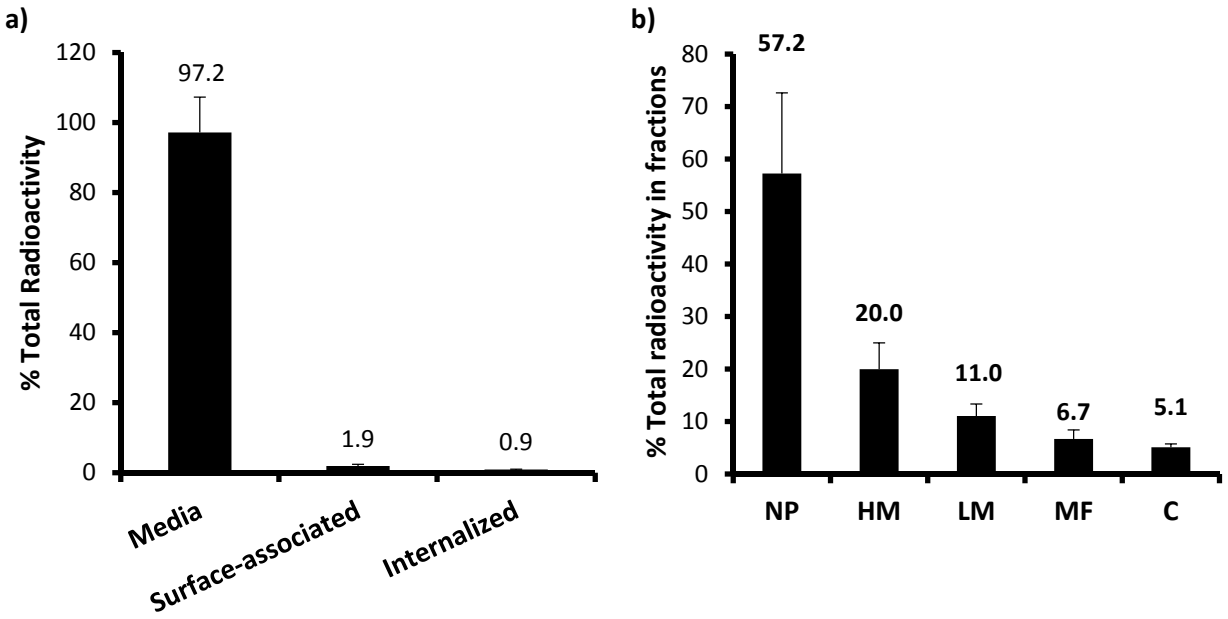

Figure 6.3. (a) [^{3}H]-labeled pHGfK copolymer uptake in HeLa cells after 6 hr incubation at 37 °C. (b) Subcellular fractionation and localization of polymer in HeLa cell lysates after 6 hr exposure to polymers n. NP = nuclear pellet; HM = heavy mitochondria; LM = light mitochondria; MF = microsomes; C = cytosol.

in HeLa cells after 4 hrs, suggesting cationic polymers may not be efficiently internalized.[22]

The cellular lysate was fractionated via differential centrifugation (Figure 6.3b) to determine intracellular distribution of the polymer after a 6 hr incubation with cells. Of the internalized polymer, 20% was found in the heavy mitochondrial fraction that contains intact mitochondria while 11% and 7% were found respectively in the light mitochondrial and microsomal fractions, which contain some mitochondria with other intracellular membrane vesicles including lysosomes, Golgi membranes, and endosomes.[29] Only 5% remained in the cytosol. In comparison, a cationic HPMA-peptide polymer with similar structure to pHGfK except displaying oligolysine instead of the GK-KLA peptide, showed lower distribution in the HM fraction (12%).[30] The GKRK sequence has been shown to bind to p32 overexpressed on many cancer lines, including glioblastoma;[19] GKRK-functionalized nanoworms have previously been shown to traffic to mitochondria in several glioblastoma cell lines.[16] This sequence may contribute towards increased trafficking of the pHGfK polymer to mitochondria compared to the HPMA-oligolysine polymers.

Table 6.3. Guanidinylated peptide and polymer IC_{50} values

	SNB-19		HeLa	
Peptide or Polymer	**IC_{50} (µg/mL)**	**IC_{50} (µM KLA)**	**IC_{50} (µg/mL)**	**IC_{50} (µM KLA)**
hRKLA	10.64	4.95	---------	---------
pHGchR	41.4	10.78	26.78	6.98
pHGfhR	44.7	10.72	26.33	6.38

6.3.5 Guanidinylation of KLA polymers

Due to the poor efficiency of cell uptake (Figure 3), pHGcK and pHGfK were guanidinylated in an attempt to increase cell internalization. Guandinylation of chitosan[31] and aminoglycosides[32] has previously been shown to significantly increase cellular uptake. In addition, a fusion peptide of oligoarginine (R_7) with KLA was shown to have more potent cytotoxic properties and to enhance permeabilization and aggregation of mitochondria.[12,33] We therefore hypothesized that conversion of the primary lysine amines of pHGcK and pHGfK to guanidines would increase cellular uptake and therefore cytotoxicity. The lysine residues on pHGcK and pHGfK were converted to homoarginine via reaction with o-methylisourea to yield guanidinylated polymer analogs pHGchR and pHGfhR, respectively.[34] Amino acid analysis confirmed complete lysine conversion as noted by the disappearance of the lysine peak and the concurrent emergence of a distinct homoarginine peak (data not shown). The toxicity of these constructs was evaluated *in vitro* in HeLa and SNB-19 cells. For both cell lines, guanidinylated polymers demonstrated 2-4 fold decrease in cytotoxicity compared to the original KLA polymers (Table 6.3). This was in contrast to guanidinylated KLA peptide (hRLA) which had significantly higher cytotoxicity (over 10-fold decrease in IC_{50}) than KLA in SNB-19 cells (Table 6.3). Additionally, HPMA-KLA copolymers lacking the GKRK sequence showed very low cytotoxicity with IC_{50} > 300 µg/mL in HeLa cells (data not shown). Therefore, the lower cytotoxicity of the guanidinylated polymers could be due to the guanidinylation of the GKRK sequence which negatively affects uptake, trafficking, and cytotoxicity, or due to reduced mitochondrial disruption due to guanidinylation of the KLA sequence.

6.3.6 Effect of polymers on mitochondrial respiration

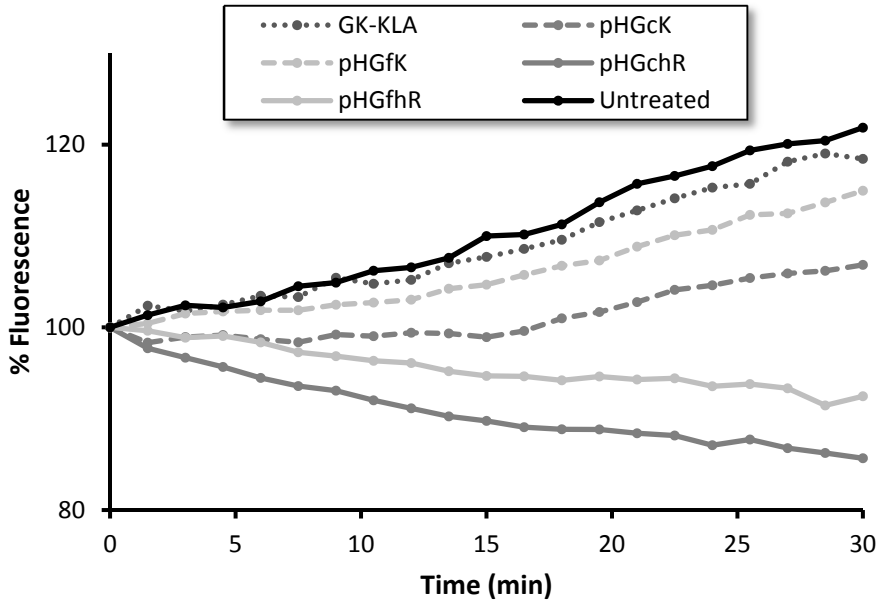

Figure 6.4. Relative fluorescence of an O_2-sensitive fluorescence probe as a measure of mitochondrial function in isolated mitochondria treated with the various polymers.

The effect of pHGcK and pHGfK and guanidinylated analogs pHGchR and pHGfhR on mitochondrial activity was therefore determined using an assay for oxygen consumption from isolated mitochondria. The function of isolated mitochondria was monitored for 30 minutes following incubation with polymers or peptide using an oxygen-sensitive, phosphorescent probe (Figure 6.4). Oxygen consumption, which correlates directly with mitochondrial respiration, was decreased by 17% when treated with GK-KLA peptide, and by 69% and 32% when treated with pHGcK and pHGfK polymers, respectively. Guanidinylated polymers have a much greater effect on mitochondrial function; no oxygen consumption was observed and slightly decreased signal, attributed to probe photobleaching, was seen. These results suggest that guanidinylation of KLA-containing polymers increases mitochondrial disruption activity but that overall cytotoxicity may be reduced due to altered intracellular trafficking. Lipophilicity and charge distribution were shown to affect cellular uptake and intracellular trafficking of cationic materials.[35] Additionally, guanidine groups bind more strongly to sulfates than primary amines, which may result in greater binding to membrane proteins such as heparan sulfates and therefore reduced trafficking to mitochondria.[36]

6.4 Conclusions and future studies

In this work, p32-targeted polymers displaying multiple pendant pro-apoptotic KLA peptides were synthesized and tested for their cytotoxicity. Targeting sequences were presented in the polymers either as fusion sequences with KLA or as separate monomers. Differences in display of the targeting peptide did not affect overall polymer toxicity; polymeric constructs are at least 10-fold more potent against cancer cell lines compared to KLA peptide. The internalization efficiency and intracellular trafficking of one polymeric KLA construct was determined by radiolabeling with subcellular fractionation analysis. Cellular uptake and intracellular localization studies show < 1% of dosed polymer is internalized within 6 hrs but that ~20% of internalized polymer is localized to fractions containing intact mitochondria. Guanidinylation of the copolymers was investigated to improve cellular uptake but despite improved ability to disrupt the function of isolated mitochondria, cytotoxicity of the guanidinylated polymers decreased relative to the original polymers. Thus, while polymeric display of pro-apoptotic peptides improves potency, there is significant room for improving uptake and mitochondrial targeting efficiency.

6.5 Acknowledgements

This was work was supported by NIH 1R01CA177272. David Chu was supported by a NIH T32 training grant (NIH CA138312). Julie Shi was supported by the National Science Foundation Graduate Research Fellowship under Grant No. DGE-0718124. We thank Profs. Anthony Convertine and Patrick Stayton for generous donation of the ECT chain transfer agent.

6.6 References

(1) Holland, E. C.: Glioblastoma multiforme: the terminator. *Proc Natl Acad Sci USA* **2000**, *97*, 6242-6244.

(2) Stupp, R.; Hegi, M. E.; Gilbert, M. R.; Chakravarti, A.: Chemoradiotherapy in malignant glioma: standard of care and future directions. *J Clin Oncol* **2007**, *25*, 4127-4136.

(3) Eramo, A.; Ricci-Vitiani, L.; Zeuner, A.; Pallini, R.; Lotti, F.; Sette, G.; Pilozzi, E.; Larocca, L. M.; Peschle, C.; De Maria, R.: Chemotherapy resistance of glioblastoma stem cells. *Cell Death Differ* **2006**, *13*, 1238-1241.

(4) Papo, N.; Shai, Y.: Host defense peptides as new weapons in cancer treatment. *Cell Mol Life Sci* **2005**, *62*, 784-790.

(5) Mader, J. S.; Hoskin, D. W.: Cationic antimicrobial peptides as novel cytotoxic agents for cancer treatment. *Expert Opin Investig Drugs* **2006**, *15*, 933-946.

(6) Nicolas, P.; Mor, A.: Peptides as weapons against microorganisms in the chemical defense system of vertebrates. *Annu Rev Microbiol* **1995**, *49*, 277-304.

(7) Hoskin, D. W.; Ramamoorthy, A.: Studies on anticancer activities of antimicrobial peptides. *BBA-Biomembranes* **2008**, *1778*, 357-375.

(8) Zasloff, M.: Antimicrobial peptides of multicellular organisms. *Nature* **2002**, *415*, 389-395.

(9) Sovadinova, I.; Palermo, E. F.; Urban, M.; Mpiga, P.; Caputo, G. A.; Kuroda, K.: Activity and mechanism of antimicrobial peptide-mimetic amphiphilic polymethacrylate derivatives. *Polymers* **2011**, *3*, 1512-1532.

(10) Leuschner, C.; Hansel, W.: Membrane disrupting lytic peptides for cancer treatments. *Curr Pharm Des* **2004**, *10*, 2299-310.

(11) Ellerby, H. M.; Arap, W.; Ellerby, L. M.; Kain, R.; Andrusiak, R.; Del Rio, G.; Krajewski, S.; Lombardo, C. R.; Rao, R.; Ruoslahti, E.; Bredesen, D. E.; Pasqualini, R.: Anti-cancer activity of targeted pro-apoptotic peptides. *Nat Med* **1999**, *5*, 1032-1038.

(12) Law, B.; Quinti, L.; Choi, Y.; Weissleder, R.; Tung, C.-H.: A mitochondrial targeted fusion peptide exhibits remarkable cytotoxicity. *Mol Cancer Ther* **2006**, *5*, 1944-1949.

(13) Mai, J. C.; Mi, Z.; Kim, S.-H.; Ng, B.; Robbins, P. D.: A proapoptotic peptide for the treatment of solid tumors. *Cancer Res* **2001**, *61*, 7709-7712.

(14) Alves, I. D.; Carré, M.; Montero, M.-P.; Castano, S.; Lecomte, S.; Marquant, R.; Lecorché, P.; Burlina, F.; Schatz, C.; Sagan, S.; Chassaing, G.; Braguer, D.; Lavielle, S.: A proapoptotic peptide conjugated to penetratin selectively inhibits tumor cell growth. *BBA-Biomembranes* **2014**, *1838*, 2087-2098.

(15) Adar, L.; Shamay, Y.; Journo, G.; David, A.: Pro-apoptotic peptide-polymer conjugates to induce mitochondrial-dependent cell death. *Polym Advan Technol* **2011**, *22*, 199-208.

(16) Agemy, L.; Friedmann-Morvinski, D.; Kotamraju, V. R.; Roth, L.; Sugahara, K. N.; Girard, O. M.; Mattrey, R. F.; Verma, I. M.; Ruoslahti, E.: Targeted nanoparticle enhanced proapoptotic peptide as potential therapy for glioblastoma. *Proc Natl Acad Sci USA* **2011**, *108*, 17450-17455.

(17) Hong, S.; Leroueil, P. R.; Majoros, I. J.; Orr, B. G.; Baker Jr, J. R.; Banaszak Holl, M. M.: The binding avidity of a nanoparticle-based multivalent targeted drug delivery platform. *Chem Biol* **2007**, *14*, 107-115.

(18) Richter, M.; Chakrabarti, A.; Ruttekolk, I. R.; Wiesner, B.; Beyermann, M.; Brock, R.; Rademann, J.: Multivalent design of apoptosis-inducing bid-BH3 peptide–oligosaccharides boosts the intracellular activity at identical overall peptide concentrations. *Chemistry* **2012**, *18*, 16708-16715.

(19) Agemy, L.; Kotamraju, V. R.; Friedmann-Morvinski, D.; Sharma, S.; Sugahara, K. N.; Ruoslahti, E.: Proapoptotic peptide-mediated cancer therapy targeted to cell surface p32. *Mol Ther* **2013**, *21*, 2195-2204.

(20) Bidlingmeyer, B. A.; Cohen, S. A.; Tarvin, T. L.: Rapid analysis of amino acids using pre-column derivatization. *J Chromatogr* **1984**, *336*, 93-104.

(21) Bulmus, V.; Woodward, M.; Lin, L.; Murthy, N.; Stayton, P.; Hoffman, A.: A new pH-responsive and glutathione-reactive, endosomal membrane-disruptive polymeric carrier for intracellular delivery of biomolecular drugs. *J Control Release* **2003**, *93*, 105-120.

(22) Shi, J.; Chou, B.; Choi, J. L.; Ta, A. L.; Pun, S. H.: Investigation of polyethylenimine/DNA polyplex transfection to cultured cells using radiolabeling and subcellular fractionation methods. *Mol Pharm* **2013**, *10*, 2145-2156.

(23) Wieckowski, M. R.; Giorgi, C.; Lebiedzinska, M.; Duszynski, J.; Pinton, P.: Isolation of mitochondria-associated membranes and mitochondria from animal tissues and cells. *Nat Protoc* **2009**, *4*, 1582-1590.

(24) Chamorro, C.; Boerman, M. A.; Arnusch, C. J.; Breukink, E.; Pieters, R. J.: Enhancing membrane disruption by targeting and multivalent presentation of antimicrobial peptides. *BBA-Biomembranes* **2012**, *1818*, 2171-2174.

(25) Chu, D. S. H.; Schellinger, J. G.; Shi, J.; Convertine, A. J.; Stayton, P. S.; Pun, S. H.: Application of living free radical polymerization for nucleic acid delivery. *Acc Chem Res* **2012**, *45*, 1089-1099.

(26) Schellinger, J. G.; Pahang, J. A.; Johnson, R. N.; Chu, D. S.; Sellers, D. L.; Maris, D. O.; Convertine, A. J.; Stayton, P. S.; Horner, P. J.; Pun, S. H.: Melittin-grafted HPMA-oligolysine based copolymers for gene delivery. *Biomaterials* **2013**, *34*, 2318-2326.

(27) Frohlich, E.: The role of surface charge in cellular uptake and cytotoxicity of medical nanoparticles. *Int J Nanomedicine* **2012**, *7*, 5577-5591.

(28) Johnson, R. N.; Chu, D. S.; Shi, J.; Schellinger, J. G.; Carlson, P. M.; Pun, S. H.: HPMA-oligolysine copolymers for gene delivery: optimization of peptide length and polymer molecular weight. *J Control Release* **2011**, *155*, 303-311.

(29) Graham, J. M.: Purification of a crude mitochondrial fraction by bensity-gradient centrifugation. In *Current Protocols in Cell Biology*; John Wiley & Sons, Inc., 2001.

(30) Shi, J.; Choi, J. L.; Chou, B.; Johnson, R. N.; Schellinger, J. G.; Pun, S. H.: Effect of polyplex morphology on cellular uptake, intracellular trafficking, and transgene expression. *ACS Nano* **2013**, *7*, 10612-10620.

(31) Zhai, X.; Sun, P.; Luo, Y.; Ma, C.; Xu, J.; Liu, W.: Guanidinylation: a simple way to fabricate cell penetrating peptide analogue-modified chitosan vector for enhanced gene delivery. *J Appl Polym Sci* **2011**, *121*, 3569-3578.

(32) Luedtke, N. W.; Carmichael, P.; Tor, Y.: Cellular uptake of aminoglycosides, guanidinoglycosides, and poly-arginine. *J Am Chem Soc* **2003**, *125*, 12374-12375.

(33) Lemeshko, V. V.: Potential-dependent membrane permeabilization and mitochondrial aggregation caused by anticancer polyarginine-KLA peptides. *Arch Biochem Biophys* **2010**, *493*, 213-220.

(34) Carlson, P. M.; Schellinger, J. G.; Pahang, J. A.; Johnson, R. N.; Pun, S. H.: Comparative study of guanidine-based and lysine-based brush copolymers for plasmid delivery. *Biomater Sci* **2013**, *1*, 736-744.

(35) Yousif, L. F.; Stewart, K. M.; Horton, K. L.; Kelley, S. O.: Mitochondria-penetrating peptides: sequence effects and model cargo transport. *ChemBioChem* **2009**, *10*, 2081-2088.

(36) Fromm, J. R.; Hileman, R. E.; Caldwell, E. E. O.; Weiler, J. M.; Linhardt, R. J.: Differences in the interaction of heparin with arginine and lysine and the importance of these basic Amino acids in the binding of heparin to acidic fibroblast growth factor. *Arch Biochem Biophys* **1995**, *323*, 279-287.

Chapter 7

DEVELOPMENT OF CYCLIC, TARGETED APOPTOTIC PEPTIDE-POLYMERS FOR TREATMENT OF GLIOBLASTOMA MULTIFORME

David S.H. Chu, Chayanon Ngambenjawong, Robert C. Rostomily, Suzie H. Pun

Abstract

Glioblastoma multiforme (GBM), the most common and deadly form of primary malignant brain tumor, lacks effective therapies. Pro-apoptotic peptides, such as KLA, have shown promise but low activity and rapid renal clearance limit clinical translation. In this work, novel cyclic peptide-polymers were developed to investigate the effects of cyclic architecture on peptide bioactivity. Multivalent peptide-polymers containing KLA and VTW, a GBM targeting peptide, were prepared by RAFT copolymerization of *N*-(2-hydroxypropyl) methacrylamide (HPMA), *N*-(3-aminopropyl) methacrylamide (APMA), and TMS-propargyl methacrylamide (TPMA) using an alkyne-functionalized chain transfer agent. Linear polymers were cyclized via copper-catalyzed "click" and peptides attached by orthogonal bioconjugation. Peptide copolymers were selectively toxic to GBM cells, showing no dose-dependent toxicity for HeLa cells. Molecular weight was shown to affect the bioactivity of cyclic polymers relative to linear analogs, with higher molecular weight cyclic polymers having increased potency compared to linear analogs.

7.1 Introduction

Glioblastoma multiforme is the most common form of primary brain cancer, but aggressive therapeutic regiments have made relatively minor improvements to the dismal prognosis of GBM over the past few decades.[1] GBM, characterized by pervasive intrusion into adjacent neural tissue, strong chemotherapeutic resistance, and anti-apoptotic phenotype, is amongst the most lethal of cancers with median survival around 9-12 months.[2-4] Current standard of care consisting of aggressive surgical resection (when tolerated) in combination with radiochemotherapy yields a modest 2-4 month increased median survival.[5,6]

Current chemotherapy regimens using alkylating agents such as carmustine and temozolomide have had limited clinical efficacy due to commonly-upregulated MGMT (methylguanine methyltransferase) expression that repairs DNA alkylation damage.[5] *In vitro* cultures of neoplastic and p53 deficient cells suggest rates of genetic mutations as high as 1/1000 cells for any given gene,[2] demonstrating that GBM maintains an aggressive proliferative phenotype despite genomic instability and heterogeneity. Therefore, therapeutic strategies divergent from DNA mutagenesis may hold promise for GBM treatment.

One alternative therapeutic strategy utilizes antimicrobial peptides as cytotoxic agents for cancer therapy; intracellular delivery of these peptides can induce mitochondrial dysfunction.[7] Mitochondrial membranes, similar in composition to bacterial membranes, are disrupted upon exposure to antimicrobial peptides, inducing mitochondrial release of cytochrome to initiate cellular apoptosis via the caspase cascade.[7] Several reported antimicrobial peptides, such as the KLA sequence (D[KLAKLAK]$_2$), induce transient pore formation and permeabilize mitochondrial membranes in a local peptide concentration-dependent manner.[7,8] Additionally, these materials have been investigated in several studies on GBM models both *in vitro* and *in vivo* and have shown promise in tumor reduction.[9-11] However, high intracellular concentrations required for therapeutic effects pose a significant barrier.

Polymeric display of apoptotic peptides can increase bioactivity and improve pharmacokinetics. Nanoworms displaying the KLA peptide increased cytotoxicity by several hundred fold *in vitro* and induced tumor regression in GBM xenograft models;[9] however, these nanoparticles had poor intratumoral penetration due to their large size. Multivalent display of BH3,[12] KLA,[9,10] and other antimicrobial peptides[13] have similarly shown increased bioactivity

compared to monomeric peptides. Methods to mediate intracellular delivery and further enhance the bioactivity of these peptides are therefore desirable.

Architecture can significantly affect the activity of polymeric carriers for peptide delivery. Constrained architectures, such as dendrimers and hyperbranched polymers, have shown increased activity of grafted ligands compared to linear analogues. Cyclic polymers are a relatively new class of materials being explored due to their interesting physical properties. Like dendrimers and hyperbranched polymers, cyclic polymers exhibit distinctive static and dynamic properties, including smaller hydrodynamic volumes, lower viscosities, and higher glass transition temperatures.[14] When administered systemically, they have longer circulation half-life than linear analogues.[15] Recent advances in polymer chemistry have made these materials scalable and tunable with regards to size and functionalization.[16,17] Additionally, cyclic homopolymers,[18] statistical copolymers, and block copolymers[19] have all been successfully synthesized. We recently demonstrated that cyclic cationic polymers of poly(2-dimethylaminoethyl methacrylate) have stronger DNA complexation and comparable transfection efficiency relative to linearly analogues but with significantly reduced cellular toxicity.[18] Therefore, cyclic architecture can potentially improve linear drug delivery platforms currently under investigation.

To date, cyclic polymers have primarily been generated by intramolecular ring-closure of linear polymers.[16] Azide-alkyne "click" chemistry has been shown to be an efficient and robust ring-closure strategy for α,ω -heterodifunctional polymers.[20] Living radical polymerizations such as atom transfer radical polymerization (ATRP) and reversible addition-fragmentation chain transfer (RAFT) polymerization are particularly well-suited for preparing cyclic polymers due to low polydispersity and control over end-group functionality.[16] ATRP has been investigated more extensively for synthesizing cyclic polymers since alkyne-functionalized initiators combined with simple post-polymerization azido conversion of the ω-terminal halide allows for efficient synthesis of heterobifunctional telechelic linear polymers. However, ATRP is limited by incompatibility with carboxylic acid or primary amine-containing monomers, and polymerization of certain monomer types, such as methacrylamides, are difficult to control.[21]

In comparison, RAFT polymerization is amenable to (1) reactions under mild conditions, including aqueous buffer, (2) cationic, anionic, and peptide macromonomers; and (3) a wide range of monomer types, including acrylates, methacrylates, acrylamides, and methacrylamides.[22,23] However, to date, there have been only a handful of reports regarding cyclic polymers synthesized

via RAFT strategies; additionally, to our knowledge, there have not been any published reports regarding cyclic polymers functionalized with bioactive molecules.

In this work, we report the synthesis of statistical cyclic copolymers containing *N*-(2-hydroxypropyl) methacrylamide (HPMA), KLA, and a glioblastoma targeting ligand (VTW), to study the effects of cyclic polymer architecture on peptide bioactivity. We previously demonstrated that methacrylamido-functionalized KLA peptides can be efficiently copolymerized with HPMA and the resulting polymers demonstrated over an order of magnitude increased cytotoxicity relative to free peptides in three cancer lines (Chapter 6). We further this work by including a glioblastoma-specific targeting ligand and investigate the effects of polymer molecular weight and architecture on activity. Cyclic, targeted pro-apoptotic polymers were synthesized via reversible addition-fragmentation chain transfer (RAFT) polymerization of HPMA, *N*-(3-aminopropyl) methacrylamide (APMA), and TMS-propargyl methacrylamide (TPMA) followed by post-polymerization ring closure of linear precursors to yield cyclic polymers. KLA and VTW were grafted post-cyclization via orthogonal conjugation chemistries. The synthesized peptide-polymer panel was evaluated for cytotoxicity *in vitro*.

7.2 Materials and Methods

7.2.1 Materials

HPMA and APMA were purchased from Polysciences (Warrington, PA). The initiator VA-044 was purchased from Wako Chemicals (Richmond, VA). 4,4'-aziobis(4-cyanovaleric acid) (ACVA) was purchased from MP Biomedical (Santa Ana, CA). Fmoc-protected amino acids, NovaPEG Rink Amide Resin, and HCTU were purchased from EMD Millipore (Billerica, MA) and N-succinimidyl methacrylate from TCI America (Portland, Oregon). 4-Cyano-4-(phenylcarbonothioylthio)pentanoic acid (CTP) was purchased from Sigma Aldrich (St. Louis, MO). 3-azido-1-propanol[24] and TPMA[25] were synthesized as previously reported. All other materials were reagent grade or better and were purchased from Sigma-Aldrich (St. Louis, MO) unless otherwise stated.

7.2.2 Synthesis of 4,4'-azobis(azidopropyl 4-cyanopentanoate) (diazido-ACVA)

Diazido-ACVA was synthesized as previously reported with minor modifications.[26] Briefly, ACVA (1 g, 3.4 mmol), 3-azidopropanol (1.08 g, 10.7 mmol) and DMAP (0.35 g, 2.9 mmol) were dissolved in 25 mL of 1:1 DCM:THF and cooled to 4 ºC. DCC (1.62 g, 7.9 mmol) in 10 mL of DCM was added dropwise over 20 minutes using an addition funnel under argon protection. The reaction mixture was stirred at 4 ºC overnight then at room temperature for 1 h. 2 drops of acetic acid were added to the reaction mixture and solution was stirred in the dark for 30 min. The solution was chilled, dicyclohexcylurea (DCU) was removed by filtration, and solvent was removed by rotary evaporation. The residue was extracted with 30 mL of diethyl ether and the ether phase was washed 5x with 20 mL of 0.1 N HCl, 3x with 20 mL saturated sodium bicarbonate, and 2x with 20 mL of ddH_2O. The ether phase was dried with anhydrous $MgSO_4$, filtered, and solvent removed by rotary evaporation to yield a viscous clear oil.

7.2.3 Synthesis of CTP-alkyne

200 mg of CTP (279.38 Da, 0.72 mmol), 37.9 mg of DMAP (122.17 Da, 0.31 mmol), and 165 mg of DCC (206.33 Da, 0.8 mmol) were added to a 50 mL round bottom flask and dissolved in 20 mL of DCM. 63 µL of propargyl alcohol (1.08 mmol) was added to the mixture and the reaction was allowed to proceed for 24 hrs at room temperature. After 24 hrs, the reaction mixture was cooled and DCU removed by filtration. The solution was concentrated by rotary evaporation to yield a deep red oil. The oil was dissolved in 60:40 acetonitrile: ddH_2O and purified via RP-HPLC using a Synergi C18 Fusion column (Phenomenex, Torrance, CA) with an isocratic 60:40 acetonitrile:ddH_2O mobile phase.

7.2.4 Synthesis of Cys-KLA and VTW-N_3 peptides

Two peptides were synthesized using (D) and (L) amino acids; C-KLA (sequence AcC(D)[KLAKLAK]$_2$, composed of N-terminal acetylation, a (L)-cysteine and (D)-amino acid KLA); and VTW-N_3 (sequence NH_2-VTWTPQAWFQWVKKK-K(N_3), composed of an N-terminal amine, only (L) amino acids, and a C-terminal lysine with the ε-amine functionalized with 5-azidopentanoic acid). To synthesize VTW-N_3, Fmoc-L-Lys(Mtt) was first coupled to NovaPEG Rink Amide resin and the Mtt protecting group removed by washing the resin 15x with 1.8% TFA

in DCM for 3 min each wash. 5-azidopentanoic acid was coupled to the deprotected ε-amine using HCTU as the activator. All subsequent amino acid coupling steps were done following standard Fmoc chemistry on an automated PS3 peptide synthesizer (Protein Technologies, Phoenix, AZ). Prior to peptide cleavage from the resin, the amino termini of the C-KLA peptide was deprotected and reacted with acetic anhydride to acetylate the terminus. Synthesized peptides were cleaved from resin by treatment of solid support with a solution of TFA/H_2O/triisopropylsilane (TIPS)/1,3-dimethoxybenzene/1,2-ethanedithiol (EDT) (87.5:2.5:2.5:5:2.5 v/v/v/v) for 2.5 hours under gentle mixing. Cleaved peptide monomers were precipitated in cold ether, dissolved in MeOH and re-precipitated twice in cold ether. Each peptide monomer was purified to > 95% purity using RP-HPLC and analyzed by MALDI-TOF MS.

7.2.5 p(HAT) RAFT kinetics study

A RAFT kinetic analysis was performed to verify polymerization conditions for the synthesis of p(HPMA-*co*-APMA-*co*-TPMA) (pHAT). 420.4 mg of HPMA (143.2 Da, 2.94 mmol), 60.1 mg of APMA (178.7 Da, 0.34 mmol), 19.7 mg of TPMA (195.11 Da, 0.10 mmol), 3.58 mg of CTP-alkyne (318 Da, 0.011 mmol), and 0.36 mg of VA-044 (323 Da, 0.0011 mmol) were dissolved in 2:1 1 M acetate buffer pH 5.1:DMF to a final volume of 3.365 mL for a monomer concentration of 1 M. The reaction solution was aliquoted equally into 4 pear-shaped flasks. Each reaction vessel was septum capped, purged for 10 min with argon, sealed with parafilm, and allowed to react in a 44 ºC oil bath for various amounts of time. At a given time point, the reaction was terminated by exposure to air. The reaction solutions were purified by precipitation into cold acetone 3x.

7.2.6 p(HAT) linear polymer synthesis

Two linear pHAT polymers were synthesized varying in the target degree of polymerization (DP). Monomer ratios of 88:10:2 (HPMA:APMA:TPMA) were used. Monomers were dissolved in 2:1 1 M acetate buffer, pH 5.1:DMF to a 1 M monomer concentration. For DP70, the monomer:CTP-alkyne:VA-044 ratio was 70:1:0.1 and for DP200 it was 200:1:0.1. The reaction solutions were transferred to round bottom flasks, capped with a rubber septum, purged with argon for 10 min, and the submerged in a 44 °C oil bath to initiate polymerization. DP70 polymers were polymerized

for 20 hrs and DP200 for 24 hrs. The polymers solutions were precipitated 3x in acetone to remove unreacted monomers.

7.2.7 Synthesis of pHAT-N_3

The ω-terminus of linear pHAT copolymers was converted to N_3 groups via radical end-capping using diazido-ACVA. pHAT copolymers were dissolved to a concentration of 1 mM polymer in DMF + 1% AcOH in a round bottom flask and 40 eq of diazido-ACVA was added. The reaction was capped, purged with argon for 20 min, and then immersed in a 70 °C oil bath for 4 hrs under gentle stirring. The end-capped polymer was recovered by precipitation in cold ether followed by centrifugation. The pellet was re-dissolved in MeOH and precipitated 2x in cold ether.

7.2.8 Cyclization of pHAT-N_3

Cyclic pHAT copolymers (cpHAT) were synthesized via azide-alkyne Huisgen "click" cycloaddition under very dilute conditions. For the DP70 copolymer, 100 mL of ddH_2O was added to a 250 mL triple head flask with a stir bar and condenser. The flask was immersed in a 100 °C oil bath and the reaction solution stirred vigorously. The water was purged for 45 min with nitrogen. 96 mg of sodium ascorbate and 80 mg of $CuSO_4 \cdot 7H_2O$ was added to the flask and the solution quickly changed to an orange-brown color. 20 mg of pHAT-N_3 was dissolved in 16 mL of ddH_2O and purged with argon for 20 min. The polymer solution was loaded into a 30 mL syringe under argon protection. The syringe was then inserted into the triple head flask and the polymer solution added slowly over 2 days using a syringe pump under gentle, continuous nitrogen purging. For the DP200 copolymer, 60 mL of ddH_2O was added to the triple headed flask. 48.3 mg of $CuSO_4 \cdot 7H_2O$ and 57.6 mg of sodium ascorbate were added. 20 mg of polymer was dissolved in 15 mL of ddH_2O, purged with argon for 20 min, loaded into a 30 mL syringe and slowly added over 2 days using a syringe pump.

After 2 days, the reaction solution was filtered using a 0.22 filter to remove copper precipitates, the volume concentrated via rotary evaporation, and then the sample dialyzed against distilled H_2O for 2 days. Product was recovered by lyophilization.

7.2.9 Conjugation of C-KLA peptide onto linear and cyclic pHAT

C-KLA peptide was grafted onto linear and cyclic pHAT copolymers via thiol-maleimide chemistry. 10 mg of the linear and cyclic pHAT copolymers were dissolved in 250 µL of DMF. 9 mg of maleimidopropionic acid NHS ester (5 eq) was dissolved in 250 µL of DMF and added to the polymers. Reaction was allowed to proceed at room temperature for 3 hrs. Polymer was precipitated in cold ether and washed 2x with acetone.

10 mg of maleimide-functionalized pHAT was dissolved in 500 µL of pH 6 PBS. 21 mg of C-KLA peptide (2 eq) was dissolved in 500 µL of pH 6 PBS and added to the pHAT polymer solutions. The reaction proceeded at room temperature for 4 hrs under gentle stirring. The polymers were then dialyzed against distilled water to purify.

7.2.10 Conjugation of VTW-N_3 peptide

VTW-N3 peptide was conjugated onto the pHAT copolymers via copper-catalyzed "click" reaction. First, TPMA was deprotected by treating polymer with 0.1 M tetrabutylammonium fluoride (TBAF) in DMF for 4 hrs. Polymer was recovered by precipitation in ether and pellet was washed 2x with 1:1 acetone:ether.

Polymer (10 mg, deprotected) was dissolved in 1 mL of ddH_2O and transferred to a 5 mL conical flask. 5 mg of VTW-N3 peptide (5 eq) was dissolved in 20 µL of ddH_2O and added to the reaction flask. Flask was purged with argon for 10 min. 1.373 mg of $CuSO_4 \cdot 7H_2O$ (10 eq) and 1.634 mg of sodium ascorbate (15 eq) were added to the reaction flasks and solutions were purged with argon for an additional 5 min. Reactions proceeded at room temperature for 48 hrs under gentle stirring. Precipitated copper was filtered out and product was purified by dialysis against distilled H_2O.

7.2.11 Size exclusion chromatography

Molecular weight analysis was carried out by size exclusion chromatography. The copolymers were dissolved at 2 mg/mL in running buffer (1:1 300 mM acetate buffer, pH 4.4:MeOH) for analysis by size exclusion chromatography-multiangle laser light scattering (SEC-MALLS).

Analysis was carried out on an OHpak SB-804 HQ column (Shodex, New York, NY) in line with a miniDAWN TREOS multiangle light scattering detector (Wyatt, Santa Barbara, CA) and an OptiLab rEX refractive index detector (Wyatt). Absolute molecular weight averages (M_n, M_w) were calculated using ASTRA software (Wyatt).

7.2.12 Amino acid analysis

The actual incorporated amount of peptide and HPMA in the final copolymers was determined through modified amino acid analysis following the method of Bidlingmeyer and coworkers.[27] Briefly, hydrolyzed polymers were run on a ZORBAX Eclipse Plus C18 (Agilent Technologies, Santa Clara, CA) HPLC column using pre-column derivatization with o-phthalaldehyde/β-mercaptopropionic acid to label hydrolyzed amino acids and 1-amino-2-propanol (hydrolyzed HPMA). Calibration curves were generated using serial dilutions of (L)-leucine, (L)-threonine, and reagent grade 1-amino-2-propanol.

7.2.13 Polymer cytotoxicity

The cytotoxicity of the polymers were evaluated *in vitro* using the MTS assay. SNB-19 (human GBM) and HeLa (human cervical cancer) cells were plated overnight in 96-well plates at a density of 3500 cells per well in 0.1 mL of growth media. Polymers at various concentrations were prepared in phosphate buffered saline (PBS) and then diluted 10-fold in complete growth media. The cells were rinsed once with PBS and incubated with 100 µL of the polymer solution for 48 hrs at 37 ºC, 5% CO_2. After 48 hrs, 20 µL of 3-(4,5-dimethylthiazol-2-yl)-5-(3-carboxymethoxyphenyl)-2-(4-sulfophenyl)-2*H*-tetrazolium (MTS) (Promega, Madison, WI) was added to each well. Cells were then incubated for 37 °C and absorbance measured after 2 hrs at 490 nm with 670 nm reference wavelength using a plate reader (Tecan Safire^2, Männerdorf, Switzerland). For polymers, IC_{50} values were determined using a nonlinear fit (four-parameter variable slope) in GraphPad Prism v.6 (San Diego, CA).

7.3 Results and discussion

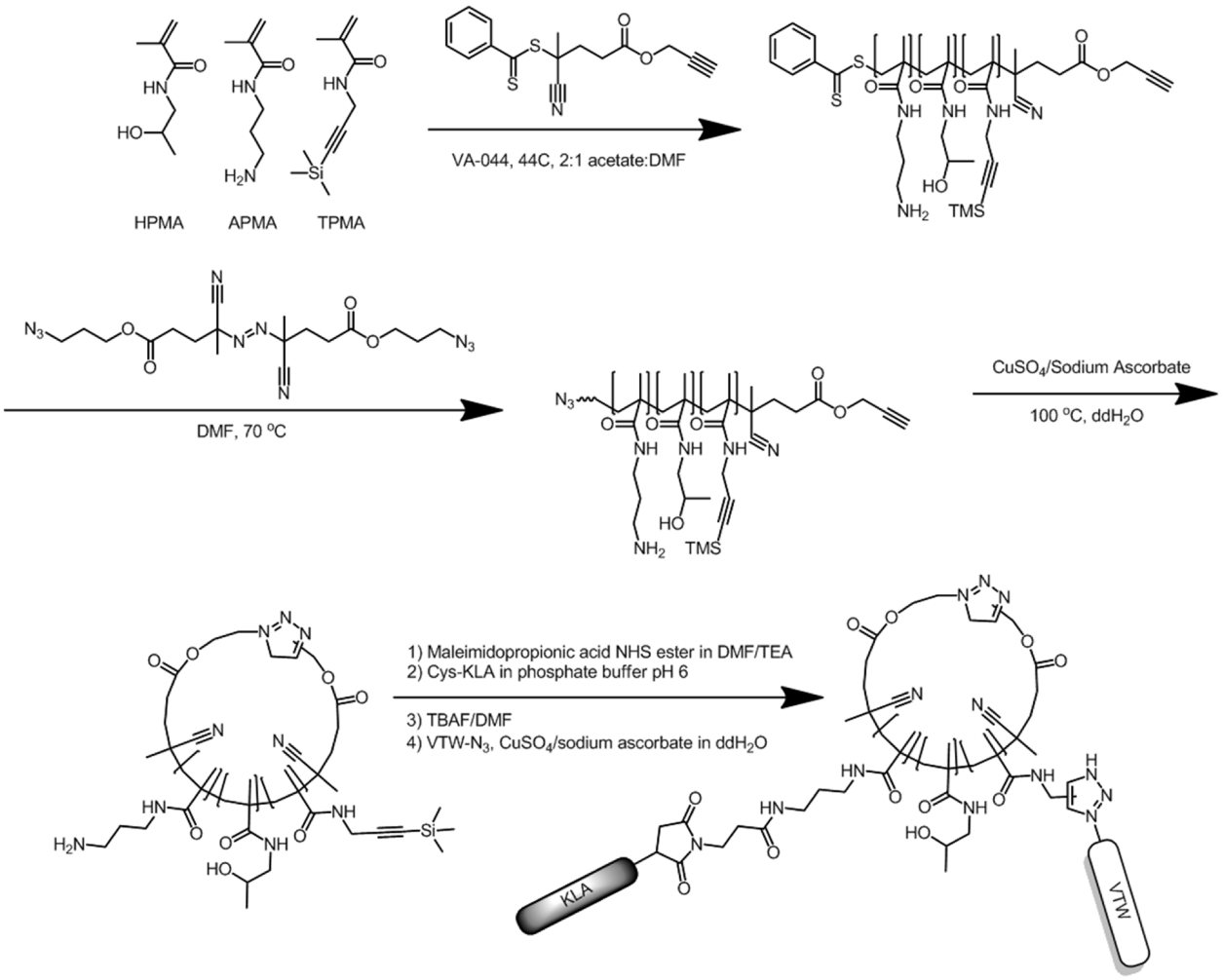

Scheme 7.1. Synthetic scheme for cyclic peptide-polymers.

7.3.1 Polymer synthesis and characterization

Cyclic HPMA-peptide copolymers were synthesized by (i) RAFT copolymerization of *N*-(2-hydroxypropyl) methacrylamide (HPMA), *N*-(3-aminopropyl) methacrylamide hydrochloride (APMA), and TMS-propargyl methacrylamide (TPMA) followed by conversion of the ω–terminus to an azide, (ii) intrachain "click" cyclization of the α-alkyne-ω-azide linear polymers, (iii) deprotection of TPMA monomers and conversion of APMA monomers to maleimide functional groups, and (iv) grafting of targeting and pro-apoptotic peptides via orthogonal conjugation chemistries (Scheme 7.1). Two cyclic polymers varying in molecular weight were

Table 7.1. Properties of pHAT copolymers

Copolymer	% APMA Feed	% TPMA Feed	DP	Mn (kDa)[a]	PDI[a]
pHAT DP70	10	2	70	14.5	1.08
cpHAT DP70	10	2	70	11.7	1.04
pHAT DP200	10	2	200	33.2	1.06
cpHAT DP200	10	2	200	29.6	1.11

[a]Determined by SEC-MALLS.

synthesized to investigate the effects of cyclic architecture on cellular toxicity of the pro-apoptotic peptide.

To generate cyclic polymers, linear copolymers were first synthesized by RAFT polymerization using an alkyne-functionalized chain transfer agent, CTP-alkyne. TPMA was synthesized by reaction of propargyl amine with methacryloyl chloride followed by protection of the alkyne with a TMS group as previously reported.[25] APMA provided a primary amine as an orthogonal functional group to the TPMA alkyne to allow for orthogonal conjugation of the two peptides while HPMA served as an inert, hydrophilic comonomer for backbone spacing between the peptide grafting sites. The resulting p(HPMA-*co*-APMA-*co*-TPMA) (pHAT) copolymers had low polydispersity and narrow molecular weight distributions (Table 7.1). A kinetic analysis of the RAFT polymerization demonstrated good control over polymerization, with increasing molecular weight and decreasing polydispersity observed as a function of reaction time (Figure 7.1).

To cyclize linear polymers, a ω-terminal azido group was introduced via radical termination of linear pHAT using a diazido radical initiator. Cyclization of linear polymers was achieved via slow addition of dilute, azido-functionalized linear pHAT to an active copper solution, yielding cyclized polymer as evidenced by delayed elution on aqueous GPC and by decreased Mn (Table 7.1, Figure 7.2). The temperature of the reaction was found significantly affect cyclization efficiency. At lower temperatures, the reaction yielded primarily intermolecular conjugates, as observed by a left-shouldering of the polymer peak by GPC (Figure 7.3), indicating formation of higher molecular weight polymer populations. Increasing the temperature during cyclization resulted in the elimination of the left shoulder and subsequently a right-shift of the polymer peak observed, demonstrating a temperature-dependence on inter- versus intramolecular "click" (Figure 7.3). This increased efficiency at higher temperatures could possibly be due to higher kinetic

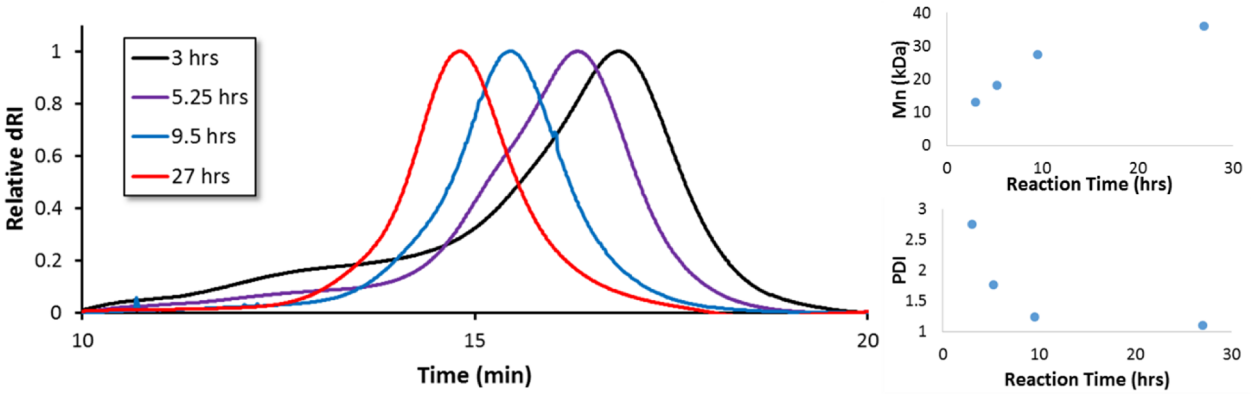

Figure 7.1. RAFT kinetics of p(HPMA-*co*-APMA-*co*-TPMA) as determined by GPC.

energy that overcomes entropic penalties and slow reaction kinetics of cyclization.

Peptides were designed to have orthogonal conjugation chemistries to allow for controlled incorporation into the polymer constructs. N-terminal cysteine modification of the KLA sequence was chosen since our previous work in Chapter 6 suggested that peptide activity is maintained on polymeric constructs following N-terminal conjugation. A C-terminal azido group was added to the VTW peptide by conjugation of 5-azidopentanoic acid to the ε-amine of a C-terminal lysine residue; the C-terminal functionalization was chosen to avoid potential loss of activity related to N-terminal conjugation.

Linear and cyclic pHAT polymers were first functionalized with the apoptotic KLA peptide via thiol-maleimide chemistry. The primary amines of the APMA were converted to thiol-reactive maleimide groups using a heterobifunctional linker and then reacted with cysteine-modified KLA peptide. Following KLA conjugation, TPMA was deprotected by treatment with tetrabutylammonium fluoride (TBAF) and then azido-VTW peptide was conjugated via copper catalyzed "click." Peptide grafting at each step results in near-uniform shifts in GPC traces, confirming successful conjugation (Figure 7.4, Figure 7.5). Final peptide-polymers, referred to as pHKV and cpHKV for linear and cyclic p(HPMA-*co*-KLA-*co*-VTW), respectively, were analyzed by GPC and amino acid analysis and results are summarized in (Table 7.2, Figure 7.4). Monomer ratios of 88:10:2 were based on previous work in Chapter 6 that suggested 10% by mole KLA was sufficient to observe increased activity in KLA-HPMA copolymers. A lower VTW mole % was targeted to avoid potential supramolecular assembly of the polymers driven by the hydrophobicity

Table 7.2. Properties of HPMA-peptide copolymers

Peptide-HPMA Copolymer	Mn (kDa)[a]	M_w/M_n[a]	% KLA[b]	% VTW[b]
pHKV DP70	44.9	1.14	10.1	3.0
cpHKV DP70	28.7	1.17	8.3	1.3
pHKV DP200	74.0	1.30	5.7	1.0
cpHKV DP200	97.8	1.57	6.1	0.6

[a]Determined by SEC-MALLS. [b]Determined by amino acid analysis.

of the peptide sequence. Linear and cyclic polymers were synthesized with comparable peptide incorporation and with slightly increased polydispersity relative to base pHAT, attributed to incomplete peptide coupling.

Cyclic polymers synthesized by ring-closure strategies have been difficult to generate in sizes greater than ~ 10 kDa in size due to high entropic penalties and decreasing ring-closure kinetics with increasing molecular weight, favoring intermolecular chain coupling.[20] However, post-polymerization grafting strategies can allow for generation of high molecular weight polymers with high efficiency; our post-polymerization peptide grafting strategy allowed for successful generation of cyclic peptide-polymers in excess of 50 kDa.

7.3.2 Cytotoxicity of polymer constructs

The cytotoxicity of the synthesized polymers was determined via MTS assay, an indirect measure of mitochondrial activity, in HeLa (human cervical cancer) and SNB-19 (human GBM) cells. A range of polymer concentrations was added to cells in order to determine the IC_{50} value (concentration of polymer for 50% growth inhibition) for each polymer. In SNB-19 cells, there was a slight trend of molecular weight dependence on the relative activity of cyclic polymers compared to their linear analogs. For DP70, higher cytotoxicity is observed with linear polymers, suggesting that the cyclic structure decreased peptide activity; however, in the larger DP200 polymers, cyclic structure show slightly enhanced cytotoxicity.

All polymers showed no dose-dependent toxicity in HeLa cells (Table 7.3, Figure 7.6), demonstrating that the VTW sequence confers specificity for GBM cells. Additionally, toxicity of constructs significantly decreases in SNB-19 cells for polymers lacking the VTW sequence, with over an order of magnitude decreased cytotoxicity (Figure 7.7). Together, this suggests that

Table 7.3. pHKV copolymer cytotoxicity

	SNB-19		HeLa	
Peptide copolymer	**IC_{50} (μg/mL)**	**IC_{50} (μM KLA)**	**IC_{50} (μg/mL)**	**IC_{50} (μM KLA)**
pHKV DP70	25.0	3.5	> 300	> 40
cpHKV DP70	35.4	6.0	> 300	> 40
pHKV DP200	42.0	10.6	> 300	> 40
cpHKV DP200	26.3	7.1	> 300	> 40

polymers are active intracellularly and not through plasma membrane-lytic methods.

7.4 Conclusions and future directions

In this work, a panel of cyclic peptide-polymers varying in molecular weight and peptide composition were synthesized and evaluated for cellular toxicity in two cell lines. As the molecular weight of the cyclic polymers increased, the bioactivity was shown increase relative to linear analogs. The VTW peptide significantly enhanced cytotoxicity in SNB-19 cells while no dose-dependent toxicity was observed in HeLa cells, suggesting high cellular selectivity. Future studies include variation of the peptide densities in these polymer constructs and elucidation of mechanism of cytotoxicity via mitochondrial disruption assays.

7.5 Acknowledgements

David Chu was supported by NIH T32 CA138312. This work was funded by NIH 1R01CA177272-01A1.

7.6 References

(1) Maher, E. A.; Furnari, F. B.; Bachoo, R. M.; Rowitch, D. H.; Louis, D. N.; Cavenee, W. K.; DePinho, R. A.: Malignant glioma: genetics and biology of a grave matter. *Gene Dev* **2001**, *15*, 1311-1333.

(2) Holland, E. C.: Glioblastoma multiforme: the terminator. *Proc Natl Acad Sci USA* **2000**, *97*,

6242-6244.

(3) Wen, P. Y.; Kesari, S.: Malignant Gliomas in Adults. *New Engl J Med* **2008**, *359*, 492-507.

(4) Salmaggi, A.; Boiardi, A.; Gelati, M.; Russo, A.; Calatozzolo, C.; Ciusani, E.; Sciacca, F. L.; Ottolina, A.; Parati, E. A.; La Porta, C.; Alessandri, G.; Marras, C.; Croci, D.; De Rossi, M.: Glioblastoma-derived tumorospheres identify a population of tumor stem-like cells with angiogenic potential and enhanced multidrug resistance phenotype. *Glia* **2006**, *54*, 850-860.

(5) Stupp, R.; Hegi, M. E.; Gilbert, M. R.; Chakravarti, A.: Chemoradiotherapy in Malignant Glioma: Standard of Care and Future Directions. *J Clin Oncol* **2007**, *25*, 4127-4136.

(6) Eramo, A.; Ricci-Vitiani, L.; Zeuner, A.; Pallini, R.; Lotti, F.; Sette, G.; Pilozzi, E.; Larocca, L. M.; Peschle, C.; De Maria, R.: Chemotherapy resistance of glioblastoma stem cells. *Cell Death Differ* **2006**, *13*, 1238-1241.

(7) Ellerby, H. M.; Arap, W.; Ellerby, L. M.; Kain, R.; Andrusiak, R.; Del Rio, G.; Krajewski, S.; Lombardo, C. R.; Rao, R.; Ruoslahti, E.; Bredesen, D. E.; Pasqualini, R.: Anti-cancer activity of targeted pro-apoptotic peptides. *Nat Med* **1999**, *5*, 1032-1038.

(8) Hoskin, D.w.; Ramamoorth, A.: Studies on anticancer activities of antimicrobial peptides. *BBA-Biomembranes* **2008**, *1778*, 357-375.

(9) Agemy, L.; Friedmann-Morvinski, D.; Kotamraju, V. R.; Roth, L.; Sugahara, K. N.; Girard, O. M.; Mattrey, R. F.; Verma, I. M.; Ruoslahti, E.: Targeted nanoparticle enhanced proapoptotic peptide as potential therapy for glioblastoma. *Proc Natl Acad Sci USA* **2011**, *108*, 17450-17455.

(10) Adar, L.; Shamay, Y.; Journo, G.; David, A.: Pro-apoptotic peptide-polymer conjugates to induce mitochondrial-dependent cell death. *Polym Advan Technol* **2011**, *22*, 199-208.

(11) Mai, J. C.; Mi, Z.; Kim, S.-H.; Ng, B.; Robbins, P. D.: A proapoptotic peptide for the treatment of solid tumors. *Cancer Res* **2001**, *61*, 7709-7712.

(12) Richter, M.; Chakrabarti, A.; Ruttekolk, I. R.; Wiesner, B.; Beyermann, M.; Brock, R.; Rademann, J.: Multivalent design of apoptosis-inducing bid-BH3 peptide–oligosaccharides boosts the intracellular activity at identical overall peptide concentrations. *Chemistry* **2012**, *18*, 16708-16715.

(13) Chamorro, C.; Boerman, M. A.; Arnusch, C. J.; Breukink, E.; Pieters, R. J.: Enhancing membrane disruption by targeting and multivalent presentation of antimicrobial peptides. *BBA-Biomembranes* **2012**, *1818*, 2171-2174.

(14) Yamamoto, T.: Synthesis of cyclic polymers and topology effects on their diffusion and thermal properties. *Polym J* **2013**, *45*, 711-717.

(15) Nasongkla, N.; Chen, B.; Macaraeg, N.; Fox, M. E.; Fréchet, J. M. J.; Szoka, F. C.: Dependence of pharmacokinetics and biodistribution on polymer architecture: effect of cyclic versus linear polymers. *J Am Chem Soc* **2009**, *131*, 3842-3843.

(16) Laurent, B. A.; Grayson, S. M.: Synthetic approaches for the preparation of cyclic polymers. *Chem Soc Rev* **2009**, *38*, 2202-2213.

(17) Brown, H. A.; Waymouth, R. M.: Zwitterionic ring-opening polymerization for the synthesis of high molecular weight cyclic polymers. *Acc Chem Res* **2013**, *46*, 2585-2596.

(18) Wei, H.; Chu, D. S.; Zhao, J.; Pahang, J. A.; Pun, S. H.: Synthesis and evaluation of cyclic cationic polymers for nucleic acid delivery. *ACS Macro Lett* **2013**, *2*, 1047-1050.

(19) Piedra-Arroni, E.; Ladavière, C.; Amgoune, A.; Bourissou, D.: Ring-opening Polymerization with Zn(C6F5)2-based lewis pairs: original and efficient approach to cyclic polyesters. *J Am Chem Soc* **2013**, *135*, 13306-13309.

(20) Zhang, J.; Li C; Wang, Y.; Zhuo R.-X.; Zhang, X.-Z.: Controllable exploding microcapsules as drug carriers. *Chem Commun* **2011**, *47*, 4457-4459.

(21) Braunecker, W. A.; Matyjaszewski, K.: Controlled/living radical polymerization: Features, developments, and perspectives. *Prog Polym Sci* **2007**, *32*, 93-146.

(22) Moad, G.; Rizzardo, E.; Thang, S. H.: Living radical polymerization by the RAFT process - a second update. *Aust J Chem* **2009**, *62*, 1402-1472.

(23) Johnson, R. N.; Chu, D. S.; Shi, J.; Schellinger, J. G.; Carlson, P. M.; Pun, S. H.: HPMA-oligolysine copolymers for gene delivery: Optimizotion of peptide length and polymer molecular weight. *J Control Release* **2011**, *155*, 303-311.

(24) Zhang, J.; Li, C.; Wang, Y.; Zhuo, R.-X.; Zhang, X.-Z.: Controllable exploding microcapsules as drug carriers. *Chem Commun* **2011**, *47*, 4457-4459.

(25) Malkoch, M.; Thibault, R. J.; Drockenmuller, E.; Messerschmidt, M.; Voit, B.; Russell, T. P.; Hawker, C. J.: Orthogonal approaches to the simultaneous and cascade functionalization of macromolecules using click chemistry. *J Am Chem Soc* **2005**, *127*, 14942-14949.

(26) Yang, J.; Luo, K.; Pan, H.; Kopečková, P.; Kopeček, J.: Synthesis of biodegradable multiblock copolymers by click coupling of RAFT-generated heterotelechelic polyHPMA conjugates. *React Funct Polym* **2011**, *71*, 294-302.

(27) Bidlingmeyer, B. A.; Cohen, S. A.; Tarvin, T. L.: Rapid analysis of amino acids using pre-column derivatization. *J Chromatogr* **1984**, *336*, 93-104.

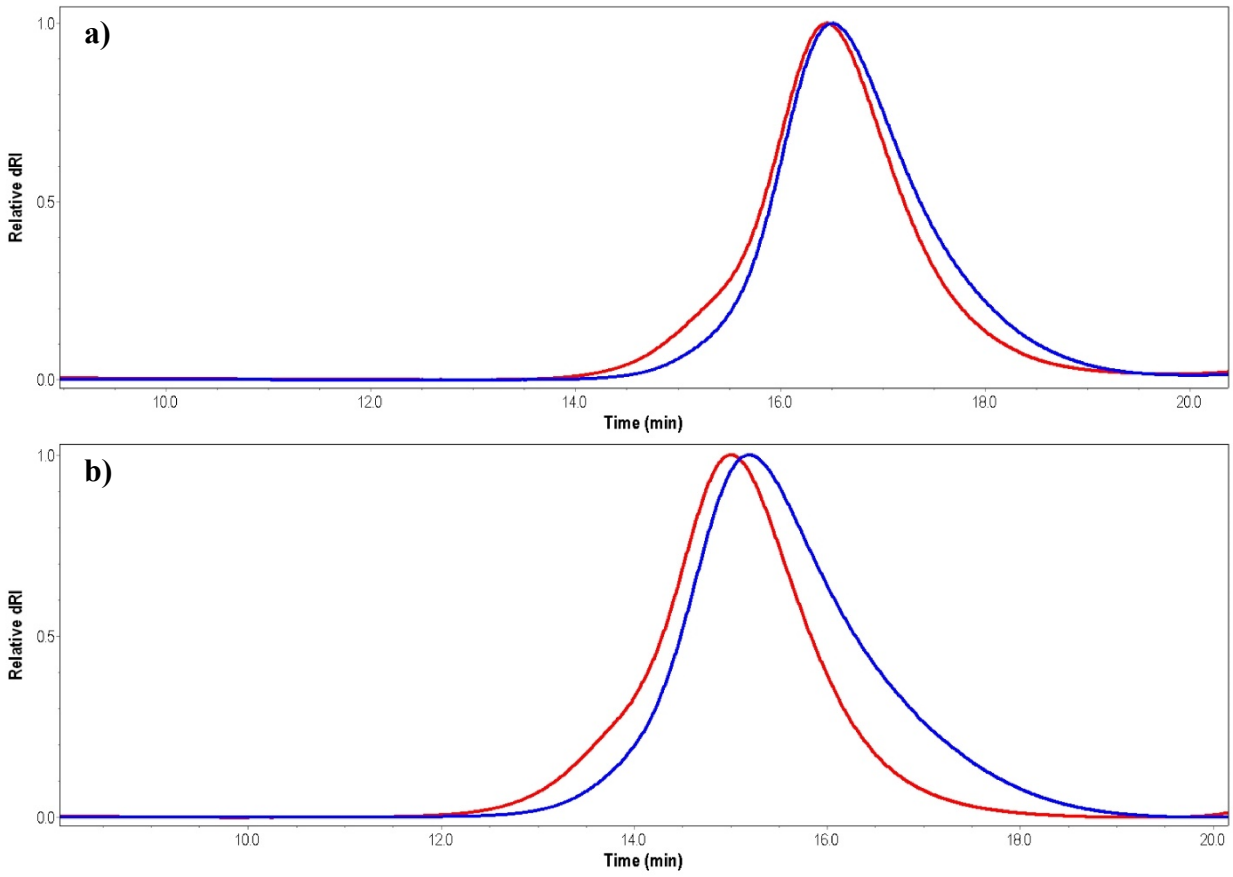

Figure 7.2. Overlaid GPC traces of (a) pHAT DP70 (red) and cpHAT DP70 (blue) and (b) pHAT DP200 (red) and cpHAT DP200 (blue).

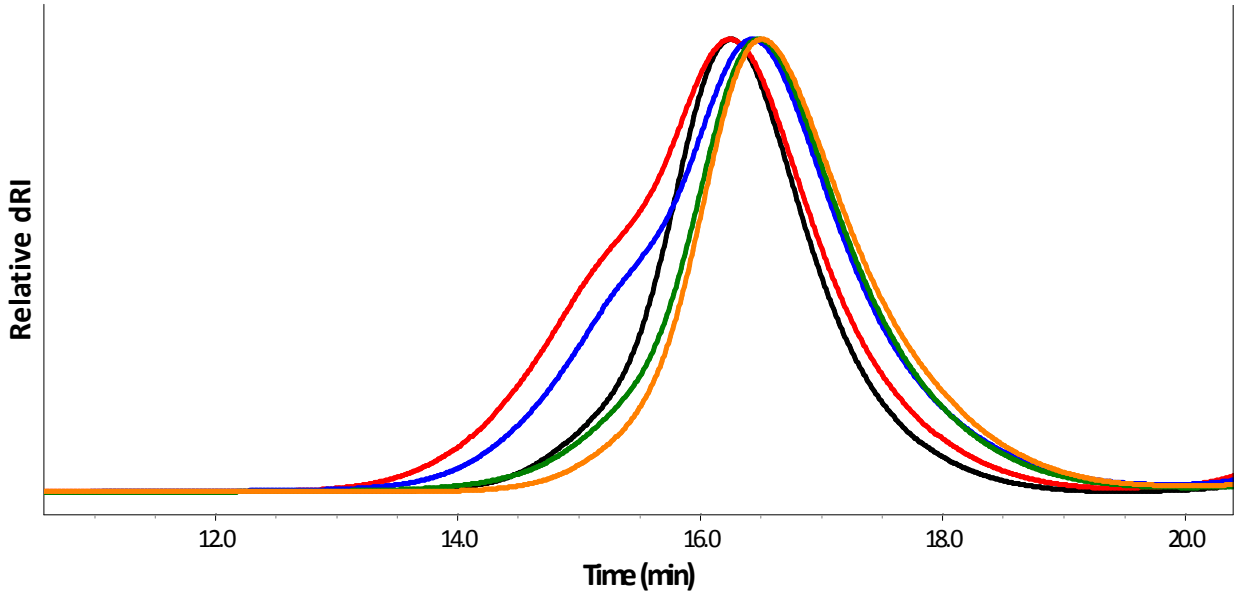

Figure 7.3. Overlaid GPC traces of pHAT DP70 cyclization products at 50 °C (red), 60 °C (blue), 80 °C (green), and 100 °C (orange) compared to unreacted pHAT (black).

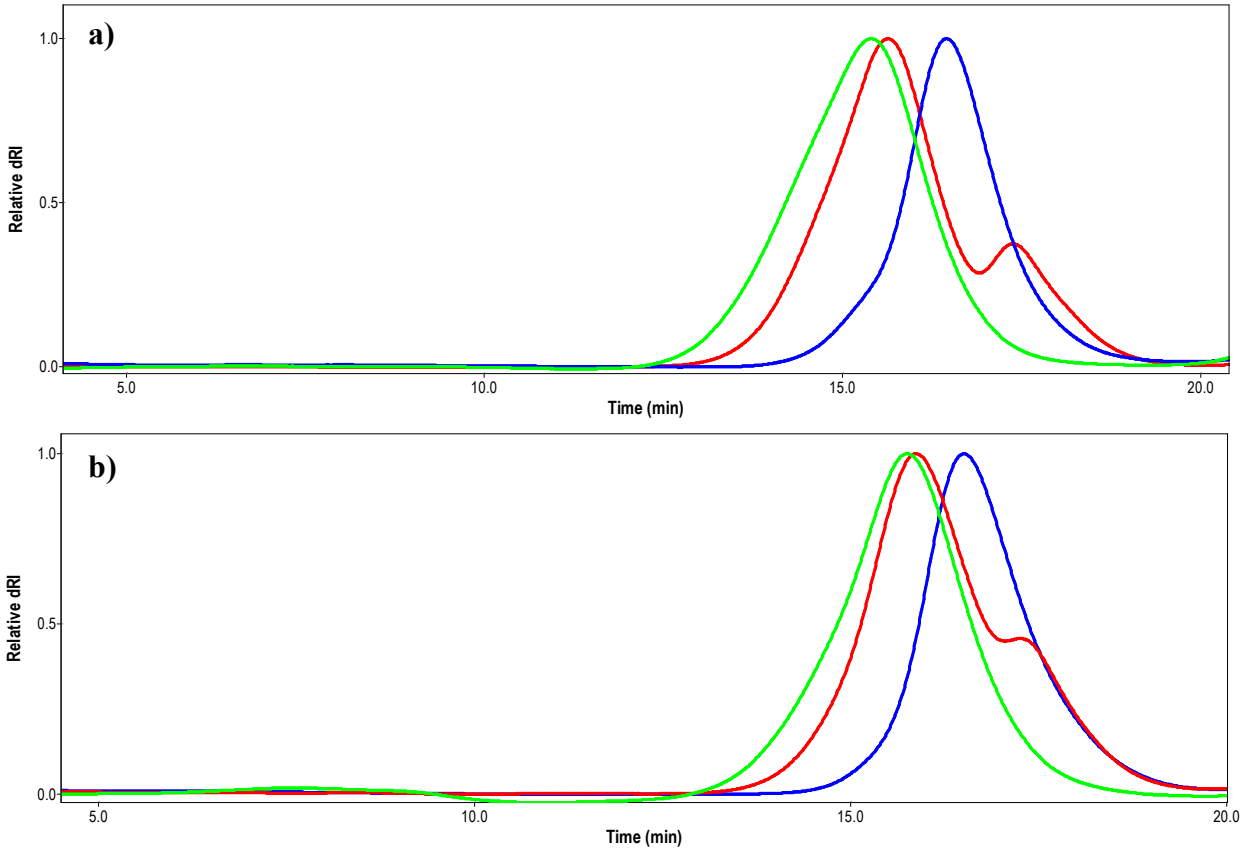

Figure 7.4. (a) Overlaid GPC traces of pHAT DP70 base copolymer (blue), following KLA conjugation (red), and after VTW conjugation (green). (b) Overlaid GPC traces of cpHAT DP70 base copolymer (blue), following KLA conjugation (red), and after VTW conjugation (green).

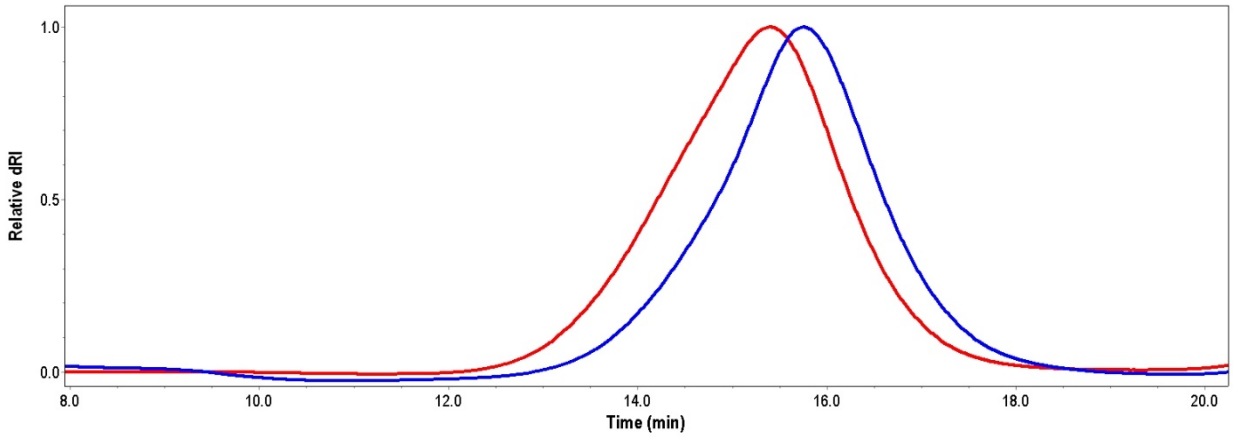

Figure 7.5. Overlaid GPC traces of pHKV DP70 (red) and cpHKV DP70 (blue).

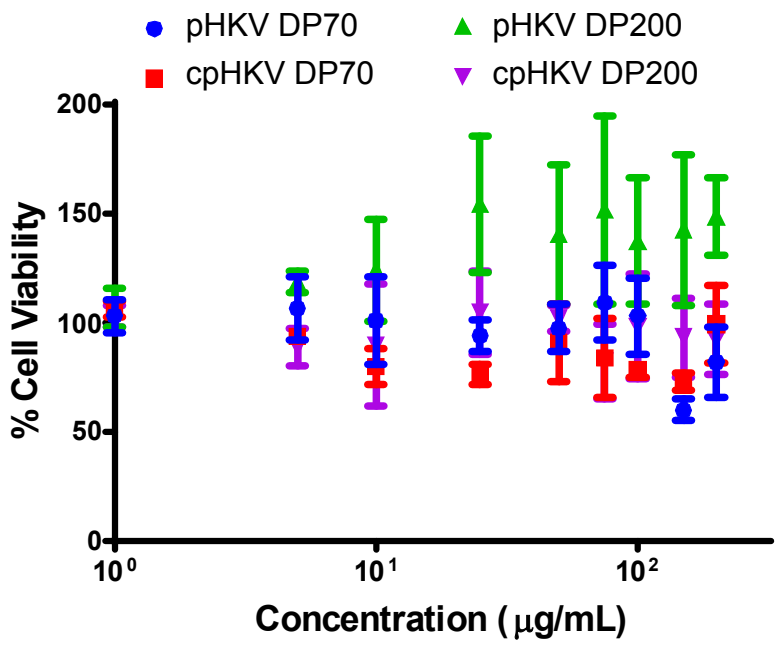

Figure 7.6. Toxicity curves for HeLa cells treated pHKV copolymers.

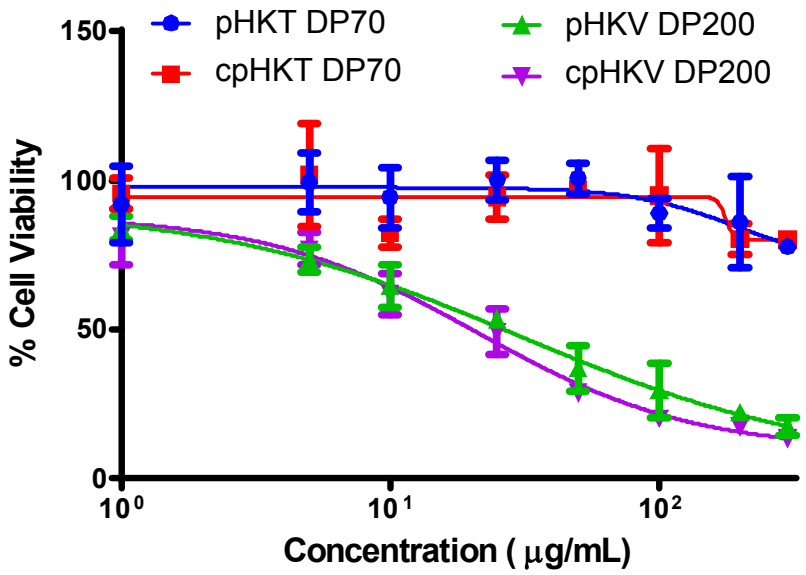

Figure 7.7. Toxicity curves of SNB-19 cells treated with pHKT DP200 (pHAT with only KLA conjugated), cpHKT DP200 (cpHAT with only KLA conjugated), pHKV DP200, and cpHKV DP200 copolymers.

Chapter 8

SUMMARY OF MAJOR FINDINGS AND RECOMMENDATIONS FOR FUTURE WORK

8.1 Summary of major findings

8.1.1 Peptide copolymers as nonviral gene delivery vectors

Peptide-based cationic polymers were developed to mediate nonviral gene delivery, with focus on incorporating polymer degradation and cellular targeting motifs. Chapter 2 summarizes previous work using living radical polymerization for developing nonviral gene delivery vectors, highlighting synthetic advantages of these techniques for developing well-controlled materials. In Chapter 3, copolymers of *N*-(2-hydroxypropyl) methacrylamide (HPMA), oligolysine, and Tet1, a neuron targeting ligand, mediated up to 80-fold enhanced luciferase expression in neuron-like differentiated PC-12 cells while not significantly affecting gene delivery to NIH/3T3 fibroblasts. These results were shown to be dependent on Tet1 incorporation, with materials containing only 1% Tet1 showing no increased transfection efficiency. However, Tet1 incorporation significantly increased the cytotoxicity of these materials in a dose-dependent manner, with higher mole % Tet1 correlating with increased cytotoxicity. In Chapter 4, HPMA-oligolysine copolymers, containing cathepsin B-sensitive linkers between the oligolysine sequence and the polymer backbone, were synthesized and evaluated. Polymers demonstrated rapid cleavage of oligolysine sequences upon treatment with cathepsin B, mediating polyplex unpackaging and DNA release within several hours. Enzyme-degradable materials were less cytotoxic while maintaining transfection efficiency comparable to non-degradable analogs.

8.1.2 Bivalirudin copolymers for spinal cord injury

In Chapter 5, MMP-responsive bivalirudin-functionalized HPMA copolymers were evaluated for direct, local administration into rat spinal cord contusion injury models. Bivalirudin peptides, linked to the polymer backbone via a MMP9-cleavable peptide linker, maintained activity while

grafted on the polymer backbone, demonstrated enzyme-mediated release upon MMP9 exposure, and had prolonged bivalirudin release from hyaluronic acid/methylcellulose (HAMC) hydrogels. Localized administration of bivalirudin copolymers physically encapsulated in HAMC hydrogels decreased cellular proliferation and astrogliosis at the lesion site while not affecting overall cell density. This therapeutic platform seems promising as a means to reduce the immediate inflammatory response, positively affect the long term scarring response, and potentially lead to a microenvironment more conducive towards functional recovery.

8.1.3 Linear and cyclic multivalent apoptotic polymers for cancer therapy

Linear and cyclic polymers displaying both cellular targeting and cytotoxic peptides were evaluated for treatment of glioblastoma multiforme. In Chapter 6, linear copolymers containing the apoptotic peptide KLA and the p32-targeting peptide GKRK demonstrated 20-80 fold increased cytotoxicity in several cancer cell lines. These materials had low hemolysis, increasing peptide potency without compromising membrane specificity. However, uptake of the polymers was low (< 1%), potentially significantly limiting the efficacy of the materials. In Chapter 7, cyclic polymers functionalized with KLA and VTW, a glioblastoma targeting ligand, were synthesized and evaluated to study the effects of polymer architecture on KLA bioactivity and cellular targeting. With lower molecular weight polymers, cyclic architecture was shown to have comparable cytotoxicity to linear analogs. However, with higher molecular weight polymers, cyclic polymers had enhanced cytotoxicity compared to linear analogs.

8.2 Recommendations for future work

8.2.1 – pH-responsive, endosomalytic peptide-polymeric micelles for nonviral gene delivery

Background and significance

In Chapters 3 and 4, we evaluated peptide-polymers for nonviral gene delivery, demonstrating that inclusion of targeting ligands and degradable linkers significantly enhanced transfection efficiency in target cells and decreased cytotoxicity. Further functionalization by inclusion of

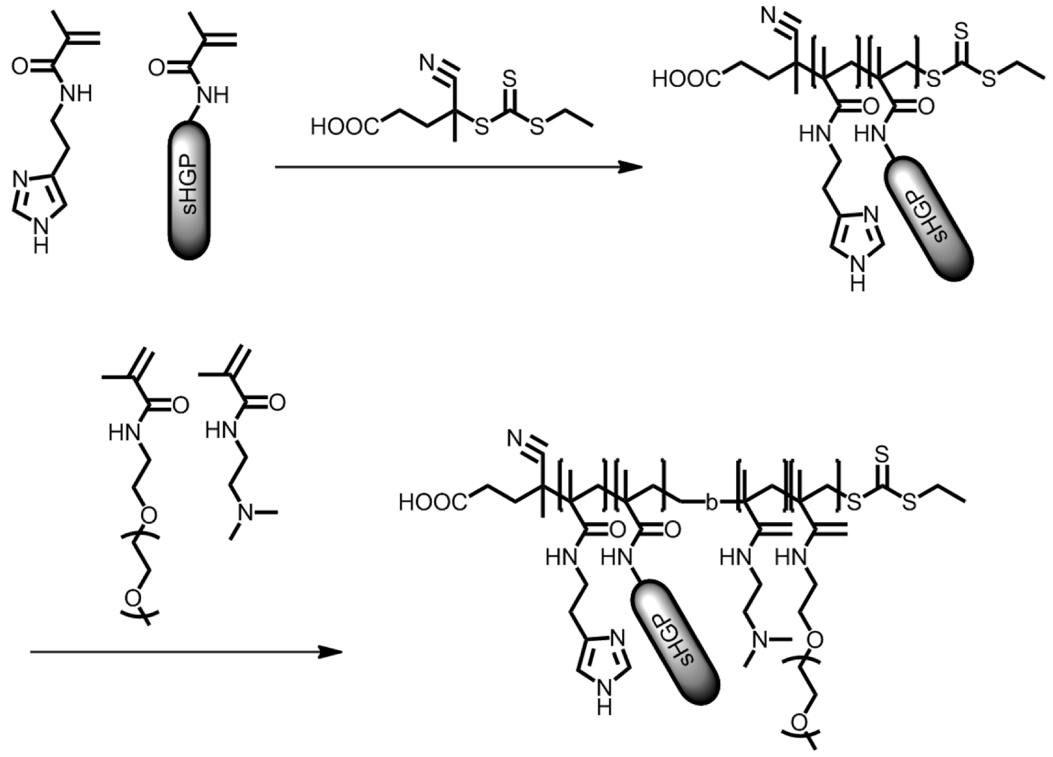

Scheme 8.1. Synthetic scheme of pH-responsive sHGP diblock copolymers.

endosomal escape moieties could mediate higher transfection efficiency. Schellinger et al demonstrated that HPMA-oligolysine diblock copolymers functionalized with the hydrophobic endosomalytic peptide sHGP formed micelles in solution, resulting in enhanced transfection efficiency with only slightly increased cytotoxicity.[1] Additionally, Wei et al demonstrated that polymeric core-shell particles improve transfection efficiency and particle stability.[2] Therefore, incorporation of the sHGP peptide into a pH-responsive hydrophobic core of core-shell particles could yield materials with high particle stability and low cytotoxicity.

Reversibly-protonable block copolymers have been investigated as pH-responsive micellar drug delivery systems. For example, polyhistidine-PEG diblock copolymers efficiently self-assemble into micelles under neutral and basic conditions but destabilize under acidic conditions due to protonation of the imidazole groups.[3,4] A similar strategy can be pursued to design diblock copolymers containing a pH-responsive hydrophobic core that would expose sHGP peptide upon acidification. This diblock copolymer would consist of a hydrophobic block containing imidazole-functionalized monomers copolymerized with sHGP, and a cationic second block to

yield core-shell polyplexes. This final polymer is expected to readily form micelles under neutral conditions but destabilize upon acidification, allowing for pH-triggered display of the sHGP peptide in the endolysosomes, potentially mediating enhanced transfection efficiency.

Aim 1: Synthesis and characterization of pH-responsive, sHGP diblock copolymers

Diblock copolymers containing a pH-responsive endosomalytic block of p(histamine methacrylamide-*co*-methacrylamido sHGP) and DMAEMA-*co*-OEGMA will be synthesized via RAFT polymerization (Scheme 8.1). Polymers will be analyzed by HNMR for conversion, GPC-MALLS for molecular weight determination, and amino acid analysis for peptide incorporation and polymer composition.

Aim 2: *In vitro* evaluation of sHGP diblock copolymers

sHGP copolymers will be evaluated *in vitro* for DNA condensation, polyplex formation, pH-responsive membrane lytic activity, and transfection efficiency. First, polymers will be incubated with DNA at various charge ratios and condensation will be analyzed via gel retardation assay. The size and zeta potential of the polyplexes will be determined using dynamic light scattering (DLS). DLS and transmission electron microscopy (TEM) will be used to verify micelle formation. pH-dependent membrane lytic activity will be determined by hemolysis assay with freshly-isolated erythrocytes at various pH. Finally, transfection efficiency will be evaluated on HeLa cells using the luciferase reporter transgene with cytotoxicity evaluated via MTS assay.

8.2.2 Polymer-loaded hydrogels for spinal cord injury

Background and significance

Hydrogels with a prolonged drug release profile are attractive for sustained drug efficacy during injury recovery. Promising results in Chapter 5 with HPMA-BM9-loaded HAMC hydrogels suggests that thrombin inhibition is a promising therapeutic strategy.[5] However, sustained thrombin inhibition was a challenge as polymers completely eluted from the hydrogel within 2

days (Figure 5.4). One strategy to prolong drug release is through direct conjugation of thrombin inhibitors to the HAMC hydrogel via environmentally-responsive linkers. Similar strategies have been investigated for MMP inhibition in cardiac injuries[6] and thrombin-responsive star-PEG hydrogels for hemostasis applications.[7] The Shoichet group has demonstrated successful immobilization of peptides, proteins, and other biomolecules onto HAMC hydrogels.[8-10] A similar approach can be utilized to incorporate potent thrombin inhibitors, like heparin, via environmentally-responsive linkers, thereby allowing for "on-demand," prolonged release of therapeutic. A formulation containing both physically encapsulated soluble inhibitors and hydrogel-immobilized molecules could allow for high concentrations of therapeutic during the primary injury response and sustained delivery during recovery.

Aim 1: Synthesis of heparin-conjugated HAMC hydrogel

Methylcellulose will be functionalized with maleimide groups as previously reported.[9] Cysteine-functionalized heparin will be synthesized by reacting heparin with the thrombin-sensitive peptide linker NH_2-Gly-Gly-(D)Phe-Pip-Arg-Ser-Trp-Gly-Cys-Gly-$CONH_2$ as previously reported.[7] Heparin will then be reacted with maleimido methylcellulose to yield heparin-methylcellulose conjugates.

Aim 2: In vitro characterization of HPMA-BM9-loaded heparin HAMC hydrogels

HPMA-BM9-loaded heparin-HAMC hydrogels will be evaluated *in vitro* for thermoresponsive gelation, HPMA-BM9 release kinetics, thrombin-mediated heparin release, and thrombin inhibition. Viscosity as a function of temperature will be measured to determine thermoresponsive gelation behavior. HPMA-BM9 hydrogel release and thrombin inhibition studies will be performed as previously described in Chapter 5. Thrombin-mediated heparin release will be quantified by treating HAMC-heparin conjugates with various amounts of thrombin and quantifying released heparin via gel electrophoresis.

Aim 3: *In vivo* evaluation of HPMA-BM9-loaded heparin-HAMC hydrogels in rat spinal cord injury.

HPMA-BM9-loaded heparin-HAMC hydrogels will be evaluated *in vivo* in rat spinal cord injury models. Shortly following spinal C4 contusion, the polymer-loaded hydrogel will be directly injected into the spinal column at the lesion site. Several markers of recovery will be investigated, including BrdU incorporation 24 hrs following injury; histological staining and cell counting in the lesion for astrocyte, microglia, and oligodendrocytes; and functional recovery as measured by several coordination tests.

8.2.3 "Janus" diblock cyclic copolymers for glioblastoma

Background and significance

Chapter 7 highlighted development of multifunctional cyclic peptide-polymers for glioblastoma. The statistical copolymers investigated had uniform display of various functional groups along the polymer backbone. Cyclizing diblock or multiblock copolymers, however, would have allowed for the synthesis of polarized cyclic polymers. Polarized display of functional groups may confer interesting physical properties, such as favoring supramolecular assembly based on the hydrophobicity of conjugated peptides, increasing bioactivity due to higher local density of peptides, and using the polymers as heterobifunctional crosslinkers. For example, small cyclic peptides have been investigated as methods to develop ordered nanotubes, where conjugation of different ligands at opposite sides of the cyclic peptide rings led to Janus nanotubes that assembled into tubular clusters to form membrane pores.[11] The physical properties conferred by polarized display of functional groups could potentially lead to interesting new drug carriers.

Aim 1. Synthesis of cyclic diblock copolymers

Linear diblock copolymers containing primary amines in one block and protected alkynes in the other will be synthesized via RAFT polymerization using an alkyne-functionalized chain transfer agent. Post-polymerization, an ω-azido group will be introduced and the polymer cyclized via copper-catalyzed "click" chemistry under dilute conditions. KLA peptide will be introduced via thiol-maleimide chemistry and VTW peptide subsequently following deprotection of the alkyne groups and copper-catalyzed click. Polymers will be characterized by GPC-MALLS for

molecular weight determination, amino acid analysis for peptide incorporation, and HNMR for conversion and to confirm click cyclization.

Aim 2. *In vitro* evaluation of diblock copolymers

Polymers will be evaluated *in vitro* for supramolecular assembly, cytotoxicity, and membrane activity. First, dynamic light scattering will be used to determine if diblock copolymers form supramolecular structures such as micelles. Cytotoxicity of the structures will be evaluated via MTS assay on SNB-19 cells treated with varying concentrations of polymer. Hemolysis assay will be performed to determine if the polymer induces plasma membrane destabilization. Purified mitochondria will be treated with polymer and assayed for O_2 respiration as an indicator of mitochondrial function.

8.3 References:

(1) Schellinger, J. G.; Pahang, J. A.; Shi, J.; Pun, S. H.: Block copolymers containing a hydrophobic domain of membrane-lytic peptides form micellar structures and are effective gene delivery agents. *ACS Macro Lett* **2013**, *2*, 725-730.

(2) Wei, H.; Volpatti, L. R.; Sellers, D. L.; Maris, D. O.; Andrews, I. W.; Hemphill, A. S.; Chan, L. W.; Chu, D. S. H.; Horner, P. J.; Pun, S. H.: Dual responsive, stabilized nanoparticles for efficient in vivo plasmid delivery. *Angew Chem Int Edit* **2013**, *52*, 5377-5381.

(3) Lee, E. S.; Shin, H. J.; Na, K.; Bae, Y. H.: Poly(L-histidine)-PEG block copolymer micelles and pH-induced destabilization. *J Control Release* **2003**, *90*, 363-74.

(4) Wu, H.; Zhu, L.; Torchilin, V. P.: pH-sensitive poly(histidine)-PEG/DSPE-PEG co-polymer micelles for cytosolic drug delivery. *Biomaterials* **2013**, *34*, 1213-22.

(5) Sellers, D. L.; Kim, T. H.; Mount, C. W.; Pun, S. H.; Horner, P. J.: Poly(lactic-co-glycolic)

acid microspheres encapsulated in Pluronic F-127 prolong hirudin delivery and improve functional recovery from a demyelination lesion. *Biomaterials* **2014**, *35*, 8895-8902.

(6) Purcell, B. P.; Lobb, D.; Charati, M. B.; Dorsey, S. M.; Wade, R. J.; Zellars, K. N.; Doviak, H.; Pettaway, S.; Logdon, C. B.; Shuman, J. A.; Freels, P. D.; Gorman Iii, J. H.; Gorman, R. C.; Spinale, F. G.; Burdick, J. A.: Injectable and bioresponsive hydrogels for on-demand matrix metalloproteinase inhibition. *Nat Mater* **2014**, *13*, 653-661.

(7) Maitz, M. F.; Freudenberg, U.; Tsurkan, M. V.; Fischer, M.; Beyrich, T.; Werner, C.: Bio-responsive polymer hydrogels homeostatically regulate blood coagulation. *Nat Commun* **2013**, *4*, DOI: 10.1038/ncomms3168.

(8) Caicco, M. J.; Cooke, M. J.; Wang, Y.; Tuladhar, A.; Morshead, C. M.; Shoichet, M. S.: A hydrogel composite system for sustained epi-cortical delivery of Cyclosporin A to the brain for treatment of stroke. *J Control Release* **2013**, *166*, 197-202.

(9) Vulic, K.; Shoichet, M. S.: Tunable growth factor delivery from injectable hydrogels for tissue engineering. *J Am Chem Soc* **2012**, *134*, 882-5.

(10) Gupta, D.; Tator, C. H.; Shoichet, M. S.: Fast-gelling injectable blend of hyaluronan and methylcellulose for intrathecal, localized delivery to the injured spinal cord. *Biomaterials* **2006**, *27*, 2370-2379.

(11) Danial, M.; My-Nhi Tran, C.; Young, P. G.; Perrier, S.; Jolliffe, K. A.: Janus cyclic peptide–polymer nanotubes. *Nat Commun* **2013**, *4*, DOI: 10.1038/ncomms3780.